The impact of glucose variation on human astrocytes

Submitted by

Paul Weightman Potter,

to the University of Exeter as a thesis for the degree of

Doctor of Philosophy in Medical Studies

In December 2018.

I certify that all material in this thesis which is not my own work has been identified and that any material that has previously been submitted and approved for the award of a degree by this or any other University has been acknowledged.

Abstract

Diabetes is a metabolic disorder dysregulating glucose homeostasis. The role of astrocytes in central glucose sensing is poorly understood. But it is recognised they take part in whole-body energy homeostasis, specifically as glucose sensors necessary for the counterregulatory response (CRR) to hypoglycaemia. Iatrogenic hypoglycaemia is the limiting factor to glycaemic control in people with type 1 or type 2 diabetes. Severe hypoglycaemia occurs approximately once per year, whereas, the incidence of minor hypoglycaemia is much greater. Hypoglycaemia impairs awareness of future hypoglycaemia and blunts the CRR, eventually causing hypoglycaemia-associated autonomic failure. The mechanisms of this process are poorly understood.

This thesis utilised isolated human astrocytes exposed to acute or recurrent low glucose (RLG) *in vitro* to mimic glucose variation in diabetes. Cellular responses were characterised of three key astrocyte functions. Firstly, is astrocyte metabolism altered by acute and RLG treatment? Secondly, do isolated human astrocytes become activated by low glucose treatment, and is this affected by RLG? Thirdly, are astrocytic inflammatory pathways altered by acute or RLG?

The key findings from this thesis shows for the first time that astrocytic mitochondrial oxidation is increased following RLG, with a concurrent increase in fatty acid dependency but decreased coupling efficiency; glycolytic function is also enhanced. Together, this indicates that astrocytes successfully adapt to low glucose to sustain intracellular nucleotide ratios. Contrary to previous work, these human astrocytes do not respond to low glucose by Ca^{2+}-dependent activation. However, the astrocytes do increase inflammatory cytokine release following acute and RLG. Lastly, for the first time an RNA-sequencing approach has been used to identify low glucose-induced differential gene expression. Together these findings support the argument that astrocytes are sensitive to low glucose and may be important in glucose sensation and the CRR.

Acknowledgements

I would like to thank first and foremost Dr Craig Beall, my primary supervisor. Without whom this thesis could not have been completed. I could not have asked for a better supervisor to guide me through my PhD. I would also like to thank the other supervisors and academics that have influenced this work including Prof Andy Randall, my second supervisor, as well as the keen scientific eye of Dr Kate Ellacott.

I would also like to thank the past and present members of the lab. Julia Vlachaki Walker, thank you for showing me the ropes and being an integral part of this project. Thank you to the rest of the lab team for putting up with me and being a part of this fantastic 'Beallacott' group. Julia, Ana, Ben, Josie, Alastair, and Nicole, thank you for making the RILD such the great working environment that it is.

Thank you to all my friends that have supported me. This includes those from my University of Bath days, especially Jenny Imm, who begun her PhD journey at the same time as me. Also, the friends I have made through Weightlifting and through American Football.

Thank you to my Father, Robert, and Brother, George, and extended family just for being my family and making me who I am today. Thank you also to my wonderful partner Jemma for tirelessly supporting and loving me over the years, and getting me to this point.

Lastly, I would like to dedicate this to my Mother, Elizabeth Weightman. While you are no longer with us I hope that you live on through me and my achievements, and you are proud of what I have done and will continue to do.

Table of contents

List of figures

Appendix A

List of tables

Appendix B

Publications arising from this thesis

Chapter 3

P.G. Weightman Potter, J.M. Vlachaki Walker, J.L. Robb, J.K. Chilton, R. Williamson, A.D. Randall, K.L.J. Ellacott and C. Beall. *Basal fatty acid oxidation increases after recurrent low glucose in human primary astrocytes*. Diabeteologia, 2019. **62**(1): p. 187-198.

Vlachaki Walker, J.M., J.L. Robb, A.M. Cruz, A. Malhi, **P.G. Weightman Potter**, M.L.J. Ashford, R.J. McCrimmon, K.L.J. Ellacott, and C. Beall, *AMP-activated protein kinase (AMPK) activator A-769662 increases intracellular calcium and ATP release from astrocytes in an AMPK-independent manner.* Diabetes, obesity & metabolism, 2017. **19**(7): p. 997-1005.

Author's declaration

All work was conducted by me, Paul Weightman Potter, at the University of Exeter Medical School laboratories with the exception of the following:

Chapter 3

- Mitotracker treatments and imaging of HPA cells was performed by Josie Robb – section 3.10, figure 3.10.
- Dr John Chilton ran the images of HPA cells stained with mitotracker through a MatLab script to determine mitochondrial number and length – section 3.10, figure 3.10.
- Julia Vlachaki Walker performed the comparisons between HPA and U373 cells basal fuel flexibility – section 3.8, figures 3.8.1, 3.8.2 and 3.8.3.

Chapter 4

- Julia Vlachaki Walker carried out the experiment and analysis where U373 cells were treated with recurrent low glucose stimulated with a higher ATP dose response – section 4.8.1, figure 4.8.1.

Chapter 5

- Julia Vlachaki Walker generated the samples used for the 24 hour low glucose treatment of U373 cells and analysed conditioned media content for macrophage-migration inhibitory factor (MIF) – section 5.5, figure 5.5.

List of abbreviations

For the convenience of the reader, listed below are the commonly used abbreviations in this thesis.

2-DG	2-deoxyglucose
3D	Three-dimensional
5HT	5-hydroxytryptamine; serotonin
6-AN	6-aminonicotinamide
6-NBDG	6-(N-(7-Nitrobenz-2-oxa-1,3-diazol-4-yl)amino)-6-Deoxyglucose
α-MSH	α-melanocyte stimulating hormone
A4	A438079
ACC	Acetyl-CoA carboxylase
ACTH	Adrenocorticotropic hormone
AD	Alzheimer's disease
ADP	Adenosine diphosphate
AGRP	Agouti-related peptide
AMP	Adenosine monophosphate
AMPK	AMP-activated protein kinase
ANLS	Astrocyte-neuron lactate shuttle
ANT	ATP/ADP antiporter
APP	Amyloid precursor protein
APS	Ammonium persulfate
ARC	Arcuate nucleus
ATP	Adenosine triphosphate
Aβ	Amyloid-β
BBB	Blood brain barrier
BDNF	Brain derived neurotrophic factor
BME	β-mercaptoethanol
BPTES	Bis-2-(5-phenylacetamido-1,3,4-thiadiazol-2-yl)ethyl sulfide
BSA	Bovine serum albumin
C1q	Complement component 1q
C3a	Complement component 3a
C3b	Complement component 3b
C5/C5a	Complement component 5a
CaMKK2	Ca2+/calmodulin-dependent protein kinase II
cAMP	Cyclic-AMP
CD40L	CD40 ligand
CD73	Cluster of differentiation 73
cDNA	Complimentary DNA
CFTR	Cystic fibrosis transmembrane regulator
CNS	Central nervous system
CoA	Coenzyme-A
COX	Cytochrome c oxidase
CPT1A	Carnitine palmitoyltransferase-a

CREB	cAMP-response element binding protein
CRR	Counterregulatory responses
CXCL1	C-X-C motif chemokine ligand 1
DAG	Diglyceride
DMH	Dorsomedial hypothamaus
DMSO	Dimethyl sulfoxide
DMV	Dorsal motor nucleus of the vagus
DNP	Dinitrophenol
DREADD	Designer receptors exclusively activated by designer drugs
EAAT1	Excitatory amino acid transporter 1
eATP	Extracellular ATP
ECAR	Extracellular acidification rate
EDTA	Ethylenediaminetetraacetic acid
EGTA	Ethylene glycol-bis(β-aminoethyl ether)-N,N,N',N'-tetraacetic acid
E-NPP	Ectonucleotide pyrophosphatase/phosphodiesterase
E-NTDPase	Ecto-nucleoside triphosphate diphosphohydrolase
ER	Endoplasmic reticulum
ETC	Electron transport chain
FA	Fatty acid
FADH2	Flavin adenine dinucleotide
FAS	Fatty acid synthase
FBS	Foetal bovine serum
FCCP	Carbonyl cyanide-p-trifluoromethoxyphenylhydrazone
FDR	False discovery rates
Fructose-2,6-P2	fructose-2,6-bisphosphate
G6P	Glucose-6-phosphate
G6PDH	Glucose-6-phosphate dehydrogenase
GABA	γ-aminobutyric acid
GAD	Glutamic acid decarboxylase
GAPDH	glyceraldehyde-3-phosphate dehydrogenase
G-CSF	Granulocyte-colony stimulating factor
GDM	Gestational diabetes mellitus
GE	Glucose excited
GECI	Genetically encoded calcium indicators
GFAP	Glial fibrillary acidic protein
GI	Glucose inhibited
GIP	Glucose-dependent insulinotropic polypeptide
GLAST	Glutamine aspartate transporter
GLP-1	Glucagon-like peptide 1
GLT-1	Glutamate transporter-1
Glut1	Glucose transporter 1
Glut2	Glucose transporter 2
Glut3	Glucose transporter 3
Glut4	Glucose transporter 4
GM-CSF	Granulocyte-macrophage colony stimulating factor
GPCR	G-protein coupled receptor

GPCR40	G-protein coupled receptor 40
GSH	Glutathione
GSK3β	Glycogen synthase 3 β
GSSH	Reduced glutathione
GWAS	Genome wide association studies
HAAF	Hypoglycaemia-associated autonomic failure
HbA1c	Glycosylated haemoglobin
HERPUD1	Homocysteine inducible ER protein with ubiquitin like domain 1
HFD	High fat diet
HK2	Hexokinase 2
HK-4	Hexokinase 4
HPA	Human primary astrocytes
HRP	Horseradish peroxidase
HSPA1A	Heat shock protein family A member 1A
IA-2	Islet antigen-2
ICAM	Intracellular cellular adhesion molecule
IFNγ	Interferon-gamma
IGF-1	Insulin like growth factor 1
IHA	Impaired hypoglycaemia awareness
IL-10	Interleukin-10
IL-12-p70	Interleukin-12-p70
IL-13	Interleukin-13
IL-16	Interleukin-16
IL-17	Interleukin-17
IL-17E	Interleukin-17E
IL-1a	Interleukin-1a
IL-1B	Interleukin-1β
IL-1ra	Interleukin-1ra
IL-2	Interleukin-2
IL-23	Interleukin-23
IL-27	Interleukin-27
IL-32a	Interleukin-32a
IL-4	Interleukin-4
IL-5	Interleukin-5
IL-6	Interleukin-6
IL-8	Interleukin-8
IMM	Inner-mitochondrial membrane
IP10	C-X-C motif chemokine ligand 10
IP3	Inositol triphosphate
IRS	Insulin receptor substrate
ISF	Interstitial fluid
I-TAC	C-X-C motif chemokine ligand 11
JNK	C-jun N-terminal kinase
kDa	kilo Daltons
KEGG	Kyoto Encyclopaedia of Genes and Genomes
KI	Knock-in

KO	Knock-out
LCFA	Long-chain fatty acid
LC-NA	Locus coeruleus-noradrenergic neurons
LDH	Lactate dehydrogenase
LDH5	Lactate dehydrogenase isomer 5
LKB1	Liver kinase B1
LOFC	Lateral orbitofrontal cortex
LRP1	Low density lipoprotein-related protein
LTP	Long-term potentiation
MAG	Monoacylglycerol
MAO	Monoamine oxidases
MAP	Mitogen activated protein
MCP-1	Monocyte chemoattractant protein-1
MCT	Monocarboxylate transporter
MIF	Macrophage-migration inhibitory factor
MIP-1A	C-C motif chemokine ligand 3
MIP-1B	C-C motif chemokine ligand 4
MnSOD	Mitochondrial superoxide
MODY	Maturity onset diabetes of the young
MPC	Mitochondrial pyruvate carrier
mTOR	Mammalian target of rapamycin
NA	Noradrenaline
NAD+	Nicotinamide adenine dinucleotide (oxidised)
NADH	Nicotinamide adenine dinucleotide (reduced)
NBT	Nitrotetrazolium blue chloride
NCX	Na+/Ca2+ exchanger
NFT	Neurofibrillary tangles
NFκB	Nuclear factor kappa B
NMDA	N-methyl-D-aspartate
NPY	Neuropeptide Y
NTS	Nucleus of the tractus solaris
OCR	Oxygen consumption rate
OGDC	Oxoglutarate or α-ketoglutarate dehydrogenase complex
OMM	Outer-mitochondrial membrane
P1	Adenosine receptor
P2	ATP receptors
PAI-1	Plasminogen activator inhibitor-1
PBS	Phosphate buffered saline
PDC	Pyruvate dehydroganse complex
PDH	Pyruvate dehydrogenase
PDK	Pyruvate dehydrogenase kinase
PEPCK	Phosphoenolpyruvate carboxykinase
PET	Positron emission topography
PFK(P)	Phosphofructokinase, platelet
PFK1	Phosphofructokinase-1
PFKFB3	6-phosphofructose-2-kinase/fructose-2,6-bisphosphatase-3

PGC1a	PPARγ coactivator-1α
Phosphofructokinase-1	PFK
PI3K	Phosphatidylinositol 3-kinase
PIP2	Phosphatidylinositol bisphosphate
PKA	Protein kinase A
PKB	Protein kinase B
PKC	Protein kinase C
PKM2	Pyruvate kinase M2
PLC	Phospholipase-C
PMCA	Plasma membrane Ca2+-ATPase
PMSF	Phenylmethanesulfonyl fluoride
PMSF	Phenylmethylsulfonyl fluoride
PMV	Portal mesenteric vein
POMC	Pro-opiomelanocortin
PP2A	Phosphatase 2A
PP2C	Protein phosphatase 2C
PPADS	Pyridoxalphosphate-6-azophenyl-2',4'-disulfonic acid
PPAR	Peroxisome proliferator-activated receptor
PPM1E	Mg2+-/Mn2+-dependent protein phosphatase 1E
PPP	Pentose phosphate pathway
PVN	Paraventricular nucleus
R5P	Ribose 5-phosphate
RANTES	C-C motif chemokine ligand 5
RH	Recurrent hypoglycaemia
RIIH	Recurrent insulin-induced hypoglycaemia
RLG	Recurrent low glucose
RNA-seq	RNA-sequencing
ROS	Reactive oxygen species
rpm	Revolutions per minute
SDF-1	Stromal cell-derived factor 1
SDHa	Succinate dehydrogenase-a
SDS-PAGE	Sodium dodecyl sulphate polyacrylamide gel electrophoresis
SERCA	Sarcoplasmic reticulum Ca2+-ATPase
sICAM-1	Soluble intracellular adhesion molecule-1
SNARE	Soluble N-ethyl maleimide-sensitive fusion protein attachment protein receptor
SOD	Superoxide dismutase
SREBP-1	Sterol regulatory element-binding protein 1
SSRI	Selective serotonin reuptake inhibitor
sTREM-1	Soluble triggering receptor expressed on myeloid cells
STZ	Streptozotocin
T172	Threonine 172
T1DM	Type 1 diabetes mellitus
T2DM	Type 2 diabetes mellitus
TAK1	TGFβ-activated kinase 1
tATP	total ATP

Tau	Microtubule associated protein tau
TBS-T	Tris buffered saline with tween
TCA	Tricarboxylic acid cycle
TEMED	N,N,N′,N′-Tetramethylethylenediamine
TMB	3,3,5,5'-tetramethylbenzidine
TNFα	Tumour necrosis factor α
TRPA1	Transient receptor potential cation channel
TU	Tuberal nucleus
UCP	Uncoupling protein
UDP	Uradine diphosphate
UTP	Uradine triphosphate
VCAM	Vascular cell adhesion molecule
VDAC	Voltage gated anion channel
VDCC	Voltage dependent calcium channels
VEGF	Vascular endothelial growth factor
VGCC	Voltage-gated calcium channels
VMN	Ventromedial nucleus of the hypothalamus
WAT	White adipose tissue
WGCNA	Weighted gene co-expression network analysis
WHO	World health organisation
XBP1	X-box binding protein 1
ZnT8	Zinc transporter 8 protein

Chapter 1

Introduction

1.1 Diabetes mellitus

Diabetes mellitus is an umbrella term used to describe a range of metabolic disorders that are characterised by faulty nutrient metabolism and insulin action. Diabetes is defined by hyperglycaemia, or high blood glucose levels. The threshold for hyperglycaemia is a fasted plasma glucose ≥7.0 mmol/l, or a 2-hour plasma glucose concentration after 75 g anhydrous glucose in an oral glucose tolerance test of ≥11.1mmol/l, or a random plasma glucose concentration of ≥11.1 mmol/l (Alberti et al. 1998). Hyperglycaemia also results in the classical symptoms of diabetes; polydipsia, polyuria, vision impairment, fatigue and nausea, as well as other severe symptoms (Alberti et al. 1998). Globally, diabetes prevalence in adults was estimated to be 8.8% in 2015 (Ogurtsova et al. 2017). The incidence of diabetes, globally, is predicted to increase to an estimated 10.4% in 2040 (Ogurtsova et al. 2017). In the United Kingdom, diabetes affects approximately 10% of adults, with an estimated cost of £23.7 billion, in 2011 (Hex et al. 2012). With a further 17% estimated increase by 2036 with associated costs of £22.9 billion (Hex et al. 2012).

Diabetes is commonly thought of as including type 1 diabetes mellitus (T1DM), type 2 diabetes mellitus (T2DM) and gestational diabetes mellitus (GDM). However, an international committee of experts solidified the definitions of the subtypes of the diabetes syndrome (ADA 2014). T1DM, T2DM and GDM are listed as polygenic disorders; where environmental factors are involved in disease pathogenesis. However, a fourth group contains “other specific types” of diabetes that includes 8 sub-categories within which are several members (ADA 2014). These other specific types include monogenic triggered diabetes, known as maturity onset diabetes of the young (MODY), as well as drug-induced pancreatic damage resulting in diabetes. T2DM is the most common subtype accounting for 90.4% of cases, whereas T1DM and other specific types account for 8.5% and 1.2% respectively, in the UK (Holman et al. 2015).

1.1.1 Type 2 diabetes mellitus

The pathogenesis of T2DM is principally characterised by insulin resistance resulting in an inability to reduce blood glucose levels. Insulin is released from the β-cell found in the islets of Langerhans within the pancreas (Hoang Do et al. 2015). Insulin is released in response to high glucose (mechanisms discussed in section 1.3.1). Once released, insulin binds to insulin receptors found in the muscle, liver, adipose tissue,

and the brain among others to increase glucose uptake, glycogen synthesis, and lipogenesis; and to decrease food intake, gluconeogenesis and lipolysis (Taniguchi et al. 2006). In T2DM, insulin sensitivity is lost resulting in reduced glucose uptake by the muscle and suppression of glucose production particularly in the liver (Stumvoll et al. 2005).

While the precise mechanisms of insulin resistance remain unknown, obesity correlates with the onset of insulin resistance and subsequent T2DM (Bastard et al. 2006). Obesity is a condition where the body has large fat deposits due to excess caloric intake relative to energy expenditure. Lipids are primarily stored in adipocytes of white adipocyte tissue (WAT) as triglycerides (Trayhurn 2007). In the absence of food intake the triglycerides are metabolised and released as fatty acids which can be an energy substrate for other cells. However, this occurs in excess during obesity. The release of fatty acids, the most common being palmitate, has been shown to impair insulin sensitivity (Vessby et al. 1994) and decrease insulin-stimulated glucose uptake in skeletal muscle (Roden et al. 1996) and liver (Boden 1997). Aside from subcutaneous adiposity, ectopic fat storage is also important for insulin resistance (Danforth Jr 2000). Both intramyocellular (Machann et al. 2004) and intrahepatic (Seppälä-Lindroos et al. 2002, Bajaj et al. 2003) lipids are associated with insulin resistance.

To compensate for a lack of insulin action, insulin secretion from β-cells increases to compensate (Wilcox 2005). Prolonged hyperglycaemia results in β-cell hyperplasia increasing the β-cell mass and therefore increasing the insulin producing capacity of the pancreas (Bonner-Weir et al. 1989). While this initial compensatory hyperinsulinaemia compensates for insulin insensitivity, β-cell dysfunction eventually occurs. People with a family history of diabetes sometimes fail to display this initial β-cell compensatory response to the onset of insulin resistance (Elbein et al. 2000). This highlights that while lifestyle and environmental factors are triggering pathogenic drivers, genetic factors also impact the likelihood of diabetes. Indeed, monozygotic and dizygotic twin studies have been used to demonstrate a heritable genetic risk for diabetes (Stumvoll et al. 2005).

1.1.2 Type 1 diabetes mellitus

While T1DM also results in hyperglycaemia, like T2DM, this is due to an absolute lack of insulin production rather than action. T1DM is an autoimmune disorder characterised by the destruction of the pancreatic β-cell, thus ablating insulin production. The resulting failure to suppress gluconeogenesis and increase glucose uptake results in fasted hyperglycaemia. At disease onset, auto-reactive T cells mediate the destruction of β-cells (Tsai et al. 2008, Willcox et al. 2009). Indeed, islet-cell auto-antibodies are present and are a positive indicator of T1DM risk (Pihoker et al. 2005). Glutamic acid decarboxylase (GAD), islet antigen 2 (IA-2), insulin, and zinc transporter 8 protein (ZnT8) are the four most commonly found auto-antibodies at disease onset (Atkinson et al. 2001).

Despite the understanding that, predominantly, T-cells mediate β-cell destruction, the precise triggers remain unknown. In 1866, it was first suggested that T1DM may be hereditary (Harley 1866). This observation is confirmed by genome wide association studies (GWAS) that show many genes to increase risk of T1DM (Jerram et al. 2017), many of which are linked to immune function (Mehers et al. 2008).

While T1DM susceptibility is influenced by genetic factors, there is only a 50% concordance between monozygotic twins in developing T1DM (Metcalfe et al. 2001). Therefore, environmental factors must be involved in initiating disease onset. One such factor may be enteroviral infection which was found in 61% of recently diagnosed T1DM patients (Richardson et al. 2009). Other factors proposed include changes in gut health and microbiota (Vaarala et al. 2008, Knip et al. 2012), as well as vitamin D deficiency (Cantorna et al. 2004). While there are multiple factors involved it remains unclear the relative importance of each in influencing disease aetiology. Therefore, genetic risk factors remain most important in predicting onset of T1DM (Concannon et al. 2009).

1.2 Pancreas

All forms of diabetes result in the same endpoint; hyperglycaemia and associated complications. While there are different triggers and mechanisms involved in diabetes they revolve around glucose homeostasis dysregulation. Therefore, an improved understanding of glucose homeostasis and the cells, tissues, organs and organ systems involved is required for the better therapies and potential cures.

The pancreas is both an endo- and exocrine organ surrounded by multiple major blood vessels that distribute the signalling molecules released (Jouvet et al. 2017). Approximately 98% of pancreatic mass is made up of acinar cells which release digestive enzymes into the duodenum (Husain et al. 2009). The remaining 2% is comprised of the α-, β-, δ-, ε- and PP-cells (Jouvet et al. 2017). In diabetes these are of the most importance as the β- and α-cells release the endocrine hormones insulin and glucagon respectively. δ-cells are also found in other organs, i.e. the stomach, and secrete somatostatin which suppresses insulin and glucagon release (Sacks et al. 1977, van der Meulen et al. 2015). ε-cells secrete ghrelin which mediates food intake, fat deposition and growth hormone release (Pradhan et al. 2013). Finally, the PP-cells release pancreatic polypeptide which autoregulates endocrine function as well as gastrointestinal secretion (Kojima et al. 2007).

1.3 Glucose homeostasis

Glucose homeostasis is tightly controlled in a healthy person even in states of extreme energy expenditure and excess. To mediate glucose homeostasis the pancreas releases the hormones insulin and glucagon to decrease or increase blood glucose respectively. However, additional neuronal mechanisms exist which regulate body weight, metabolism and food intake (Schwartz et al. 2005, Prodi et al. 2006). Furthermore, while classically thought of an energy store, adipose tissue is being recognised as a regulator of metabolism (Rosen et al. 2006). For example, adipocytes release leptin which decreases food intake and enhances energy expenditure. A principle target site of leptin function are the leptin receptors found in the brain in the mediobasal hypothalamus where it supresses orexigenic and activates anorexigenic pathways (Rosen et al. 2006). Lastly, the gastrointestinal tract and gut hormones regulates glucose homeostasis as well (Drucker 2007). For example, glucose-dependent insulinotropic polypeptide (GIP) and glucagon-like peptide-1 (GLP1), released from the gut, modulate meal-stimulated insulin secretion from β cells in a glucose dependent manner (Drucker et al. 2006).

While there are several excellent overviews of glucose homeostasis and how it is altered by diabetes, (Rosen et al. 2006, Marty et al. 2007, Watts et al. 2010, Jouvet et al. 2017), due to the breadth and depth of the literature, a fully comprehensive review is not within the scope of this thesis. Instead the following brief review presents an outline of peripheral glucose homeostatic mechanisms and focuses

more closely on neural regulation of glucose homeostasis. The role of astrocytes and their impact on glucose homeostasis will be discussed in detail.

1.3.1 Glucose homeostasis: insulin release and action

The release of insulin from β-cells is dependent on sensing elevated glucose concentrations. In a healthy human β-cell glucose is uptaken via glucose transporter 1 (Glut1) and Glut3 (McCulloch et al. 2011). Glucose is metabolised through glycolysis and further metabolised by the mitochondria to generate ATP. This increases the ATP/ADP ratio in the β-cell. The K_{ATP} channel is closed by this elevation of ATP depolarising the cell membrane which opens the voltage-gated calcium channels (VGCC) allowing the influx of Ca^{2+} and thus increasing $[Ca^{2+}]_i$. This promotes the fusion of insulin granules with the cell membrane and the release of the insulin contained within (Orci et al. 1973, Komatsu et al. 2013).

β-cell insulin release is also modulated by fatty acids and amino acids. For example, L-glutamate, in isolation, does not alter insulin release, but enhances insulin secretion in the presence of L-leucine (Newsholme et al. 2006, Newsholme et al. 2014). Fatty acids can regulate insulin release from β-cells in three known distinct pathways. Firstly, fatty acid metabolism contributes to ATP production, through mitochondrial metabolism, closing K_{ATP} channels (Prentki et al. 2013). Secondly, long-chain fatty acids (LCFA) can directly activated the G-protein coupled receptor (GPCR) 40 (GPCR40), found in β-cells, to increase insulin release (Mancini et al. 2013). Lastly, during fatty acid metabolism, monoacylglycerol (MAG) is produced with activates Munc13-1, an insulin granule exocytosis activator [14].

Non-pancreas derived hormones such as the incretins regulate β-cell metabolism. Incretins include GLP-1, and GIP, secreted by K and L cells respectively in the gut (Meier et al. 2005). While GLP-1 augments insulin secretion, and suppresses glucagon secretion from α-cells, GIP increases glucagon secretion (Meier et al. 2003).

Released insulin acts across the body to enhance energy consumption and suppress energy production. Insulin receptors are found throughout the body, including the brain, liver, adipose, and muscle (Ullrich et al. 1985). When insulin binds to the receptor, the α-subunit conformationally changes allowing for β-subunit auto-phosphorylation and phosphorylation of insulin receptor substrates (IRS). Once the

α-subunit of the β-subunit auto-phosphorylates and further phosphorylates IRS. This activates mitogen-activated protein (MAP) kinase signalling pathway as well as the phosphatidylinositol 3-kinase (PI3K)-protein kinase B (PKB) signalling pathway which regulates cell growth, gene expression, lipogenesis, glycogenesis and glucose uptake (Frasca et al. 2008).

Insulin also decreases blood glucose by increasing glycogen storage in a process known as glycogenesis. Upon binding to the insulin receptor, the subsequent activation of protein kinase C (PKC) disinhibits glycogen synthase by inhibiting its phosphorylation by glycogen synthase kinase 3-β (GSK3-β) (Lochhead et al. 2001). The principle sites of glycogen storage are in the liver and muscle (Wasserman 2009). However, glycogen stores are also found in the brain in astrocytes (Brown 2004). These small cerebral stores of glycogen can also be increased by insulin stimulation (Muhič et al. 2015). It is generally considered that insulin enters the brain from the periphery and originates from the pancreas via insulin-receptor mediated active transport (Schwartz et al. 1992, Baura et al. 1993, Woods et al. 2003, Banks 2004). However, based on analysis of cultured rodent neurons (Devaskar et al. 1994), and *in situ* hybridisation techniques showing the expression of insulin and preproinsulin mRNA in the rodent brain (Schechter et al. 1996) indicates that the brain may also produce some portion of this insulin (Gerozissis 2008). Insulin binds to insulin receptors found on the neurons and glia in networks associated with feeding, reproduction or cognition (Baskin et al. 1983, Brüning et al. 2000, Gerozissis 2003). The intact hypothalamic insulin signalling mechanisms are required for the full systemic effect of insulin on reducing endogenous glucose production (Obici et al. 2002b, Prodi et al. 2006). For example, central insulin action can stimulate muscle glycogen synthesis (Perrin et al. 2004).

Insulin upregulates lipogenic gene expression by activating sterol regulatory element-binding protein 1 (SREBP-1) (Lane et al. 1990, Assimacopoulos-Jeannet et al. 1995, Nakae et al. 1999), and also increases leptin release from adipocytes by increasing gene expression (Malmstrom et al. 1996, Koopmans et al. 1998, Saad et al. 1998). Leptin is a satiety hormone that correlates strongly with BMI and fat mass (Considine et al. 1996, Dagogo-Jack et al. 1996). While leptin binds to type 1 cytokine receptors found throughout the body (Cirillo et al. 2008), it mainly acts on the hypothalamus to both inhibit neuropeptide Y and stimulate satiety (Elias et al.

1999, Elmquist et al. 1999, Fekete et al. 2000). Therefore, suppressing food intake and increasing anabolic processes.

1.3.2 Glucose homeostasis: glucagon release and action

Glucagon contradicts the actions of insulin by increasing endogenous glucose production, glycolysis and lipolysis. Glucagon, released from the α-cells of the pancreas, binds to the glucagon receptor, a GPCR found throughout the body; liver, pancreas, brain, heart, adrenal glands, thyroid and skeletal muscle (Hansen et al. 1995, Brubaker et al. 2002). Once activated the glucagon receptor stimulates adenylate cyclase to increase $[cAMP]_i$, activating protein kinase A (PKA), which phosphorylates and activates glycogen phosphorylase (Exton 1987, Johnson 1997) and catalyses the breakdown of glycogen to generate glucose-6-phosphate. Glucose exits myocytes and hepatocytes via Glut2 to raise blood glucose levels (Nordlie et al. 1999). Additionally, glucagon increases blood glucose by inhibiting glucose storage. Glucagon inhibits glycogen synthase activity (via PKA activation) which also activates glycogen phosphorylase (Ciudad et al. 1984, Roach 1990). Glucagon also inhibits glycolysis in the liver by inhibiting phosphofructokinase-1 (PFK1) (Pilkis et al. 1991, Okar et al. 1999). Glucagon can stimulate hepatic gluconeogenesis via phosphoenolpyruvate carboxykinase (PEPCK) and the activation of cAMP-response element binding protein (CREB) via PKA. CREB activation increases gene transcription of, for example, PEPCK (Herzig et al. 2001, Yoon et al. 2001).

1.4 Central regulation of glucose homeostasis

The sensitivity of the brain to low glucose was identified in the 1950s (Mayer 1953). The brain can control glucose homeostasis, by altering glucose production and utilisation, and food intake. The hypothalamus is the centre of glucose homeostasis, feeding and energy expenditure in the brain (Schwartz et al. 2000, Spiegelman et al. 2001, Flier 2004, Schwartz et al. 2005, Stanley et al. 2005), with the action of glucose sensing neurons being identified in the 1960s by Oomura *et al* (Oomura et al. 1969). It is optimally located at a part of the blood-brain barrier (BBB) that is more permeable to nutrients and is located close to the Willis polygon making the hypothalamus one of the first brain areas to be supplied with arterial blood (Leloup et al. 2016). To facilitate the increased permeability of the BBB in this area the capillaries are specialised with semi-permeable endothelial cells unlike normal blood vessels (Rodriguez et al. 2010). The hypothalamus is comprised of distinct nuclei

that coordinate energy balance: arcuate nucleus, ventromedial nucleus (VMN) and the paraventricular nucleus (PVN). Additionally the hindbrain is also involved in regulating energy balance, including the nucleus of the tractus solaris (NTS; nucleus of the solitary tract) and the dorsal motor nucleus of the vagus (DMV) (Grill et al. 2012). Together these nuclei integrate neuronal (e.g. vagal nerve), hormonal (e.g. leptin, ghrelin, and insulin) (Baskin et al. 1999, Beverly et al. 2000, Bellinger et al. 2002), and nutritional inputs (e.g. glucose (Beverly et al. 2000, Routh et al. 2014), fatty acids (Obici et al. 2002a, Lam et al. 2005a), and amino acids (Su et al. 2012)) to modulate food intake, energy expenditure, and fat deposition (Morton et al. 2006).

1.4.1 Metabolism sensing neurons

The detection of energy state within the brain depends on neuronal signalling from glucose excited (GE) and glucose inhibited (GI) neurons (Song et al. 2001, Levin et al. 2004). The current understanding of hypothalamic glucose-excited (GE) neurons sensing stems from the "β-cell model" of glucose sensing (described in 1.3.1). Briefly, in the β-cells of the pancreas, glucose is taken up by Glut-2 and metabolised by hexokinase-4 (HK-4; glucokinase). In a dose-dependent manner, glucose uptake increases the ratio of ATP:ADP within the cell. This closes the K_{ATP} channels depolarising the cell with further Ca^{2+} influx. Conversely, in low glucose the K_{ATP} channel is open and hyperpolarises the cell preventing firing. Glucose-inhibited (GI) neurons, on the other hand, are hyperpolarised by high glucose levels and depolarised by low glucose (Routh 2002). The key molecule mediating glucose sensing in these cells is AMP-activated protein kinase (AMPK) (Murphy et al. 2009). AMPK acts as an intracellular 'fuel-gauge' (McCrimmon 2008), which is activated by the relative abundance of AMP, which displaces ATP and prevents dephosphorylation of AMPK. Once activated, AMPK blocks the cystic fibrosis transmembrane regulator (CFTR) Cl^- ion channel (Murphy et al. 2009), thus activating voltage dependent calcium channels (VDCC) which depolarises the cell and stimulates neurotransmitter release (Beall et al. 2012b). Other evidence suggests that tandem-pore K^+ channels (K_{2P}) mediates orexin GI neuronal firing (Burdakov et al. 2006). Additionally, in orexin GI neurons the intracellular supply of glucose or ATP, and preventing Ca^{2+} influx did not inhibit their firing suggesting that the glucose-sensing mechanism required extracellular signalling to alter firing rates (Burdakov et al. 2006).

In addition to glucose, neurons also sense changes in other nutrients, including fatty acids and amino acids, which can be modulated by hormones (insulin, leptin, ghrelin) and neurotransmitters (5HT, NA) to moderate feeding and energy balance (Watts et al. 2010, Toda et al. 2017). Pro-opiomelanocortin (POMC) neurons, for example, release POMC to regulate metabolism (Parton et al. 2007). This can be cleaved to produce α-melanocyte stimulating hormone (α-MSH; involved in satiety (Varela et al. 2012)), adrenocorticotropic hormone (ACTH; regulating glucocorticoid secretion (Bornstein et al. 2008)), β-endorphin, and opioid peptides (Smith et al. 1988). POMC mutations result in an obese phenotype, indicating its role in metabolism (Coll et al. 2004). POMC neurons are found within the hypothalamus, in the arcuate nucleus (ARC), and the hindbrain, in the NTS. Low glucose attenuates POMC neuron firing rates in *ex vivo* slices from mice (Parton et al. 2007), similar to a glucose excited cell phenotype (Ibrahim et al. 2003). This is mediated by the K_{ATP} channel (Parton et al. 2007) where, as glucose levels decrease, the ATP:AMP ratio decreases which opens the K_{ATP} channel increasing hyperpolarisation. POMC neurons are also activated by leptin, endocannabinoids, nicotine, serotonin, fatty acids and amino acids, and inhibited by ghrelin and glucocorticoids (Toda et al. 2017). Interestingly, insulin has been reported to both suppress (Plum et al. 2006, Williams et al. 2010) and activate (Qiu et al. 2014) POMC neurons.

Neuropeptide Y (NPY)/ agouti-related peptide (AGRP) neurons are similarly found in ARC and the hindbrain (Akabayashi et al. 1993, Akabayashi et al. 1994, Sergeyev et al. 2000, Elmquist 2001, Fraley et al. 2003, Li et al. 2004, Li et al. 2006). However, NPY/AGRP neurons are a population of orexigenic neurons that stimulate feeding behaviour (Gropp et al. 2005, Wu et al. 2009), unlike the anorexigenic POMC neurons (Sohn 2015). For example, NPY/AGRP pharmacogenetic or optogenetic activation increases food intake in mice (Aponte et al. 2011, Krashes et al. 2011). Ghrelin and glutamate released from excitatory neurons increase the firing rate of NPY/AGRP neurons (Enriori et al. 2007, Sohn 2015). NPY/AGRP neurons primarily release γ-aminobutyric acid (GABA) (Krashes et al. 2013) which suppresses POMC neurons (Cowley et al. 2001). The inhibitory function of the NPY/AGRP neurons suggests their role as inhibitors of the anorexigenic centres of the CNS.

1.4.2 Glucose sensing networks

The schema by which sensory input is integrated and actioned upon by the brain is achieved via the basic principle of sensory motor integration first proposed by Sherrington (Sherrington 1906). Firstly, sensory neurons, i.e. GE or GI neurons, centrally or peripherally, detect an initial stimulus. Secondly, this is relayed and processed by integrative networks for higher level processing, or directly to pre-motor control neurons which directly project to defined motor neurons allowing for reflexive responses. Lastly, the motor neurons, that mediate the output from the brain to effector cells (i.e. pancreatic α- and β- cells).

1.4.2.1 Glucose sensing networks: glucose sensors

Glucose sensing cells can be found centrally, in the hypothalamus (Oomura et al. 1969), hindbrain (Adachi et al. 1984), and in the periphery, in the hepatic portal mesenteric vein (PMV), gut and oral cavity (Niijima 1989, Thorens et al. 2004, Fujita et al. 2005) and in the pancreatic β-cells (MacDonald Patrick et al. 2005). Interestingly, many of the glucose-sensitive cells in the hypothalamus (Shimizu et al. 1983) and hindbrain (Adachi et al. 1984) respond to changes in glucose within the PMV via vagal afferents. Indeed, hindbrain hypoglycaemia-induced FOS activation is greatly reduced by chemically preventing neurotransmission from the PMV (Bohland et al. 2014). In the hindbrain there several glucose sensing areas (Lynch et al. 2000, Andrew et al. 2007) including the area postrema (Funahashi et al. 1993), nucleus of the tractus solaris (NTS) and the dorsal nucleus of vagus nerve (DMX) (Mizuno et al. 1984, Balfour et al. 2006). Within the hypothalamus, glucose-sensing areas include the lateral hypothalamus (Oomura et al. 1964), and the ventromedial hypothalamus including the ventromedial nucleus of the hypothalamus (VMN), arcuate nucleus (Arc), paraventricular nucleus (PVN), tuberal nucleus (TU), and lateral hypothalamus all of which are critical for counterregulatory responses (CRR) to hypoglycaemia (Borg et al. 1995, Borg et al. 1997, Beverly et al. 2000, Song et al. 2001, Chan et al. 2006, Chan et al. 2008).

1.4.2.2 Pre-motor control and their targets

The pre-motor neurons project directly to their respective neuroendocrine and pre-autonomic neurons within the hypothalamus, hindbrain and spinal cord. Viral tracer studies in the pancreas, and adrenal gland identified regions of the hypothalamus (Jansen et al. 1997, Buijs et al. 2001) and hindbrain (Kerman et al. 2003, Kerman et

al. 2006, Kerman et al. 2007) as containing pre-motor neurons. Within the hindbrain several regions have been identified, including the NTS, locus coeruleus and A5 catecholamine cell group. These groups then activate pre-autonomic parasympathetic (e.g. the NTS activating the pancreas), or both the parasympathetic and sympathetic networks (Watts et al. 2010).

Regions of the hypothalamus project into the hindbrain and spinal cord (Saper et al. 1976, Swanson et al. 1980) which can regulate CRR (Motawei et al. 1999). Specifically, the PVN, lateral hypothalamus, and retrochiasmatic area contribute to CRR by pre-autonomic control of the pancreas and adrenal gland (Watts et al. 2010). Injections of noradrenaline, opiate agonists or neuropeptide Y into the PVN increased plasma adrenaline and glucose levels (Kiritsy-Roy et al. 1986, Leibowitz et al. 1988), demonstrating the role of the PVN to regulate glucose concentrations. The PVN integrates signals from the ARC (Sawchenko et al. 1983, Broberger et al. 1998b), lateral hypothalamus (Watts et al. 1999) and dorsal-medial hypothalamus (Thompson et al. 1996). The corticotropin-releasing hormone pre-motor neurons of the PVN trigger the release of adrenocorticotropic hormone (ACTH) which stimulates the synthesis and release of glucocorticoids which are important for counterregulation (Cryer 1997a). Glucocorticoids, including cortisol, stimulate gluconeogenesis in the liver, reduce glucose uptake and stimulate lipolysis (Munck 1971, Exton et al. 1972). The lateral hypothalamus projects to the spinal cord and hindbrain (Saper et al. 1976), as well as the pancreas adrenal gland (Jansen et al. 1997, Buijs et al. 2001, Kerman et al. 2006), and liver (Yi et al. 2010). Furthermore, the lateral hypothalamus projects to other hypothalamic regions involved in CRR, including the VMN (Canteras et al. 1994), ARC (Broberger et al. 1998a, Broberger et al. 1998b), and PVN (Sawchenko et al. 1983, Watts et al. 1999). Lastly, the retrochiasmatic area projects to the pancreas and adrenal gland. But it is unknown the extent of its role in CRR.

1.4.2.3 Integrative networks of glucose regulation

There is a good comprehension of the general mechanisms of glucose sensing and that central networks mediate glucose homeostasis (Ritter et al. 2003, Saberi et al. 2008). For example, the hindbrain contains all the necessary components for glucose homeostasis as sympathoadrenal responses remain following decerebration and 2-DG-glucoprivation in rats (DiRocco et al. 1979). Additionally, specific

glucoprivation within the hindbrain triggers counterregulatory responses (Cechetto et al. 1988, Cardin et al. 2001). Within the hindbrain chatecholaminergic (adrenaline or NA releasing cells) widely innervate the CNS (Ungerstedt 1971) including the hypothalamus and spinal cord (Watts et al. 2010, Ritter et al. 2011) and *vice versa*.

The hypothalamus is well known for its control of metabolism (Bellinger et al. 2002, Evans et al. 2004b). The VMN, alongside metabolism, also integrates sexual behaviour and territoriality (Yang et al. 2013). The dendrites extend beyond its nuclear borders, which likely contributes to its diverse functions (Millhouse 1973). However, retrograde viral tracer studies have failed to demonstrate the VMN as innervating the liver, pancreas or adrenal gland directly (Jansen et al. 1997, Buijs et al. 2001). These studies utilised pseudorabies viral tracer techniques where the neurotropic virus can propagate from an initial injection site along neurons; afterwards the pseudorabies virus presence in neurons is identified immunohistochemically. However, it does interact with pre-autonomic hypothalamic neurons in the lateral hypothalamus and PVN (Sawchenko et al. 1983, Canteras et al. 1994, Watts et al. 2010). Furthermore, retrograde viral studies in the pancreas showed first order neurons in the hindbrain, second order neurons locus coeruleus as well as the paraventricular nucleus of the hypothalamus (PVN), and lastly third-order neurons in the VMN and Arc indicating their role in the glucose regulatory network (Buijs et al. 2001). This signifies the importance of the VMN in regulating the pancreas indirectly via pre-autonomic neurons.

The Arc is another region that is part of the greater integrative network of glucose homeostasis (Watts et al. 2010). Being a small region there are few tracing studies of its projections, however it does contain NPY/AGRP and POMC neurons. These neurons project to the telencephalon and other nuclei within the hypothalamus (Broberger et al. 1998b, Haskell-Luevano et al. 1999). Within the hypothalamus, Arc neurons project to the lateral hypothalamus and the PVN which directly links the Arc with pre-autonomic control networks (Sawchenko et al. 1983, Broberger et al. 1998a). These neurons are also found in the dorsomedial hypothalamus (DMH) (Broberger et al. 1998b, Haskell-Luevano et al. 1999), and the hindbrain (Kenny 2011, Blevins et al. 2013).

Together these networks, both central and peripheral, interact to provide a complex and integrative system for regulating glucose homeostasis (figure 1.1). These networks allow for autonomic responses to changes in glucose, but also allow for modulatory input from other brain regions (Loewy 1991, Saper 2002). However, as the hindbrain can regulate glucose homeostasis without forebrain input (DiRocco et al. 1979) this suggests some hierarchical structure to the overall central glucoregulatory network.

Figure 1.1

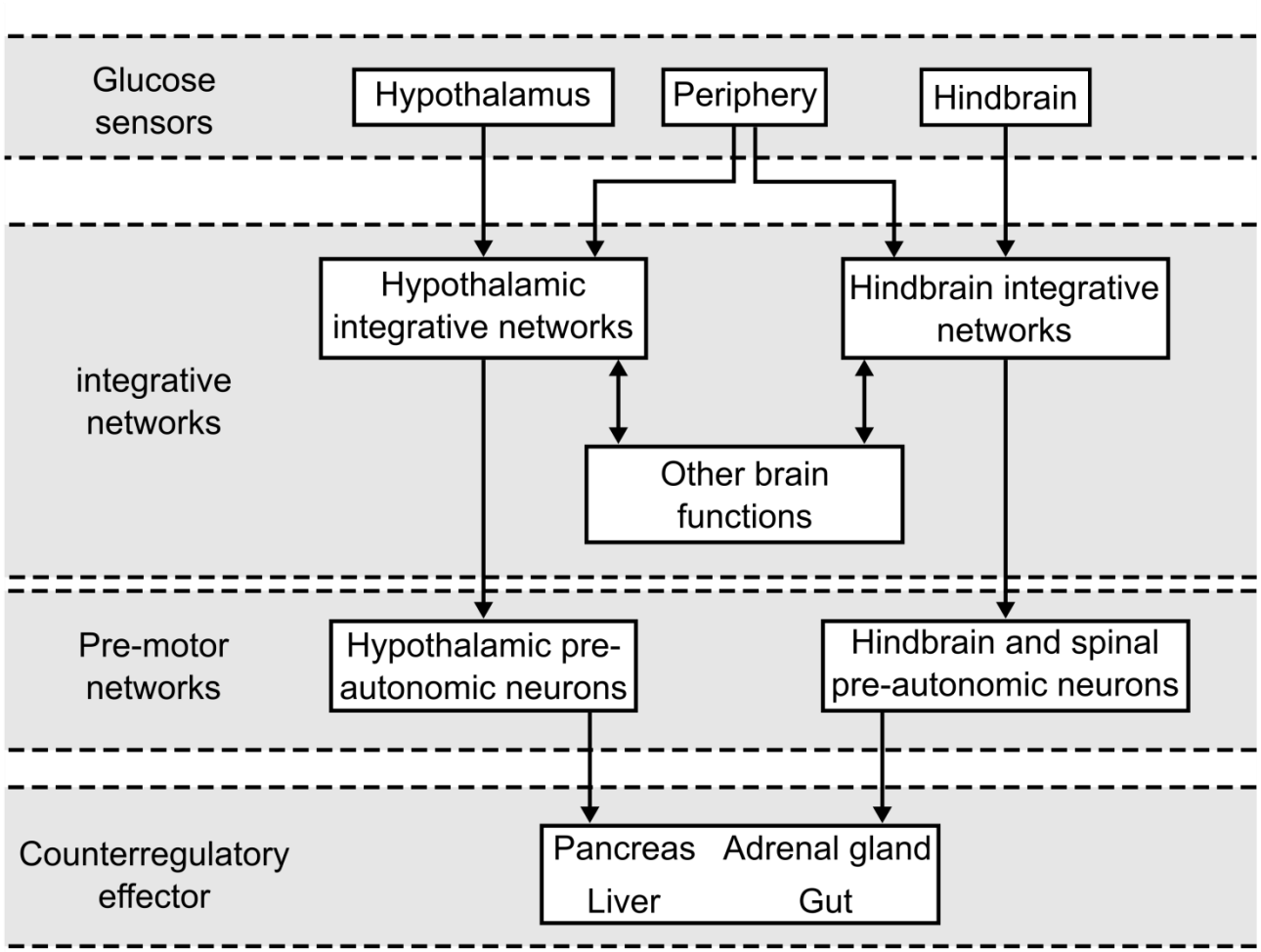

Figure 1.1. Integrative networks of glucose homeostasis

A schematic representation of how glucose homeostasis involves multiple levels of complexity. Initial glucose sensation by in the brain and periphery activates pre-motor neurons whilst being further integrated by the hypothalamus and hindbrain. At this level other brain functions can be influenced by and influence the response to fluctuations in glucose homeostasis. The pre-motor networks drive autonomic and neuroendocrine functions in a reflexive manner. Together these central systems mediate counterregulation through effector organs and tissues.

1.5 Complications of diabetes

Effective glucose homeostasis in diabetes fails primarily due to the loss of insulin action either by the loss of production or insulin sensitivity. The negative consequences of diabetes and faulty glucose homeostasis are of both short- and long-term significance. Hyperglycaemia leads to the classical symptoms previously mentioned: ketoacidosis, nonketotic hyperosmolar syndrome, polyuria, polydipsia, and blurred vision (Association 2012). Longer-term sequelae of hyperglycaemia have been thoroughly reviewed and are not the focus of this introduction. For interest, the reader is directed to these reviews: (Brownlee 2001, Brownlee 2005, Forbes et al. 2013). Briefly, these may include neuropathy, with risks ulceration; nephropathy, leading to renal failure; Charcot joints; autonomic dysfunction; and increased risks of cardiovascular, peripheral vascular and cerebrovascular diseases (Alberti et al. 1998, Association 2012). This thesis and introduction focus on the effects of hypoglycaemia, specifically those affecting the central nervous system (CNS), which will be reviewed in detail below.

1.5.1 Management of hyperglycaemia in diabetes

To counteract hyperglycaemia caused by the loss of insulin action (through depletion or insensitivity) either exogenous insulin is supplied or other glucose lowering agents. Sulfonylureas, for example stimulate insulin release by blocking K_{ATP} channels on β-cells (Madison et al. 1959, Ashcroft 1996). Metformin, another common drug used in the treatment of diabetes reduces endogenous glucose production and improves hepatic insulin sensitivity (Hundal et al. 2000, Moghetti et al. 2000, Zhou et al. 2001).

A side effect of anti-hyperglycaemic medicine usage is iatrogenic hypoglycaemia, particularly in patients treated with intensive insulin therapy. Indeed, iatrogenic hypoglycaemia is major barrier to effective glycaemic control (Cryer 2008). Patients often fear hypoglycaemia, and deliberately allow their blood glucose levels to be high to avoid hypoglycaemia, despite the known consequences of this action (Driscoll et al. 2016).

1.5.2 Acute effects of hypoglycaemia

Hypoglycaemia is defined by blood glucose levels of <4 mmol/l amount. A single episode of hypoglycaemia can induce a range of symptoms including, tremor,

anxiety, sweating, tiredness, hunger and paraesthesia, and cognitive symptoms: behavioural changes, cognitive dysfunction, seizures and coma. If untreated, hypoglycaemia can result in severe brain damage or death. An estimated 2-4% of deaths in those with T1DM have been caused by hypoglycaemia (Cryer 1997b, Laing et al. 1999). Additionally, inpatients' with diabetes that experience hypoglycaemia during their stay increases the length of hospitalisation and cost of stay (McEwan et al. 2015).

1.5.3 Frequency of hypoglycaemia in T1DM and T2DM

The awareness of hypoglycaemia is often lost following repeated episodes. This leads to the clinically recognised condition of impaired hypoglycaemia awareness, which increases the likelihood of hypoglycaemia occurrence. Iatrogenic hypoglycaemia is more common in those with T1DM, who will experience mild hypoglycaemia twice a week and one severe episode, requiring medical attention, per year (Donnelly et al. 2005). This equates to a rate of 0.62-1.70 hypoglycaemic episodes per year in T1DM (Reichard et al. 1991, MacLeod et al. 1993, Group 1998), compared to 0.03-0.73 episodes per year in those with T2DM (Reichard et al. 1991, Abraira et al. 1995, Saudek et al. 1996).

1.6 Counterregulatory response

To restore euglycaemia multiple mechanisms converge to raise blood glucose concentrations in a process known as the CRR. Firstly, insulin production, from β-cells is reduced as glucose drops below 4.6 mmol/l. Secondly, counterregulatory hormones like glucagon, adrenaline and noradrenaline are released when glucose drops below 3.8 mmol/l. Thirdly, if glucose concentrations fall below 3.2 mmol/l, the onset of neurological symptoms occurs, i.e. confusion and anxiety (Zammitt et al. 2005). The brain will increase sympathoadrenal outflow activating pre-autonomic nerve fibres which activates the adrenal medulla to release adrenaline and noradrenaline (Strack et al. 1989, Buijs et al. 1999). Neuroglycopenia will also induce hypothalamic-pituitary-adrenal activation releasing growth hormones, cortisol and glucocorticoids. In combination, these responses to falling glucose levels increase glucose production, decrease glucose clearance, increase the release of gluconeogenic precursors, such as lactate, and increase appetite (Mastorakos et al. 1993, de Guia et al. 2014). However, in those with diabetes this process is fundamentally altered.

1.6.1 Perturbations of counterregulatory response in diabetes

The first aspect of counterregulation, modulation of endogenous insulin levels, is lost in T1DM and advanced T2DM where an individual has become insulin dependent. Secondly, after approximately 5 years of diabetes disease duration glucagon production is lost in response to hypoglycaemia in T1DM (Bolli et al. 1983, Cryer et al. 2003) and in advanced T2DM as well (Gerich et al. 1973, Segel et al. 2002, Drucker et al. 2006). Interestingly, this is not due to a lack of α-cells as they are present in normal numbers and are functional in other scenarios, such as exercise (Wali et al. 2015). Given that glucagon production is possible the α-cells have not lost the ability to synthesis and secrete glucagon, instead there is a loss of the signals that trigger this event. One proposed explanation is that the loss of endogenous β-cells prevents the α-cells' responses to falling insulin levels, especially in the context of the inhibitory effect of exogenously supplied insulin (Taborsky et al. 1998).

Glucagon stimulates the breakdown of hepatic glycogen stores to produce glucose and increases glucose levels (Drucker et al. 2006). The release of glucagon from α-cells relies on signalling from other cells within the pancreatic islet and CNS inputs (Taborsky et al. 1998). For example, α-cells are suppressed by insulin and specific KO of the insulin receptor on α-cells results in hyperglucagonaemia (Kawamori et al. 2009). Additionally, central input from the hypothalamus and hindbrain increase glucagon secretion (Tong et al. 2007, Fan et al. 2009).

Catecholamines, adrenaline and noradrenaline are released during CRR from the adrenal gland (DeRosa et al. 2004), which act on adrenergic receptors in the liver to enhance hepatic glucose output (Exton 1987). However, in both T1DM and advanced T2DM the magnitude of the adrenaline response is diminished and begins at a lower glucose concentration (Segel et al. 2002). The adrenal response to hypoglycaemia is primarily mediated by central hypoglycaemia detection and autonomic outflow activating adrenaline and noradrenaline release (McCorry 2007). See figure 1.2 for an outline of these processes.

1.6.2 Recurrent hypoglycaemia counterregulation

In addition to pathological changes to the glucoregulatory systems induced by diabetes, antecedent hypoglycaemia in healthy humans reduces CRR to subsequent

hypoglycaemia (Davis et al. 1997, Davis et al. 2000). This increases the likelihood of future hypoglycaemia as the awareness of hypoglycaemia is impaired leading to hypoglycaemia-associated autonomic failure (HAAF) (Cryer 2005). Repeated antecedent hypoglycaemia results in an acute reduction of adrenalin, pancreatic polypeptide (a marker of parasympathetic nervous system activity), and muscle sympathetic nerve activity (a direct marker of sympathetic nerve system activation) in humans with T1DM, T2DM and healthy controls (Cryer 2008). Fortunately, hypoglycaemia awareness can be regained with strict glycaemic control and hypoglycaemia avoidance in some patients (Cranston et al. 1994). Nevertheless, the mechanisms by which blunted CRR occurs are not completely understood and as such, hypoglycaemia remains a limiting factor in maintaining euglycaemia in diabetes (Cryer 2004).

Figure 1.2

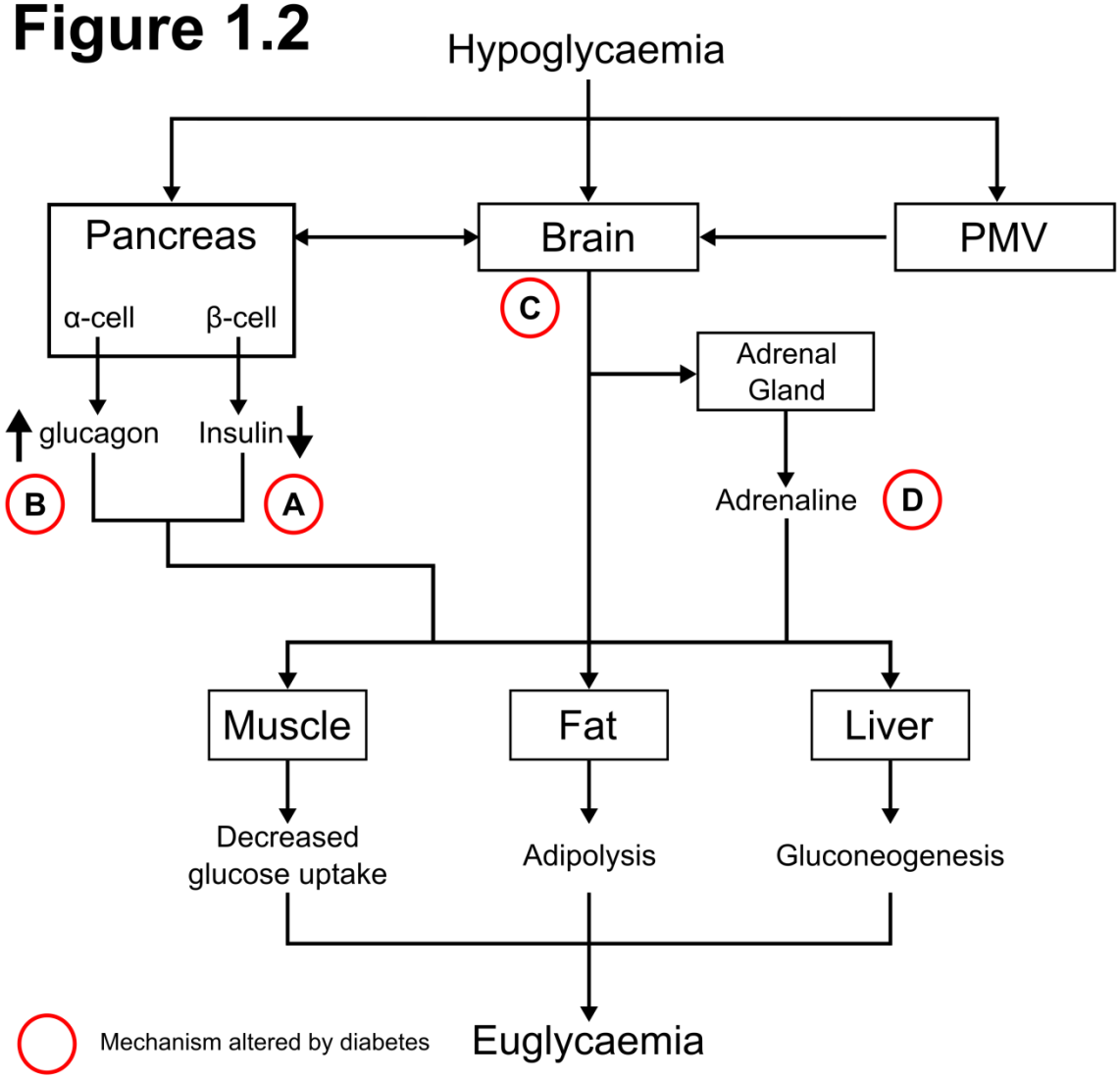

Figure 1.2. Counterregulation in health and disease

Hypoglycaemia is first detected by glucose sensors both peripherally, in the pancreas and portal mesenteric vein (PMV), and centrally in the brain. The initial responses in the pancreas include the suppression of insulin production from β-cells and an increase of glucagon from α-cells. The brain also integrates the peripheral and central sensing of hypoglycaemia to modulate sympatho-adrenal outflow stimulating the adrenal gland, and direct interaction with the pancreas. In concert, these tissues and organs act on the muscle, fat, and liver tissues to decrease glucose uptake, increase adipolysis and gluconeogenesis. The brain also increases food intake. Together these actions restore euglycaemia. **A**. in T1DM or advanced T2DM where exogenous insulin is supplied, production increased, or insulin action is enhanced by insulin sensitising drugs, insulin levels are unable to be reduced resulting in hyperinsulinaemia. **B**. in T1DM and advanced T2DM the pancreatic glucagon response is lost to hypoglycaemia which is perhaps due to failures of intra-pancreatic signalling and reduced CNS alterations. **C**. blunting of glucosensation results in a suppression of sympatho-adrenal outflow and neuroglycopenia symptoms. **D**. The alterations to CNS also lead to a reduced adrenal output of cortisol and adrenaline, which are important mediators of the counterregulatory response.

1.6.2.1 Glycogen supercompensation

As mentioned previously glycogen is a carbohydrate store that is readily broken down as glucose levels fall and increased during high blood glucose states. Glycogen, in the brain, is mostly stored in astrocytes (Brown 2004). Astrocyte glycogen content is modulated by many signals including noradrenaline and serotonin, insulin, and blood glucose concentrations (Magistretti et al. 1993, Gruetter 2003). During hypoglycaemia in humans (Oz et al. 2009) and rodents (Choi et al. 2003) glycogen is broken down within astrocytes to provide energy for neurons in the form of lactate according to the astrocyte-neuron lactate shuttle hypothesis (ANLS) (Pellerin et al. 2012). When lactate is provided exogenously, in the presence of peripheral hypoglycaemia, CRR is blunted (Borg et al. 2003), therefore, glucose sensing neurons may not detect the energy deficit when lactate is provided by astrocytes. It was originally hypothesised by Choi and Gruetter (Choi et al. 2003) that following hypoglycaemia astrocytic glycogen stores may increase in size to pre-empt future metabolic stress. This hypothesis is supported by evidence that in rats glycogen levels are elevated 20 hours after glucopaenia in the hypothalamus (Alquier et al. 2007), or following an episode of hypoglycaemia (Choi et al. 2003). However, other groups have found that glycogen supercompensation did not occur in rats following acute or recurrent hypoglycaemia, even though a faulty CRR was detected (Herzog et al. 2008). Furthermore, hypoglycaemia awareness and brain glycogen content in the brain are not correlated in humans with T1DM diabetes (Öz et al. 2012). While the discrepancies in the literature have not been resolved, it is more important to know whether or not manipulation of glycogen levels will provide a therapeutic benefit to people. For example, would increasing brain glycogen stores protect neural function or prevent the detection of hypoglycaemia?

1.6.2.2 Blunting of AMPK activation

AMPK is expressed in both neurons and astrocyte populations (Turnley et al. 1999), and is involved in energy homeostasis and CRR (McCrimmon 2008). For example, the use of the AMPK activator AICAR stimulates VMN GI neurons, similarly to a low glucose treatment, even in 2.5 mM glucose (euglycaemia) (Canabal et al. 2007). GI neurons also produce nitric oxide during low glucose stimulation which is attenuated by AMPK inhibition (Canabal et al. 2007). Nitric oxide signalling is required for the closing of the CFTR and is therefore necessary for GI neuron function (Murphy et al.

2009). Interestingly, AMPK activation during acute hypoglycaemia in the VMN enhanced CRR and improved CRR in rats with blunted CRR (McCrimmon et al. 2006a). Similarly, AMPK inhibition by siRNA prevents CRR to hypoglycaemia (Mccrimmon et al. 2006b). Furthermore, the selective KO of the active AMPK subunit (α-1) prevented glucose sensitivity in POMC and AGRP neurons (Claret et al. 2007).

Normal AMPK activity is suppressed by repeated neuroglycopenia, intracerebroventricular 2-DG injections over 4 days *in vivo* (Alquier et al. 2007). Interestingly, activation of AMPK in CRR-blunted rats can improve counterregulatory responses to future hypoglycaemia (McCrimmon et al. 2006a, Alquier et al. 2007). Furthermore, recent work shows that recurrent insulin-induced hypoglycaemia (RIIH) increases AMPK protein expression in several hypothalamic nuclei while the normal increase in AMPK phosphorylation was lost (Mandal et al. 2017). Taken together these data indicate AMPK activity is suppressed following RIIH or repeated neuroglycopenia suggesting a failure of glucose sensing activity. While this likely contributes to blunted CRR, given AMPK activation improves CRR (McCrimmon et al. 2006a, Alquier et al. 2007), the mechanisms by which AMPK phosphorylation is diminished remains unclear. One potential explanation could be glycogen supercompensation (as described above) (Alquier et al. 2007) may delay the onset of AMPK activation enhancing short-term energy supplies from glycogenolysis and glycolysis (Pellerin et al. 2012).

1.6.2.3 Alterations in brain glucose uptake

The brain utilises approximately 20% of a human body's total caloric intake (Rolfe et al. 1997). Most of this comes from the metabolism of carbohydrates of which the brain preferentially uses (Benarroch 2014). The source of glucose for the brain is from the vasculature supplying the brain. Glucose is transported across the blood brain barrier (BBB) via Glut-1 which then directly enters the neuron via Glut-3 or is indirectly transported into astrocytes by Glut-1 and metabolised to lactate; which is transported to neurons by monocarboxylate transporter 1 (MCT1) and MCT2 (Benarroch 2014).

Glucose uptake is reduced during acute hypoglycaemia. However, recurrent, long duration, hypoglycaemia in humans prevented this reduction in a future hypoglycaemic clamp study (Boyle et al. 1994). An additional study showed brain

glucose uptake was unchanged during hypoglycaemia in patients with T1DM who also had low glycosylated haemoglobin (HbA1c), impaired hypoglycaemia awareness, and blunted CRR, compared to patients with T1DM and higher HbA1C values (Boyle et al. 1995). This has also been investigated in rodent models where sustained, but not acute, hypoglycaemia reversibly increased glucose uptake into the brain during hypoglycaemia (McCall et al. 1986). Indeed cerebral glucose levels are maintained in humans with T1DM and IHA (Criego et al. 2004). Together this suggests glucose uptake into the brain is enhanced, which may explain the maintenance of cognitive function and absence of hypoglycaemia-associated symptoms. A rodent study of chronic hypoglycaemia demonstrated that the increased brain glucose uptake may be due to increased Glut-1 mRNA expression and BBB permeability-surface area (Kumagai et al. 1995).

1.6.2.4 Altered neuronal transmission

Within the VMN, glucose sensing can be directly manipulated by the addition of glucose or 2-DG which inhibit or enhance CRR (Borg et al. 1995, Borg et al. 1997). It has been suggested that blunted CRR may be partly due to a failure in the sensitivity of GE and GI neurons to glucose (Parekh 2009). K_{ATP} channels are a necessary part of GE neuron glucose detection (Parton et al. 2007) and modulate GABA levels. K_{ATP} channel blockers decrease CRR to both central and systemic hypoglycaemia through increasing GABAergic inhibitory tone (Evans et al. 2004a, Chan et al. 2007). Conversely, K_{ATP} channel openers improve CRR in hypoglycaemia naïve rats and those with blunted CRR by attenuating GABA levels (McCrimmon et al. 2005, Chan et al. 2007).

1.6.2.5 GABA and glutamate signalling

As mentioned previously, GABA is an important inhibitory neurotransmitter in the brain with importance in the energy balance centres of the brain (Cowley et al. 2001). For example, inhibition and activation of GABA receptors in the VMN amplifies and suppresses CRR respectively (Chan et al. 2006). Additionally, GABA levels are suppressed by K_{ATP} activation with a corresponding increase in glucagon and adrenaline responses to hypoglycaemia (Chan et al. 2007). During hypoglycaemia, GABAergic inhibitory tone within the VMN decreases but is increased by RH (Chan et al. 2008). Conversely, glutamatergic neurotransmission is increased by acute hypoglycaemia, but diminished by RH (Chowdhury et al. 2017).

Glutamatergic neurotransmission is necessary for glucagon release and avoidance of hypoglycaemia (Tong et al. 2007). Furthermore, in people with T1DM and HAAF, glutamate concentrations do not decline as expected during hypoglycaemia in the occipital lobe (Terpstra et al. 2014). While the precise mechanisms remain unclear, the interplay between GABA and glutamatergic neurotransmission is altered by RH. Together, failure in each system results in diminished CRR (Tong et al. 2007, Potapenko et al. 2012).

1.7 Astrocytes

While much of the literature discussed so far focusses primarily on neurons, astrocytes have also been shown to sense metabolic hormones and nutritional state (Chowen et al. 1999, Cheunsuang et al. 2005, Marty et al. 2005, McDougal et al. 2013a, McDougal et al. 2013b, Angelova et al. 2015, Chen et al. 2016, García-Cáceres et al. 2016, Rogers et al. 2016, Turovsky et al. 2016).

Astrocytes are non-electrically excitable neural cells which have a supporting role in the brain. They are a part of the tripartite synapse, where their fine processes ensheaths the synaptic cleft to regulate neurotransmission (Papouin et al. 2017). However, the number of synapses in intimate association with astrocytes varies within the rodent brain between an estimated 30-90% depending on the brain region (Papouin et al. 2017) indicating a wide range of uses in the CNS. Additionally, astrocytes have a heterogeneous morphological structure which can define different subtypes of glia. Protoplasmic, fibrous, surface-associated, gomori, perivascular and marginal, and radial astrocytes are the major sub-classifications of astrocytes (Verkhratsky et al. 2017). Even within each subtype astrocytes can have heterogeneous functions. Within the hippocampus, for example, there are protoplasmic GluR and GluT astrocytes; GluR astrocytes express ionotropic glutamate receptors whereas GluT astrocytes lack the receptors but express glutamate transporters (Matthias et al. 2003). Dissimilarly, perivascular astrocytes do not commonly interact with neurons, instead they interact with the cerebral vasculature through their end-feet which form a part of the blood brain barrier (Liu et al. 2013). Lastly, gomori astrocytes, found in the hypothalamus and hippocampus, highly express Glut2 allowing for rapid uptake of glucose which may contribute to metabolic sensing of the hypothalamus (Young et al. 2004). Astrocytes also have

important roles in ion, water and pH homeostasis, and inflammation (Verkhratsky et al. 2017).

1.7.1 Astrocyte calcium signalling

Astrocytic activation is fundamentally linked to the flow of Ca^{2+} ions. The generation of a high to low calcium gradient is essential for calcium signalling which occurs both extracellularly to cytoplasm, as well as between intracellular compartments, i.e. the endoplasmic reticulum (ER), and the cytoplasm (Verkhratsky et al. 2012). The cellular machinery which enables gradient formation can include Ca^{2+} channels, buffers, pumps and exchangers (Verkhratsky et al. 2012). Ca^{2+} influx can be both compartmentalised into microdomains or apply to a broader whole cell response (Berridge 2006, Verkhratsky et al. 2012). For example, influx of Ca^{2+} into the cytoplasm from the extracellular space or from internal stores can be highly spatially restricted or cascade on to the rest of the cell. Alternatively, after increased $[Ca^{2+}]_{i,}$ secondary downstream signalling occurs leading to changes in gene transcription (Fields et al. 2005), metabolism (Denton et al. 1972, Hubbard et al. 1996, Territo et al. 2000), and propagation to other cells (Verkhratsky 2006, Verkhratsky et al. 2006). Aside from Ca^{2+} influx, metabotropic GPCRs induce the production of inositol triphosphate (IP_3) which triggers IP_3-induced Ca^{2+} release from the ER (Hamilton et al. 2008). The increase in intracellular IP_3 can also be propagated intercellularly via gap-junctions to stimulate long-range calcium waves (Cornell-Bell et al. 1990). IP_3-induced Ca^{2+} release is important in the exocytosis of vesicles from astrocytes as an ER calcium inhibitor prevented the calcium dependent release of glutamate from astrocytes (Innocenti et al. 2000, Jeremic et al. 2001). Astrocytes propagate calcium signalling through the glial syncytium through calcium waves enabling the dissemination of a signal from an initial stimulus to other astrocytes (Scemes et al. 2006).

1.7.2 Gliotransmission

The release of neurotransmitters such as glutamate was thought to be the exclusive role of neurons. However, astrocytes also release neurotransmitters in response to stimuli in a Ca^{2+}-dependent manner (Zhang et al. 2005a, Savtchouk et al. 2018). *In vitro* studies first demonstrated Ca^{2+}-dependent astrocytic exocytosis of neurotransmitters (Parpura et al. 1994, Parpura et al. 1995, Araque et al. 1998a, Araque et al. 1998b, Araque et al. 1999, Araque et al. 2000, Parpura et al. 2000,

Araque et al. 2001). This expanded to the use of pharmacological activation of endogenous receptors that activate Gq-GPCRs to increase $[Ca^{2+}]_i$ from intracellular stores (Parpura et al. 1994, Jeftinija et al. 1996, Montana et al. 2006). While debate remains (see Savtchouk and Volterra arguing for (Savtchouk et al. 2018) and Fiacco and McCarthy arguing against (Fiacco et al. 2018)), glutamate, D-serine, purines are proposed to be released during gliotransmission (Haydon et al. 2006, Di Castro et al. 2011, Harada et al. 2015).

Exocytotic release of stored vesicles in astrocytes, as in other cells, requires Ca^{2+}-sensitive machinery such as the soluble *N*-ethyl maleimide-sensitive fusion protein attachment protein receptor (SNARE) complex (Montana et al. 2006). Inhibition of this process prevents the release of glutamate from astrocytes (Montana et al. 2006).

It is well established that astrocytes recycle glutamate (Danbolt 2001, Oliet et al. 2001) known as the glutamate-glutamine cycle. Briefly, astrocytes uptake glutamate, convert it to glutamine by glutamine synthetase, and export it to neurons where it is converted back to glutamate by glutaminase (Rudy et al. 2015). Importantly, neurons lack the machinery to synthesise glutamate or GABA directly from glucose (Hertz et al. 1999), thus require astrocytes to perform this function. Astrocytes can also release glutamate directly in a Ca^{2+}-dependent fashion. Importantly, failure of the glutamate-glutamine cycle leads to excitotoxicity (Halassa et al. 2007).

D-serine is amino acid proposed to be released from astrocytes that co-agonises NMDA receptors (Mothet et al. 2005, D'Ascenzo et al. 2014, Paul et al. 2014). However, recent evidence suggests that this is not the case and serine racemase, which synthesises D-serine, is almost exclusively found in neurons and not astrocytes (Miya et al. 2008, Benneyworth et al. 2012). Furthermore, while astrocytes *in vitro* release D-serine, this has been attributed to changes in expression resulting in non-physiological serine racemase expression (Wolosker et al. 2016). Instead it is proposed that astrocytes produce L-serine, the precursor to D-serine, which is shuttled to neurons which subsequently synthesise D-serine (Wolosker et al. 2016).

Lastly, purines, including ATP, ADP, and adenosine have long been known to be neurotransmitters and act through a process known as purinergic signalling

(Burnstock 1972, Burnstock 2016). Aside from being the energy currency of the cell, ATP acts as a signalling molecule often regarded as a danger signal (Trautmann 2009). Extracellular ATP, or following hydrolysis by ectonucleotidases, ADP and adenosine bind to purinergic receptors. Briefly, these are categorised into P2X, ionotropic, P2Y metabotropic receptors. A specific class of adenosine sensitive receptors are called P1 or adenoreceptors (Burnstock 2016). Together these modulate $[Ca^{2+}]_i$ by direct influx of ions opening voltage dependent calcium channels, or through Gq-GPCRs which trigger calcium release from intracellular stores (Tomic et al. 1996). Astrocytes release ATP from vesicles (Zhang et al. 2007b, Abbracchio et al. 2009), pannexin hemi-channels (Bao et al. 2004) and P_2X_7 receptors (Suadicani et al. 2006).

As gliotransmission is calcium dependent, systems that modulate astrocytic calcium can affect gliotransmitter release. Circulating hormones can directly affect gliotransmission; for example, insulin receptor KO in astrocytes in mice caused anxiety, obesity (Brüning et al. 2000, Fisher et al. 2005) and a decrease in ATP exocytosis (Cai et al. 2018). Additionally, other factors like pH, O_2/CO_2, and metabolic availability increase astrocytic $[Ca^{2+}]_i$ which could then influence gliotransmission (Verkhratsky et al. 2017). For example, hypoxia/hypoglycaemia triggers the release of adenosine in the CNS including astrocytes (Ciccarelli et al. 1999). Furthermore, adenosine receptor antagonists, i.e. caffeine, can prevent normal CRR in response to 2-DG glucoprivation (Minor et al. 2001) and prevent hypoglycaemia-induced neuronal death (Turner et al. 2004).

1.7.3 Astrocyte and neuronal metabolism

Neurotransmission is an energetically costly process (Laughlin et al. 1998, Attwell et al. 2001). In neurons glucose is completely metabolised by oxidative phosphorylation in the mitochondria (Waagepetersen et al. 1998, Bouzier-Sore et al. 2006). Kety and Schmidt noted, however, there was a discrepancy between estimated and actual glucose utilisation rates by the brain; glucose utilisation exceeded oxygen consumption (Kety et al. 1948). Therefore, glucose was being used partly in an oxygen independent manner, i.e. glycolysis. This has been largely attributed to astrocytes which are more glycolytic than neurons (Bélanger et al. 2011, Pellerin et al. 2012). Astrocytic involvement in neurotransmission incurs metabolic costs; when glutamate is released from neurons some of this is uptaken by astrocytes and this

stimulates lactate release and increases glucose utilisation (Pellerin et al. 1994, Sibson et al. 1998, Schurr et al. 1999, Voutsinos-Porche et al. 2003). Despite high metabolic demands, astrocytes are more glycolytic in comparison to neurons. This is partly due to their expression of 6-phosphofructo-2-kinase type 3 (PFKFB3) which is almost absent in neurons (Herrero-Mendez et al. 2009). This enzyme generates fructose-2,6-bisphosphate which activates phosphofructokinase-1 (PFK) accelerating glycolysis. Interestingly, forced increases in neuronal glycolysis via PFKFB3 overexpression causes increased ROS, which was attributed to decreased pentose phosphate pathway (PPP) mediated anti-ROS defence (Herrero-Mendez et al. 2009). Astrocytes also contain glycogen stores, unlike neurons, which can be utilised in the absence of glucose to maintain glycolysis (Wender et al. 2000, Brown 2004). Pyruvate is the end-product of glycolysis which enters the mitochondria for complete oxidation. Alternatively, lactate dehydrogenase (LDH) converts pyruvate to lactate. In astrocytes, thanks to LDH5 isoform, the majority of pyruvate is converted to lactate (Bittar et al. 1996); which can then be exported via monocarboxylate transporters (MCT) 1 and 4 to supply neurons with lactate as a metabolic substrate (Steinman et al. 2016). Neurons express LDH1 which favours the conversion of lactate into pyruvate (Bittar et al. 1996) which can then be completely oxidised in the mitochondria.

1.7.4 Astrocyte-neuron lactate shuttle hypothesis

The supply of lactate to neurons is a part of the astrocyte-neuron lactate shuttle (ANLS), proposed by Pellerin and Magistretti (Pellerin et al. 1994). The ANLS hypothesises that neuronal activity results in a corresponding increase in astrocytic glycolysis to provide lactate to neurons as a metabolic substrate (Pellerin et al. 1994, Pellerin et al. 2012). This was demonstrated, initially, by glutamate stimulating astrocytic metabolism due to co-transport of Na^+ ions activating the Na^+/K^+-ATPase using ATP. The resulting increased glucose uptake produces lactate which is transported to and metabolised in neurons (Pellerin et al. 1994, Pellerin et al. 2012).

Interestingly, in streptozotocin-induced diabetes in rats MCT 1 and 2 expression increased and even more so following RH, increasing brain lactate uptake (Aveseh et al. 2014). Additionally, in humans with T1DM compared to healthy controls lactate uptake into the brain is similarly increased (Mason et al. 2006, De Feyter et al. 2013). Together these data suggest an enhanced ANLS induced by diabetes and/or

RH. For example, RH blunts the CRR (Aveseh et al. 2014) and direct infusion of lactate into the hypothalamus also blunts the CRR during systemic hypoglycaemia (Borg et al. 2003) then is it plausible that enhanced lactate production and/or utilisation may be blunting of CRR following RH.

1.7.5 Glucose sensing role of astrocytes

While CNS glucose sensing has been known for over 60 years, this has mostly been attributed as a function of neurons (Mayer 1953, Oomura et al. 1969, Watts et al. 2010). Nonetheless, relatively recently, astrocytes are being recognised as sensors of metabolic hormones, local energy balance, and glucose (Marty et al. 2005, McDougal et al. 2013a, McDougal et al. 2013b, Chen et al. 2016, Rogers et al. 2018). Marty *et al*, were the first group to identify astrocytes as being important low glucose sensors (Marty et al. 2005). Their work studied a mouse Glut2 KO model and found extrapancreatic Glut2 glucose-sensing mechanism to be important in hypoglycaemia-induced glucagon secretion. 2-DG-induced glucoprivation increased c-FOS activation in the NTS in control but not Glut2 KO mice and selective re-expression of Glut2 in GFAP expressing cells rescued the Glut2 KO phenotype.

More recently, McDougal *et al*, demonstrated that isolated NTS-astrocytes *in vitro* respond to glucose withdrawal and 2-DG glucoprivation (McDougal et al. 2013a). Furthermore, inhibition of astrocytes using fluorocitrate, an astrocyte anti-metabolite, prevented gastric motility in response to glucoprivation (McDougal et al. 2013b). Furthermore, activation or inhibition of GFAP-expressing glia in the ARC increases and suppresses food intake, respectively (Chen et al. 2016). This was shown to be dependent on NPY/AgRP but not POMC neurons, as specific inhibition of the NPY/AgRP neurons prevented increased food intake (Chen et al. 2016). Furthermore, astrocytes were necessary for hindbrain-derived CRR which was blocked by the addition of fluorocitrate (Rogers et al. 2016). The addition of adenosine receptor, blockers also prevented CRR suggesting that purinergic gliotransmission is also necessary for CRR (Rogers et al. 2016). Purinergic gliotransmission was also required for activation of glucose-sensing neurons in *ex vivo* mouse hindbrain slices containing the NTS (Rogers et al. 2018). Again, inhibition of astrocytes with fluorocitrate inhibited the activation of these neurons (Rogers et al. 2018). Importantly, upon glucoprivation, astrocytes Ca^{2+} increase occurred approximately 40 seconds before neurons suggesting they are the initiators

of glucose detection. Together these seminal studies demonstrate the necessity of astrocytes in glucose sensing and counterregulation.

1.8 Inflammation

Inflammation is an integral aspect of both T1DM and T2DM (Wellen et al. 2005). It is well established that inflammatory responses require metabolic involvement; for example, mobilisation of lipid stores are necessary for acute-phase responses (Khovidhunkit et al. 2004). Furthermore, malnutrition, both over- and under-nutrition negatively affects inflammation. People in starvation, for example, have immune suppression (Chandra 1996, Blackburn 2001, Khovidhunkit et al. 2004). The modern epidemic of obesity is also resulting in a rise of inflammatory diseases, including T2DM diabetes (Heilbronn et al. 2008).

Although both T1DM and T2DM both involve inflammatory pathways, they are fundamentally different in aetiology. T1DM is an auto-immune response where the body fails to recognise “self” antigens, leading to the selective destruction of the pancreatic β-cells. This is thought to stem from both genetic (Habib et al. 2012) and environmental factors (Cantorna et al. 2004, Knip et al. 2012, Ghazarian et al. 2013) involving failures in the gut (Vaarala et al. 2008), thymus (Geenen 2012), and lymph nodes (Yip et al. 2014). Conversely, T2DM strongly correlates with obesity which is characterised by chronic low grade inflammation (Heilbronn et al. 2008). A key inflammatory-obesity mediator is the cytokine TNF-α which is overexpressed in adipose and muscle tissue in obesity (Hotamisligil et al. 1993, Hotamisligil et al. 1995, Saghizadeh et al. 1996, Sethi et al. 1999). Interestingly, TNF-α treatment *in vitro* or *in vivo* impairs insulin action which can be reversed by disruption of TNF-α or its receptor (Hotamisligil et al. 1993, Uysal et al. 1997). For example, the incubation of murine adipocytes with TNF-α decreased expression of Glut1 and Glut2 reducing glucose uptake, and blocking TNF-α receptor activity increased insulin-stimulated glucose utilisation in mice (Hotamisligil et al. 1993).

1.8.1 Peripheral and central inflammatory processes

In the periphery the immune response is mediated by dedicated immune cells; natural killer cells, lymphocytes, T cells, and B cells. While historically the brain has been regarded as an immunoprivileged site, absent of peripheral immune cells, it is now understood that T-cells, for example cross the BBB into the CNS (Louveau et al.

2015). Within the CNS glial cells, astrocytes and microglia, are the first responders to a CNS insult (Gadani et al. 2015). Both astrocytes and microglia are activated by ATP which triggers the release of cytokines (Panenka et al. 2001, Kataoka et al. 2008) as well as ATP-induced ATP release from astrocytes (Davalos et al. 2005, Roth et al. 2013).

1.8.2 Hypoglycaemia as an inflammatory stimulus

As previously mentioned, undernutrition can alter the immune system (Chandra 1996, Blackburn 2001, Khovidhunkit et al. 2004), and hypoglycaemia can stimulate the release of proinflammatory, prothrombotic and pro-atherogenic cytokines in man (Gogitidze Joy et al. 2010, Wright et al. 2010). Interestingly, non-esterified fatty acids are released during hypoglycaemia and can induce vascular inflammation (REF). Typically RH blunts normal responses to acute hypoglycaemia; however, RH appears to exacerbate cytokine release (Joy et al. 2015). RH also stimulates microglial activation in diabetic rats (Won et al. 2012). In acute glucose/oxygen deprivation astrocytes suppressed the release of interferon-γ, an inflammatory cytokine, from microglia (Kim et al. 2010). Given the metabolic expense of inflammatory processes (Romanyukha et al. 2006), it is plausible this suppression of inflammation is to conserve energy.

1.8.3 Inflammatory modulation of the hypothalamus

A high-fat diet (HFD) for 20 weeks in rats increases CNS inflammation via increased NF-κB signalling and reactive oxygen species (ROS) production (Zhang et al. 2005b). In the hypothalamus, 16 weeks of HFD upregulates the release of inflammatory cytokines TNF-α, IL-1β and IL-6 in rats (De Souza et al. 2005). Conversely, blockade of hypothalamic NF-κB signalling reduces insulin resistance in a mouse diet-induced obesity model (Zhang et al. 2008). This implicates hypothalamic inflammation as a central mediator of obesity and regulation of food intake more generally. Indeed, cytokines including TNF-α, IL-1β and IL-6 also stimulate the hypothalamic-pituitary-adrenal axis (Chrousos 1995, Tsigos et al. 1997). IL-6, for example, is released during hypoglycaemia in healthy humans (Dotson et al. 2008), but also in obesity (Park et al. 2010). Additionally, IL-6 administration also stimulates ACTH release and hypothalamic-pituitary-adrenal axis activation (Naitoh et al. 1988, Späth-Schwalbe et al. 1994). Given that hypothalamic-pituitary-adrenal axis increases plasma glucose concentrations, IL-6 is an important

factor in CRR and obesity-related elevated blood glucose. Interestingly, the largest source of IL-6 in the CNS are astrocytes (Van Wagoner et al. 1999). Therefore, astrocytes may be contributing to restoring glucose levels through activation of the hypothalamic-pituitary-adrenal axis.

1.8.4 Astrogliosis

Astrogliosis is a defence mechanism in response to noxious stimuli like trauma or ischaemia (Burda et al. 2014). This typically involves changes to astrocyte morphology (Sofroniew 2009) and an alteration to gene expression (Zamanian et al. 2012). Typical markers of astrocytes, glial fibrillary acid protein (GFAP) and vimentin have increased expression which corresponds to morphology becoming more ramified. Additionally, cytokine release, including IL-6, TNF-α, and IFN-γ increases with the magnitude of astrogliosis (Kıray et al. 2016). Importantly, astrogliosis is stimulus specific and not a homogenous response. In one study, while approximately 50% of astrogliosis-induced gene expression was the same, the remaining 50% differed depending on whether astrogliosis was induced by ischaemia or lipopolysaccharide (LPS) injection (Zamanian et al. 2012), highlighting the adaptive capabilities of astrocytes.

While neuronal NF-κB signalling disruption can protect against hypothalamic inflammation caused by HFD, a similar result can be found in astrocytes (Buckman et al. 2015, Douglass et al. 2017). Interestingly, fasting also triggers astrogliosis and activation (Daumas-Meyer et al. 2018). Inflammation has a metabolic demand (Romanyukha et al. 2006) which in astrocytes is met by adaptive metabolic responses (Iglesias et al. 2017). For example, glucose/oxygen deprivation of *in vitro* primary rat astrocytes increases both glycolysis and lactate production by >50% (Amaral et al. 2010), which may be due to increased Glut1 expression (Vannucci et al. 1998). Additional glycolytic upregulation is reported to come from increased PFKFB3 and glyceraldehyde-3-phosphate dehydrogenase (GAPDH) (Mazzola et al. 2001, El Kadmiri et al. 2014, Fu et al. 2015).

Inflammatory stimuli like HFD (Zhang et al. 2005b) and hypoglycaemia (McGowan et al. 2006) increase ROS production. This can lead to DNA damage (Singh et al. 2004) and mitochondrial dysfunction (Lin et al. 2006). A major anti-oxidant defence mechanism is the pentose phosphate pathway (PPP) which diverts glucose-6-

phosphate out of glycolysis to generate NADPH and ribose-5-phosphate (R5P) (Stincone et al. 2015). The NADPH is used to generate reduced glutathione (GSH) which ~~is~~ neutralises ROS (Winterbourn et al. 1994). Astrocytes increase PPP activity in response to traumatic brain injury (Bartnik et al. 2005). As glucose is required for the PPP the upregulation of glucose uptake transporters, like Glut1 (Vannucci et al. 1998), may be required. Indeed, reactive gliosis also upregulates the expression of metabolic related genes which may address the increased metabolic demands of their inflammatory response. With the aforementioned roles of inflammation modulating energy-homeostasis in the body and the CNS, astrocytes could be important and under-appreciated mediators of these processes that have not been fully investigated.

1.9 Summary and project aims

Astrocytes are no longer seen as passive bystanders in the functions of the CNS. Previously it was known astrocytes are important in sensing circulating metabolic hormones, such as leptin (Cheunsuang et al. 2005) and insulin (García-Cáceres et al. 2016), as well as oxygen (Angelova et al. 2015) and carbon dioxide (Turovsky et al. 2016). However, important gaps in the knowledge remain. In the following chapters the work presented aims to characterise the responses of isolated human astrocytes to physiologically and pathophysiologically relevant glucose concentrations. To investigate the effects of acute or recurrent low glucose (RLG) human primary astrocytes (HPA) and U373 human astrocytoma cell lines were used. The overarching hypothesis was that astrocytic function would be altered by glucose variation. Specifically, the aims of this thesis were; firstly, to test whether human astrocytes respond to low glucose in an AMPK dependent manner and how this is affected by RLG. Secondly, to test whether astrocytic mitochondrial and glycolytic metabolism enhanced to compensate for low glucose availability. Thirdly, to test whether isolated human astrocytes are activated by low glucose exposure and how this is affected by RLG. Lastly, to investigate if astrocytic cytokine release is differentially regulated by RLG treatment.

Chapter 2

Materials and Methods

2.1 Materials

2.1.1 Chemicals

Table 2.1

Chemical	Supplier	Catalogue number
0.05% (w/v) Trypsin-EDTA	Fisher	25300-062
100% ethanol (for RNA extraction)	Thermo Fisher	E/0650DF/17
6-(N-(7-Nitrobenz-2-oxa-1,3-diazol-4-yl)amino-6-Deoxyglucose (6-NBDG)	Cayman Chemical	CAY13961-5
A438079	Biotechne	2972
Adenosine diphosphate (ADP)	Sigma-Aldrich	A2754
Adenosine triphosphate (ATP)	Sigma-Aldrich	A9187
Ammonium persulfate	Sigma-Aldrich	A3678
ATP:ADP ratio kit	Sigma-Aldrich	MAK135
ATPlite luminescence assay system	PerkinElmer	6016947
Benzamidine	Sigma-Aldrich	12072
Bio-Rad protein assay dye reagent	Bio-Rad	500-0006
BioTrace Nitrocellulose membrane	VWR	732-3031
Bovine serum albumin	Sigma-Aldrich	A2153
Bromophenol blue sodium salt	Sigma-Aldrich	B5525
DAPI	Molecular Probes	D1306
Dimethyl Sulfoxide HYBRI-MAX (DMSO)	Sigma-Aldrich	D2650-5X5ML
Direct-zolTM RNA MiniPrep kit	Zymo Research	R2050
D-mannitol	Sigma-Aldrich	M4125
DMEM glucose free	Fisher	11966
DMEM high glucose	Sigma-Aldrich	D5671
DMEM low glucose	Sigma-Aldrich	31885
DMEM, no glucose or phenol red	Fisher	12307263
EGTA	Melford	e1102
Ethylenediaminetetraacetic acid disodium salt (EDTA)	Sigma-Aldrich	E1644
Fluo-4 direct calcium assay reagent	Life Technologies	F10471
Foetal bovine serum (FBS)	Gibco	11573397
Fura-2 AM	Life Technologies	F1221
Gentamicin	Thermo Fisher	15750060
Glucose	Sigma-Aldrich	G7021
Gluteraldehyde	Thermo	11423488
Glycerol	Sigma-Aldrich	49767
Glycine	Melford	G0709
Glycogen kit (fluorometric)	Cell Biolabs, Inc	MET-5023

Grade 3MM Chr blotting paper	Fisher	11330744
HEPES	Sigma-Aldrich	H0877
Human cytokine array panel A	R&D systems	ARY005
Interleukin-13 (IL-13) ELISA	Biotechne	DY213-05
Lactate dehydrogenase (LDH)	Sigma-Aldrich	L1254
L-glutamine	Fisher	25030-024
L-lysine	Thermo	10016203
Macrophage migration inhibitory factor (MIF) ELISA	RayBiotech	ELH-MIF-1
Methanol	Sigma-Aldrich	34860-2.5L-R
Mito fuel flex test kit	Agilent	103260-100
Mito stress test kit	Agilent	103015-100
MitoTracker Red CMXRos	Molecular Probes	M7512
N,N,N′,N′-Tetramethylethylenediamine (TEMED)	Sigma-Aldrich	T7024
NaCl Sodium Chloride	Sigma-Aldrich	S7653
NaF Sodium Fluoride	Sigma-Aldrich	S7920
NaVO4 Sodium Orthovanodate	Sigma-Aldrich	S6508
Noradrenaline	Abcam	ab120717
Normal donkey serum	Sigma-Aldrich	S30-100ML
Paraformaldehyde	Sigma-Aldrich	P6148-1KG
Penicillin-streptomycin	Fisher	15070-063
Phenylmethanesulfonyl fluoride (PMSF)	Sigma-Aldrich	P7626
Phosphate buffered saline (PBS) tablets	Fisher	10209252
Plasminogen activator inhibitor-1 (PAI-1) ELISA	Sigma-Aldrich	RAB0429
Poly-L-lysine hydrobromide	Sigma-Aldrich	P1274
Pyridoxalphosphate-6-azophenyl-2',4'-disulfonic acid tetrasodium salt (PPADs)	BioTechne	625
ProtoGel (30% w/v) acrylamide	Scientific Laboratory Supplies	NAT1260
SeeBlue plus 2 pre-stained protein standard	Life Technologies	LC5925
Semicarbazied hydrochloride	Sigma-Aldrich	S2201
Serotonin hydrochloride (5HT)	Cambridge Bioscience	CAY14332
Skimmed milk powder	Oxoid	LP0031
Sodium dodecyl sulphate (SDS)	Melford	B2008
Sucrose	Melford	S0809
Tris	Melford	B2005
Triton X100	VWR	M143-1L
TRIzol	Invitrogen	15596026
Tween-20	Sigma-Aldrich	P2287
β-mercaptoethanol (BME)	Sigma-Aldrich	M3148
β-Nicotinamide adenine dinucleotide sodium salt	Sigma-Aldrich	N0632

2.1.2 Equipment

Table 2.2 Equipment

Equipment	Supplier
PHERAstar® *FS* microplate reader	BMG Labtech
Seahorse XFe96 bioanalyser	Agilent
DM4000 B LED Fluorescent microscope	Leica
DMi8 confocal microscope	Leica
Odyssey® CLx	Licor
Mini-PROTEAN® Tetra system	Bio-Rad
TC20™ Automated Cell Counter	Bio-Rad
Eclipse TE 2000-S	Nikon
79000 Series Filter Set	Chroma
ORCA-ER Digital Camera	Hamamatsu
Lambda DG4	Sutter Instrument Company
2200 Tapestation	Agilent
HiSeq 2500	Illumina

Table 2.3 Cell culture materials

Equipment and apparatus	Supplier	Catalogue number
96-Well Microplate, Round Wells, Flat Bottom, PS (Sterile)	Starlab	E2996-1600
FluoroNunc F96-MicroWell Plate, with lid, sterile (50 pack)	VWR	732-2699
Greiner 96-well plate TC treated with lid clear sterile	Scientific Laboratory Supplies	G655180
T25	Starstedt	83.3911.001
T75	Starstedt	83.3911.002
T175	Starstedt	83.3912
35 mm dish	Thermo Fisher	150318
60 mm dish	Starstedt	83.3901
10 cm dish	Starstedt	83.3902
12 well plate	Starstedt	83.3921
24 well plate	Starstedt	83.3922

2.1.3 Primary antibodies

Table 2.4 Primary Antibodies

Primary antibodies	Supplier	Catalogue number
CPT1-a	Cell Signalling technologies (CST)	15184-1-AP

EAAT1	St John's Laboratory	STJ92813
FAS	CST	3180S
G6PD	Source Bioscience	GTX101212S
GFAP	Dako	z0334
Glut-1	Millipore	07-1401
HK1	CST	2024
HK2	CST	2867
HK3	Abcam	ab126217
pSer79 ACC	CST	3661
pThr172 AMPK	CST	2535
PDHe1	CST	3205P
PFKP	CST	5412
PGC1-a	CST	2178S
PKM2	CST	4053P
SDHa	CST	11998
VDAC	CST	4661S
Vimentin	Sigma-Aldrich	V6630
β-actin	Biotechne	NB600-501

2.1.4 Secondary antibodies

Table 2.5 Secondary antibodies

Primary antibodies	**Supplier**	**Catalogue number**
Alexa fluor™ 680 goat anti-mouse IgG	Invitrogen	A21057
Anti-mouse Alexa fluor 568	Invitrogen	A10037
Anti-IgG (Rabbit) Goat Polyclonal Antibody	VWR	ROCK611-132-122
Anti-rabbit Alexa fluor 488	Invitrogen	A21206

2.2 Methods

2.2.1 Cell culture

Cells were cultured using aseptic technique to avoid contamination and incubated at 37°C in a humidified atmosphere containing 95% air and 5% CO_2. Human astrocytoma U373 cells were obtained from the European Collection of Authenticated Cell Cultures (EACC), human neuroblastoma SH-SY5Y cells were gifted by Professor Rory McCrimmon of the University of Dundee, and mouse hypothalamic immortalised neuronal GT1-7 cells were gifted by Dr Pamela Mellon of

the University of San Diego. Human primary astrocytes (HPA) were gifted by Dr Janet Holley and Professor Nicholas Gutowski from the University of Exeter. HPA cells were originally isolated from normal subventricular deep white matter blocks immediately post-mortem following consent from next-of-kin and with ethical approval from the North and East Devon Research Ethics Committee from a 17-year old male (Holley et al. 2005). Astrocytes were isolated from approximately 2 cm^3 tissue blocks modifying methods previously used (McCarthy et al. 1980, Noble et al. 1984a, Noble et al. 1984b). Media components for each cell type are listed in table 2.6:

Table 2.6 Media components

Cell type	Medium name	Medium constituents
HPA	Stock	Sigma DMEM (31885), 10 % (v/v) Sigma Foetal Bovine Serum (FBS, 11573397), 2 mM L-glutamine, and 25 ug/ml gentamicin. Contains 5.5 mM glucose.
HPA	2.5 mM glucose	Sigma DMEM (11966) and 2.5 mM glucose.
HPA	0.1 mM glucose	Sigma DMEM (11966) and 0.1 mM glucose.
HPA	2.5 mM glucose with serum	Sigma DMEM (11966), 1% (v/v) Sigma FBS (11573397), 22.5 mM mannitol, and 2.5 mM glucose.
HPA	0.1 mM glucose with serum	Sigma DMEM (11966), 1% (v/v) Sigma FBS (11573397), 24.9 mM Mannitol, and 0.1 mM glucose.
U373, SH-SY5Y and GT1-7	Stock	Sigma DMEM (D5671), 10 % (v/v) Sigma FBS, 4% (v/v) L-glutamine, and 2% PenStrep. Contains 25 mM glucose.
U373, SH-SY5Y and GT1-7	7.5 mM glucose	Sigma DMEM (11966), 10 % (v/v) Sigma FBS 11573397), 2% penStrep, and 2% (v/v) L-glutamine.
U373, SH-SY5Y and GT1-7	2.5 mM glucose	Sigma DMEM (11966), and 2.5 mM glucose.
U373, SH-SY5Y and GT1-7	0.1 mM glucose	Sigma DMEM (11966), and 0.1 mM glucose.

U373 cells were passaged every 3-7 days and maintained at 50-85% confluency in T-75 flasks. HPA cultures were passaged weekly to fortnightly and kept between 70-100% confluency in T-175 flasks. To aid with adhesion, plastic ware used to culture HPAs was coated with poly-L-lysine (PLL) used at 4 mg/ml for >30 minutes. Cell cultures were passaged by removal of media, gentle washing with warm PBS, incubating with 0.05% Trypsin-EDTA (3-5 ml for T-75s and 7-10 ml for T-175s) for 3-5 minutes at 37 °C, trypsinisation was ceased with the addition of stock medium (5ml for T-75s and 10ml for T-175s) to the flask. Cells were pelleted by centrifugation at 1000 rpm for 5 minutes. The pellet was resuspended in 1 ml of medium and then a further 2-5 ml. For U373 cultures, 1 ml of cell-suspension would then be added to a new T-75 and 9 ml of stock medium added. For HPA cultures, $1x10^6$ cells were counted using the TC20^{TM} Automated Cell Counter (Bio-Rad) and topped up to a total of 25 ml of stock media. Stock flasks were given fresh media every 48-72 hours to maintain nutrient supply. For experiments, U373 cultures were incubated in 7.5 mM glucose containing media, HPAs were plated in stock medium the night before experimentation. To ensure a suitable and consistent confluency, cells were seeded at the densities found in table 2.6.

Table 2.7 Seeding densities

Cell type	Culture vessel	Cells seeded
HPA	96 well plate	$2 x10^4$
HPA	24 well plate	$5 x10^4$
HPA	60 mm dish	$2.5 x10^5$ for 4 day RLG. $4.5 x10^5$ for next day treatment and collection
U373	60 mm dish	$4.5 x10^5$ for next day treatment and collection $2.5 x10^5$ for 4 day RLG
HPA	10 cm dish	$6.5 x10^5$ for next day treatment and collection $1 x10^6$ for 4 day RLG

HPA	T75	1 x10^6 for stock or 4 day RLG or 7.5x10^5 for RLG plus recovery
U373	T75	1:3-1:5 from previous flask
HPA	T175	1 x10^6 for stock culturing
SH-SY5Y	T75	1 x10^6 for stock culturing
SH-SY5Y	60 mm dish	4.5 x10^5 for next day treatment and collection
GT1-7	T75	1 x10^6 for stock culturing
GT1-7	96 well plate	5 x10^4

When suitable confluency was attained cell cultures were split and used within a range of passage numbers: HPA cells p7-20, U373 cells p16-p30, SH-SY5Y cells p10-20, and GT1-7 cells p50-56.

2.2.2 Glucose variation treatments

2.2.2.1 Acute low glucose

Cells were seeded the day before experiments and incubated overnight; HPA in stock medium and U373 in 7.5 mM glucose containing medium. On the day of experimentation the overnight media was aspirated and cells washed with warm PBS and replaced with 2.5 mM glucose containing DMEM 11966 media. During the characterisation of AMPK pathway activation by low glucose in HPA cells it was noted that cellular morphology was altered by the withdrawal of FBS, therefore, in experiments HPA media was supplemented with 1% serum, and 22.5 or 24.9 mM mannitol for 2.5 and 0.1 mM glucose concentrations respectively, to reduce osmotic stress. The cells were incubated for 2-hours before washing with warm PBS and replaced with either 2.5 or 0.1 mM glucose containing DMEM 11966 media. Cells were then cultured for 30 or 180 minutes. For experiments including the addition of noradrenaline (NA) and serotonin (5HT) a final concentration of 50 µM was added from a stock of 100 mM and 50 mM (vehicle was H_2O) respectively into the treatment media. Cells were incubated for 30 minutes before termination of the treatment. In all instances, following treatments conditioned media and cell lysates were collected (see 2.2.2.4).

2.2.2.1.1 Repeated sampling of U373 cells exposed to acute low glucose

U373 cells were seeded the day before experimentation into 60 mm dishes and incubated in medium containing 7.5 mM glucose. On the day of experimentation media was aspirated and the cells washed with 1.5 ml of warmed PBS and replaced with 1.5ml 2.5 mM glucose containing media with 22.5 mM mannitol and incubated for 2 hours at 37°C. Medium was aspirated; cells washed with 1.5 ml of warmed PBS and incubated for 3 hours in 1.5 ml 2.5 mM glucose with 22.5 mM mannitol containing media at 37°C. After this first, baseline, period 1 ml of conditioned media was collected and frozen at -20°C. The rest of the medium was aspirated and the cells washed with 1.5 ml warmed PBS. The cells were then incubated in 1.5 ml of 2.5 or 0.1 mM glucose with 22.5 or 24.9 mM mannitol containing media respectively at 37°C for 3 hours. 1 ml of conditioned media was collected from both control (2.5 mM glucose) and low glucose (0.1 mM glucose) treated cells and frozen. The remaining media was aspirated and the cells washed with 1.5 ml warmed PBS. There was then a final 3 hour incubation of cells in 1.5 ml 2.5 mM glucose, 22.5 mM mannitol containing media at 37°C. 1 ml of conditioned media was then collected and frozen, the remaining medium aspirated and the cells lysed and collected using 65 µl of lysis buffer. Cell samples were frozen and stored until protein quantification. Conditioned media samples were stored frozen until a human MIF ELISA was performed.

2.2.2.2 Recurrent low glucose

Each day cells were exposed to 2 hours of media containing 2.5 mM glucose then 3 hours of medium containing 2.5 or 0.1 mM before being recovered in stock medium or 7.5 mM glucose containing medium overnight for HPA and U373 respectively. The control and acute low glucose groups were treated with media containing 2.5 mM glucose, whereas, the antecedent RLG and RLG treated groups received 0.1 mM glucose media for 3 hours each day for the first three days. On the fourth day control and antecedent RLG were treated with 2.5 mM glucose media, whereas, acute low glucose and RLG were treated with 0.1 mM glucose media. See figure 2.1A for a depiction of the treatments. The treatment period on the last day varied between 15, 30 or 180 minutes depending on the experiment performed. At the end of treatment conditioned media and cell lysates were then collected.

2.2.2.2.1 Antecedent recurrent low glucose for Seahorse analysis

For analysis of cellular metabolism using the Seahorse XFe96 HPA and U373 cells were seeded into T75 flasks 3 days, and the day before glucose variation, respectively. Control and RLG cells were treated with 2.5 mM glucose for 2 hours and then medium containing 2.5 or 0.1 mM glucose for 3 hours. Each night cells were recovered in stock medium or medium containing 7.5 mM glucose for HPA and U373 cells respectively. On the fourth day of this treatment cells were recovered for 2 hours and then split and seeded at $2x10^4$ cells per well into a Seahorse 96-well microplate and incubated overnight in stock medium or medium containing 7.5 mM for HPA and U373 cells respectively.

2.2.2.2.2 Recurrent low glucose treatment of HPA for RNA extraction

HPA samples generated for RNA extraction were cultured in 60 mm dishes and treated to control, acute low glucose, antecedent RLG, or RLG as previously described. At the end of the treatment period, cells were trypsinised at 37°C and centrifuged for 5 minutes at $1x10^3$ RPM to pellet the cells. Supernatant was then removed and cells resuspended in PBS. One half of the cell suspension was transferred to a new tube where an additional 250 µl of TRIzol™ was added. The other half was kept for analysis of DNA at a later date. Samples were then stored at -80°C until DNA and RNA extraction took place.

2.2.2.3 Recurrent low glucose with recovery

HPA cells were seeded at $7.5x10^5$ cells per T75 flask and incubated overnight in stock media. For the next 7 days control, RLG and RLG plus recovery treatment groups were treated with media containing 2.5 mM glucose for 2 hours, 3 hours of treatment media, and recovered overnight in stock media. On days 1-4, control and RLG cells were treated with medium containing 2.5 mM glucose for 3 hours and RLG plus recovery were treated with medium containing 0.1 mM glucose. On days 5-8, control and RLG + recovery cells were treated with medium containing 2.5 mM glucose and RLG cells were treated with medium containing 0.1 mM glucose. On day 8, after the final treatment, conditioned media and cell lysates were collected. For assessment of cellular metabolism, cells were recovered for 2 hours in stock media before being split and seeded into Seahorse 96 well plates at $2x10^4$ cells per well and incubated overnight in stock medium. See figure 2.1B for a depiction of the cell treatment protocol.

Figure 2.1

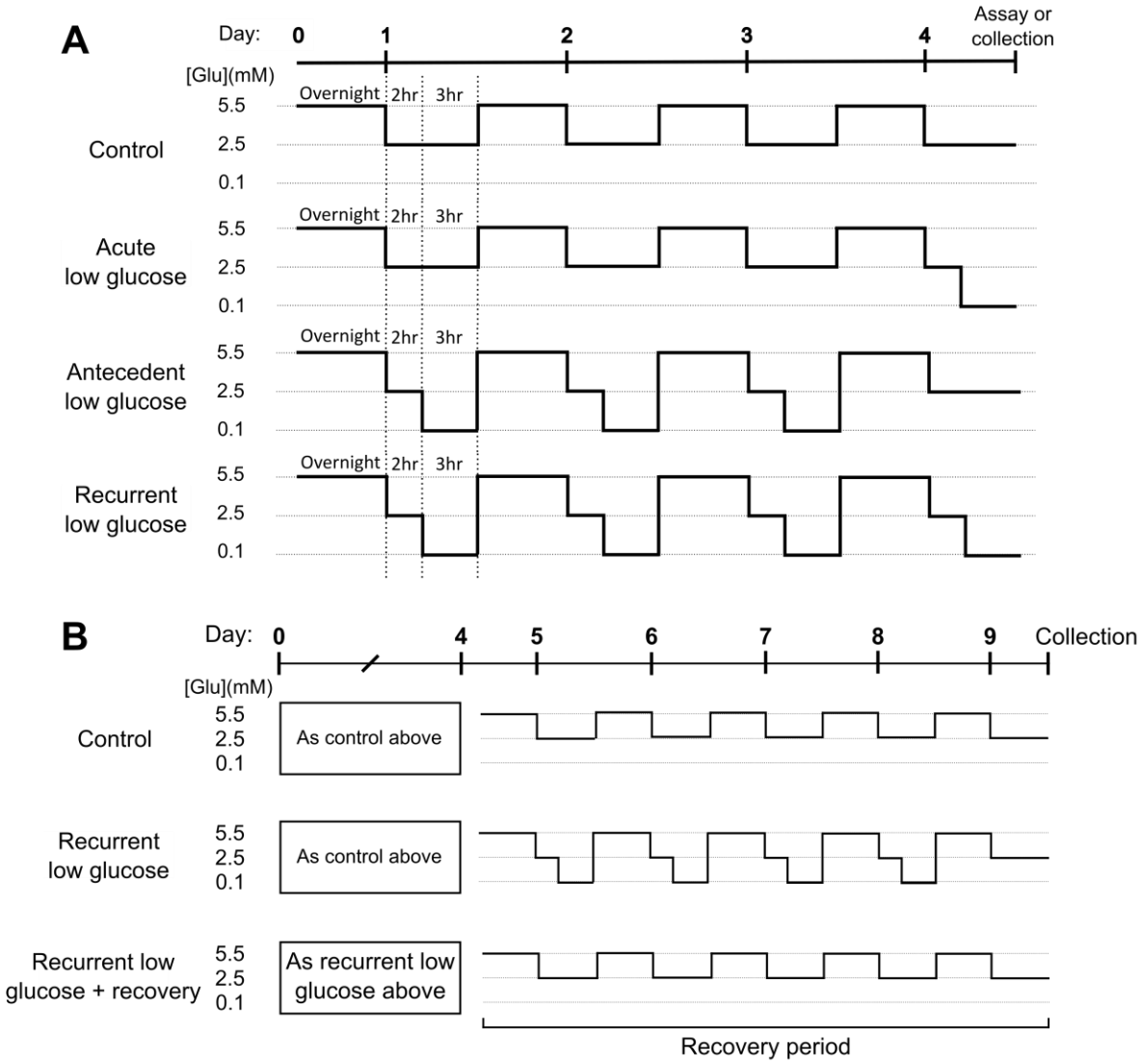

Figure 2.1 Recurrent low glucose (RLG) model

To replicate the glucose variation seen in a person with type 1 diabetes undergoing intensive insulin therapy, human primary astrocytes were exposed to the following RLG treatments. **A**. Each day cells are incubated in 2.5 mM glucose containing media for 2 hours and then treated with either 2.5 or 0.1 mM glucose containing media for 3 hours before recovery overnight in stock media (5.5 mM glucose for HPA), or 7.5 mM glucose for U373 cells. This is repeated for 4 days. The control group is never treated with 0.1 mM glucose containing media. The acute low glucose group receives one bout of 0.1 mM glucose containing media on the fourth day. Antecedent low glucose is treated with low glucose each day for three days and on the fourth day maintained in 2.5 mM glucose. The RLG group is treated with 0.1 mM glucose each day. **B**. To test whether cells could recover from RLG treatment human primary astrocytes were cultured for 8 days with a 4-day recovery period following RLG treatment. Control cells were never incubated in 0.1 mM glucose. RLG cells were treated like control cells for days 1-4 and then treated like RLG cells for days 5-8. RLG plus recovery cells were treated like RLG cells for days 1-4 and then like control cells for days 5-8.

2.2.2.4 Preparation of cell lysates

Lysis buffer contained EDTA and EGTA to chelate Mg^{2+} and Ca^{2+} ions, removing an essential cofactor for many protein kinases. Ca^{2+} chelation also inhibits calcium-dependent proteases, phosphatases, and kinases. To inhibit serine/threonine protein kinases sodium fluoride and sodium pyrophosphate were used. Tyrosine phosphatases were inhibited by sodium orthovanadate. Furthermore, benzamidine and phenylmethylsulfonyl fluoride (PMSF) was added to inhibit other protease activity. The complete lysis buffer constituents were: 25 mM Tris HCl (pH 7.4), 0.5 M NaF, 0.1 M NaCl, 1 mM EDTA (pH 8), 5 mM EGTA (pH 8), 1% (v/v) Triton X100, 10 mM NaPPi, 269 mM sucrose, 1 µl/ml β-Mercaptoethanol (BME), 1 mM $NaVO_4$, 1 mM benzamidine, and 0.1 mM PMSF.

After experimental conditions were completed media samples were collected and immediately cooled in wet ice or snap frozen with dry ice. Cells culture vessels were placed on top of a bed of ice to keep them cold, and ice cold lysis buffer added. Lysis was further aided by mechanical disruption of the cells using scraping. Sample lysate was then collected and retained in a 1.5 ml Eppendorf tube and cooled in wet ice or snap frozen in dry ice. Cell lysates were frozen and thawed before they were centrifuged at 1.48 $x10^4$ rpm for 15 minutes at 4°C to removed insoluble material. Supernatants were transferred to fresh 1.5 ml Eppendorf tubes and protein content quantified by the Bradford method.

2.2.2.5 Determination of protein content

Protein concentration was determined using the Bradford method (Bradford 1976). Briefly, 1 µl of sample was added in triplicate in a 96 well plate and 200 µl of 1 in 5 diluted Bradford reagent (BioRad) was added. The resulting solution was mixed by orbital shaking at 500 rpm for 5 minutes prior to measurement. Measurement was achieved by measuring absorbance at 595 nm was measured using the PHERAstar® *FS*. Samples were compared to a standard curve generated from known concentrations of bovine serum albumin (BSA).

2.2.3 SDS-PAGE separation of proteins

Sodium dodecyl sulphate polyacrylamide gel electrophoresis (SDS-PAGE) was used to separate proteins of different molecular weights in a sample. Proteins were linearised and a negative charge applied using SDS, allowing for their

electromagnetic attraction to an anode. An electrical current was applied to the samples and pulled the sample through the poly-acrylamide gel. By varying the concentration of acrylamide in the gel (table 2.7), different matrix sizes could be created. Gels containing a higher percentage of polyacrylamide, with small matrix sizes, allowed for optimal resolution of smaller molecular weight proteins and the inverse is also true.

2.2.3.1 Preparation of hand cast gels

Table 2.8 Hand cast gel compositions

	4%	**7%**	**10%**	**12%**
ddH_2O	1.4 ml	2.64 ml	2.075 ml	1.71 ml
1.5 M Tris	-	1.575 ml	1.575 ml	1.575 ml
0.5 M tris	0.625 ml	-	-	-
30% Acrylamide	0.425 ml	1.315 ml	1.875 ml	2.24 ml
10% SDS	25 µl	55 µl	55 µl	55 µl
20% APS	25 µl	27.7 µl	27.7 µl	27.7 µl
TEMED	2.675 µl	5.5 µl	5.5 µl	5.5 µl

Hand cast gels were made using mini-PROTEAN® Tetra equipment supplied by Bio-Rad. TEMED and 20% ammonium persulfate (APS) were added in quick succession last to initiate acrylamide polymerisation. Before the gel had polymerised the resolving (7-12% mixtures) gel was poured and a layer of water added to level out the gel. Once the resolving gel had set the water was removed and the stacking (4%) gel was added and well combs put in place.

Wells were loaded at 10 µg of sample protein in sample buffer. Once loaded the gels were run at 90 V for 15 minutes, until the samples had passed through the stacking gel. The gels were then exposed to 150 V for 1 hour and 30 minutes to 2 hours depending on the molecular weight of the protein of interest.

Table 2.9 SDS-PAGE buffers

Buffer	**Recipe**
Sample buffer	Immediately prior to use 1 µl/ml of BME was added to 4x sample

	buffer which was then added to make a 1x final solution with samples diluted to a desired concentration of protein. 125 mM Tris/HCl (pH 6.8), 0.4 ml/ml 10% SDS, 0.2 ml/ml glycerol, and a small amount of bromophenol blue, made up in ddH_2O.
Running buffer	A 10x stock was diluted to 1x before use. 10 x stocks were made with 250 mM Tris, 1.9 M glycine, and 34.7 mM SDS made up in ddH_2O.
Transfer buffer	0.2 ml/ml methanol, 48 mM tris, and 39 mM glycine was made up in ddH_2O
Tris-buffered saline with tween 20 (TBS-T)	20mM Tris/HCl (pH 7.4), 152 mM NaCl, 0.05% v/v Tween-20 made up in ddH_2O

2.2.3.2 Transfer of proteins to nitrocellulose membranes

Upon completion of SDS-PAGE protein was transferred to nitrocellulose membranes by electrotransfer. A nitrocellulose membrane was placed onto the gel and sandwiched by filter paper and fibre pads on both sides. To electrotransfer the proteins in the gel onto the membrane, the membrane was placed between the gel and an anode whilst bathed with transfer buffer. Similarly to SDS-PAGE, an electrical current, 100 V for 1 hour and 15 minutes, was applied to attract the still negatively charged proteins towards the anode.

2.2.3.3 Immunodetection

Following the completion of electrotransfer membranes were incubated in 5% (w/v) dried milk or 5% (w/v) BSA in TBS-T for 1 hour at room temperature with gentle rocking. This allowed for all the nitrocellulose membrane's free protein binding sites to be bound and prevent non-specific binding of the antibodies used. Primary antibodies were then incubated using the specific protocols as outlined in table 2.9. After these protocols were completed primary antibodies were removed and the membranes washed for 6 x 5 minute washes in TBS-T to remove remaining un-bound primary antibody. Membranes were then incubated in TBS-T containing IRDye secondary antibodies for 1 hour at room temperature. Following the

incubation membranes were washed with TBS-T for 6 x 10 minutes. To visualise the Immunodetection the Odyssey® CLx (Licor) was used to scan the blots.

Table 2.10 Antibody protocols:

Antibody	Dilution	Solution	Source
pAMPK	1:1000	2.5% (w/v) BSA in TBS-T	Rabbit
pACC	1:1000	2.5% (w/v) BSA in TBS-T	Rabbit
HK1	1:1000	2.5% (w/v) BSA in TBS-T	Rabbit
HK2	1:1000	2.5% (w/v) BSA in TBS-T	Rabbit
HK3	1:1000	2.5% (w/v) BSA in TBS-T	Rabbit
PFKP	1:1000	2.5% (w/v) BSA in TBS-T	Rabbit
VDAC	1:1000	2.5% (w/v) BSA in TBS-T	Rabbit
SDHa	1:1000	2.5% (w/v) BSA in TBS-T	Rabbit
PGC1-a	1:1000	2.5% (w/v) BSA in TBS-T	Rabbit
Glut-1	1:1000	5% (w/v) BSA in TBS-T	Rabbit
PDHe1	1:1000	5% (w/v) BSA in TBS-T	Rabbit
PKM2	1:1000	5% (w/v) BSA in TBS-T	Rabbit
CPT1-a	1:1000	2.5% (w/v) BSA in TBS-T	Rabbit
Vimentin	1:1000	2.5% (w/v) BSA in TBS-T	Mouse
FAS	1:1000	2% (w/v) Milk in TBS-T	Rabbit
G6PD	1:1000	2.5% (w/v) BSA in TBS-T	Rabbit
EAAT1	1:1000	2.5% (w/v) BSA in TBS-T	Rabbit
β-actin	1:10000	2.5% (w/v) BSA in TBS-T	Mouse
Anti-Rabbit	1:10000	TBS-T	Goat
Anti-mouse	1:10000	TBS-T	Goat

2.2.3.4 Analysis of western blots

Densitometric analysis was done using Image Studio™ Lite; regions of interest were drawn around the detected bands, including regions for background signal detection, and the signal measured using pixel intensity. For all proteins of interest signal was normalised to the loading control, β-actin. The β-actin was used to account for errors in protein quantification and sample loading. Samples were then normalised to the control, which was designated as 1, and relative levels of protein or phosphorylated

protein were analysed using one-sample T-tests. Statistical significance was determined if the $P<0.05$.

2.2.4 Extracellular flux analysis

2.2.4.1 Seahorse XFe96

The Seahorse XFe96 measures in real time oxygen consumption rate (OCR) and extracellular acidification rate (ECAR) of live cells in a 96 well plate. OCR is a measure of mitochondrial respiration whereas ECAR is a measure of glycolysis. OCR is generated by the use of oxygen in the electron transport chain within the mitochondria. ECAR is generated by the production of lactate and H^+ by glycolytic processes. HPA or U373 cells were seeded at $2x10^4$ cells per well at least 16-24 hours before the assay was performed. The assay began, after pre-treatments when needed, by replacing the medium with low buffered Seahorse basal medium with an additional 2.5 mM glucose, 2 mM L-glutamine, and 2.5 mM pyruvate. Note that in the case of the glucose dose response experiments, the cells were cultured with no glucose in the Seahorse media, which was then injected back in during the experiment. The low buffered medium allows for the unregulated change of pH in the medium which can be measured by the Seahorse probes. Once the medium was replaced, the cells were incubated at 37°C for 1 hour in atmospheric oxygen and CO_2 conditions to further reduce the buffering capacity of the medium by eliminating CO_2 mediated buffering. During this de-gassing process a Seahorse cartridge was loaded with any compounds that were to be injected during flux analysis. Once completely loaded the cartridge was placed in the Seahorse machine and an equilibration and calibration process was performed. After de-gassing, equilibration and calibration the cells were loaded and OCR and ECAR flux was measured. 3 minute mix and 3 minute measure cycles were used during the assay. Prior to any injections 3-4 baseline measurements were taken to ensure stability. Following assay completion the plate was removed and the medium aspirated. The cells were lysed with 100 µl of 50 mM NaOH and the protein content of the wells was quantified by the Bradford method as previously described. OCR and ECAR measurements were normalised to well protein content.

2.2.4.2 Mitochondrial stress test

The Mito Stress test was performed using the manufacturer's instructions (Agilent). The Mito Stress test is performed by the sequential addition of mitochondrial inhibitors to test different mitochondrial parameters. Following measurement of basal OCR, oligomycin, an ATP-synthase inhibitor, was injected at 10 µM. The resulting decrease in OCR was a measure of ATP-production-associated OCR. After 4 mix and measure cycles carbonyl cyanide-p-trifluoromethoxyphenylhydrazone (FCCP), an ionophore that transports H^+ through the inner mitochondrial membrane, uncoupling respiration driving maximal oxygen consumption, was added at a final concentration of 5 µM. The increase in OCR gave a measure of maximal respiration, and when basal respiration was subtracted gave a measure of spare respiratory capacity. After a further 4 mix and measure cycles rotenone and antimycin A were added at 5 µM each. These are complex 1 and 3 inhibitors respectively, which ablates the remaining function of the electron transport chain, thus eliminating mitochondrial oxygen consumption, allowing the measurement of non-mitochondrial OCR. Cytoplasmic oxygenases are the principle source of non-mitochondrial oxygen consumption. When non-mitochondrial OCR is subtracted from basal OCR it reveals the mitochondrial component of OCR. One can further calculate other mitochondrial parameters including proton leak and coupling efficiency. See table 2.10 for a list of measurable parameters and their calculations. The basal ECAR readings can also be of value, showing at baseline differences in glycolytic activity.

Table 2.11 Cellular metabolic parameter calculations

Parameter	**Equation**
Non-mitochondrial OCR	Minimum rate after rotenone and antimycin A injection
Basal Respiration	(last rate measurement before first injection) – (non-mitochondrial respiration rate)
Maximal respiration	(maximum rate measurement after FCCP injection) – (non-mitochondrial respiration rate)
H^+ (proton) leak	(minimum rate measurement after

	oligomycin injection) – (non-mitochondrial respiration rate)
ATP-production-associated OCR	(last rate measurement before oligomycin injection) – (minimum rate measurement after oligomycin injection)
Spare respiratory capacity	(maximal respiration) – (basal respiration)
Spare respiratory capacity as a %	(maximal respiration) / (basal respiration) x 100
Coupling efficiency	(ATP production rate) / (basal respiration rate) x 100

Figure 2.2

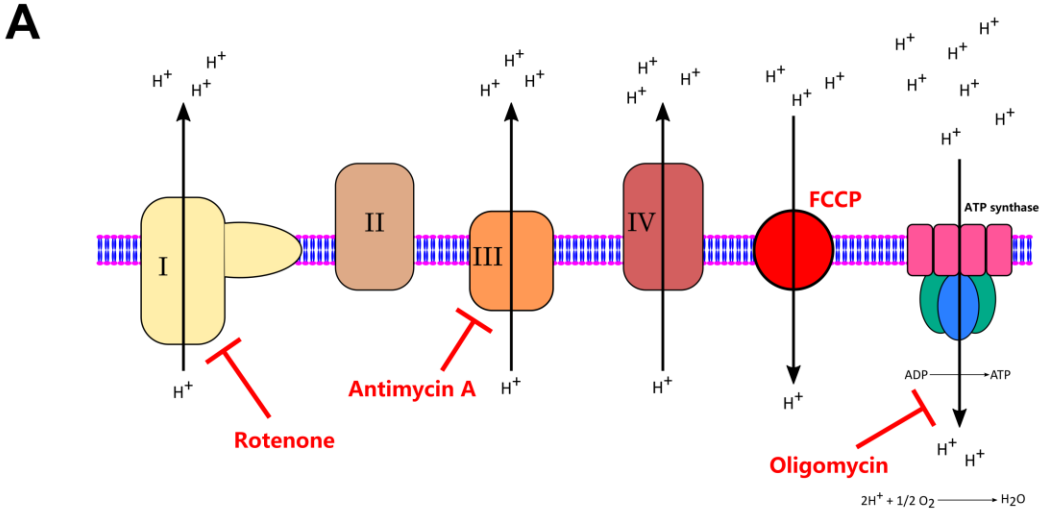

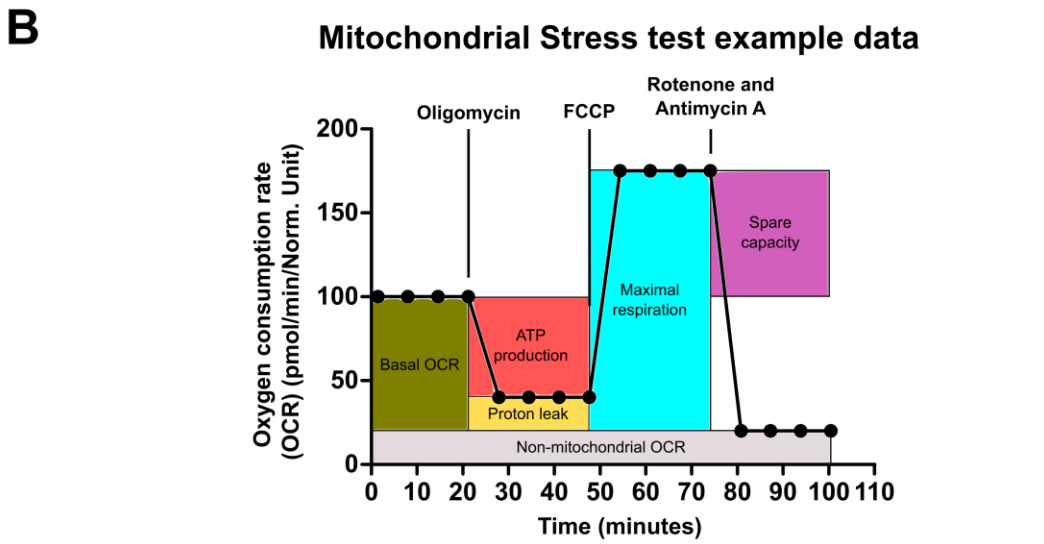

Figure 2.2. Mitochondrial stress test

The mitochondrial stress test enables the measurement of some key mitochondrial parameters in real time from a live population of cells. **A**. A depiction of the electron transport chain containing complex I, II, III and IV as well as ATP synthase. Complexes I, III and IV pump protons across the inner mitochondrial membrane into the inter mitochondrial membrane space to generate a proton gradient. ATP synthase allows the flow of protons back across the inner mitochondrial membrane and uses the proton motive force to generate ATP by the addition of P_i to an ADP molecule. During this process the mitochondria consume oxygen to convert H^+ into H_2O. The Seahorse can detect the consumption of oxygen from the media, and thus estimate mitochondrial function. By the sequential addition of mitochondrial inhibitors, specific mitochondrial metabolic functional parameters can be calculated. Oligomycin inhibits ATP synthase, FCCP uncouples flow of protons across the inner mitochondrial membrane driving maximal oxygen consumption, and rotenone and antimycin A inhibit complexes I and III ablating remaining mitochondrial function. **B**. The addition of these inhibitors causes changes to oxygen consumption rates and through a series of calculations the parameters of mitochondrial function can be quantified. Figure adapted from existing schematic found on https://www.agilent.com/en/products/cell-analysis/seahorse-xf-consumables/kits-reagents-media/seahorse-xf-cell-mito-stress-test-kit, retrieved 23rd of November 2018.

2.2.4.3 Mitochondrial fuel flex test

The Mitochondrial Fuel Flex test was carried out following the manufacturer's instructions (Agilent). The Mitochondrial Fuel Flex test allows measurement of differential fuel usage by mitochondria; pyruvate, glutamine, and long-chain fatty acids (LCFAs). The test elucidates the fuel specific dependency, capacity and flexibility by the sequential inhibition of either the pathway of interest or the other two pathways. To inhibit glucose fuel utilisation UK5099 was added at a final concentration of 2 µM which blocks the transport of pyruvate into the mitochondria via mitochondrial pyruvate carrier. Bis-2-(5-phenylacetamido-1,3,4-thiadiazol-2-yl)ethyl sulphide (BPTES) was used at 3 µM to inhibit glutamine oxidation via allosteric inhibitor of glutaminase, which converts glutamine to glutamate which is subsequently converted to α-ketoglutarate and oxidised by the TCA cycle. Etomoxir was used at 4 µM to inhibit LCFA usage by inhibiting carnitine palmitoyl-transferase 1A (CPT1A), the rate limiting enzyme in the uptake of LCFAs into the mitochondria. To calculate dependency the pathway of interest is inhibited and OCR was allowed to stabilise before inhibition of the remaining two pathways. The decrease in OCR is indicative of the inability of mitochondria to compensate for the loss of this substrate therefore a measure the mitochondria's dependency on that substrate. A cell's capacity to use a fuel can be calculated by inhibiting the two alternative pathways leaving the cells to use the remaining fuel pathway at their maximal rate. Fuel flexibility can be calculated by subtracting the fuel dependency from fuel capacity. To carry out the test on HPA and U373 cells, they were exposed to RLG using the protocol previously described. On the day before experimentation split and seeded into Seahorse 96 well plate and cultured overnight in stock medium for the HPAs and medium containing 7.5 mM glucose for the U373 cells.

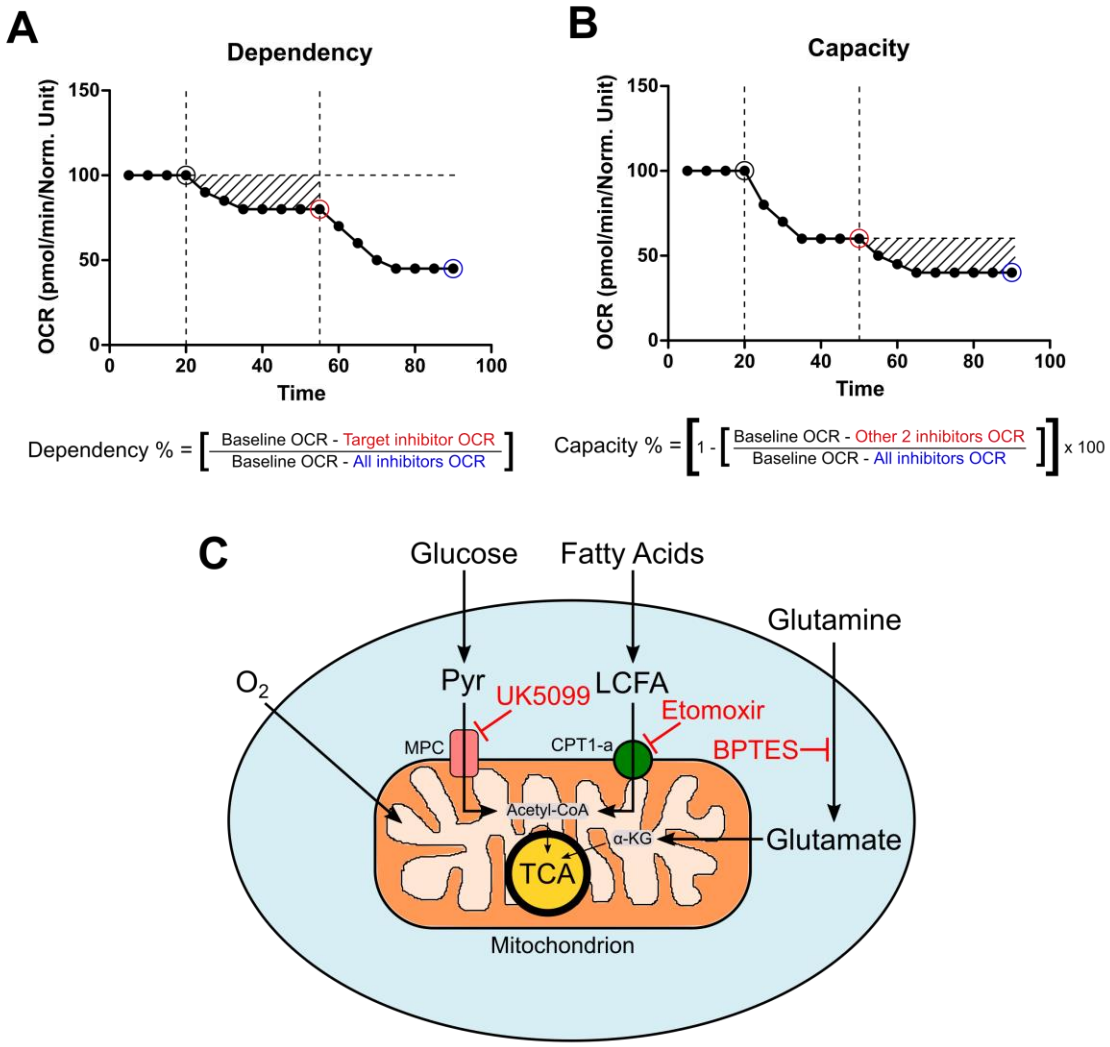

Figure 2.3. Mitochondrial fuel flex test

The mitochondrial fuel flex test measures the ability of mitochondria to metabolise different fuel sources. **A**. Fuel dependency can be calculated from inhibiting the pathway of interest and measuring the decrease in oxygen consumption rate (OCR), considering the contribution of the other two pathways. **B**. To measure the capacity for metabolising a fuel substrate the other two pathways are inhibited so the cells rely solely on the pathway of interest. **C**. To inhibit the substrate usage the three main pathways by which mitochondria metabolise substrates can be inhibited sequentially. Pyruvate (Pyr) uptake is inhibited by UK5099 which blocks the mitochondrial pyruvate carrier (MPC). Long chain fatty acid (LCFA) uptake is inhibited by etomoxir which blocks carnitine palmitoyl transferase 1a (CPT1a). Glutamine metabolism is inhibited by BPTES which inhibits glutaminase. Figure adapted from schematics found in the Seahorse XF Mito Fuel Flex Test Kit User Guide, published 1st of November 2018 by Agilent.

2.2.4.4 Glucose dose response

To study the effect of reintroduction of glucose following RLG HPA and U373 cells were exposed to the RLG model previously described and the day before experimentation seeded into the Seahorse 96 well plate and incubated in stock or medium containing 7.5 mM glucose respectively. On the day of experiment, the medium of the de-gas step, which normally containing 2.5 mM glucose, 2.5 mM pyruvate and 2 mM L-glutamine, contained no glucose. The cells were incubated for 60 minutes outside of the Seahorse XFe96 before being put in and baseline measurements were taken for a further 20 minutes before glucose was injected into the wells. The glucose injections were 0.5, 2.5 and 5.5 mM glucose. OCR and EFCAR were continually measured a further 60 minutes.

2.2.4.5 Inhibition of the pentose phosphate pathway (PPP) using 6-aminonicotinamide (6-AN)

The PPP runs in parallel to glycolysis and produces CO_2 as a by-product during the synthesis of NADPH and ribulose-5-phosphate (Stincone et al. 2015). CO_2 is released from the cell and this contributes to ECAR (Mookerjee et al. 2015). The rate limiting step of the PPP is the conversion of glucose-6-phosphate to phosphogluconolactone by glucose-6-phosphate dehydrogenase (G6PD).

To study the impact of the PPP on cellular metabolism, HPA cells were exposed to control and RLG as previously described. Two hours after the cells had been seeded into the Seahorse 96 well plate, and 15 hours before analysis in the Seahorse XFe96 analyser vehicle containing DMSO (0.01%), and 250 or 500 µM 6-aminonicotinamide (6-AN) were added into the wells. 6-AN is a selective inhibitor of G6PD and therefore inhibits the PPP. The inhibition of the PPP should result in a decrease in CO_2 production and therefore a decrease in ECAR. If there is a large decrease in ECAR it would suggest that there is a lot of PPP activity and *vice versa*. Therefore, changes to ECAR induced by 6-AN can be used as a preliminary method for the estimation of PPP activity.

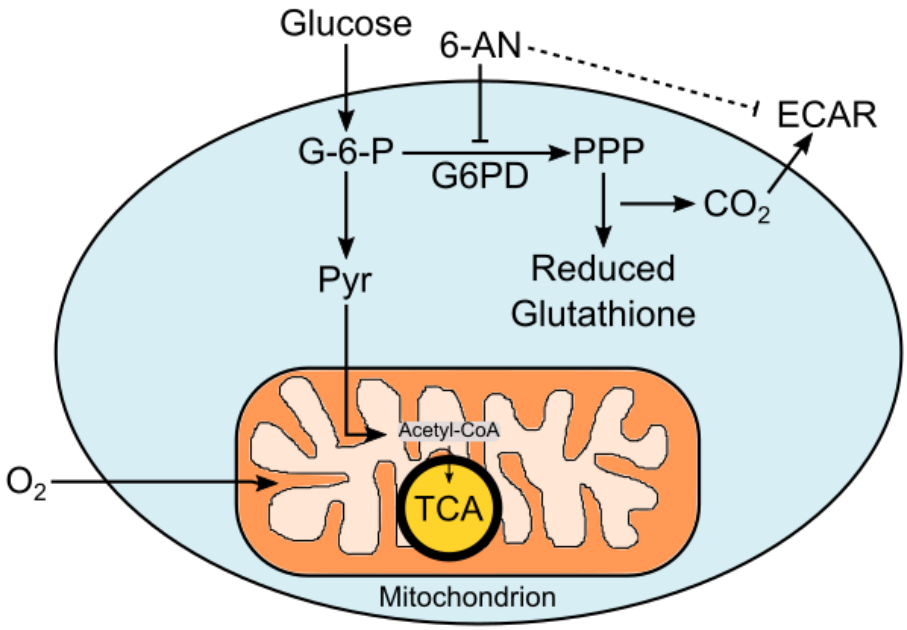

Figure 2.4 Effects of 6-aminonicotinamide (6-AN) on the pentose phosphate pathway (PPP)

During the PPP carbon dioxide is produced which contributes to extracellular acidification rate (ECAR). The rate limiting step in the PPP is the conversion of glucose-6-phosphate into phosphogluconolactone by the enzyme glucose-6-phosphate dehydrogenase (G6PD). Using the inhibitor 6-AN, this will block PPP activity which will inhibit ECAR. The changes to ECAR will be detectable by the Seahorse XFe96 analyser and can be used as a proxy for PPP activity.

2.2.5 Immunocyctochemistry

2.2.5.1 GFAP and vimentin

For experiments resulting in fluorescent imaging, cells were cultured on 13 mm round glass coverslips. Adhesion of HPA cells was aided by the addition of poly-L-lysine. Following treatment, cells were fixed by methanol. Medium was aspirated and immediately replaced with methanol kept at -20°C and incubated for 90 seconds. The methanol was then aspirated and cells were washed with PBS. Cells were permeabilised with lysine buffer (PBS, 10% normal donkey serum, 50 mM L-lysine, 0.2% Triton X-100). Cells were incubated overnight at 4°C with primary antibodies, anti-vimentin (Sigma, V6630, #102M4831 1:500 in lysine buffer), or anti-GFAP (Dako, z0334, #20035994, 1:100 in lysine buffer). The following day, primary antibodies were washed off with PBS and secondary anti-mouse (Alexa fluor 568, Invitrogen, A10037, #1827879 1:500 in PBS for vimentin) or anti-rabbit (Alexa fluor 488, Invitrogen, A21206, #1927937 1:500 in PBS for GFAP) were added to the cells for 1 hour at room temperature. The anti-body containing solution was washed off briefly with PBS and cells were co-stained with DAPI. Coverslips were mounted in fluoroshield mounting medium, dried, and imaged by fluorescence microscopy (Leica DM4000 B LED; x40).

2.2.5.2 Measurement of mitochondrial morphology with MitoTracker Red CMXRos

HPAs were cultured on 13 mm round glass coverslips coated with poly-L-lysine in 24 well plates for 4 days, seeded at $5x10^4$ cells per well and exposed to the RLG model previously described. On the fourth day of RLG treatment during the initial incubation of the cells for 2 hours in medium containing 2.5 mM glucose was modified so that the first 15 minutes contained MitoTracker Red CMXRos (50 nM; Molecular Probes, M7512, #1785958). After 15 minutes the medium was aspirated, the cells washed with 500 µl PBS and replaced with medium containing 2.5 mM for a further 1 hour and 45 minutes. After 3 hours 2.5 or 0.1 mM glucose treated cells were fixed with 4% PFA and 0.25% glutaraldehyde solution for 20 minutes. Cells were permeabilised with lysine buffer and stained with DAPI nuclear stain (Molecular Probes, D1306, 0.2mg/mL in PBS). Coverslips were briefly submersed in water and excess liquid

removed prior to mounting in fluoroshield mounting medium (Abcam, ab104135, #GR311329-1). Note that the fourth day of RLG, addition of MitoTracker Red CMXRos, fixing and staining of the cells was carried out by Josephine Robb and included here for completeness. Confocal microscopy (Leica DMi8; x63/oil immersion lens) was used to obtain Z-stacks of cells. After maximum projections were generated using LAS X software (v1.9.0.13747), images were thresholded, mean, median, and the total number of objects per image was calculated using a custom MatLab script (work carried out by Dr Jon Chilton, but included here for completeness). Data from the script were analysed using one-way ANOVA with post-hoc Bonferroni multiple comparisons tests in GraphPad Prism (v5.01).

2.2.6 Measurement of intracellular nucleotides

2.2.6.1 Total ATP levels

Total ATP levels were measured using ATPlite (Perkin Elmer, #6016941) with minor modifications as previously described (Vlachaki Walker et al. 2017). Briefly, this assay uses a luciferase assay that luminesces based on ATP content in the sample. Media samples were taken from the 60 mm dishes and 100 µl of this was loaded in triplicate into the wells of a black walled 96 well plate (VWR). To generate a standard curve fresh medium was added to the standard wells and known amounts of ATP added ranging from 0.01 to 10 µM. Mammalian cell lysis solution was added to all wells, and the plate shaken for 5 minutes. ATP substrate solution was then added to all wells and shaken for a further 5 minutes. The plate was dark adapted for 10 minutes to reduce auto-luminescence of the plate prior to measuring luminescence.

2.2.6.2 ATP:ADP ratios

ATP:ADP ratios were calculated using a luminescence assay (Sigma; #MAK135). Briefly, $1x10^3$ cells were seeded into black walled 96 well plates and exposed to 2.5 mM or 0.1 mM glucose levels for 15-180 minutes and nucleotide ratios assayed as per manufacturer's instructions. The assay is performed using two steps. Firstly, cells are lysed releasing ATP and ADP. The luciferase, ATP and substrate react to produce light which is a direct measure of $[ATP]_i$. The second step converts ADP to ATP through an enzymatic reaction which then reacts with the luciferase and substrate to emit light.

2.2.7 Measurement of extracellular lactate

Quantification of lactate in the conditioned media of HPA, U373 and SH-SY5Y neuroblastoma cells was carried out using an absorbance based plate assay. Following cell treatments supernatant was collected and frozen. Samples were defrosted on ice and centrifuged for 5 minutes at $1x10^3$ RPM. Supernatants were moved to fresh 1.5 ml Eppendorf tubes and 100 µl of sample was aliquoted, in triplicate, into a clear bottomed 96 well plate. A standard of known lactate concentrations was also loaded into the plate in triplicate. 100 µl of reaction buffer was added to each well and incubated for 1 hour at 37°C with intermittent shaking. Absorbance was read at 340 nm and the concentration in samples was determined by comparison against the standard.

The reaction buffer contained lactate dehydrogenase (LDH) and NAD^+. LDH converts lactate to pyruvate and NADH which can be detected by a change in absorbance at 340 nm. The recipe for the reaction buffer is as follows: 0.2 M glycine, 0.2 M semicarbazide hydrochloride. The pH of the solution was adjusted to 10 using 10N NaOH. On the day of assay, 2.5 U/ml LDH, and 3 mM NAD^+ are added just prior to use.

2.2.8 Calcium imaging

2.2.8.1 Fluo-4 Direct™

Fold changes in intracellular calcium were measured using the cell-permeable Ca^{2+} sensitive dye fluo-4 Direct™ (Thermo Fisher) as previously described (Vlachaki Walker et al. 2017). Cells were incubated in medium containing 2.5 or 0.1 mM glucose for 2 hours and then loaded with 1 x Fluo-4 Direct™ for 1 hour in phenol red free DMEM (Fisher) medium containing 2.5 or 0.1 mM glucose supplemented with 5 mM L-glutamine. After the 1 hour loading period the plate was loaded into the PHERAstar® *FS* microplate reader. Fluorescence was measured with excitation at 485 nm and emission at 520 nm. Measurements were taken every 0.2 seconds with vehicle (phenol red free DMEM with 25 mM HEPES), or drug injections occurring at 30 seconds, and continually measured for an additional 95 seconds. Compounds injected and the concentrations used are listed in table 2.11. Changes to Ca^{2+}-dependent fluorescence were normalised to the first measurement set to a value of

1. For analysis the peak fold-change response was used to measure the magnitude of change in $[Ca^{2+}]_i$.

Table 2.12 Compounds used during Fluo-4 experiments

Compound	Treated cell lines	Concentrations used (μM)
ATP	HPA, U373, GT1-7	5, 10, 20, 50, 100
ADP	U373	5, 10, 20
Noradrenaline (NA)	HPA, U373	10, 50 and 100

2.2.8.2 Fura-2 AM

To measure $[Ca^{2+}]_i$ in single cells, the cell permeable ratiometric calcium sensitive dye Fura-2 AM was used as previously described (Vlachaki Walker et al. 2017). Briefly, cells were loaded with Fura-2 AM (2 μM) for 60 minutes. The dye was washed off using NaCl HEPES based normal saline containing 2.5 or 0.1 mM glucose. During imaging cells were continuously perfused in a low volume chamber with NaCl HEPES based normal saline with either 2.5 or 0.1 mM glucose, and/or supplemented with ATP. Ratiometric calcium imaging was carried out by alternating exposures of excitation at 340 and 380 nm and emission at 510 nm. This was performed on the TE 2000-S Eclipse microscope (Nikon), using the 79001-ET Fura2 filter set (Chroma), the lamda DG4 light source (Sutter Instrument Company), and an ORCA-ER digital camera (Hamamatsu). Images were analysed using Volocity software (v5.5).

The recipe for NaCl HEPES based normal saline is as follows: NaCl 135 mM, KCl 5 mM, HEPES 10 mM, $MgCl_2$ 1 mM, $CaCl_2$ 2 mM, glucose 2.5 or 0.1 mM dissolved in double distilled H_2O and the pH adjusted to 7.4 using 1 M NaOH.

2.2.9 Measurement of 6-NBDG uptake

6-(N-(7-Nitrobenz-2-oxa-1,3-diazol-4-yl)amino-6-Deoxyglucose (6-NBDG) is a non-hydrolysable fluorescent glucose analogue that is transported into cells by GLUT-1. Once inside the cell fluorescence the dye can be excited by 485 nm of light and emission of 520 nm measured. To measure its uptake by HPA cells, following control or RLG treatment 6-NBDG was added at 600 μM for 15 minutes in 2.5 mM glucose before being washed off and fluorescence measured.

2.2.10 Measurement of glycogen

Glycogen content of HPA and U373 cells exposed to control or RLG was measured using a fluorometric kit (Cell Biolabs, Inc.) as per manufacturer's instructions. Briefly samples were compared against a standard curve of known glycogen content. HPA cells were exposed to control or RLG treatments; after the last 3 hour glucose exposure the cells were washed with ice cold PBS and, scraped and collected with ice cold PBS and snap frozen in dry ice. Samples were sonicated and centrifuged for 10 minutes at $1x10^4$ g for 10 minutes at 4°C. Samples were then loaded into a colourless 96 well plate in triplicate. Separate wells were exposed to amyloglucosidease and the other half were not, to measure endogenous background. This converts glycogen to glucose which is converted to D-gluconic acid by glucose oxidase releasing H_2O_2 which can be measured by a fluorometric probe.

2.2.11 Measurement of cytokines in conditioned media

Assessment of extracellular cytokines was achieved using the human cytokine array panel A (R&D Systems, ARY005) under the manufacturer's instructions. HPA cells were exposed to control or RLG conditions as previously described, without the addition of 1% serum and mannitol to the treatment media. Briefly, conditioned media from the cells was collected and incubated on the membranes supplied by the kit with bound anti-bodies specific for 36 different human cytokines. Membranes were washed and signal developed using horseradish peroxidase conjugated secondary antibodies on X-ray film. Densitometric analysis was carried out using Image Studio Lite (v5.2, Li-cor).

2.2.12 Quantifying cytokines in conditioned media using enzyme-linked immunosorbent assays (ELISAs)

To quantify IL-13, PAI-1 and MIF concentrations in conditioned media a targeted ELISA was used under manufacturer's instructions (Biotechne, Sigma-Aldrich and RayBiotech respectively). All kits used a sandwich ELISA methodology. The PAI-1 and MIF ELISA plates were pre-coated with a capture antibody, the IL-13 kit required the overnight incubation of the plate coated with a supplied capture antibody. Unknown samples and standards of known concentration were loaded into the wells and incubated for a specific amount of time. Following this, unbound antigens were washed out of the wells and a specific biotinylated anti-target antibody was added to the well. Following an incubation period, unbound primary antibody was washed

from the well. A conjugated streptavidin-horse radish peroxidase (HRP) secondary antibody was added. Following incubation, unbound enzyme-antibody-antibody conjugates were washed off the plate. 3,3,5,5'-tetramethylbenzidine (TMB) substrate reagent was added to each well and incubated to generate a reaction product. Upon the addition of an acidic stop solution, 0.2 M sulphuric acid, the reaction product becomes yellow in colour with a peak absorbance at 450 nm. The absorbance of light at 450 nm was immediately read in each well using the PHERAstar® *FS* microplate reader.

Mean absorbance values were calculated across technical replicates from each ELISA and the average zero standard was subtracted from each. A standard curve was produced by fitting a model curve to standard data, which was then used to predict the concentrations of the unknown samples. The model curve fitting was achieved using a four parameter logistic regression model. To see example standard curves for each ELISA please see appendix C.

2.2.13 RNA-sequencing

RNA-sequencing is a technique being increasingly used to measure the entire transcriptome of biological samples (Kukurba et al. 2015). This improves on quantitative PCR and microarray techniques that are comparatively slower. An overview of the RNA-sequencing pipeline is given in figure 2.5, and discussed in detail in the sections below.

2.2.13.1 Isolation of RNA

RNA extraction was completed by Samuel Washer and included here for completeness. Total RNA extraction was completed using the Direct-zol^{TM} RNA MiniPrep kit (Zymo Research, California, USA). Prior to RNA extraction, RNA PreWash, and RNA wash buffer were prepared by adding 10 ml and 48 ml of 100 % ethanol (Thermo Fisher) respectively.

Samples generated from 2.2.2.2.2, containing TRIzol, were thawed on ice and homogenised by trituration. 250 µl of 100% ethanol was added to each sample, mixed and then transferred to a Zymo-Spin^{TM} IIC Column in a collection tube and centrifuged at 1.2x10^{4} g for 30 seconds. Any flow-through was discarded and the spin column moved to a new collection tube. 400 µl of RNA Wash Buffer was added and the column centrifuged, as before, and flow-through discarded. To remove any

DNA contamination DNase I and DNA digestion buffer were added to each spin column and incubated for 15 minutes at room temperature. RNA PreWash was added, and the tubes centrifuged at $1.2x10^4$ g for 30 seconds and the flow through discarded. This was done a second time. RNA wash buffer was added, and the tubes centrifuged at $1.2x10^4$ g for 2 minutes to completely remove any wash buffer. To elute the RNA, DNase and RNase-free water was added to the column and centrifuged for 30 seconds at $1.2x10^4$ g. RNA quantity and quality was checked using the 2200 TapeStation (Agilent Technologies) and samples stored at -80°C until further use.

2.2.13.2 RNA-sequencing by the Exeter sequencing service

RNA library preparation and sequencing was performed by the Exeter Sequencing Service and Computational core facilities at the University of Exeter. Prior to RNA sequencing libraries were enriched for mRNA using poly-A isolation. Once prepared RNA was sequenced using the HiSeq 2500 (Illumina, Cambridge, UK) This facility was funded by the Medical Research Council Clinical Infrastructure award (MR/M008924/1), Wellcome Trust Institutional Strategic Support Fund (WT097835MF), Wellcome Trust Multi User Equipment Award (WT101650MA) and BBSRC LOLA award (BB/K003240/1). The author thanks the generous support from the aforementioned funders and the service provided by the sequencing service.

2.2.13.3 Quality control

Raw data quality control was performed by the Exeter Sequencing Service using FastQC. This determines a Phred score which is a metric for the quality of base identification during the sequencing procedure (Ewing et al. 1998a, Ewing et al. 1998b). The Phred score is logarithmically linked to error probabilities (Ewing et al. 1998a), meaning a Phred score of 10, 20, and 30 has a base call accuracy of 90, 99 and 99.9% respectively. All samples had a Phred score of >30.

2.2.13.4 Spliced transcripts alignment to a reference (STAR) alignment

To align the reads generated from RNA sequencing to the human genome (Homo sapiens GRCh38, STAR alignment software (v2.4.0.1) was used (Dobin et al. 2013, Dobin et al. 2015). STAR is comprised of two principle phases, seed searching, and clustering, stitching and scoring. Seed searching involves sequentially searching for a maximal mappable prefix.

Once aligned to a reference genome, STAR clusters, stitches and scores the seeds generated from the first step. Firstly, STAR clusters seeds by proximity to 'anchor' seeds. The reads that are successfully mapped are stitched together. The stitching process is guided by a local alignment scoring system where the highest scoring stitched combination is reported as the best alignment for a read.

The success of read mapping can be measured as the percentage of uniquely mapped reads, which is the percentage of reads successfully mapped reads compared to the total number of reads input into the software. A score of >80% is considered good (Dobin et al. 2015).

2.2.13.5 Read summarisation by featureCounts

Once reads have been successfully aligned to the reference genome, the number of reads mapping to a genome feature, i.e. a gene, can be counted by a process known as read summarisation, using featureCounts software (v1.6.1) (Liao et al. 2014). The featureCounts algorithm works by firstly overlapping reads with predefined genomic features. Any reads that overlap multiple features are removed. A hash table of the reference sequence names is generated allowing for reference sequence names to be found quickly within the input files. After hashing, a two-level hierarchy of genomic bins and features is derived that allows for a quick comparison of query reads against. The read counts generated from this procedure provides a summary of overall expression level of a gene. Note that this method does not distinguish between different isoforms of the same gene due to high genomic overlap.

2.2.13.6 DESeq2

Once the abundance of reads has been calculated differential gene expression analysis was performed using DESeq2 software (1.16.1). The original authors of the software Love *et*. *al*., 2014 give a full explanation of DESeq2 in their original paper (Love et al. 2014). Briefly, genes with low read counts, due to stochastic changes in read counts, can have large variance and give false positives with little physiological significance. Therefore, genes with <5 reads across each sample were excluded from further analysis. Raw read count data is input into DESeq2 software which internally corrects and normalises for library size. A series of contrasts were performed between groups of interest using wald-tests that determine whether or not the log2 fold-change is significantly different between groups from 0. These contrasts

were performed between the following groups: cells treated with 0.1 versus 2.5 mM glucose on the last day (i.e. control and antecedent RLG versus low glucose and RLG), cells treated with control and RLG prior to the last day of study (i.e. control and acute low glucose versus antecedent RLG and RLG), as well as individual groups control versus low glucose, control versus antecedent RLG, control versus RLG, low glucose versus antecedent RLG, low glucose versus RLG, and antecedent RLG versus RLG. The false discovery rates within each contrast were controlled for using Benjamini-Hochberg corrections (Benjamini et al. 1995). These analyses gave lists of differentially expressed genes that were subsequently analysed.

2.2.13.7 Gene ontology analysis

Differentially expressed genes were further analysed using the web-based enrichment analysis software Enrichr (Chen et al. 2013, Kuleshov et al. 2016). This software uses a Fisher exact test to measure overlap between genes of interest input by the user and known gene ontologies derived from data bases such as the Gene Ontology Consortium (The Gene Ontology et al. 2000, The Gene Ontology Consortium 2017) or the Kyoto Encyclopaedia of Genes and Genomes (KEGG) (Kanehisa et al. 2000, Kanehisa et al. 2016, Kanehisa et al. 2017). These multiple comparisons performed in this process are corrected for using Benjamini-Hochberg corrections (Chen et al. 2013, Kuleshov et al. 2016). In this thesis differentially expressed gene lists derived from DESeq2 were input as a crisp data set rather than a fuzzy data set (i.e. one that includes membership weightings). Fuzzy data sets require further computational analysis to generate and only slightly improve enrichment scores (Kuleshov et al. 2016). Therefore in the interests of first-pass analysis crisp data sets were used.

2.2.14 Statistical analysis

Excluding the data generated by RNA-sequencing, which is discussed above, statistical analysis was carried out using GraphPad Prism v7.03. For the comparison of two groups unpaired two-tailed student's t-tests were used. For the comparison of three or more groups one-way ANOVA tests were used with post hoc Bonferonni multiple comparisons test to determine confidence intervals between groups. To compare groups to a hypothetical mean (i.e. fold-change or baseline) one-sample t-tests were used set to the appropriate hypothetical value. In all instances p values were determined as significant by an α level of 0.05.

Figure 2.5

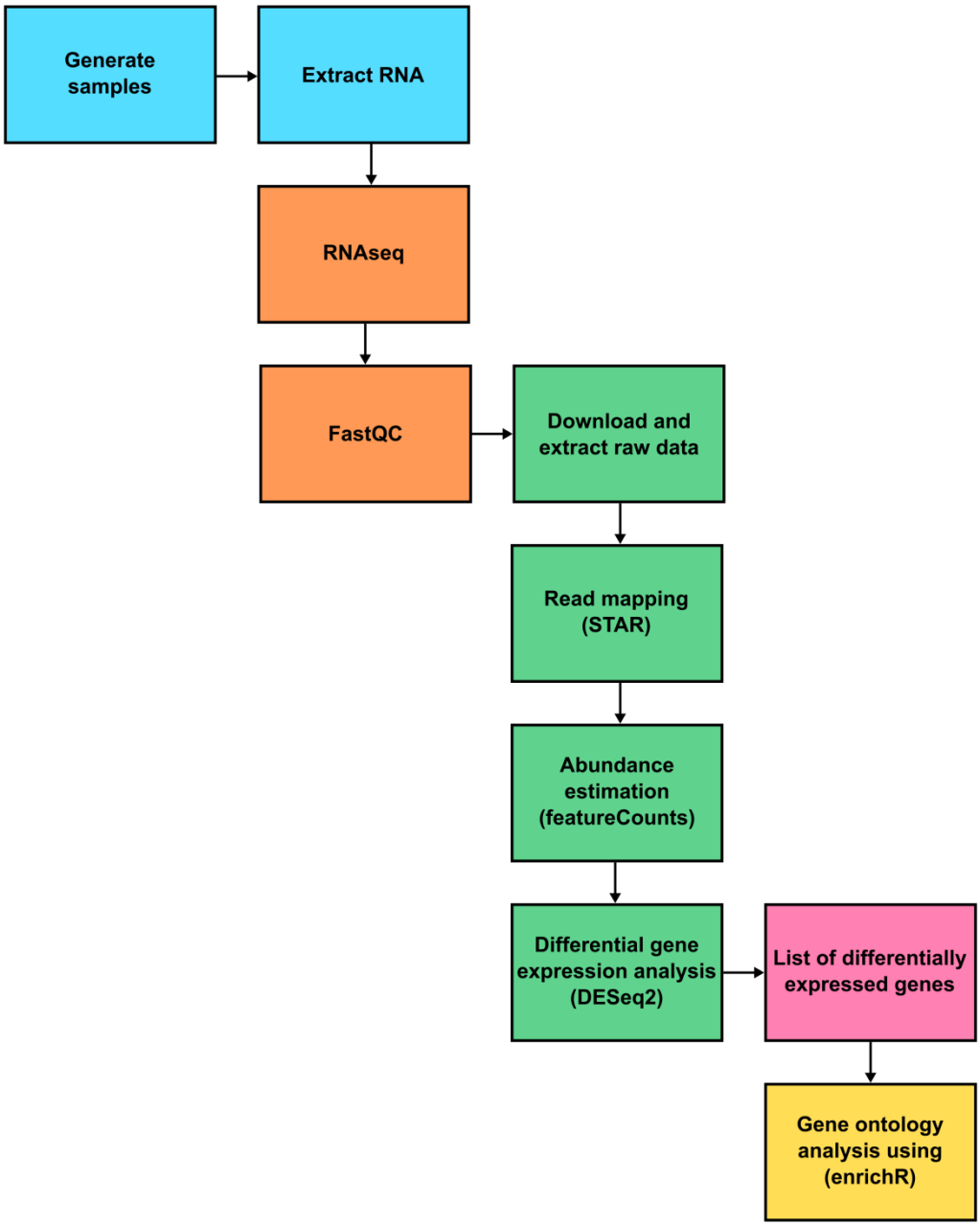

Figure 2.5. RNA-sequencing pipeline overview

Firstly, samples were generated by exposing human primary astrocytes to control, acute low glucose, antecedent recurrent low glucose (RLG), and RLG. RNA was extracted and sent to the Exeter Sequencing Service to perform RNA-sequencing using the HiSeq 2500. Raw output data quality control is performed using FastQC. If the raw data is of sufficient quality, the reads are mapped to the reference human genome GRCh38 using spliced transcripts alignment to a reference (STAR) alignment. Gene abundance is estimated using featureCounts and differential gene expression analysis performed using DESeq2. The list of differentially expressed genes undergoes secondary analysis by searching for enriched gene ontologies using the web-based program Enrichr.

Chapter 3

Human astrocytes have increased mitochondrial and glycolytic rates following recurrent glucose variation *in vitro*

Introduction

Hypoglycaemia in T1DM is a major barrier to glycaemic control and still a significant concern for those affected. Acutely, hypoglycaemia is dangerous and can result in coma, seizures and death if left untreated; also known as ‘dead-in-bed’ syndrome accounting for approximately 6% of deaths in people under 40 years of age with T1DM (Secrest et al. 2011). However, more insidious risks are an increase in cardiovascular events (Robinson et al. 2004, Chow et al. 2014a) and dementia (Mancardi et al. 1983, Renkawek et al. 1999, Booth et al. 2017). Moreover, hypoglycaemia blunts the counterregulatory response to future hypoglycaemia (Heller et al. 1991, Segel et al. 2002). This can lead to reduced symptom awareness resulting in deeper, more frequent hypoglycaemia; causing IHA. However, strict avoidance of hypoglycaemia can improve hypoglycaemia awareness to some extent (Fanelli et al. 1993, Cranston et al. 1994, Dagogo-Jack et al. 1994, Fritsche et al. 2001).

The principal site of counterregulation is in the central nervous system (CNS), in particular the cells of the ventromedial nucleus of the hypothalamus (VMN) (Borg et al. 1995), the arcuate nucleus of the hypothalamus (ARC) (Wang et al. 2004), and the dorsal vagal complex (Filippi et al. 2012). Pharmacological (Muller et al. 1972) or chemical (Shor-Posner et al. 1986, Lu et al. 1993) inhibition of adrenergic hindbrain neurons impairs or ablates the normal responses to neuroglycopenia. The hypothalamus also detects glucose directly; hypothalamic glucose transporter inhibition induces hyperphagia in rats (Glick et al. 1968). More recently, Levin et. al., demonstrated the chemical and genetic manipulation of glucose-sensing neurons in the VMN alters the CRR to insulin-induced hypoglycaemia (Levin et al. 2008). In the ARC there are neuropeptide Y (NPY) and pro-opiomelanocortin (POMC) neurons, which have opposite effects on energy metabolism. NPY neurons are orexigenic and increase food intake and reduce energy consumption (Shintani et al. 2001), whereas, POMC neurons are anorexigenic, decreasing food intake and increasing energy expenditure (Cowley et al. 2001). Glucose-sensing neurons can be classified as glucose excited (GE) or glucose inhibited (GI). Populations of POMC neurons are GE and increase firing in response to high interstitial glucose (Ibrahim et al. 2003). Populations of NPY neurons, conversely, are GI and activated by low glucose (Mountjoy et al. 2007). Synaptic glutamate release from neurons of the VMN is

necessary for CRR to insulin-induced hypoglycaemia (Tong et al. 2007). Astrocytes have also been demonstrated to be important in glucose-sensing and the CRR. For example, astrocyte activation can be induced by glucoprivic stimuli, such as 2-deoxyglucose (2-DG), where consequent neuronal modulation increases gastric emptying (McDougal et al. 2013b). Moreover, in a global KO of glucose transporter 2 (Glut-2), the selective re-expression of Glut-2 in astrocytes, but not neurons, restored CRR in rodents (Marty et al. 2005). Lastly, using chemogenetic manipulation of astrocytes Chen *et al*, were able to bi-directionally control food intake, highlighting the importance of astrocytes in whole-body energy homeostasis (Chen et al. 2016).

The ability to sense low glucose is mediated in part by the activation of AMP-activated protein kinase (AMPK) (McCrimmon et al. 2006a). AMPK, found in many tissues, is a cellular fuel-gauge which when activated increases catabolism and decreases anabolism. As AMP and ADP increase within a cell AMPK is activated and phosphorylated at threonine 172. AMPK is phosphorylated at this site by at least three kinases liver kinase B1 (LKB1), Ca^{2+}/calmodulin-dependent protein kinase II (CaMKK2) and TGFβ-activated kinase 1 (TAK1) (Hardie et al. 2012). ATP allosterically inhibits AMPK activation forming a negative feedback loop as intracellular 'energy' levels increase. ATP blocks the action of upstream kinases and permits access to phosphatases, protein phosphatase 2C (PP2C) and Mg^{2+}-/Mn^{2+}-dependent protein phosphatase 1E (PPM1E), that dephosphorylate threonine 172. When AMP and ADP reach high concentrations, they displace ATP and block the action of phosphatases, thus activating AMPK during low energy situations. While AMPK is known to be important in glucose-sensing neurons (McCrimmon et al. 2006a), it remains unclear the extent to which it is involved in astrocyte glucose-sensing.

AMPK is necessary for normal cellular function during increased energy demands. During energetic stress, according to the astrocyte-neuron lactate shuttle hypothesis, astrocytes are able to provide metabolic support to neurons in the form of lactate via monocarboxylate transporter 1 (MCT1) and MCT4 on astrocytes, and MCT2 on neurons (Pellerin et al. 1994, Pellerin et al. 1998, Pellerin 2003, Bergersen 2007). However, there is some disagreement in the literature concerning the extent of this phenomenon and whether it occurs in physiological and/or pathological circumstances (Chih et al. 2003, Mangia et al. 2009, Figley 2011). Importantly,

astrocytes can store small amounts of glycogen, which have been shown to be broken down in *ex vivo* brain slices in response glucose withdrawal in order to bolster energy supplies; some of which may be provided to neurons via lactate (Wender et al. 2000, Brown et al. 2005). Astrocytes also line the blood-brain barrier (BBB), in combination with pericytes and endothelial cells, and therefore may be exposed to glucose changes before neurons, perhaps being first to act to falling glucose levels (Virgintino et al. 1997). Indeed, astrocytes have been shown to mediate glucose uptake from microvessels, demonstrating a regulatory role (Maxwell et al. 1989). *In vitro* cultures of brain endothelial cells the uptake of glucose can be upregulated by the release of gliotransmitters which may couple astrocyte sensing of neuronal activity and the increased supply of glucose at the BBB (Braet et al. 2004, Leybaert et al. 2004, Leybaert 2005). Furthermore, the release of these factors from astrocytes may be triggered by hypoglycaemia which may serve as a mechanism to sustain neuronal energy supply (Régina et al. 2001).

Astrocyte and neuronal metabolism are markedly different. Neurons utilise primarily, the more efficient, oxidative phosphorylation to generate ATP, whereas, astrocytes can rapidly increase glycolytic rates (Bélanger et al. 2011). This is partly due to a higher expression of 6-phosphofructo-2-kinase type 3 (PFKFB3), which can enhance glycolysis (Almeida et al. 2004, Snyder et al. 2004). Glycolysis in astrocytes is also more likely to result in lactate production rather than pyruvate (Walz et al. 1988, Peng et al. 1994) due to the presence of lactate dehydrogenase (LDH) isoform 5 (LDH5), which has a higher affinity for pyruvate resulting in net lactate production (Bittar et al. 1996). This contrasts with neurons, which only have LDH1 (also found in astrocytes) which favours lactate catabolism (Bittar et al. 1996). The increased metabolic flexibility of astrocytes makes them highly adaptable to different nutrient states and able to react to increased energy demands associated with neurotransmission (Pellerin et al. 1994, Fray et al. 1996).

A consequence of oxidative phosphorylation is the generation of reactive oxygen species (ROS) (Murphy 2009). While neurons have an increased reliance on mitochondrial respiration, they are more sensitive to oxidative stress-induced cell death (Bolanos et al. 1997). A significant cytosolic mechanism for ameliorating ROS is the pentose phosphate pathway (PPP) (Stincone et al. 2015). In neurons, the PPP accounts for ~5% of glucose metabolism compared to ~60-70% in astrocytes

(Allaman et al. 2010, Takahashi et al. 2012). The PPP operates in parallel to glycolysis, diverging when glucose-6-phosphate (G6P) is converted by the rate-limiting enzyme G6P dehydrogenase (G6PDH) to phosphogluconolactone (Glaser et al. 1955). The PPP is composed of the oxidative phase and the non-oxidative phase (Stincone et al. 2015). The oxidative phase consists of phosphogluconolactone being further broken down to 6-phosphogluconate and onto ribose-5-phosphate (R5P), contributing to DNA and RNA synthesis (Stincone et al. 2015). During the conversion of G6P to R5P, two nicotinamide adenine dinucleotide phosphate (NADPH) molecules are produced which is the major source of NADPH within the cell (Dickens et al. 1951). This also produces CO_2 which contributes to extracellular acidification rates (ECAR), detectable by the Seahorse XFe^{96} extracellular flux analyser (Mookerjee et al. 2015). The PPP can also re-join glycolysis, via the production of fructose-6-phosphate and glyceraldehyde-3-phosphate, allowing for further contributions to ECAR. In theory, the glucose shunted away from glycolysis would be prevented from undergoing complete oxidation by the mitochondria and, therefore, detectable by changes to OCR also.

The NADPH produced by the PPP is used as a reducing agent involved in fatty acid synthesis and production of reduced glutathione (GSH) from glutathione disulphide (GSSG) (Panday et al. 2014). GSH is a major cellular antioxidant which converts H_2O_2 to GSSG and water by GSH peroxidase (Stincone et al. 2015). It is known that the PPP is upregulated as a part of the oxidative stress response (Stincone et al. 2015). For example, high-glucose-induced stress in astrocytes *in vitro* leads to an elevation in PPP activity (Takahashi et al. 2012). The PPP requires glucose, therefore in hypoglycaemia PPP may not be as active leading to a decrease in ROS defence. Indeed, hypoglycaemia (McGowan et al. 2006), and glucose deprivation (Rose et al. 1998) have been shown to increase oxidative stress in the brain. AMPK is activated by hypoglycaemia (McCrimmon et al. 2004) which in turn upregulates fatty acid oxidation (Merrill et al. 1997). Increased fatty acid oxidation also increases ROS. Therefore, in the absence of glucose PPP activity may be reduced while there is an increase in ROS leading to cellular stress. However, little is known about how acute or recurrent low glucose may affect the PPP, especially in astrocytes.

More broadly there is growing recognition of astrocytic involvement and activation in other CNS diseases, such as obesity (Horvath et al. 2010, Thaler et al. 2012),

Alzheimer's disease (Mancardi et al. 1983), and Parkinson's disease (Renkawek et al. 1999, Booth et al. 2017). A general marker of astrocyte activation is astrogliosis which occurs in many of these disease states (Pekny et al. 2016). Interestingly, astrogliosis also occurs during fasting and fed states (Horvath et al. 2010, Thaler et al. 2012, Daumas-Meyer et al. 2018). Astrogliosis manifests as a ramification of astrocyte intermediate filaments glial fibrillary acid protein (GFAP) and vimentin, which increases morphological complexity. Vimentin fragmentation has also been shown to occur in response to inflammatory stimuli (Darlington et al. 2008).

Despite an increased awareness of the importance of astrocytes in physiological and pathophysiological conditions, little is known about the intrinsic responses of astrocytes to either acute low glucose or RLG exposure. It was hypothesised there would be astrocytic AMPK pathway activation to maintain energy homeostasis. AMPK pathway activation should in turn activate catabolic processes, like fatty acid metabolism (Ronnett et al. 2009). Indeed, it has previously been shown that hypoglycaemia can increase the expression of fatty acid oxidation-related genes (Poplawski et al. 2010, Poplawski et al. 2011). Mitochondrial and glycolytic metabolic rates were determined, in real-time, using the Seahorse extracellular flux analyser. Other metabolic components were measured including, glycogen levels, intracellular nucleotide levels, and the expression of metabolic enzymes. The novel findings from this work show that human astrocytes intrinsically adapt to RLG stress by increasing basal oxygen consumption, glycolytic rates, and fatty acid metabolism, at the expense of decreased coupling efficiency.

Overall aim and objectives

Fundamentally, RH deprives cells or glucose to generate ATP. Therefore to sustain neural function changes in cellular metabolic activity must occur; activation of AMPK, metabolic substrate switching, or changes to fuel utilisation. Still, little is known about how human astrocytes respond to acute or recurrent low glucose. Therefore, the overarching aim of this chapter was to investigate changes to human astrocyte metabolic functions after acute and recurrent low glucose treatments including:

- Is AMPK phosphorylated by low glucose treatment in HPA and U373 cells and how is this affected by RLG?

- Does RLG induce and alter astrogliosis in HPA cells as measured by altered GFAP and Vimentin expression?
- Does RLG alter mitochondrial function? If so, can this be recovered?
- Does RLG induce glycogen supercompensation in isolated HPA cells?
- Does RLG alter glucose uptake, lactate release or glycolytic function in human astrocytes?

Results

3.1 HPA AMPK and ACC phosphorylation is increased by low glucose

AMPK is a physiological fuel gauge that is activated by low glucose levels and the increase of AMP within a cell. AMPK activation and phosphorylation at threonine 172 is necessary for sensing of hypoglycaemia (McCrimmon et al. 2008). However, it is unknown whether human astrocytes respond in a similar manner. As such HPAs were exposed to 5.5, 2.5 and 0.1 mM glucose for 30 minutes, representative of hyperglycaemia, euglycaemia, and hypoglycaemia respectively. Changes in AMPK pathway phosphorylation were assessed by Western blotting cell lysates. Treatment with 0.1 mM glucose increased phosphorylation of AMPK at threonine 172 (figure 3.1A,C). Further to this, ACC, a downstream target of phosphorylated AMPK, had increased phosphorylation at serine 79 (figure 3.1B). Interestingly, there were no significant differences between 5.5 and 2.5 mM glucose treated cells.

Figure 3.1

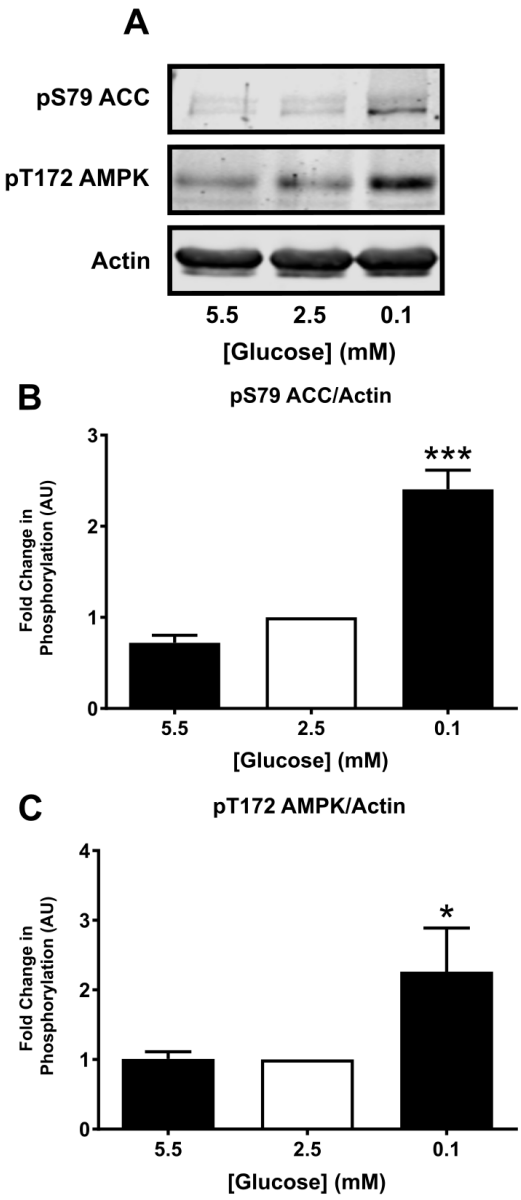

Figure 3.1. Human primary astrocyte (HPA) AMP-activated protein kinase (AMPK) and acetyl-CoA carboxylase (ACC) phosphorylation is increased by low glucose.

A. Representative immunoblots from HPA exposed to 5.5, 2.5 or 0.1 mM glucose for 30 minutes probed for pS79 ACC (top panel), pT172 (middle panel), and actin (bottom panel) (n=8). **B**. Densitometric analysis of immunostaining for pT172 AMPK normalised to actin as a loading control. **C**. Densitometric analysis of immunostaining for pS79 ACC normalised to actin as a loading control. *P<0.05;***P<0.001 vs 2.5 mM glucose treated cells. One-way ANOVA with post hoc Bonferroni multiple comparisons tests. Error bars represent standard error of the mean (SEM).

3.2 HPA and U373 astrocytoma AMPK and ACC phosphorylation is increased by low glucose

It was noticed that serum withdrawal during experiments, regardless of glucose concentration, resulted in morphological changes resembling astrogliosis in the HPA cells. Therefore to reduce morphological changes and differences induced by serum withdrawal and osmolarity, 1% serum and mannitol were included in the treatment media. U373 medium did not include 1% serum or any mannitol as they did not react to serum withdrawal.

The aim of this experiment was, firstly, to test whether the increase in AMPK and ACC phosphorylation in 0.1 mM glucose was altered by the presence of 1% serum and osmotic controls. Secondly, it tests whether AMPK and ACC phosphorylation similarly increased with 0.1 mM glucose treatment in U373 cells. After 30 minutes of exposure to 2.5 or 0.1 mM glucose containing media, there was a significant increase in both pT172 AMPK and pS79 ACC in HPA and U373 cell lysates (figure 3.2A-F). These data also show the increase in pT172 AMPK in response to low glucose is preserved in the presence of serum or mannitol.

Figure 3.2

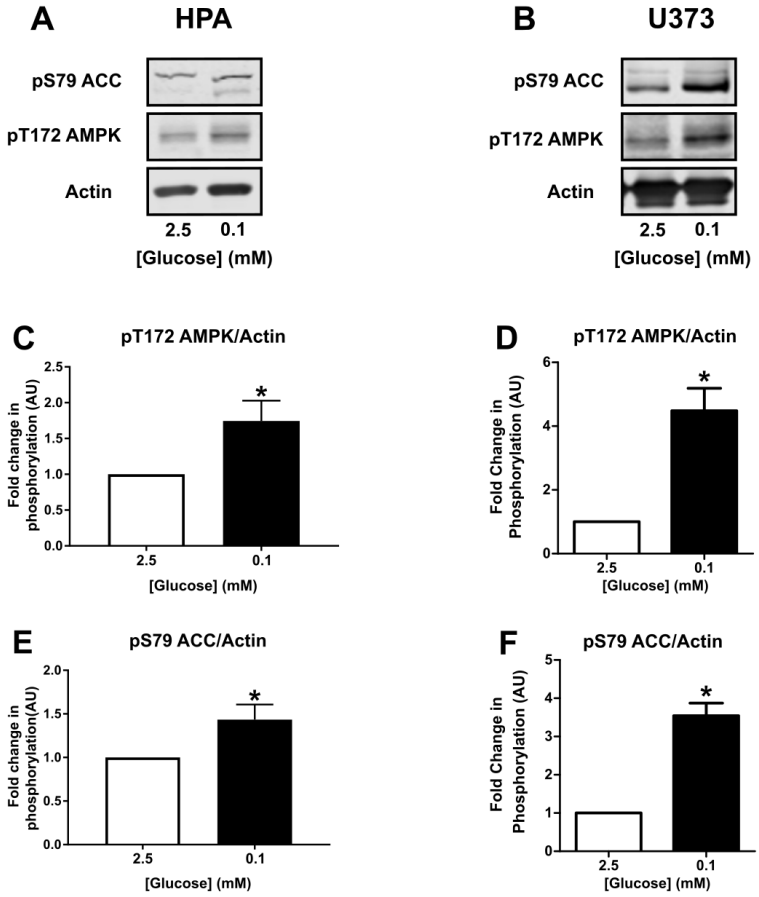

Figure 3.2. Human primary astrocytes (HPA) and U373 human astrocytoma AMP-activated protein kinase (AMPK) and acetyl-CoA carboxylase (ACC) phosphorylation is increased by low glucose.

Representative immunoblots from HPA (**A**; n=7 and U373 astrocytoma cells (**B**; n=3) exposed to 2.5 or 0.1 mM glucose media for 30 minutes, including added 1% foetal bovine serum and 22.5 or 24.9 mM mannitol respectively for HPA samples. **C**, **D**. Densitometric analysis of immunostaining for pT172 AMPK normalised to actin as a loading control. **E**, **F**. Densitometric analysis of immunostaining for pS79 ACC normalised to actin as a loading control. *P<0.05; ***P<0.001 vs 2.5 mM glucose treated cells. One-sample t-test in comparison to control. Error bars represent standard error of the mean (SEM).

3.3 HPA AMPK pathway activity after RLG

It has been previously shown that recurring insulin-induced hypoglycaemia blunts the activation of AMPK (Mandal et al. 2017). To test whether this occurred in HPAs, cells were exposed to control or RLG for three days and on the last day treated with 2.5 mM or 0.1 mM glucose for 15 or 30 minutes. Changes in AMPK pathway activation in cell lysates was measured by Western blotting. After 15 minutes of 0.1 mM glucose treatment both pT172 AMPK, and pS79 ACC did not increase significantly (figure 3.3A,B,D). After 30 minutes of 0.1 mM glucose treatment pT172 AMPK and pS79 ACC increased significantly (figure 3.3A,C,E). Interestingly, RLG + 2.5 mM glucose had a significantly higher pT172 AMPK than control + 2.5 mM (figure 3.3C). Similarly, RLG + 0.1 mM glucose, while not significantly different from RLG + 2.5 mM glucose, was higher than control + 2.5 mM glucose (figure 3.3C). This shows that while the absolute amount of AMPK phosphorylation remains similar after low glucose treatment, the increase in pT172 AMPK in response to 0.1 mM glucose is lost following RLG. Despite the altered AMPK response, the change in phosphorylation of ACC in response to low glucose was maintained (figure 3.3E).

Figure 3.3

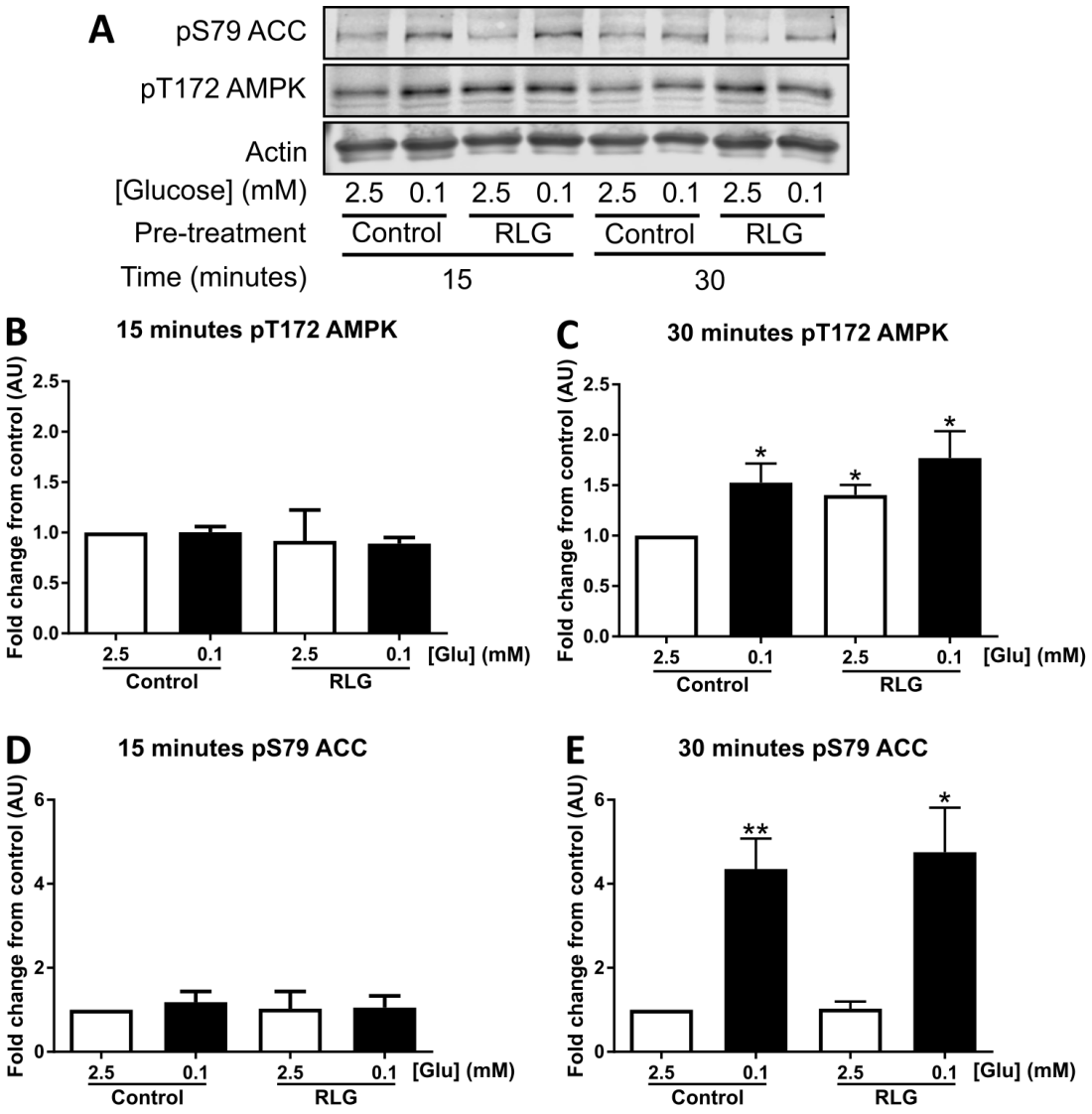

Figure 3.3. Human primary astrocyte (HPA) AMP-activated protein kinase (AMPK) pathway activity after recurrent low glucose (RLG).

A. Representative immunoblots probed for pS79 acetyl-CoA carboxylase (pACC; top panel; n=7), pT172 AMPK (pAMPK; middle panel; n=6), and actin (bottom panel) from HPA cells treated with RLG where the last exposure to either 2.5 or 0.1 mM glucose lasted for 15 or 30 minutes. **B**, **C**. Densitometric analysis of immunostaining for pAMPK normalised to actin as a loading control after 15 or 30 minutes of treatment respectively. **D**, **E**. Densitometric analysis of immunostaining for pACC normalised to actin as a loading control after 15 or 30 minutes of treatment respectively. *P<0.05, **P<0.01 vs 2.5 mM glucose with control pretreated cells. One sample t-test in comparison to control. Error bars represent standard error of the mean (SEM).

3.4 Effects of acute or recurrent low glucose on HPA GFAP

Astrogliosis occurs in astrocytes in response to overnutrition (Horvath et al. 2010, Thaler et al. 2012) and fasting (Daumas-Meyer et al. 2018). This results in the ramification of astrocytic intermediate filaments and an altered cellular morphology. Therefore, expression of GFAP in HPA cells following exposure to RLG was measured. GFAP content was determined following a 3-hour exposure to 2.5 or 0.1 mM glucose on the last day. In contrast to expectations, no significant difference in GFAP immunostaining was observed between control and low glucose treated cells (figure 3.4A,B).

3.5 RLG increases HPA vimentin content

The expression of vimentin, another intermediate filament, is also increased by astrogliosis (Pekny et al. 2005) and can be fragmented following inflammatory stimuli (Darlington et al. 2008). To determine the effect of RLG on cellular vimentin cells were exposed to control or RLG with an additional 3-hour exposure to 2.5 or 0.1 mM glucose. Vimentin fragmentation and expression increased significantly in cell lysates after RLG, determined by Western blotting (figure 3.5C). Additionally, there was an increase in lighter vimentin-positive bands detectable indicating increased fragmentation (figure 3.5C). Cellular distribution of vimentin, however, was not significantly altered by RLG (figure 3.5A,B).

Figure 3.4

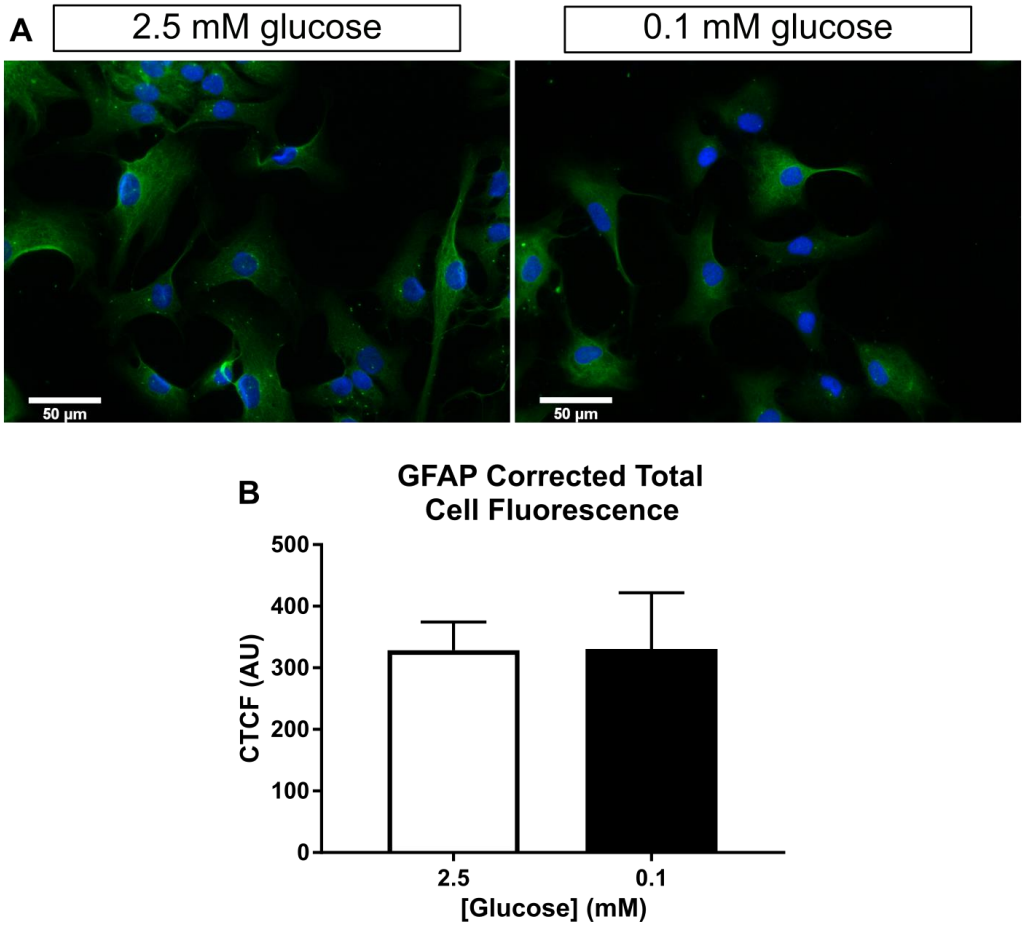

Figure 3.4. Human primary astrocytes (HPA) are positive for glial fibrillary acidic protein (GFAP) and GFAP is unaltered by low glucose.

A. HPA cells stained with a GFAP antibody (green) and DAPI to identify nuclei (blue). Scale bar: 50 µm. **B**. Quantified correct total cell fluorescence (CTCF) of GFAP immunofluorescence (control group, n=5; low glucose, n=4). Error bars represent standard error of the mean (SEM).

Figure 3.5

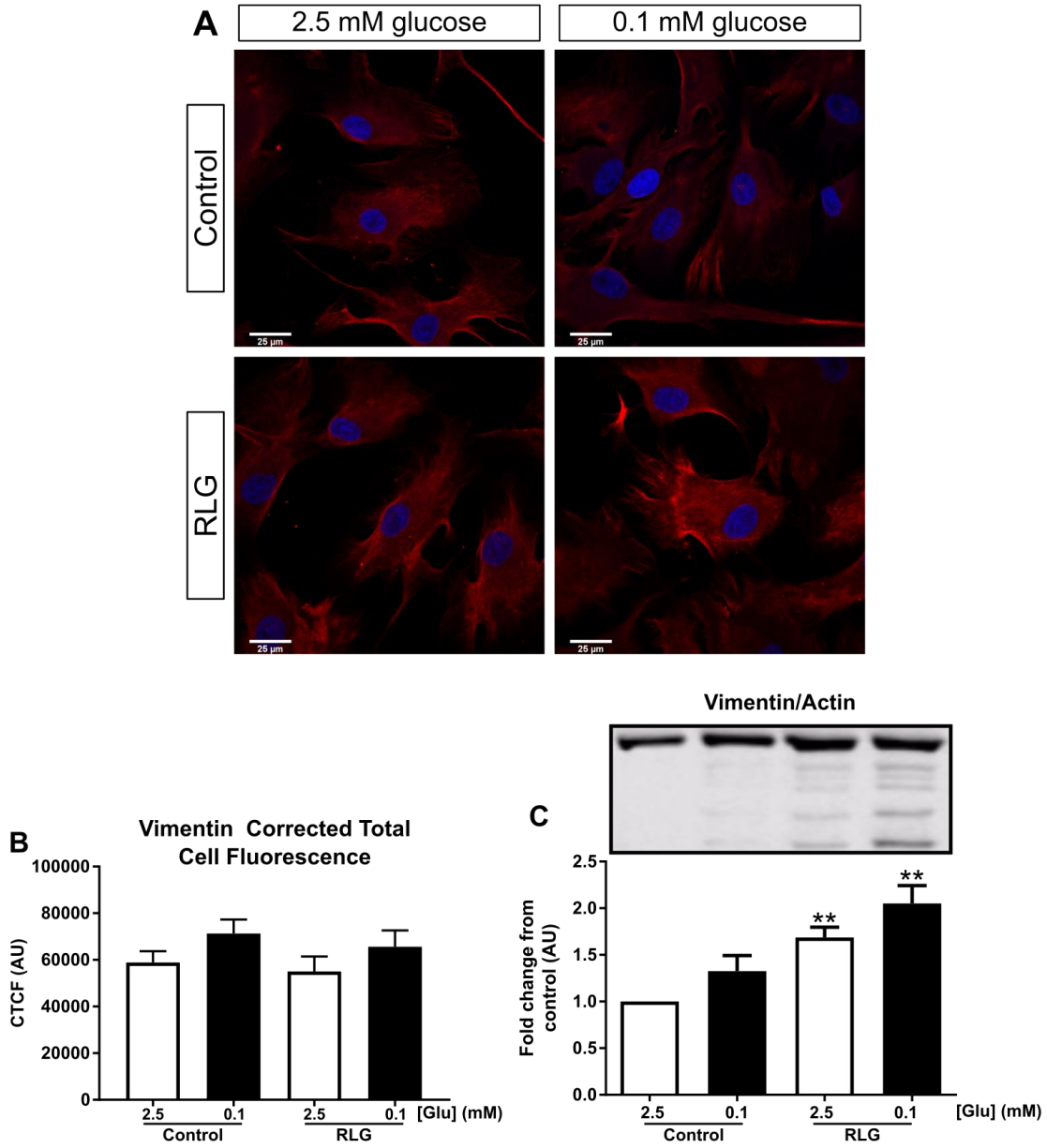

Figure 3.5. Recurrent low glucose (RLG) does not affect vimentin staining in human primary astrocytes (HPA), but increases vimentin expression.

A. Representative images of HPA cells (n=11-12) exposed to RLG with and without additional 0.1 mM glucose exposure stained with a vimentin antibody (red) and DAPI to identify nuclei (blue). Scale bar: 50 µm. **B**. Quantified corrected total cell fluorescence (CTCF) of vimentin immunofluorescence. Error bars represent standard error of the mean (SEM). **C**. Representative immunoblots and densitometric analysis from HPA cells exposed to 2.5 or 0.1 mM glucose for 3 hours following control or RLG and probed for vimentin (n=5). **P<0.01 vs 2.5 mM glucose with control pretreated cells. Error bars represent standard error of the mean (SEM). One-way ANOVA with one-sample t-tests in comparison to control.

3.6 The effects of RLG on HPA and U373 mitochondrial and glycolytic phenotype

To investigate the effects of RLG on human astrocytes a mitochondrial stress test was performed. Briefly, HPA and U373 were exposed to 4 days of three hours exposures to either control (2.5 mM) or low (0.1 mM) glucose each day before being seeded into a 96 well plate compatible with the Seahorse XFe96 extracellular flux analyser where their OCR and ECAR was measured following the injection of mitochondrial inhibitors. During the assay the glucose concentration in the media was 2.5 mM.

3.6.1 RLG increases baseline mitochondrial metabolism and reduces mitochondrial coupling efficiency.

HPA and U373 baseline OCR was elevated following RLG exposure (figure 3.6.1A-D), demonstrating sustained alterations to cellular metabolism lasting up to 24 hours after the last low glucose exposure. Upon addition of the ATP-synthase inhibitor oligomycin, the resulting decrease to ATP production associated-OCR was diminished in RLG treated HPA. Thus, the fraction of basal OCR contributing to ATP-production was reduced in HPA, but not U373 (figure 3.6.1E,F). FCCP, an ionophore used to uncouple flow of H^+ across the inner mitochondrial membrane from ATP production was added to maximally drive ETC oxygen consumption. In both control and RLG, OCR increased to ~200% of baseline, however, the RLG treated cells had an augmented FCCP-sensitive increase to OCR. In the HPAs, the reduction in spare respiratory capacity was mediated by increased basal metabolism (figure 3.6.1F). In contrast, U373 cells had an increased spare respiratory capacity (figure 3.6.1H). Injection of rotenone and antimycin A, complex I and III inhibitors respectively, were used to ablate remaining mitochondrial function. This resulted in significantly increased non-mitochondrial OCR in HPA but not U373 cells (figure 3.6.1.1A,B). These measurements permitted calculation of proton leak and coupling efficiency. The latter significantly decreased in HPA cells (figure 3.6.1.1E), mediated by significantly increased proton leak (figure 3.6.1.1C). While proton leak was elevated in U373 cells (figure 3.6.1.1D) this did not lead to a change in coupling efficiency (figure 3.6.1.1F).

3.6.2 RLG increases baseline ECAR of HPA but not U373 cells

Basal ECAR was elevated in HPA cells but not in U373 cells (figure 3.6.2A-D).

3.7 The effects of RLG on HPA basal state mitochondrial fuel oxidation

Astrocytes are metabolically flexible cells, and it was shown previously RLG changes mitochondrial and glycolytic functions. To test whether the changes in mitochondrial function were due to changes in substrate utilisation a mitochondrial fuel flex test was used. Mitochondrial fuel dependency, capacity and flexibility of three key substrate metabolic pathways; pyruvate, glutamine, and fatty acids following RLG exposure, were examined using the mitochondrial fuel flex test. In each assay the glucose concentration was 2.5 mM glucose.

Figure 3.6.1

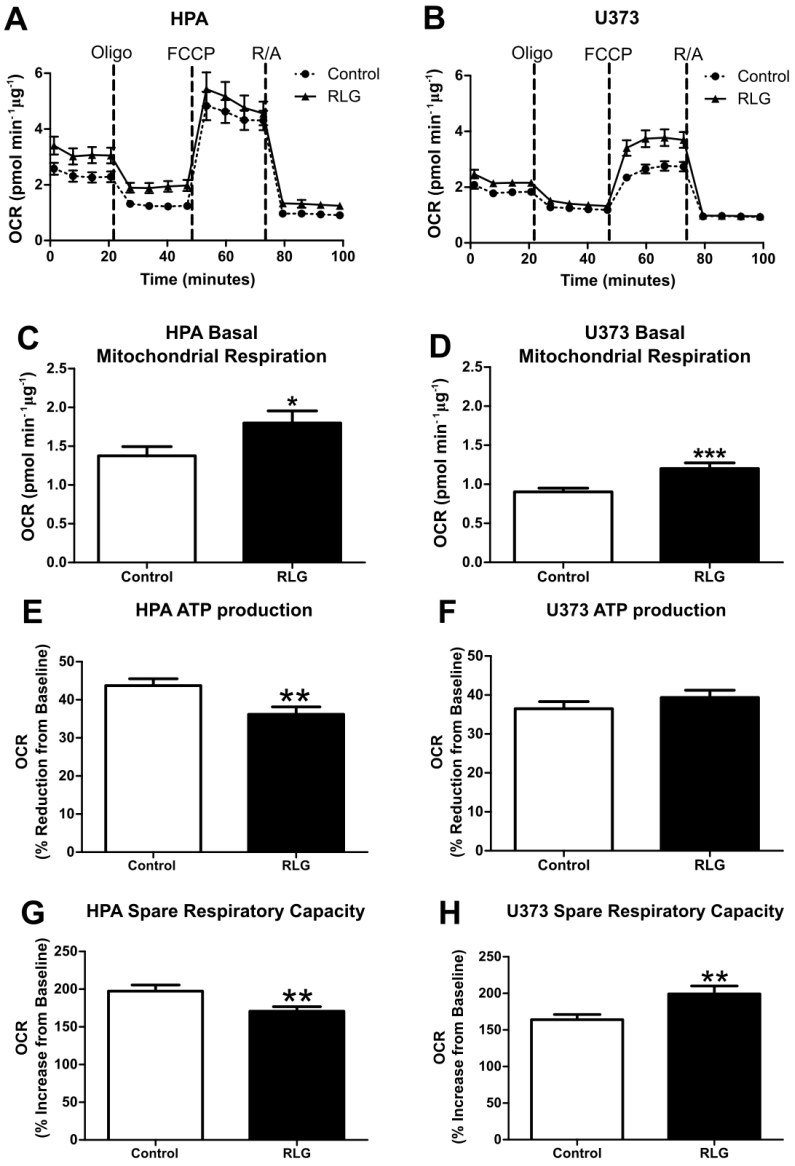

Figure 3.6.1. Recurrent low glucose (RLG) increases baseline mitochondrial metabolism in human primary astrocytes (HPA) and U373 astrocytoma cells.

Oxygen consumption rate (OCR) of HPA during a mitochondrial stress test (**A**; control group, n=36; RLG group, n=39, across three separate assays) and U373 cells (**B**) following RLG (control group, n=40; RLG group, n=43, across separate assays). Cells were exposed to oligomycin (10 µM; Oligo), FCCP (5 µM) and a combination of rotenone (5 µM; R) and antimycin A (5 µM; A). **C**, **D**. Mean basal OCR in control and RLG treated astrocytes. **E**, **F**. ATP production determined from the oligomycin dependent change in OCR. **G**, **H**. Spare respiratory capacity calculated from the difference between maximal and basal respiration. *P<0.05, **P<0.01 vs control. Error bars represent standard error of the mean. Unpaired two-tailed student's t-tests

Figure 3.6.1.1

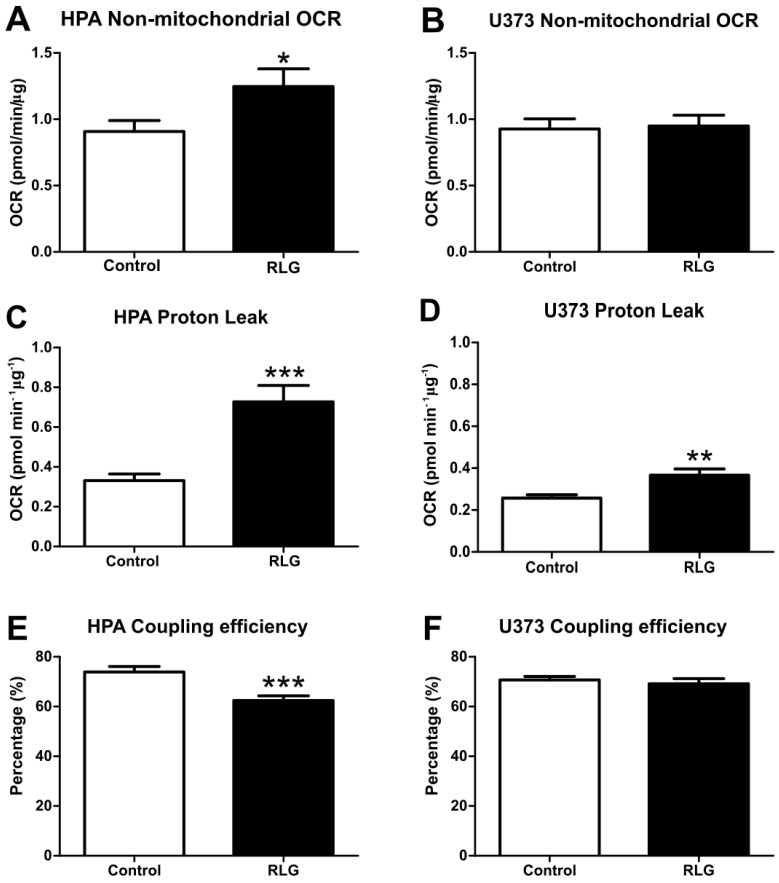

Figure 3.6.1.1. Recurrent low glucose (RLG) increases proton leak in human primary astrocytes (HPA) and U373 astrocytoma cells.

Oxygen consumption rate (OCR) of HPA during a mitochondrial stress test. **I**, **J**. Non-mitochondrial OCR determined after the addition of all inhibitors. **K**, **L**. Proton leak, calculated from the oligomycin-insensitive (i.e. not ATP-synthase linked) OCR minus non-mitochondrial respiration. **M**, **N**. Coupling efficiency calculated from the ratio of oligomycin sensitive OCR and basal OCR expressed as a percentage. *P<0.05; **P<0.01, ***P<0.001 vs control. Unpaired two-tailed student's t-test. Error bars represent standard error of the mean (SEM).

Figure 3.6.2

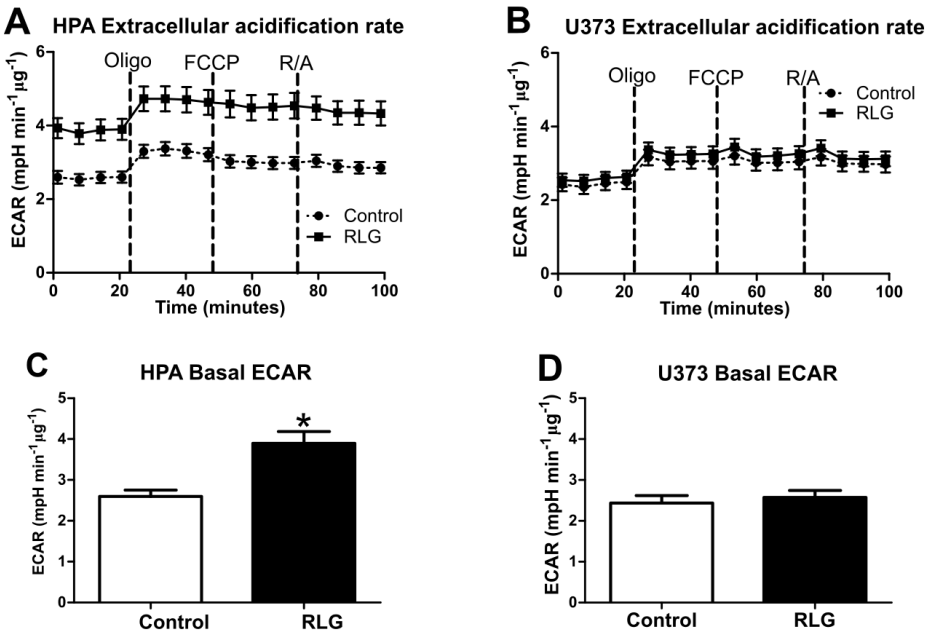

Figure 3.6.2. Recurrent low glucose (RLG) increases baseline extracellular acidification rates (ECAR) of human primary astrocytes (HPA) but not U373 astrocytoma cells.

ECAR of HPA (**A**; control group, n=36; RLG group, n=39, across three separate assays) and U373 cells (**B**) following RLG (control group, n=40; RLG group, n=43, across separate assays). Cells were exposed to oligomycin (10 µM), FCCP (5 µM) and a combination of rotenone and antimycin A (5 µM). **C**, **D**. Mean basal ECAR in control and RLG treated HPA and U373 cells respectively. *P<0.05 vs control. Unpaired two-tailed student's t-test. Error bars represent standard error of the mean (SEM).

3.7.1 RLG increases HPA fatty acid dependency

Inhibition of fatty acid uptake into the mitochondria using etomoxir to block CPT1a caused OCR to decrease in HPA cells. This response was significantly augmented in RLG treated HPA cells (figure 3.7.1A). The addition of BPTES and UK5099, to block glutamine and pyruvate usage by the mitochondria respectively, was used to maximally stimulate fatty acid utilisation. Fatty acid dependency was calculated by:

$$Fatty\ Acid\ Dependency\ (\%) = \left(\frac{Baseline\ OCR - Etomoxir\ Reduced\ OCR}{Baseline\ OCR - All\ inhibitors\ reduced\ OCR}\right) x\ 100$$

Fatty acid dependency was significantly higher in RLG compared to control (figure 3.7.1C). However, fatty acid capacity was not altered (figure 3.7.1D). FA capacity was calculated by:

$$Fatty\ Acid\ Capacity\ (\%) = \left(1 - \left(\frac{Baseline\ OCR - BPTES\ and\ UK5099\ reduced\ OCR}{Baseline\ OCR - All\ inhibitors\ reduced\ OCR}\right)\right) x\ 100$$

Fatty acid flexibility, the difference between dependency and capacity, was significantly reduced by RLG (figure 3.7.1E)

Figure 3.7.1

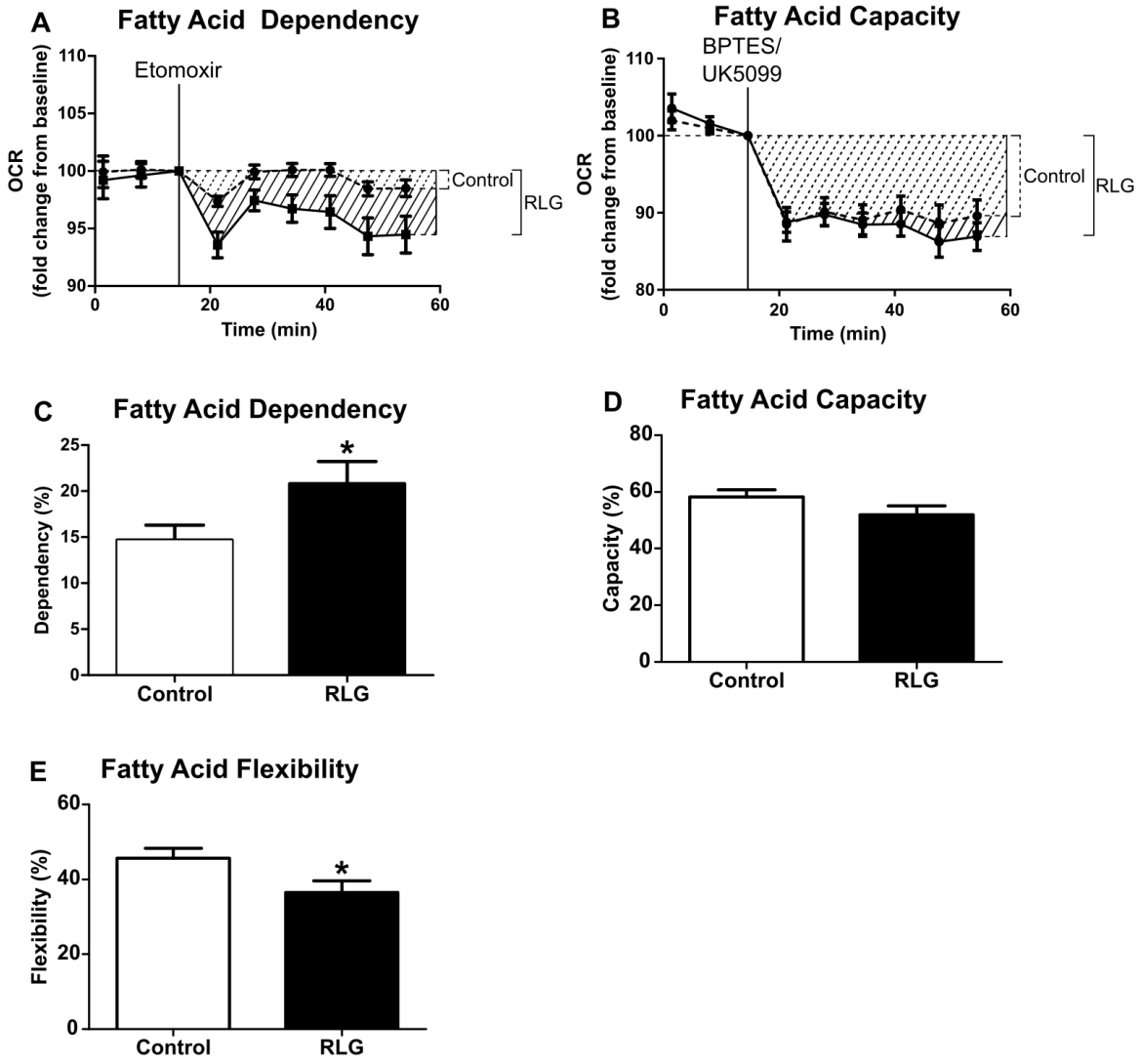

Figure 3.7.1. Recurrent low glucose (RLG) increases fatty acid (FA) dependency in human primary astrocytes (HPA).

A. The oxygen consumption rate (OCR) of HPA after RLG (control group, n=21; RLG group, 24) and the inhibition of carnitine palmitoyltransferase 1-α (CPT1-α) using etomoxir (4 μM) to measure changes in FA dependency. **B**. OCR following inhibition of mitochondrial pyruvate carrier and glutaminase using UK5099 (2 μM) and BPTES (3 μM) respectively to determine FA capacity. **C**. FA dependency, determined as its contribution to basal OCR, is increased by RLG. **D**. FA capacity, determined as its maximal contribution to OCR following inhibition of complete pyruvate and glutamine oxidation pathways, remains unchanged. **E**. FA flexibility, calculated as the difference between capacity and dependency, is decreased by RLG. *P<0.05 vs control. Unpaired two-tailed student's t-test. Error bars represent standard error of the mean (SEM).

3.7.2 RLG does not change the mitochondrial utilisation of pyruvate in HPA

Inhibition of pyruvate uptake into the mitochondria via mitochondrial pyruvate carrier (MPC) using UK5099 decreased OCR in HPA cells (figure 3.7.2A). The addition of etomoxir and BPTES, to block fatty acid and glutamine usage by the mitochondria respectively, was used to maximally stimulate fatty acid utilisation. While there was a decrease in OCR the remaining OCR was not different between control and RLG (figure 3.7.2B). Pyruvate dependency was calculated by:

$$Pyruvate\ Dependency\ (\%) = \left(\frac{Baseline\ OCR - UK5099\ \ Reduced\ OCR}{Baseline\ OCR - All\ inhibitors\ reduced\ OCR}\right) x\ 100$$

Pyruvate dependency (figure 3.7.2C) was not significantly different in RLG treated cells. Pyruvate capacity was unchanged by RLG (figure 3.7.2D), as calculated by:

$$Pyruvate\ Capacity\ (\%) = \left(1 - \left(\frac{Baseline\ OCR - BPTES\ and\ etomoxir\ reduced\ OCR}{Baseline\ OCR - All\ inhibitors\ reduced\ OCR}\right)\right) x\ 100$$

Pyruvate flexibility, the differences between dependency and capacity, was not significantly altered by RLG (figure 3.7.2E).

Figure 3.7.2

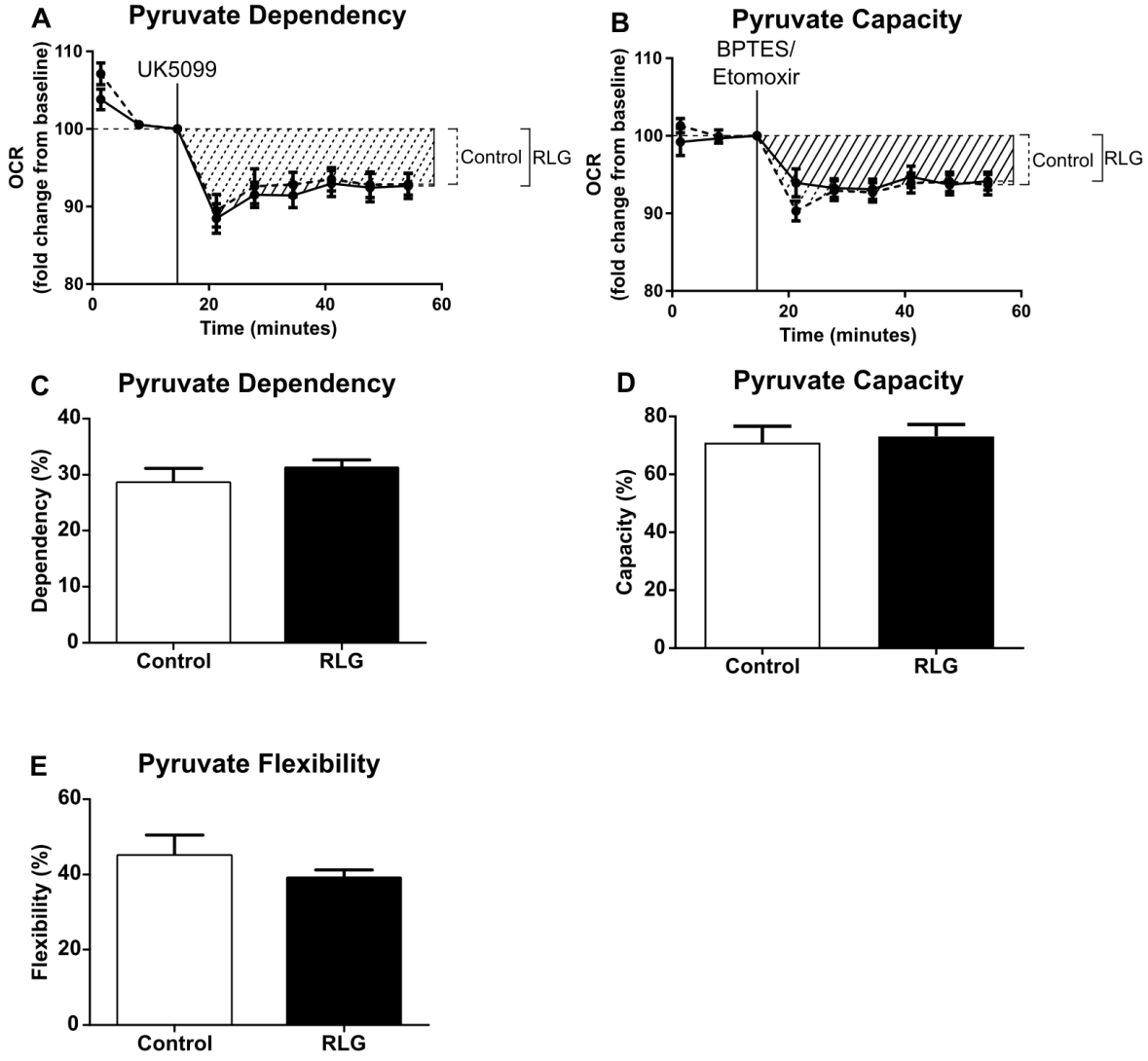

Figure 3.7.2. Recurrent low glucose (RLG) does not change pyruvate utilisation in human primary astrocytes (HPA).

A. The oxygen consumption rate (OCR) of HPA after RLG (control group, n=21; RLG group, 24) and the inhibition of mitochondrial pyruvate carrier using UK5099 (2 μM) to measure changes in pyruvate dependency. **B**. OCR following inhibition of carnitine palmitoyltransferase 1-α (CPT1-α) and glutaminase using etomoxir (4 μM) and BPTES (3 μM) respectively to determine pyruvate capacity. **C**. Pyr dependency, determined as its contribution to basal OCR, is unchanged. **D**. Pyruvate capacity, determined as its maximal contribution to OCR following inhibition of complete fatty acid and glutamine oxidation pathways, is unchanged. **E**. Pyruvate flexibility, calculated as the difference between capacity and dependency, is unchanged. Unpaired two-tailed student's t-test. Error bars represent standard error of the mean (SEM).

3.7.3 RLG increases HPA glutamine flexibility

Inhibition of glutamine usage by the mitochondria via glutaminase was blocked with the selective inhibitor BPTES. This caused a decrease in HPA OCR (figure 3.7.3A). The addition of UK5099 and etomoxir to inhibit pyruvate and fatty acid oxidation respectively was used to maximally stimulate glutamine utilisation (figure 3.7.3B). Fatty acid dependency was calculated by:

$$Glutamine\ Dependency\ (\%) = \left(\frac{Baseline\ OCR - BPTES\ \ Reduced\ OCR}{Baseline\ OCR - All\ inhibitors\ reduced\ OCR}\right)\ x\ 100$$

Neither glutamine dependency or capacity were significantly changed by RLG (figure 3.7.3C,D). Glutamine capacity was calculated by:

$$Glutamine\ Capacity\ (\%) = \left(1 - \left(\frac{Baseline\ OCR - UK5099\ and\ etomoxir\ reduced\ OCR}{Baseline\ OCR - All\ inhibitors\ reduced\ OCR}\right)\right)\ x\ 100$$

Due to a trending decrease in glutamine dependency but no change to glutamine capacity, this amounted to a significant increase in glutamine flexibility following RLG (figure 3.7.3E).

Figure 3.7.3

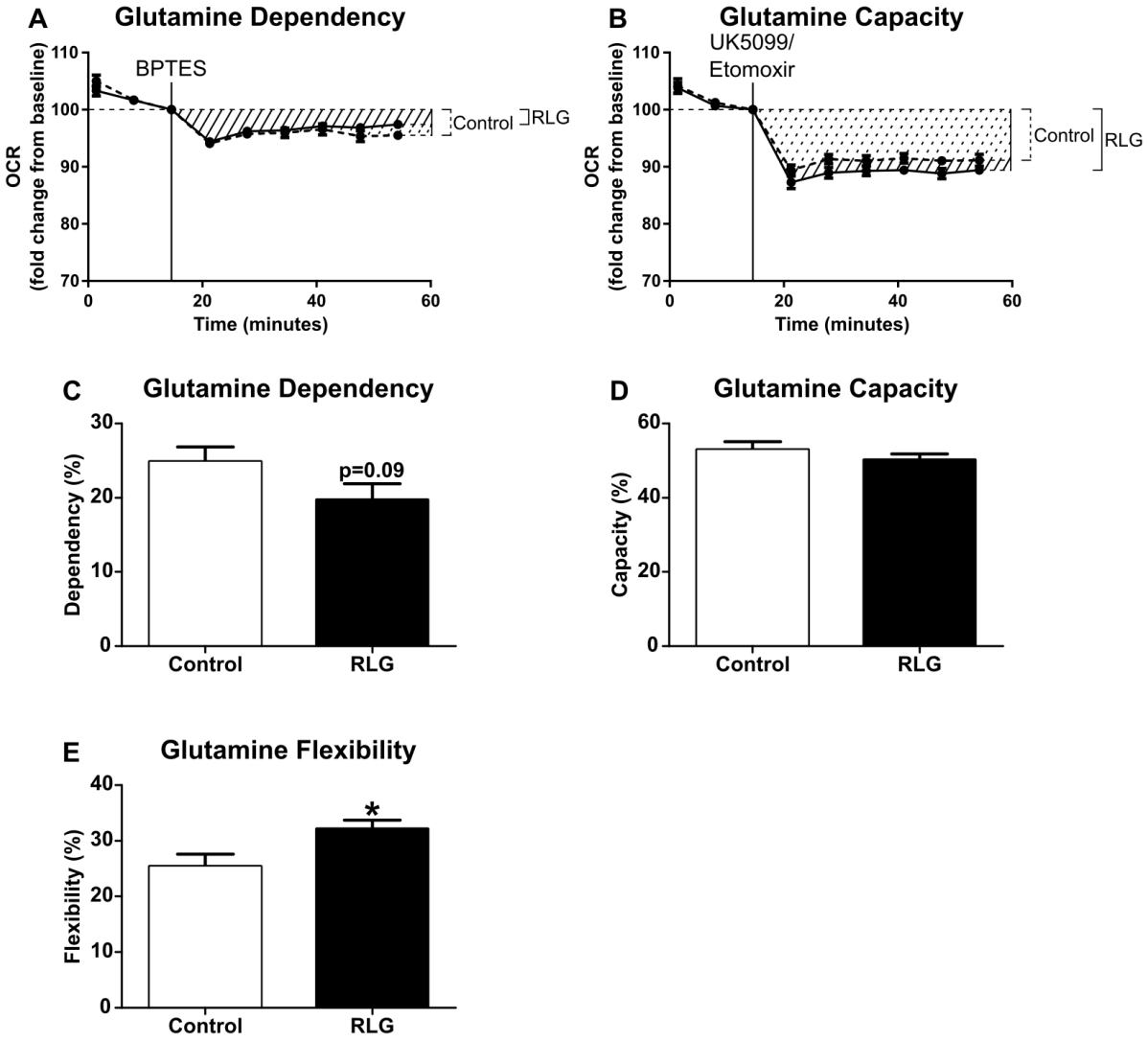

Figure 3.7.3. Recurrent low glucose (RLG) does not change glutamine utilisation in human primary astrocytes (HPA).

A. The oxygen consumption rate (OCR) of HPA after RLG (control group, n=21; RLG group, 24) and the inhibition of glutaminase using BPTES (3 μM) to measure changes in glutamine dependency. **B**. OCR following inhibition of carnitine palmitoyltransferase 1-α (CPT1-α) and mitochondrial pyruvate carrier using etomoxir (4 μM) and UK5099 (2 μM) respectively to determine glutamine capacity. **C**. Glutamine dependency, determined as its contribution to basal OCR, non-significantly trends to decrease with RLG. **D**. Glutamine capacity, determined as its maximal contribution to OCR following inhibition of complete fatty acid and glucose oxidation pathways, is unchanged by RLG. **E**. Glutamine flexibility, calculated as the difference between capacity and dependency, is increased by RLG. *P<0.05 vs control. Unpaired two-tailed student's t-test. Error bars represent standard error of the mean (SEM).

3.8 A comparison of basal mitochondrial substrate oxidation between HPA and U373 cells

HPA and U373 cells were noted to have different responses to the same stimuli. To discern the source of this variation a direct comparison of mitochondrial fuel utilisation was examined. HPA are primary cells and should be more reflective of the physiological state, whereas, U373 are cancerous cells. Cancer cells have fundamentally altered metabolic profile (Warburg et al. 1936). To evaluate the differences between cell types, a Mitochondrial Fuel Flex test was performed under basal conditions, containing 2.5 mM glucose. These experiments were completed by Julia Vlachaki-Walker and included for completion.

3.8.1 U373 cells are less dependent on and more flexible with fatty acid oxidation than HPA

As described previously, fatty acid dependency was measured by inhibition of CPT1a resulting in a decrease to basal OCR (figure 3.8.1A). Fatty acid dependency was significantly lower in U373 cells compared to HPAs (figure 3.8.1C). Addition of UK5099 and BPTES were used to block pyruvate and glutamine utilisation allowing for fatty acid capacity to be calculated (figure 3.8.1B). Fatty acid capacity was not significantly different between cell types (figure 3.8.1 D). As there was no change in fatty acid capacity but there was a large decrease in dependency, U373 cells had a higher fatty acid flexibility compared to HPA (figure 3.8.1 E).

Figure 3.8.1

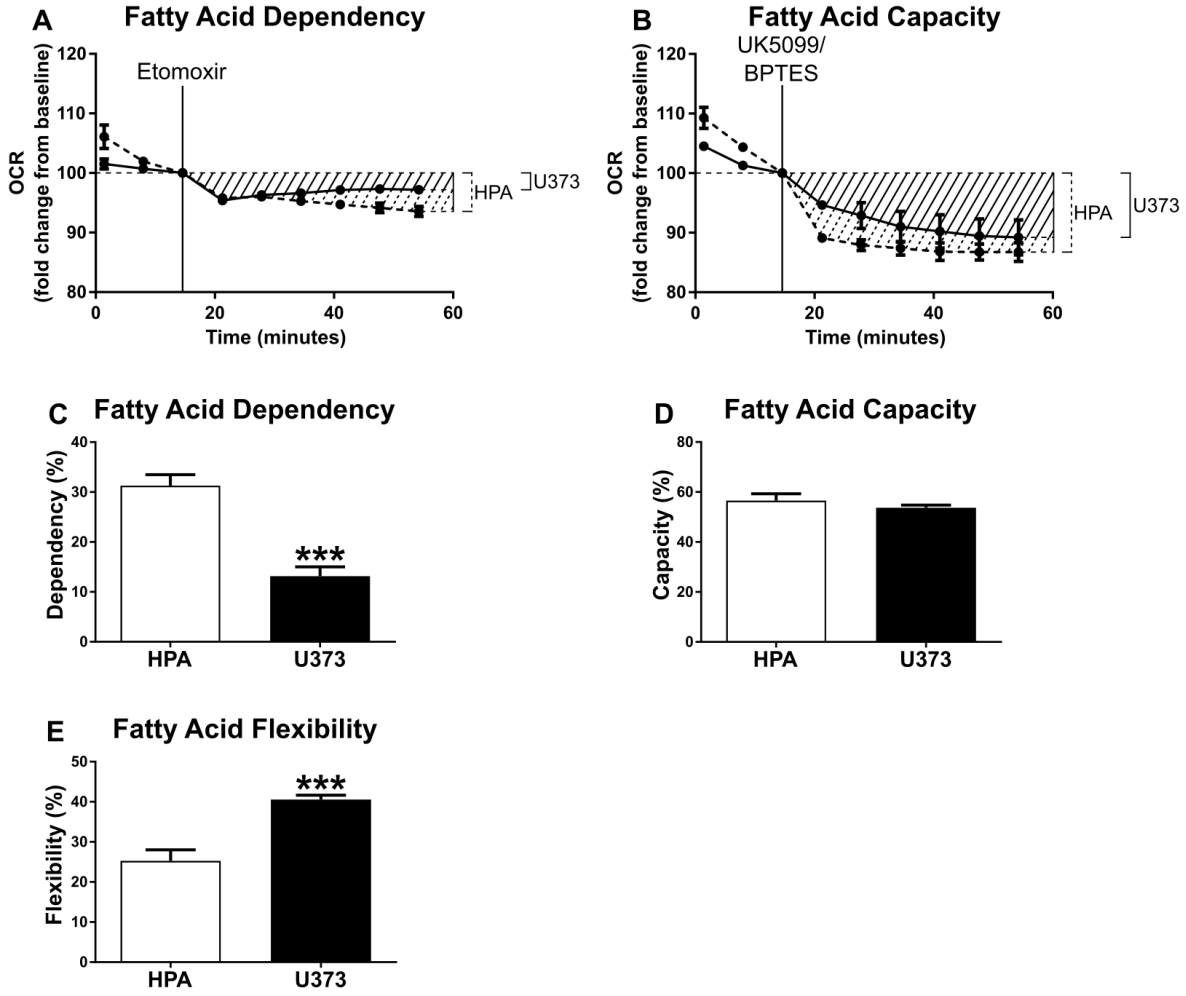

Figure 3.8.1. U373 astrocytoma cells are less dependent on fatty acid (FA) oxidation than human primary astrocytes (HPA).

A. The oxygen consumption rate (OCR) of HPA and U373 cells after the inhibition of carnitine palmitoyltransferase 1-α (CPT1-α) using etomoxir (4 μM) to measure changes in FA dependency. **B**. OCR following inhibition mitochondrial pyruvate carrier and glutaminase using UK5099 (2 μM) and BPTES (3 μM) respectively to determine FA capacity. **C**. FA dependency, determined as its contribution to basal OCR, is lower in U373 cells (n=20). **D**. FA capacity, determined as its maximal contribution to OCR following inhibition of complete pyruvate and glutamine oxidation pathways, is not significantly different between cell types (n=19). **E**. FA flexibility, calculated as the difference between capacity and dependency, is higher in U373 cells (n=19). ***P<0.001 vs control. Unpaired two-tailed student's t-test. Error bars represent standard error of the mean (SEM).

3.8.2 U373 cells are less dependent on pyruvate than HPA

As previously described pyruvate dependency was measured by blocking the MPC with UK5099 which resulted in OCR to decrease (figure 3.8.2A). Pyruvate dependency was significantly lower in the U373 cells compared to HPAs (figure 3.8.2C). Pyruvate capacity was measured by blocking glutamine and fatty acid utilisation with BPTES and etomoxir respectively, decreasing OCR (figure 3.8.2B). Pyruvate capacity and flexibility were not significantly different between cell types (figure 3.8.2D,E).

3.8.3 U373 cells have a higher capacity and flexibility to oxidise glutamine than HPA

As discussed previously glutamine dependency is determined by the addition of BPTES decreasing OCR by inhibiting glutaminase (figure 3.8.3A). Glutamine dependency was not significantly different between cell types (figure 3.8.3C). Glutamine capacity was determined by the inhibition of mitochondrial fatty acid and pyruvate uptake using etomoxir and UK5099 respectively, decreasing OCR (figure 3.8.3B). Glutamine capacity was significantly higher in U373 cells (figure 3.8.3D). Glutamine flexibility, the difference between dependency and capacity, was significantly higher in U373 cells than HPA (figure 3.8.3E)

Figure 3.8.2

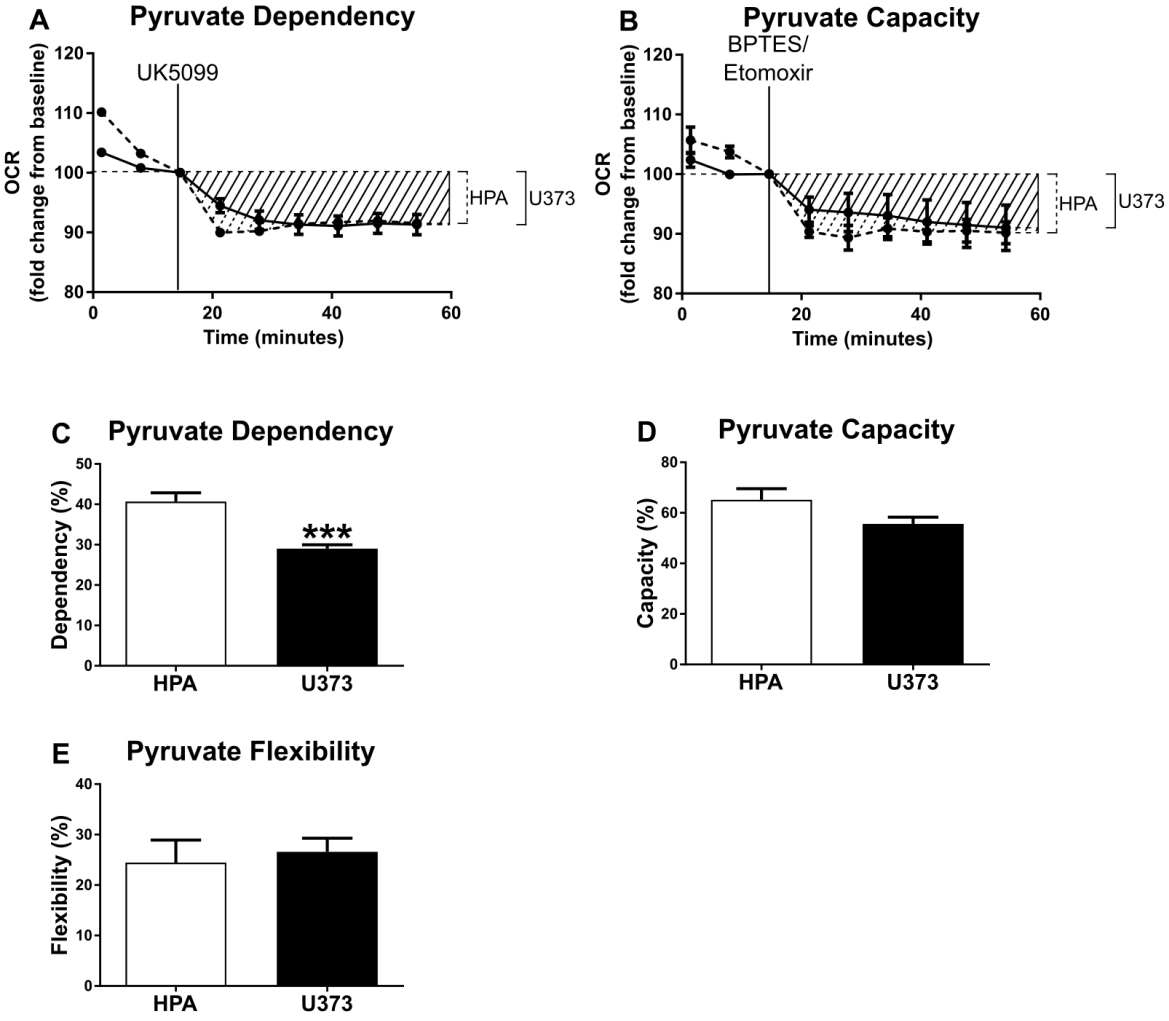

Figure 3.8.2. Fuel flex test U373 astrocytoma cells are less dependent on pyruvate oxidation than human primary astrocytes (HPA).

A. The oxygen consumption rate (OCR) of HPA and U373 cells after the inhibition of mitochondrial pyruvate carrier using UK5099 (2 μM) to measure changes in pyruvate dependency. **B**. OCR following inhibition carnitine palmitoyltransferase 1-α (CPT1-α) and glutaminase using etomoxir (4 μM) and BPTES (3 μM) respectively to determine pyruvate capacity. **C**. Pyruvate dependency, determined as its contribution to basal OCR, is lower in U373 cells (HPA n=22; U373 n=21). **D**. Pyruvate capacity, determined as its maximal contribution to OCR following inhibition of complete fatty acid and glutamine oxidation pathways, is unchanged (HPA n=16; U373 n=18). **E**. Pyruvate flexibility, calculated as the difference between capacity and dependency, is unchanged (HPA n=15; U373 n=18). ***P<0.001 vs control. Unpaired two-tailed student's t-test. Error bars represent standard error of the mean (SEM).

Figure 3.8.3

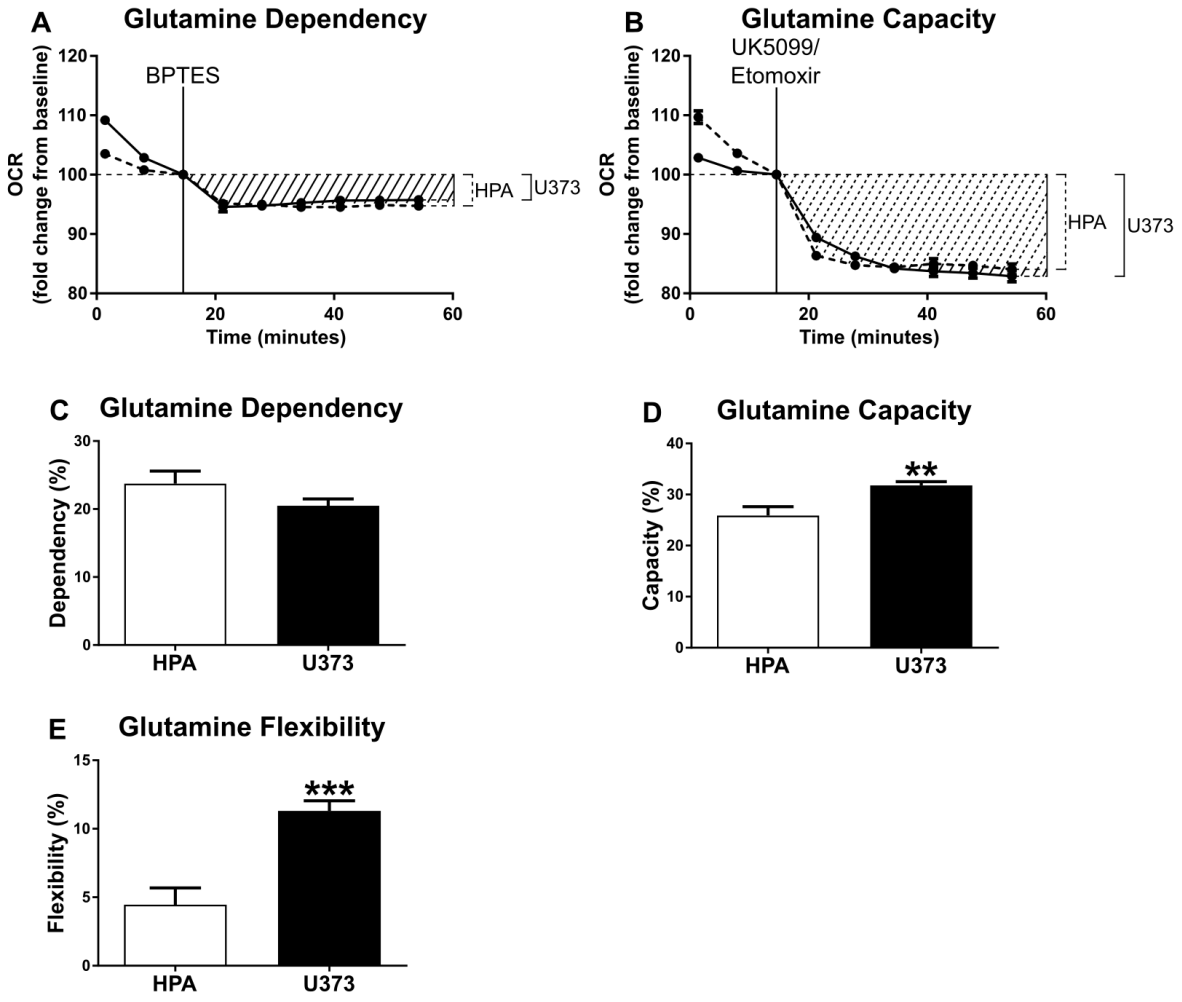

Figure 3.8.3 Fuel flex test U373 astrocytoma cells have a higher glutamine oxidation capacity than human primary astrocytes (HPA).

A. The oxygen consumption rate (OCR) of HPA and U373 cells after the inhibition of glutaminase (3 μM) to measure changes in glutamine dependency. **B**. OCR following inhibition of carnitine palmitoyltransferase 1-α (CPT1-α) and mitochondrial pyruvate carrier using etomoxir (4 μM) and UK5099 (2 μM) respectively to determine glutamine capacity. **C**. Glutamine dependency, determined as its contribution to basal OCR, is not significantly different between cell types (HPA n=19; U373 n=20). **D**. Glutamine capacity, determined as its maximal contribution to OCR following inhibition of complete fatty acid and glucose oxidation pathways, is higher in U373 cells (n=23). **E**. Glutamine flexibility, calculated as the difference between capacity and dependency, is higher in U373 cells (n=23). **P<0.01; ***P<0.01 vs control. Unpaired two-tailed student's t-test. Error bars represent standard error of the mean (SEM).

3.9 RLG does not alter HPA mitochondrial enzyme expression

To investigate why mitochondrial metabolism was altered, total levels of mitochondrial proteins were assessed after RLG treatment. Succinate dehydrogenase (SDHa; figure 3.9A), voltage-dependent anion channel (VDAC; figure 3.9B), fatty acid synthase (FAS; figure 3.9C), and carnitine palmitoyltransferase-α (CPT1α; figure 3.9D) expression was measured and RLG treated cells were not significantly different from control treated cells. This suggests that total mitochondrial content is not altered following RLG.

3.10 Acute and RLG does not alter HPA mitochondrial number or length.

Given substantial alterations to mitochondrial function and activity being induced by RLG, mitochondrial morphology was examined using mitotracker DsRed. Interestingly, no significant differences were found between treatments (figure 3.10A,B), indicating that differences in mitochondrial activity are not caused by changes in the mitochondrial filamentous network.

3.11 Recovery from low glucose increases glycolysis and is enhanced following RLG in HPA

Given that there was an increase in basal ECAR in HPA cells, the effects of glucose reperfusion following RLG were examined. On the day of the study, cells were acutely incubated in glucose-free medium to examine the effect of glucose reperfusion. ECAR and OCR were measured during the addition of 0.5, 2.5 and 5.5 mM glucose.

Figure 3.9

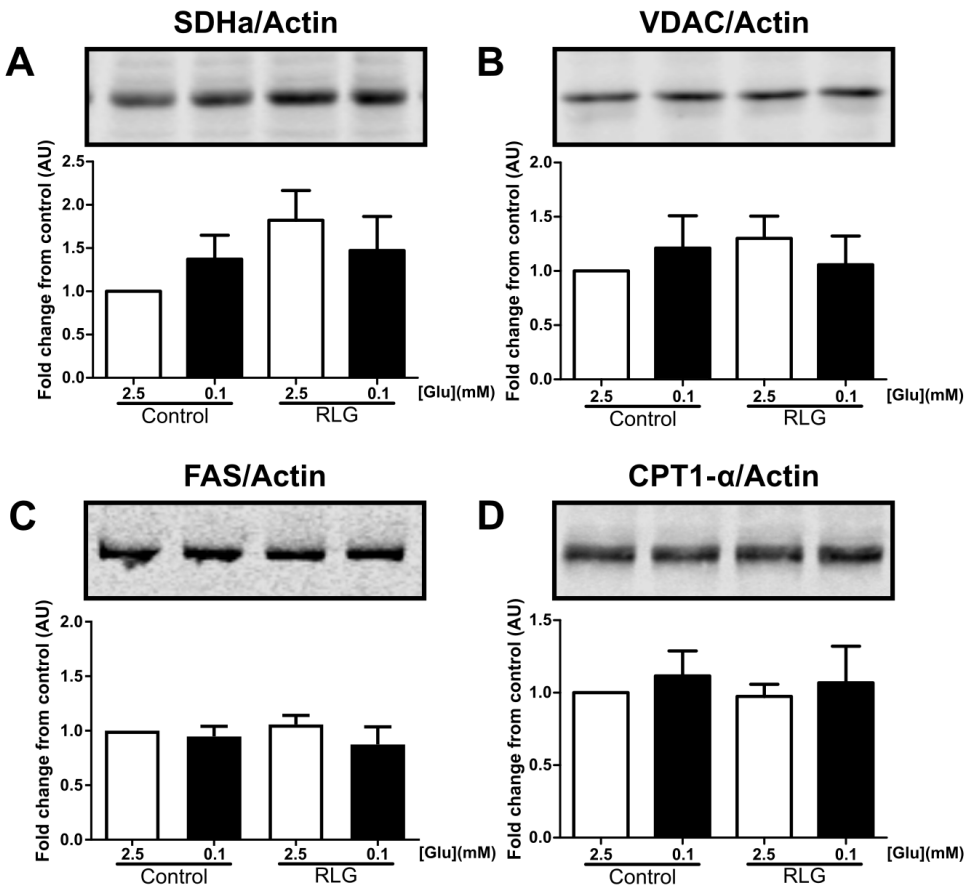

Figure 3.9. Expression of key mitochondrial markers are not altered by acute or recurrent low glucose exposure (RLG) in human primary astrocytes (HPA).

Representative immunoblots and densitometric analysis from HPA cells exposed to 2.5 or 0.1 mM glucose for 3 hours following control or RLG and probed for succinate dehydrogenase-a (**A**; SDHa), voltage dependent anion channel (**B**; VDAC), fatty acid synthase (**C**; FAS) carnitine palmitoyltransferase 1-α (**D**; CPT1-α) were not altered by acute or recurrent low glucose exposure (n=3-4). Error bars represent standard error of the mean (SEM). One-way ANOVA with one-sample t-tests in comparison to control.

Figure 3.10

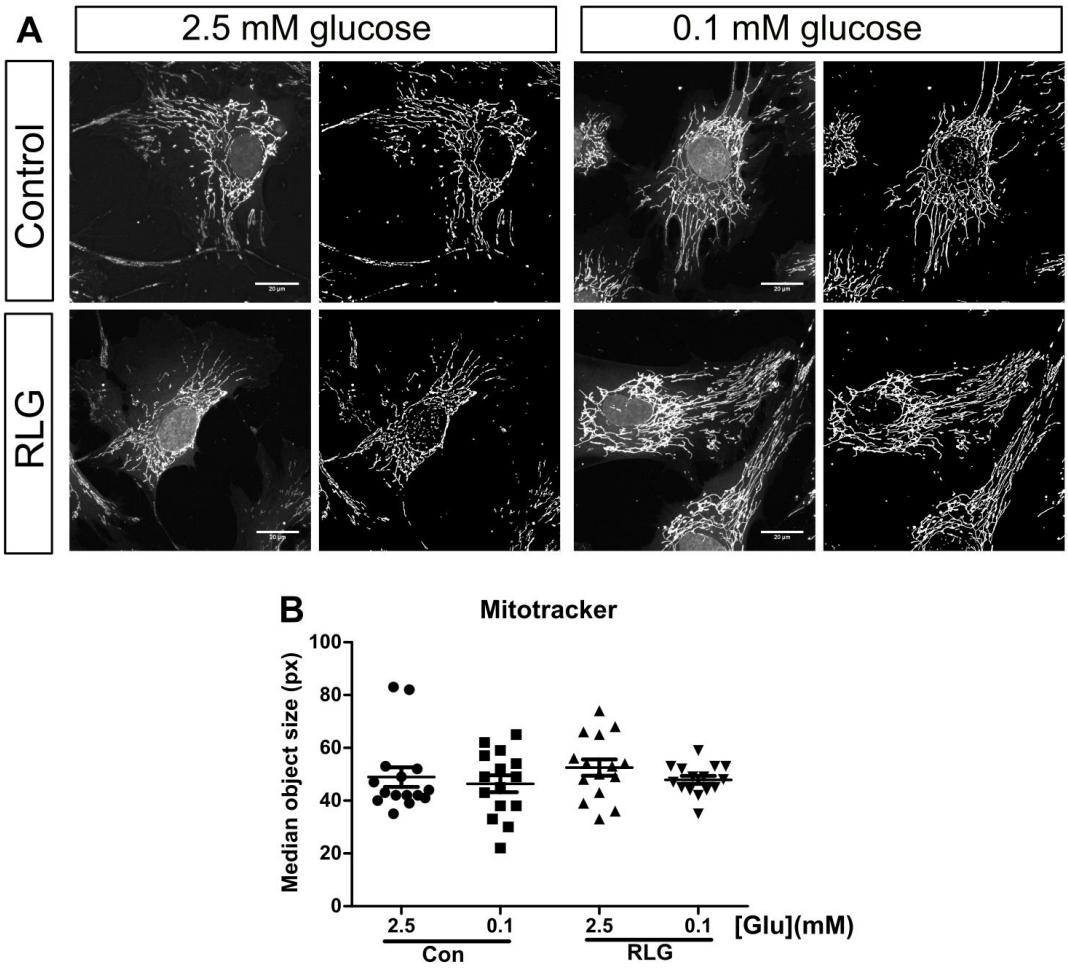

Figure 3.10. Acute and recurrent low glucose (RLG) does not alter human primary astrocyte (HPA) mitochondrial number or length.

A. Representative confocal images of HPA exposed to 2.5 or 0.1 mM glucose for 3 hours following control or RLG. Raw confocal images are shown on the left hand side, with extracted signal images shown on the right. **B**. Quantification of median object size (in pixels) using a custom MatLab script (15 images across 3 separate experiments). Error bars represent standard error of the mean (SEM). Scale bar is 20 μm.

3.11.1 RLG augments activation of ECAR and reduction of OCR during glucose reperfusion in HPA

Glucose reperfusion increased ECAR which was larger in 2.5 and 5.5 compared to 0.5 mM glucose (figure 3.11.1A-C). Interestingly, there was a corresponding decrease in OCR as cellular metabolism shifts from oxidative phosphorylation towards glycolysis, like the Warburg effect where cells have elevated glycolytic activity in the presence of ample oxygen (3.11.1D-F) (Warburg et al. 1936). In RLG treated cells, the increase in ECAR and decrease in OCR was enhanced at 2.5 mM and 5.5 mM glucose (3.11.1A-F). These results are consistent with increased basal ECAR following RLG and show an enhanced Warburg-like effect.

3.11.2 RLG does not affect ECAR or OCR during glucose reperfusion in U373 cells

Next, glycolytic re-activation after control or RLG treatment and complete glucose withdrawal in U373 cells was examined. Interestingly, ECAR and OCR changed equally in all glucose concentrations used in both control or RLG pre-treated cells (figure 3.11.2 A-F). Unlike in HPA cells, RLG did not augment ECAR or OCR in response to glucose reperfusion.

Figure 3.11.1

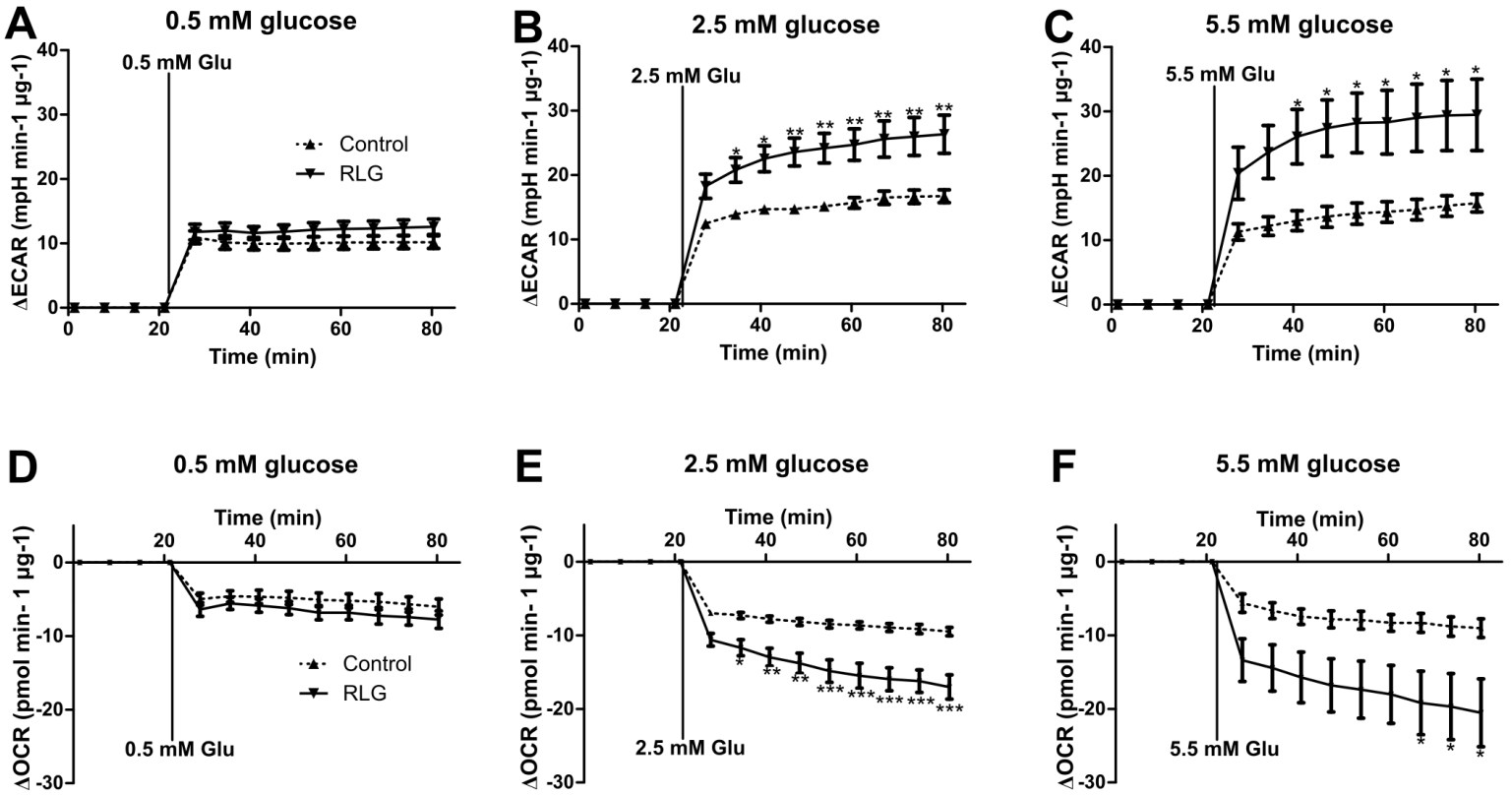

Figure 3.11.1. Recurrent low glucose (RLG) increases glycolytic re-activation after acute low glucose exposure in human primary astrocytes (HPA).

Extracellular acidification rate (ECAR) increased in HPA cells after control or RLG on re-introduction of 0.5 mM glucose (**A**), 2.5 mM glucose (**B**) and 5.5 mM glucose (**C**). Oxygen consumption rate (OCR) decreased on addition of 0.5 mM glucose (**D**), 2.5 mM glucose (**E**) and 5.5 mM glucose (**F**). *P<0.05; **P<0.01; ***P<0.001 (control group, n=8-10; RLG group, n=9-10). Two-way ANOVA with post hoc Bonferroni multiple comparisons tests. Error bars represent standard error of the mean (SEM).

Figure 3.11.2

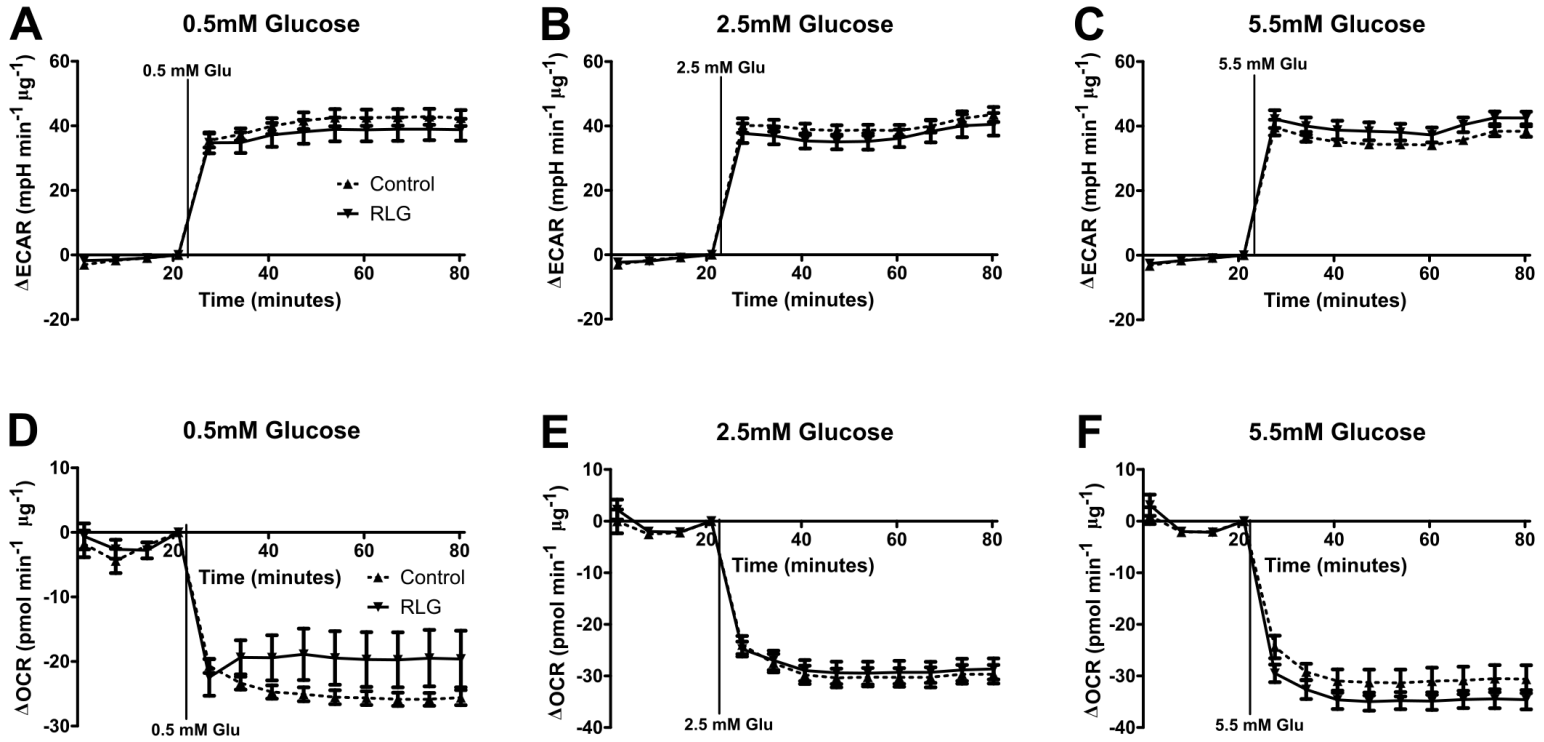

Figure 3.11.2. Recurrent low glucose (RLG) does not alter glycolytic re-activation after acute low glucose exposure in U373 cells.

Extracellular acidification rates (ECAR) increased in U373 cells after control or RLG on re-introduction of 0.5 mM glucose (**A**), 2.5 mM glucose (**B**) and 5.5 mM glucose (**C**) although this was not significantly different between control and recurrent low glucose (RLG) treated cells. Oxygen consumption rate (OCR) decreased on addition of 0.5 mM glucose (**D**), 2.5 mM glucose (**E**) and 5.5 mM glucose (**F**), which was not significantly different between control and RLG (control group, n=10-12; RLG group, n=9-11). Two-way ANOVA with post hoc Bonferroni multiple comparisons tests. Error bars represent standard error of the mean (SEM).

3.12 Prior RLG does not alter 6-NBDG uptake by human primary astrocytes HPA

To test whether RLG-induced changes to ECAR were due to enhanced glucose uptake, the non-hydrolysable fluorescent dye, 6-NBDG, which enters the cell by glucose transporters, was used. HPA cells were treated to control or RLG and then assayed in 2.5 mM glucose. There was no significant difference in 6-NBDG uptake between control and RLG treated cells (figure 3.12A). This suggests the changes to ECAR are not due to increased glucose uptake.

3.13 RLG does not alter glycogen storage in HPA or U373 astrocytoma cells

Astrocytes are the primary source of glycogen in the CNS (Maxwell et al. 1965, Cataldo et al. 1986, Oe et al. 2016). This can be utilised to buffer energy supply during external energy deprivation. Glycogen content has been speculated to super-compensate following RH which leads to blunting of CRR (Cryer 2005). Therefore, human astrocytes' glycogen content was measured after prior treatment to control or RLG in 2.5 mM glucose. No significant differences were found between control and prior RLG in HPA (figure 3.13A) or U373 (figure 3.13B).

3.14 HPA glycolytic pathway component expression is unchanged by RLG

As alterations to ECAR were found after RLG, key components of the glycolytic pathway were investigated. No significant differences were found in the expression of glucose transporter-1 (Glut-1; figure 3.14A), hexokinase 1 (HKI; figure 3.14B), hexokinase 2 (HKII; figure 3.14C), hexokinase 3 (HKIII; figure 3.14D), phosphofructokinase, platelet (PFK(P); figure 3.14E), or pyruvate kinase M2 (PKM2; figure 3.14F).

Figure 3.12

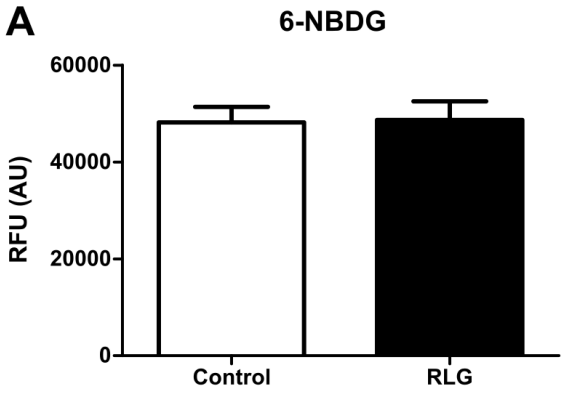

Figure 3.12. Prior recurrent low glucose (RLG) does not alter 6-(N-(7-Nitrobenz-2-oxa-1,3-diazol-4-yl)amino)-6-Deoxyglucose (6-NBDG) uptake by human primary astrocytes (HPA).

A. Fluorescent signal from labelled glucose analogue 6-NBDG incubated with HPA cells for 15 minutes remains unchanged after control or RLG conditions (n=7). Error bars represent standard error of the mean (SEM).

Figure 3.13

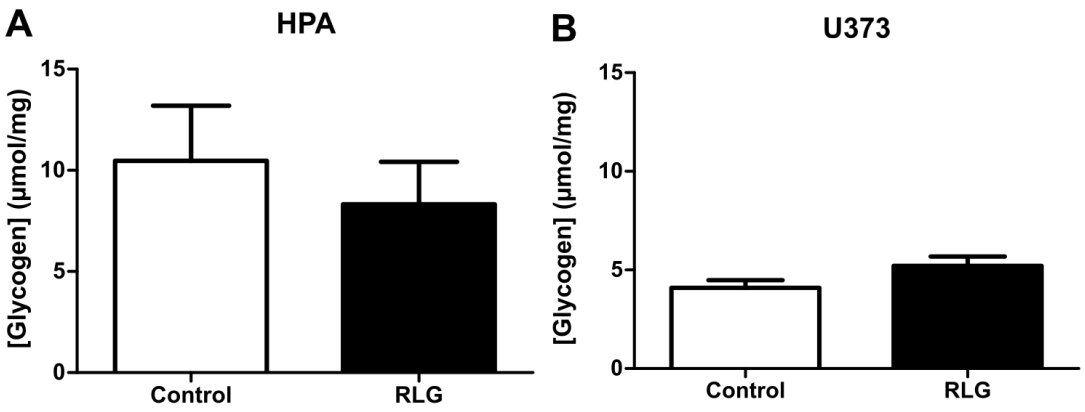

Figure 3.13. Recurrent low glucose (RLG) does not alter glycogen storage in human primary astrocytes (HPA) or U373 astrocytoma cells.

Glycogen content of HPA (**A**; n=5) and U373 (**B**; n=5) after control or RLG. Error bars represent standard error of the mean (SEM).

3.15 Maintenance of total ATP and ATP:ADP ratios by HPA and U373 astrocytoma cells during acute and RLG

The effect of low glucose on intracellular energy levels was determined by measuring total ATP (tATP) as well as the ratio of ATP:ADP. HPA and U373 were exposed to RLG with and without a further exposure to 0.1 mM glucose for 15, 30 and 180 minutes. Even after 180 minutes, there were no significant changes to tATP or ATP:ADP within the HPAs (figure 3.15A,C) and U373s (figure 3.15B,D). Similarly, the basal ratios between control and RLG were not changed.

3.16 Acute low glucose exposure alters lactate release in HPA

Astrocytes are thought to provide lactate to neurons during either situation of high ATP demand (e.g. high synaptic activity), or during metabolic stress (e.g. hypoglycaemia) (Pellerin et al. 1994, Pellerin et al. 1998, Pellerin 2003). To investigate whether lactate released from HPA cells was altered by low glucose the cells were cultured in medium containing 2.5 or 0.1 mM glucose for 30 minutes. While there was no significant change to lactate levels, however, if the 25-fold reduction in glucose concentration is considered there is a large relative increase in lactate released (figure 3.16A-B). This suggests that HPAs may respond to low glucose by maintaining lactate release.

Figure 3.14

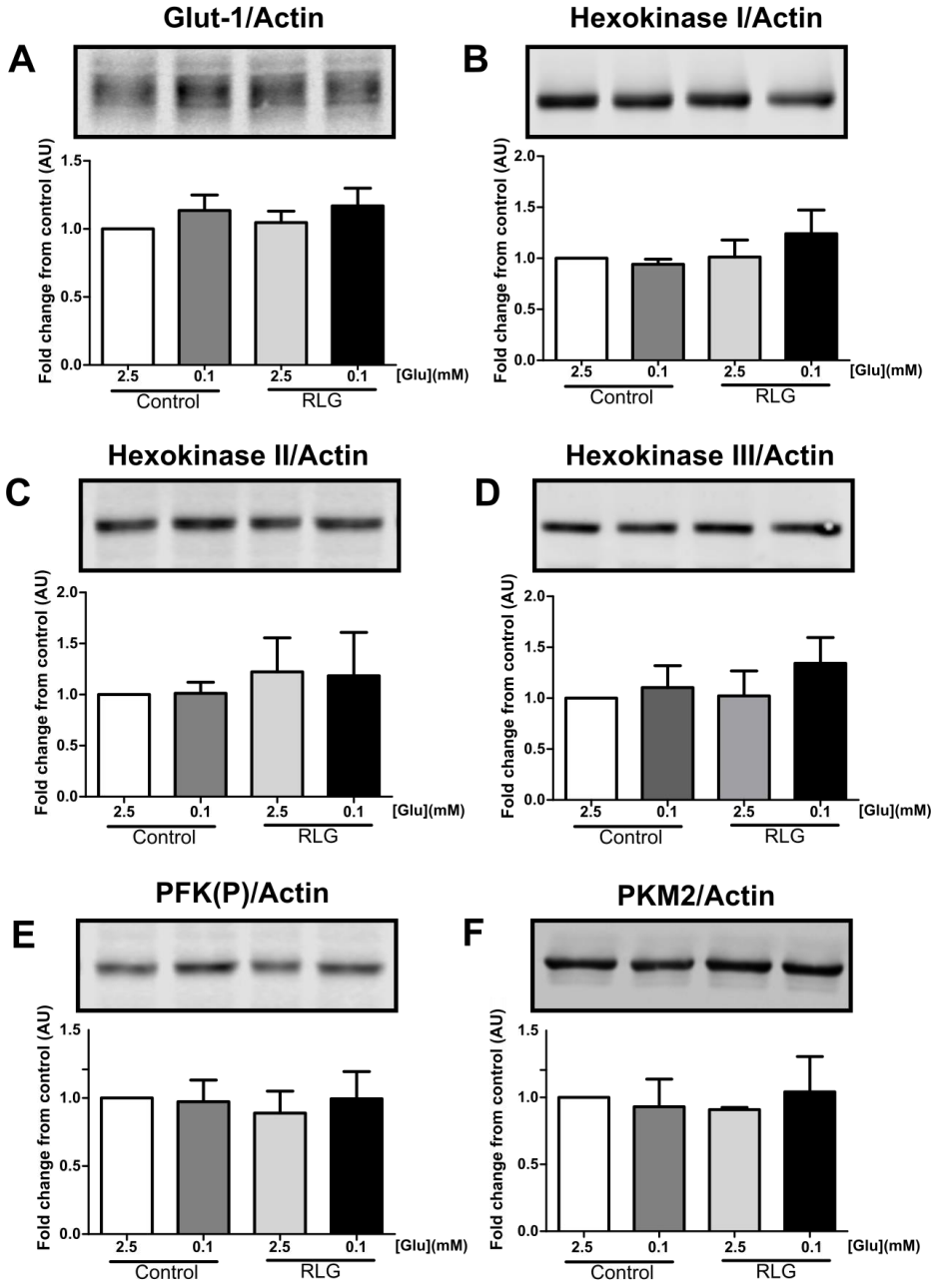

Figure 3.14. Expression of key glycolytic markers are not altered by acute or recurrent low glucose exposure (RLG) in human primary astrocytes (HPA).

Representative immunoblots and densitometric analysis from HPA cells exposed to 2.5 or 0.1 mM glucose for 3 hours following control or RLG and probed for glucose transporter 1 (**A**; GLUT-1), hexokinase I (**B**; HKI), hexokinase II (**C**; HKII), hexokinase III (**D**; HKIII), phosphofructokinase-platelet (**E**; PFK(P), and pyruvate kinase M2 (**F**; PKM2) were not altered by acute or recurrent low glucose exposure (n=3-4). Error bars represent standard error of the mean (SEM).

Figure 3.15

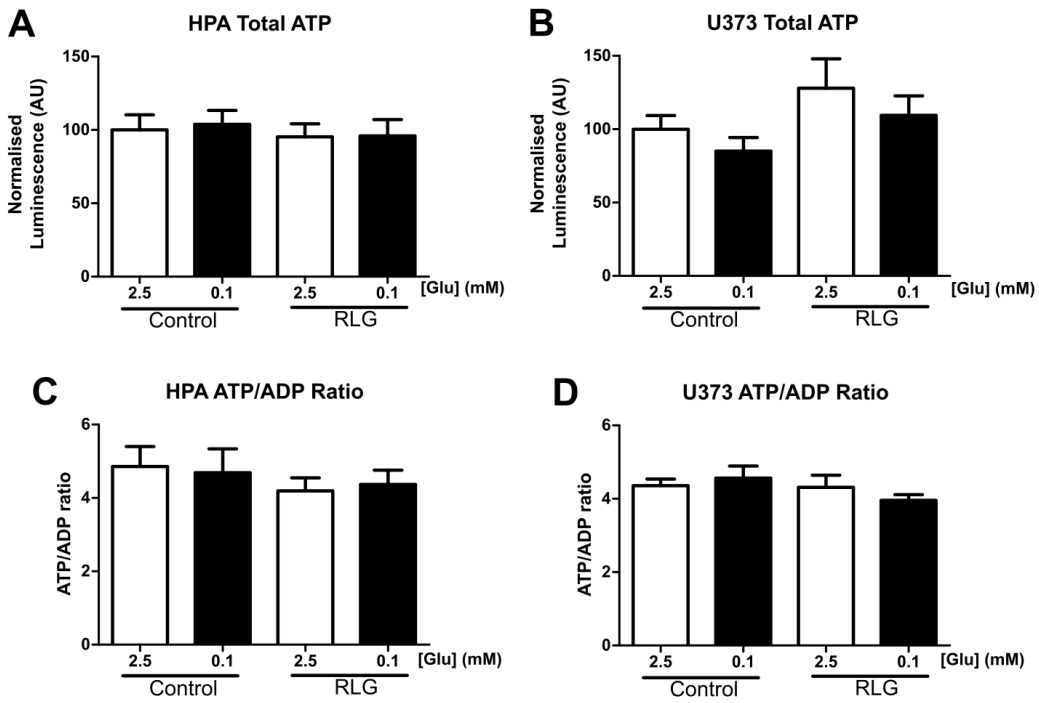

Figure 3.15. Acute and recurrent low glucose (RLG) does not modify intracellular ATP and ATP/ADP ratios in human primary astrocytes (HPA) and U373 astrocytoma cells.

Total intracellular ATP levels in human primary astrocytes (HPA; **A**, n=6) and U373 astrocytoma cells (**B**; n=6) exposed to 2.5 or 0.1 mM glucose for 3 hours after control or RLG. Intracellular ATP/ ADP ratios in HPA (**C**; n=6) and U373 astrocytoma cells (**D**; n=4) exposed to 2.5 or 0.1 mM glucose for 3 hours after control or RLG. Error bars represent standard error of the mean (SEM).

3.17 The effect of prior RLG on lactate release from HPA and U373 astrocytoma cells during 3 hours of 2.5 or 0.1 mM glucose

To test whether RLG exposure modulated lactate release from astrocytes HPA and U373 cells were exposed to RLG and lactate was measured in the conditioned media. Interestingly, 0.1 mM glucose resulted in an absolute decrease in lactate concentrations within the medium compared to 2.5 mM. However, RLG did not alter the change in lactate concentrations in 0.1 mM glucose, compared to control pre-treated cells treated to 2.5 mM glucose (figure 3.17A,B). However, if the 25-fold reduction in glucose concentration is considered there is a large relative increase in lactate released (figure 3.17C,D). It is important to note that the length of treatment for this study was 3 hours rather than 30 minutes as in figure 3.16.

3.18 RLG reduces HPA PPP activity

As ECAR was increased by RLG but there were no changes to glucose uptake, glycogen content, or the expression of glycolytic enzymes, an alternative metabolic pathway for glucose was investigated. The PPP is in parallel to glycolysis, separating when glucose-6-phosphate (G6P) is converted by rate-limiting enzyme G6P dehydrogenase to phosphogluconolactone. The PPP is a major source of cellular NADPH that is vital for antioxidant defence mechanisms (Takahashi et al. 2012, Stincone et al. 2015). As the PPP requires glucose, it is upregulated in neurons and astrocytes in response to high glucose *in vitro* (Takahashi et al. 2012), it was speculated that there would be a decrease in PPP activity in low glucose. To test this, 6-aminonicotinamide (6-AN), a G6P dehydrogenase inhibitor, was added to cells at 250, and 500 µM for 16 hours. Basal OCR and ECAR were then measured for 60 minutes after a 20-minute equilibration period in 2.5 mM glucose. The anticipated outcome of inhibiting PPP would be decreased ECAR and increased OCR, as glucose could undergo complete oxidation by the mitochondria. Therefore if the response is augmented by RLG it would suggest increased PPP activity. Interestingly, RLG augmented the 6-AN-dependent increase to OCR at 250 µM in comparison to control, but this was not seen with 500 µM (figure 3.18A). Conversely, RLG did not affect the decrease in ECAR caused by 6-AN at either 250 or 500 µM (figure 3.18B). Taken together these results indicate that PPP activity was increased, contradicting our original hypothesis.

3.19 Maintaining glucose levels following RLG partially recovers metabolic adaptations in HPA

It has previously been shown that strict avoidance of hypoglycaemia restores hypoglycaemia awareness in those with T1DM (Cryer 1994). To test whether the metabolic adaptations made by HPA cells could be recovered, HPAs were exposed to RLG with an additional 4-day recovery period. In this period cells were maintained in 5.5 mM glucose for 19 hours and 2.5 mM glucose for a total of 5 hours. Cells were incubated overnight in 5.5 mM glucose to provide sufficient glucose such that the glucose did not fall sufficiently below 2.5 mM glucose. To assess changes to metabolism, increased basal OCR, basal ECAR, proton leak, and decreased coupling efficiency, a mitochondrial stress test was performed on control, RLG or RLG with recovery treated cells. Basal OCR was elevated following RLG, whereas OCR after the recovery period was comparable to control (figure 3.19A,B). However, coupling efficiency was still reduced (figure 3.19C) and proton leak, while trending towards recovery, did not reach statistical significance (figure 3.19D). The increase to basal ECAR following RLG remained unchanged by a recovery period (figure 3.19E,F). Taken together these data show that while basal OCR can be restored by a recovery period, basal ECAR and coupling efficiency remain altered in HPA cells.

Figure 3.16

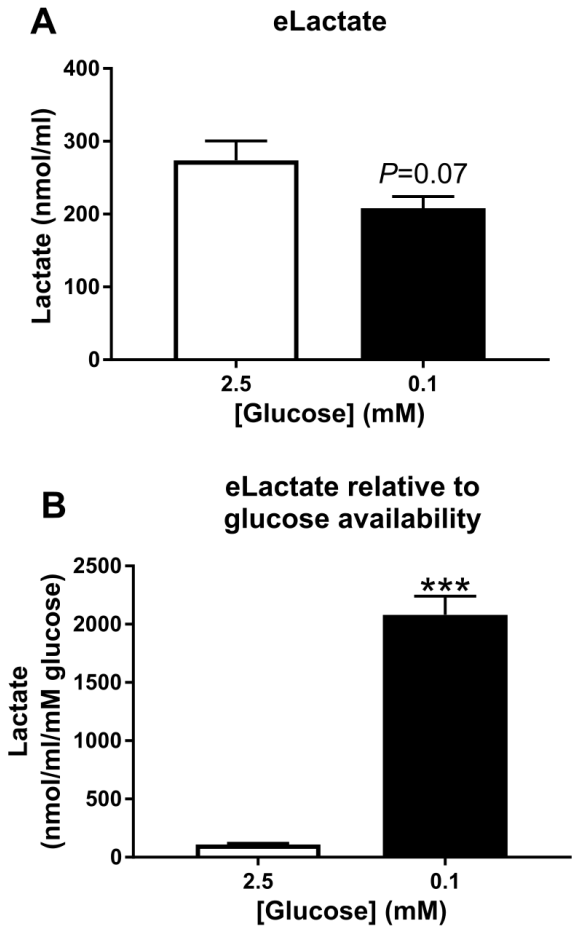

Figure 3.16. Acute low glucose exposure to human primary astrocytes (HPA) alters lactate release.

A. HPAs were exposed to media containing 2.5 (n=7) or 0.1 (n=6) mM glucose supplemented with 1% FBS and 22.5 or 24.9 mM mannitol for 30 minutes. The conditioned media was assayed for lactate content. **B**. Extracellular lactate content was normalised to the amount of glucose available in the media, the 25-fold reduction in glucose in the low glucose group results in a significantly, relative, increase in lactate release. ***P<0.001 vs control. Two-tailed unpaired student's t-test. Error bars represent standard error of the mean (SEM).

Figure 3.17

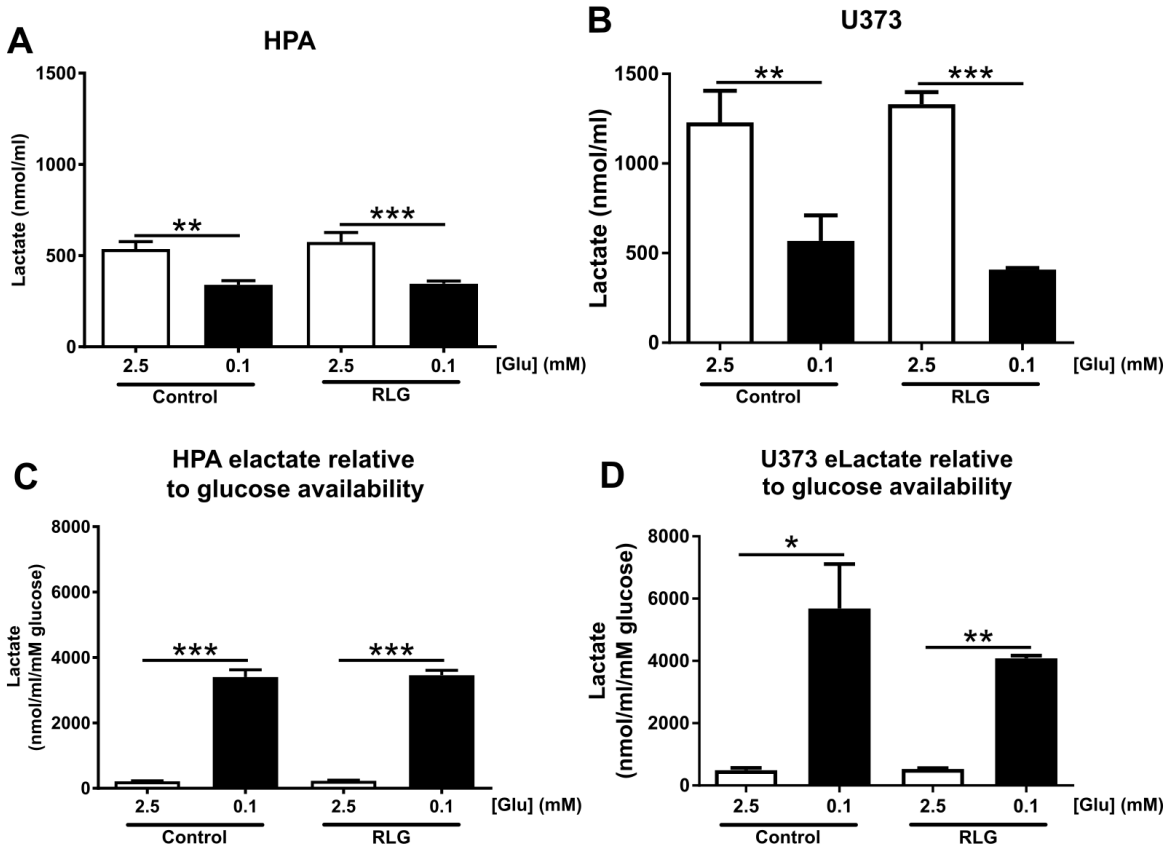

Figure 3.17. The effect of prior recurrent low glucose (RLG) on lactate release from human primary astrocyte (HPA) and U373 astrocytoma cells during 3 hours of 2.5 or 0.1 mM glucose.

Extracellular lactate levels measured from conditioned media from human primary astrocytes (HPA; **A**; n=8) and U373 (**B**; n=6) following control or RLG with an additional exposure to 2.5 or 0.1 mM glucose for 3 hours. Extracellular lactate levels normalised to glucose availability from conditioned media from HPA (**C**; n=8) and U373 (**D**; n=6) following exposure to 2.5 or 0.1 mM glucose containing media for 3 hours. One-way ANOVA with post hoc Bonferroni multiple comparisons tests. *P<0.05; **P<0.01; ***P<0.001 between highlighted groups. Error bars represent standard error of the mean (SEM).

Figure 3.18

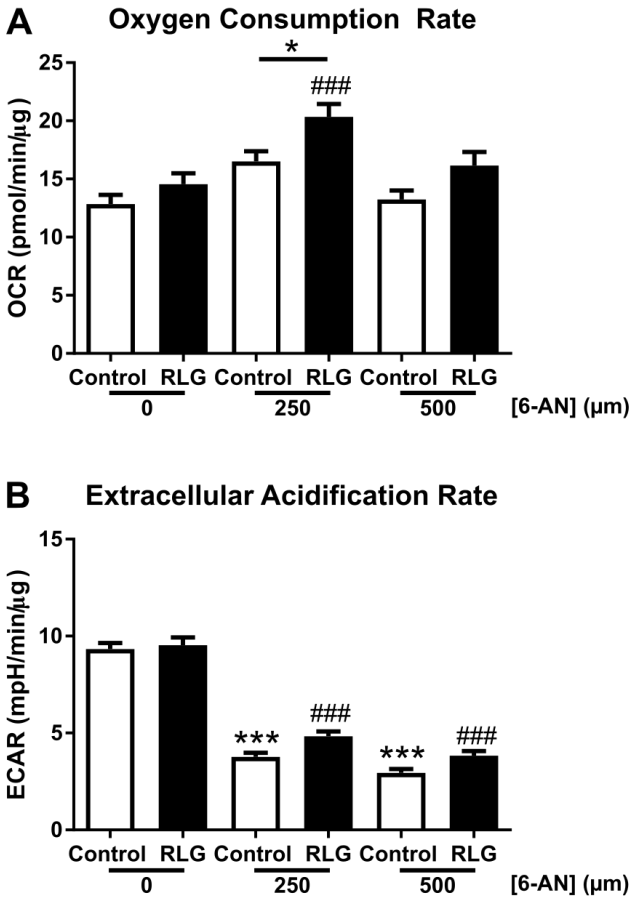

Figure 3.18 Recurrent low glucose (RLG) increases 6-aminonicotinamide (6-AN) sensitive oxygen consumption rate (OCR) in human primary astrocytes (HPA).

6-AN used as an inhibitor of the pentose phosphate pathway by inhibiting glucose-6-phosphate dehydrogenase increases OCR and decreases extracellular acidification rate (ECAR) in HPA. HPA cells were exposed to RLG and then given 250, 500 µM 6AN for 16 hours prior to measurement of basal OCR (**A**) and ECAR (**B**). Control and RLG vehicle n=30; control and RLG 250 uM 6-AN n=32; control and RLG 500 µM 6-AN n=29. One-way ANOVA with post hoc tukey tests. *P<0.05, ***P<0.001 difference from vehicle treated control cells, ###P<0.001 difference from vehicle treated RLG.

Figure 3.19

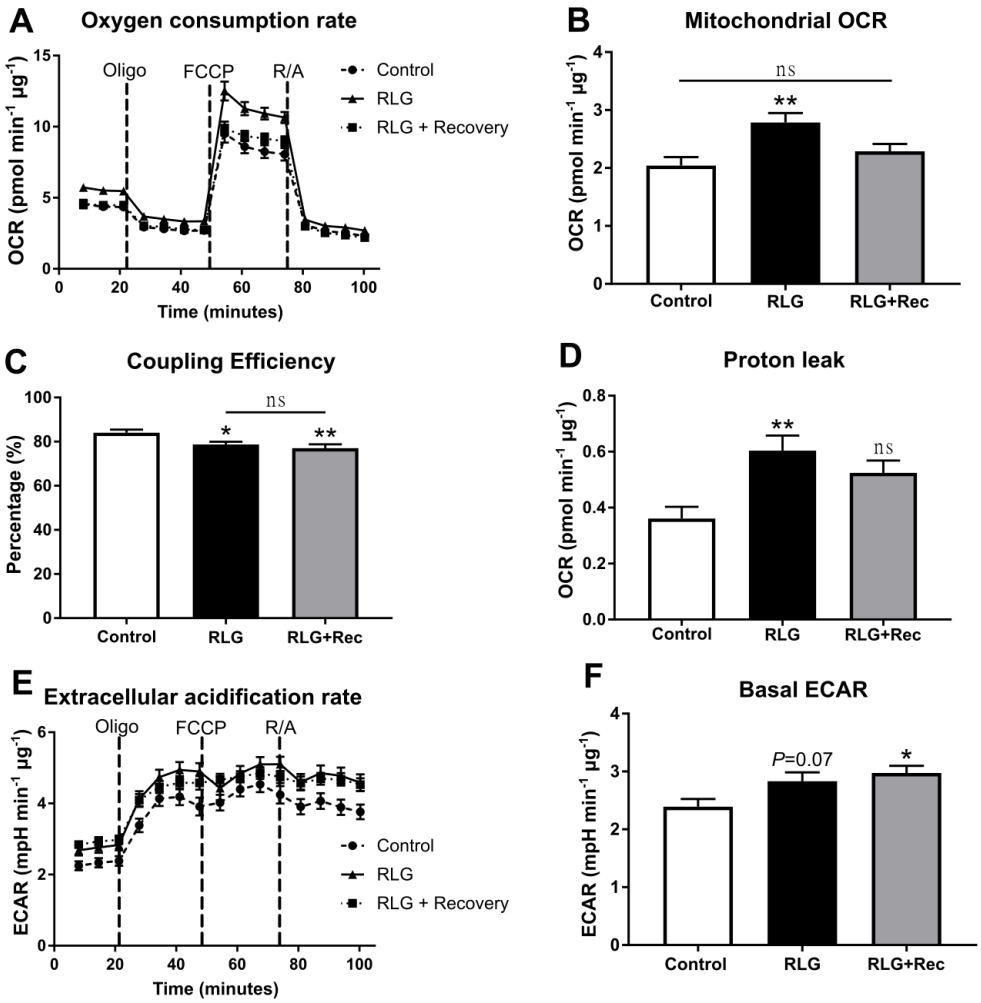

Figure 3.19. Maintaining glucose levels following recurrent low glucose (RLG) partially recovers metabolic adaptations in human primary astrocytes (HPA.

A. Oxygen consumption rate (OCR) of human primary astrocytes (HPA) following RLG with a 4 day recovery after the last low glucose exposure (control group, n=31; RLG group, n=31; RLG + recovery group, n=26). Cells were exposed to oligomycin (10 µM), FCCP (5 µM) and a combination of rotenone and antimycin A (5 µM). **B**. Mean basal OCR (**P<0.01 vs control). **C**. Coupling efficiency calculated from the ratio of oligomycin sensitive OCR and basal OCR expressed as a percentage. **D**. Proton leak, calculated from the oligomycin-insensitive (i.e. not ATP-synthase linked) OCR minus non-mitochondrial respiration, from HPA cells (**P<0.01 vs control; ns, not significant vs control and vs RLG). **E**. Extracellular acidification rate (ECAR) analysis measured during mitochondrial stress tests (control group, n=31; RLG group, n=31; RLG + recovery group, n=26). **F**. Mean baseline ECAR in HPA cells following RLG and RLG plus recovery (RLG+Rec; *P<0.05 vs control). One-way ANOVA with post hoc Bonferroni multiple comparisons tests. Error bars represent standard error of the mean (SEM).

Discussion

Astrocytes are metabolically flexible cells, which, for example, can rapidly upregulate glycolysis, partly due to increased expression of PFKFB3 which can stimulate glycolysis during stress (Almeida et al. 2004, Snyder et al. 2004). Furthermore, transcriptional analysis of astrocytes showed ~34% of astrocytic genes, in comparison to neuronal, were metabolism related, aiding in their metabolic flexibility (Lovatt et al. 2007). Astrocytes are also intimately associated with the blood-brain barrier (BBB) (Virgintino et al. 1997) and are part of the tripartite synapse (Araque et al. 1999) making them ideally situated to modulate neuronal function. This study gives for the first time a characterisation of the intrinsic metabolic changes of human primary astrocytes (HPA) and U373 human astrocytoma cells in response to acute and recurrent low glucose (RLG).

AMPK activity is necessary for GI neurons to sense low glucose (McCrimmon et al. 2006a). It was therefore examined whether AMPK activation also occurred in human astrocytes in response to physiologically relevant glucose levels. Indeed both HPA and U373 cells had increased phosphorylation of AMPK at threonine 172, as well as increased phosphorylated ACC (a downstream target of AMPK (DAVIES et al. 1990)), indicating increased AMPK activity (Hawley et al. 1996). Importantly culturing HPA cells with 2.5 mM glucose did not increase AMPK phosphorylation compared to 5.5 mM glucose. This shows that culturing HPA cells in 5.5 and then 2.5 mM as a part of the RLG model does not activate AMPK. Therefore, the increase in AMPK phosphorylation is also specific to the euglycaemia-like to hypoglycaemia-like glucose concentrations.

To model recurrent hypoglycaemia seen in T1DM HPA and U373 cells were given recurrent bouts of low glucose exposure (0.1 mM for 3 hours/day) for 4 days; termed recurrent low glucose (RLG). Interestingly, RLG increased basal phosphorylation of AMPK in 2.5 mM glucose compared to controls such that it was comparable to a low glucose exposure without prior RLG. While AMPK phosphorylation was elevated by antecedent RLG a further low glucose exposure did not further elevate AMPK phosphorylation; blunting the fold change from baseline in response to low glucose as would normally occur (Hardie et al. 2012). This corroborates evidence from a rat model of recurrent insulin-induced hypoglycaemia (RIIH) which had decreased AMPK phosphorylation compared to acute insulin-induced hypoglycaemia, within the

mediobasal hypothalamus (Mandal et al. 2017). Interestingly, there was also an increase in total AMPK content induced by RIIH, which implies an AMPK-dependent energy sensor failure caused by RIIH. In the present study ACC phosphorylation, indicating downstream activity of AMPK, was unchanged by RLG; while pAMPK was elevated in 2.5 mM glucose following RLG, there is no increase in pACC, and while pAMPK was unchanged with a further bout of low glucose, pACC was robustly increased. This is interesting as it suggests a disconnection between phosphorylation of AMPK and its downstream target ACC. Why elevated pAMPK would not result in increased pACC remains unknown. When phosphorylated, ACC is inhibited and unable to produce malonyl-CoA as a substrate for fatty acid biosynthesis. Therefore if pACC was also elevated by antecedent RLG it would inhibit the elevated fatty acid oxidation found in this study. Taken together though these results show that HPA and U373 are able to react to pathophysiologically relevant (Claret et al. 2007, Beall et al. 2012b) glucose concentrations, but increased pAMPK in response to low glucose is blunted by antecedent RLG.

Astrogliosis is a phenomenon whereby cellular morphology becomes ramified with an increase in cytoskeletal components. Astrogliosis occurs in response to a range of different stimuli including CNS injury (Burda et al. 2016), CNS diseases (Pekny et al. 2016), and energy changes; both fasting and high caloric intake exposure increase astrogliosis (Horvath et al. 2010, Thaler et al. 2012, Daumas-Meyer et al. 2018). Therefore, it was hypothesised that HPA cells would respond to acute low glucose and/or RLG with increased astrogliosis and increased expression of glial intermediate filaments GFAP and vimentin. Vimentin expression and fragmentation increased in an additive manner to each low glucose exposure, but there was no change in vimentin distribution. Importantly the fragmentation of vimentin was not due to sample degradation as actin was not degraded. Cleavage of vimentin can be due to caspase activity (Darlington et al. 2008). Caspase activity is commonly associated with programmed cell death and inflammation (Galluzzi et al. 2016), as well as models of hypoglycaemia: oxygen-glucose-deprivation (Nath et al. 2002), and acute and recurrent insulin-induced hypoglycaemia (Ouyang et al. 2000, Cardoso et al. 2013). Therefore, the fragmentation of vimentin here may be indicating an inflammatory response mediated by caspase activity.

AMPK pathway activation increases catabolic processes, including fatty acid oxidation, to restore energy homeostasis (Ronnett et al. 2009). As AMPK was phosphorylated in HPA and U373 cells during low glucose, it was anticipated this would increase mitochondrial and glycolytic pathway activity. Interestingly, significant increases in basal mitochondrial oxygen consumption in both HPA and U373 were found, which is, at least partly, mediated by increased fatty acid oxidation. While fatty acids are a high energy substrate, glucose is primarily used by neurons and glia (Dienel 2012, Pellerin et al. 2012). This is because fatty acid oxidation is known to increase reactive oxygen species (ROS) (St-Pierre et al. 2002). The ROS generated by β-oxidation is also particularly detrimental to neurons as they are more sensitive to oxidative stress than other neural cells (Bolanos et al. 1997). A mitochondrial defence to increased ROS is to uncouple proton flow across the inner mitochondrial membrane, mediated by uncoupling proteins or the ATP/ADP antiporter (ANT; (Skulachev 1998)). Furthermore, proton leak has been demonstrated to occur when isolated mitochondria are treated with fatty acids (Tonkonogi et al. 2000). In the present study, RLG also increased proton leak which also likely contributed to a decreased coupling efficiency. Previously, β-oxidation genes have been shown to increase with acute hypoglycaemia but this is subsequently blunted by RH (Poplawski et al. 2011). This contrasts our findings of increased fatty acid oxidation following RLG in human astrocyte mono-cultures. However, it is worth noting that those measurements were taken from whole rodent mediobasal hypothalamus containing multiple cell types. Perhaps the change to astrocytic fatty acid oxidation is being masked by responses from other cells, i.e. neurons, which may have a different cell-type dependent response to RH. A key regulatory molecule for these and related processes is AMPK. Chronic elevation of basal AMPK activity seen in this model has been shown in rat myocytes, where AMPK increases mitochondrial enzyme expression and cytochrome c oxidase (COX) activity, indicating enhanced oxidative capacity (Winder et al. 2000, Ljubicic et al. 2011). This corroborates with our data showing increased fatty acid oxidation dependency, but not mitochondrial biogenesis, following RLG where AMPK baseline activation may play an important role.

García-Cáceres *et al*, demonstrated that a loss of insulin receptors on astrocytes led to impaired astrocytic glucose uptake (García-Cáceres et al. 2016). This was

accompanied by fewer and smaller mitochondrial filaments, suggesting heightened mitophagy (García-Cáceres et al. 2016). Furthermore, in our study, increases to basal mitochondrial OCR could suggest a change in mitochondrial number and/or network morphology, however, no significant differences in protein expression of VDAC, SDHa, or CPT1-a or any change to mitochondrial filamentous networks were found. Normally, mitochondria are dynamic organelles that undergo fusion and fission in a continual manner to partition off unhealthy regions which are then targeted for mitophagy (Youle et al. 2012). RLG increased proton leak and decrease coupling efficiency indicating some mitochondrial stress. As these changes persist up to 4 days since the last low glucose exposure it suggests there is a failure to fully resolve mitochondrial stress. This may be due to a failure to appropriately partition unhealthy mitochondria by mitochondrial fission. On the other hand, the mitochondrial stress induced by low glucose may not be sufficient to elicit changes on a network level. Additionally, cells were recovered into serum containing media which may provide sufficient insulin and growth factors to recover from each bout of low glucose.

Given that astrocytes are known to alter glycolysis in response to low glucose and supply neurons with lactate (Pellerin 2003), it was hypothesised that RLG would alter glycolytic flux. RLG exposure increased basal ECAR in HPA cells but not U373 cells. Moreover, glucose reperfusion-induced a larger activation of ECAR in HPA cells after RLG, and a concomitant decrease in OCR, with 2.5 and 5.5 mM glucose. However, there was no difference in response between 2.5 and 5.5 mM glucose. This shows that supplying excess glucose does not result in further glucose utilisation, and somewhere between 0.5 and 2.5 mM glucose, there was a saturation of glycolytic machinery. The U373 cells also increased ECAR and decrease OCR in response to glucose reperfusion; however, RLG did not significantly differ from controls. Interestingly, the ECAR response to glucose in U373 cells was twice as large as in HPA cells. ECAR is a simple measure of the rate of extracellular acid produced by cells which mainly comes from lactate release and the formation of $lactate^-$ and H^+ (Blouin et al. 2010, Mookerjee et al. 2015). However, the complete breakdown of glucose via oxidative phosphorylation and the TCA cycle produces six CO_2 molecules. These contribute to ECAR via the reversible hydration and

dissociation into bicarbonate and protons (Divakaruni et al. 2014, Sakamaki et al. 2014):

$$H_2O + CO_2 \leftrightarrow H_2CO_3 \leftrightarrow H^+ + HCO_3^-$$

As RLG did not induce changes to basal lactate release in HPA cells it is probable the difference in basal ECAR in HPA cells is likely due to the contribution of CO_2 from, at least in part, elevated mitochondrial respiration. Interestingly, cytosolic processes can also produce CO_2 while consuming oxygen, for example, the PPP when converting 6-phosphogluconate to D-ribulose-5-phosphate (Stincone et al. 2015).

Given notable discrepancies in how HPA and U373 respond to acute and recurrent low glucose the capacity of the mitochondria to utilise different substrates was assessed in basal conditions. Cancerous cells are known to have a markedly different metabolic profile to their non-cancerous counterparts (Warburg et al. 1936, Dettmer et al. 2013, DeBerardinis et al. 2016). Due to a process known as the Warburg effect, cancerous cells are termed aerobically glycolytic; meaning an increased reliance on glycolysis to generate ATP even with ample oxygen present (Warburg et al. 1936). Nevertheless, while U373 cells are metabolically altered by virtue of being cancerous, they were used because the cells proliferated quickly and were easy to maintain. This allowed preliminary studies to be carried out before the use of slower growing HPA cells. Additionally as the HPA cells are a rare resource and U373 cells are more widely used it was important to compare the HPAs to a more well understood cell line. The comparison between cell types may also be of interest to those that study cancer biology. Interestingly, the HPA cells were more dependent on pyruvate oxidation than the U373 while pyruvate oxidation capacity and flexibility were similar. This suggests that more of the pyruvate generated by HPA goes into the mitochondria for oxidation, in comparison to U373 cells, where they are less dependent on pyruvate. Pyruvate either enters the mitochondria or is converted to lactate, therefore, pyruvate is likely being converted to lactate in the U373 cells as predicted by the Warburg hypothesis (Liberti et al. 2016). When studying metabolic changes induced by disease-relevant stimuli it is important to consider the differences in metabolic phenotype between primary and cancerous cell lines; for example, glucose withdrawal induces cell death in glioblastoma cells but

not in normal human astrocytes (Jelluma et al. 2006). Indeed even long-term cell culture impacts primary cell metabolism (Dettmer et al. 2013). Nevertheless, primary cells more accurately represent physiology and are more appropriate for studies into metabolic disorders.

RLG induced an increase to HPA basal ECAR and enhanced ECAR reactivation following acute low glucose withdrawal. Interestingly, brain glucose uptake, measured using the labelled glucose analogue [^{18}F]fluorodeoxyglucose, increases during hypoglycaemia in people with T1DM (Cranston et al. 2001b), and in those with diabetes with intact hypoglycaemia awareness, but, this is lost with IHA (Cranston et al. 2001a, Dunn et al. 2007). RH also reduces cerebral blood flow to these regions in subjects with T1DM compared to healthy controls (Mangia et al. 2012). To test whether glucose uptake was altered by RLG in HPA cells the uptake of the non-hydrolysable fluorescent glucose analogue 6-NBDG was measured. Interestingly, there was no change in 6-NBDG accumulation following antecedent RLG suggesting no change in glucose uptake. Therefore, glucose uptake is not the cause of increased basal ECAR and increased ECAR reactivation following glucose withdrawal.

Expression of HK2 has been reported to be decreased in STZ induced diabetic rats, which was restored upon normalisation of blood glucose levels (Burcelin et al. 1993). This suggests high glucose suppresses HK2 expression, but the effects of low glucose on glycolytic machinery expression are unknown. In this study, no changes to HK1, HK2, HK3, PFK(P), and PKM2 were found showing that increased glycolytic rates were not due to increased expression of glycolytic enzymes. However, enzymatic expression may not accurately reflect their activity. Therefore, activity rates for each enzyme should be determined before ruling out their involvement in modulating ECAR. Another mechanism by which glycolytic rates might be increased would be through increased translocation of HK2 to the mitochondria. HK2 has been previously shown to interact with VDAC (Arzoine et al. 2009), perhaps giving it better access to ATP needed to fuel its conversion of glucose to glucose-6-phosphate (Bustamante et al. 1977). This could be assessed by comparing the amount of HK2 found in a mitochondrial fraction following RLG. To see specifically if there is an increased interaction with VDAC, co-immunoprecipitation could be performed. Nevertheless, these data show HPA and U373 metabolism is altered by RLG.

While hypoglycaemia is a significant obstacle to optimal glycaemic control, strict avoidance of blood glucose levels of <3 mM can recover hypoglycaemia awareness (Fanelli et al. 1993, Cranston et al. 1994, Dagogo-Jack et al. 1994). To test whether the changes to HPA metabolism induced by RLG could be resolved in a similar fashion a 4-day recovery period was introduced with exposures to euglycaemia-like glucose concentration (2.5 mM) each day. Increases to basal OCR were restored to normal, but, coupling efficiency remained decreased and proton leak partially recovered. The restoration of some aspects of HPA metabolism reflects, in part, the recovery seen by avoidance of hypoglycaemia in humans. Nevertheless, there has not been a complete restoration to normal function, as some metabolic adaptations have persisted. However With enough time, weeks to months, a complete recovery may take place. An additional issue with the RLG model is that only four low glucose exposures are used which contrasts potentially decades of glucose variation seen in T1DM. However, even one exposure to hypoglycaemia in healthy humans decrease CRR (Burcelin et al. 1993, Davis et al. 1997), therefore repeated exposures to hypoglycaemia or low glucose are not required for blunting of CRR.

Glycogen is stored primarily in astrocytes (Brown 2004) and is metabolised to generate lactate (Dringen et al. 1993). Lactate is then supplied to neurons and used as a metabolic substrate (Gruetter 2003, Brown 2004, Cloix et al. 2009). During hypoglycaemia or recurrent 2DG induced glucoprivation, brain glycogen in rodents is significantly reduced (Choi et al. 2003, Canada et al. 2011) and following restoration of euglycaemia glycogen stores increased above pre-hypoglycaemic levels; super-compensation had occurred. Choi et. al., hypothesised this increased glycogen store could be metabolised during future hypoglycaemia delaying the onset of CRR (Choi et al. 2003). The increase in glycogen breakdown would lead to an increase in lactate production for neurons. However, lactate delivery to the VMN during peripheral hypoglycaemia prevents the onset of CRR (Borg et al. 2003). Conversely, Herzog et. al., did not observe any glycogen supercompensation in rats after either acute or recurrent hypoglycaemia (Herzog et al. 2008). Additionally, no correlation has been found in humans between brain glycogen content and hypoglycaemia awareness (Öz et al. 2012). Despite RLG altering HPA metabolism, no changes in glycogen levels were found, supporting the current literature. However, glycogen turnover is necessary for normal brain function (Hertz et al. 2003, Gibbs et al. 2007,

Suzuki et al. 2011, Duran et al. 2013) and therefore a model including neurotransmitter dynamics and/or co-culturing neurons with astrocytes should be employed to completely address this question.

Lactate is readily used by neurons as a metabolic substrate in euglycaemia. As hypoglycaemia ensues, lactate levels are maintained in both new-born dogs (Vannucci et al. 1981) and humans without diabetes (Abi-Saab et al. 2002). While lactate is maintained, glucose levels within the CNS do decrease, but there is an approximate 30-minute lag before CNS levels change (Abi-Saab et al. 2002). Given sufficient hypoglycaemia duration lactate levels do fall (Lewis et al. 1974). Interestingly the lactate concentration in the brain of people with T1DM and IHA decrease during hypoglycaemia compared to people with T1DM and healthy controls with normal hypoglycaemia awareness (Wiegers et al. 2016). The depletion of brain lactate suggests it is being oxidised and used as a fuel substrate, which prevents the onset of CRR and awareness of hypoglycaemia. This supports data by Borg et. al., showing an injection of lactate into the VMN prevents the onset of CRR in the presence of peripheral hypoglycaemia (Borg et al. 2003). Furthermore, the injection of lactate into the periphery can reverse insulin-induced hypoglycaemic stupor-coma and decrease the rate of brain glucose utilisation suggesting it is used as a fuel by the brain (Thurston et al. 1983). In the present study astrocytes were able to maintain lactate release in low glucose for 30 minutes, but, by 3-hours of low glucose exposure lactate concentration had significantly decreased. However, the decrease in lactate release did not relate to the 25-fold reduction in glucose concentration showing there was an increase in lactate release relative to glucose availability. This effect was unaltered by prior RLG. The source of lactate in the absence of extracellular glucose is likely from the breakdown of glycogen stores (Dringen et al. 1993). When glycogen is converted to G6P it is unlikely to then be converted to glucose due to low G6P phosphatase activity in astrocytes (Stephens et al. 1976, Pertsch et al. 1988), therefore, G6P continues through glycolysis to produce lactate. Further, to lactate production glycogenolysis and subsequent glycolysis produce ATP. In this study up to 3-hours of low glucose, with or without prior RLG, did not alter ATP:ADP ratios or total ATP in HPA or U373 cells. In chronic (Vannucci et al. 1981) and severe acute (McCall et al. 1986) hypoglycaemia, ATP levels are sufficiently maintained, with a concurrent reduction in carbohydrates implicating their

utilisation as a fuel source. As previously discussed, glycogen content may contribute to sustaining intracellular nucleotide levels. However, 4 mM L-glutamine was present in the experimental medium used in this study, additionally 1% serum in HPA media. It is likely that a combination of intracellular glycogen and the nutrients present in the medium all contribute to sustaining intracellular ATP levels in low glucose. In addition to this, the mitochondrial and glycolytic adaptations seen may be compensatory to maintain cellular energy balance. Taken together these data demonstrate the ability of human astrocytes *in vitro* to increase lactate release relative to glucose availability and sustain intracellular nucleotide levels suggesting they do adapt to acute low glucose exposure.

A parallel glucose metabolic pathway is the pentose phosphate pathway (PPP). The NADPH produced from the PPP is used to generate reduced glutathione (GSH) (Panday et al. 2014), a major cellular antioxidant (Stincone et al. 2015). This pathway is upregulated in astrocytes compared to neurons (Allaman et al. 2010, Takahashi et al. 2012), and is active as a part of the oxidative stress response (Stincone et al. 2015), i.e. high-glucose-induced stress *in vitro* (Takahashi et al. 2012) or following hypoglycaemia (McGowan et al. 2006) or glucose deprivation (McCrimmon et al. 2004). However, glucose is required for the PPP which detracts from ATP generation via glycolysis. Therefore, it was unclear whether the PPP would be increased, due to increased ROS, or decreased due to a lack of glucose supply. To test PPP activity the rate-limiting enzyme G6P dehydrogenase (G6PDH) was inhibited using 6-AN for 16 hours. PPP inhibition should result in an increase in OCR and a decrease in ECAR as PPP reduces oxygen consumption and contributes to ECAR. Interestingly, the increase to OCR was augmented by prior RLG, suggesting increased PPP activity induced by prior RLG. However, 6-AN inhibition of the PPP would disrupt a major cellular ROS defence mechanism and predispose a cell to oxidative stress which may affect the results. While preliminary, these data indicate that PPP activity is enhanced by RLG. To further investigate PPP activity of G6PDH could be assessed with an activity assay (Glock et al. 1953), radioactively labelled glucose tracer studies with mass spectroscopy could be used to measure glucose flux through the PPP (Kruger et al. 2003).

An important function of astrocytes is to recycle the excitatory neurotransmitter glutamate and subsequent processing through the glutamate-glutamine cycle

(Danbolt 2001, Oliet et al. 2001). Glutamate is detoxified by its conversion to glutamine by glutamine synthetase in an ATP-dependent reaction (Schousboe et al. 2013) which is mainly expressed in astrocytes (Norenberg et al. 1979). Glutamine is recycled to neurons and converted to glutamate by glutaminase and loaded into synaptic vesicles to complete the cycle (Schousboe et al. 2013, Schousboe 2018). Astrocytes sequester excess glutamate from the synaptic cleft via excitatory amino acid transporter 1 (EAAT1) (Kirischuk et al. 2016). Three Na^+ ions are co-transported with glutamate, which needs to be balanced by the ATP-dependent Na+/K+ ATPase (Cholet et al. 2002, Kirischuk et al. 2016). Thus there is a significant metabolic cost for astrocytes to maintain ion homeostasis during the glutamate-glutamine cycle; estimated to be approximately 20% of astrocytic ATP production (Silver et al. 1997). Tight regulation of glutamate is important as in excess it leads to neurotransmission failure and excitotoxicity (Ankarcrona et al. 1995, Yang et al. 1997). Glutamate stimulation has been shown to impair astrocytic mitochondrial function; decreasing spare respiratory capacity and increasing lactate production (Yan et al. 2017), which, when combined with the data in the current study, suggests that mitochondrial dysfunction could potentially be exacerbated following recurrent bouts hypoglycaemia in the presence of glutamate. Knock down of the astrocytic glutamate transporters glutamine aspartate transporter (GLAST) and glutamate transporter-1 (GLT-1) increases excitotoxicity in rats (Rothstein et al. 1996). Additionally, recent observations showed that RH reduces astrocytic glutamate recycling likely through reduced glutamate uptake, which led to the failure of glutamatergic neurotransmission during subsequent hypoglycaemia (Chowdhury et al. 2017). Based on the findings presented here, it is possible that mitochondrial dysfunction could reduce glutamate uptake due to the metabolic demands on the Na^+/K^+-ATPase, which requires further study. In addition, astrocytes also uptake GABA from the synaptic cleft in *ex vivo* slices of rat cortex (Iversen et al. 1968). However, GABA uptake is not associated with a significant metabolic cost (Chatton et al. 2003b), and as such may not be affected by any mitochondrial dysfunction. Interestingly, during RH a relative increase of GABA within the VMN occurs (Chan et al. 2008) which is less metabolically taxing for astrocytes (Chatton et al. 2003a). Therefore, a relative excess of GABA to glutamate may result in suppression of neurotransmission contributing to CRR, though further investigation is required to test this hypothesis.

It is worth noting that there is marked heterogeneity of astrocyte phenotype within the brain, including protoplasmic, fibrous, interlaminar, polarised, and varicose projection astrocytes (Verkhratsky et al. 2017). The range of astrocyte subtypes impact their function, for example, mouse hypothalamic astrocytes express more genes for lipid oxidation in comparison to cortical astrocytes that favour lipid synthesis, for example *SREBP-1* (Boisvert et al. 2018). Additionally, glycogen levels, found in mouse astrocytes, within the cortex and hippocampus are higher than hypothalamus and other thalamic regions (Oe et al. 2016). This may be reflective of differences in regional demand for energy supply, or perhaps the brain regions that have higher glycogen are not directly involved in glucose sensing they need to maintain their function during low glucose, whereas the hypothalamus needs to be more reliant on interstitial glucose concentrations. The subtype and regional differences in astrocyte functions could, therefore, result in differential reactions to a low glucose stimulus.

Diabetic encephalopathy is being increasingly recognised as part of the long-term sequelae of diabetes (Sima 2010). Furthermore, evidence from epidemiological studies implicates diabetes, and hypoglycaemia increasing the risk of cognitive dysfunction (McCrimmon et al. 2012). It is unknown by what mechanisms RH increases the risk of dementia, but glucose metabolism is altered in several ways in Alzheimer's disease (AD). For example, there is a reduction in glucose transporter 1 (Glut-1) and 3 (Glut-2) expression in the brains of patients with AD (Simpson et al. 1994). In an APP-overexpressing mouse model of AD that were Glut-1 deficient had a faster onset of neurodegeneration and amyloid-β (Aβ) pathology (Winkler et al. 2015), implicating glucose uptake in the pathogenesis of AD. Patterns of glucose uptake deficiencies have been found in frontotemporal dementia (Grimmer et al. 2004, Diehl-Schmid et al. 2007), Parkinson's disease (Kuhl et al. 1984, Peppard et al. 1990), and AD (Chase et al. 1984, Duara et al. 1986, McGeer et al. 1986, Castellano et al. 2015) which worsens with disease progression. Interestingly the decline in glucose uptake is not limited to pathology as healthy elderly subjects had widespread decreases in glucose uptake compared to healthy subjects (Garraux et al. 1999). In human brains, there is a reduction of glycolytic flux, resulting in an accumulation of tissue glucose levels, both of which correlated with severity of AD (An et al. 2018). Glucose hypometabolism also increases amyloid precursor protein

(APP) mRNA expression in primary rat cortical astroglial cells (Shi et al. 1997). Moreover, hypoglycaemia increases ROS (McGowan et al. 2006) which is known to be important in the onset of dementia (Huang et al. 2016). By increasing plasma glucose levels in patients with AD, memory improvements can be made (Craft et al. 1999, Craft et al. 2003). In the present study, RLG increases ECAR, indicating increased glycolytic flux. This may have been generated by increased CO_2 production by mitochondria, driven by increased fatty acid oxidation, rather than a change in glycolysis. It is interesting to speculate that the changes seen in astrocyte metabolism in response to RLG may impact dementia-related pathways given enough time.

This study for the first time shows human astrocytes respond to a physiologically relevant glucose range by activation of the AMPK pathway. In response to RLG, human astrocytes intrinsically adapt their metabolism; increasing mitochondrial respiration, mediated in part by fatty acid oxidation, as well as glycolytic rates. This does, however, generate a mild to moderate mitochondrial stress seen as an increase in proton leak and decreased coupling efficiency. Nevertheless, human astrocytes can successfully sustain intracellular nucleotide ratios and maintain lactate release in low glucose. Lastly, following RLG a 4-day recovery period restored mitochondrial oxygen consumption, but coupling inefficiency and elevated basal ECAR remained. While it is difficult to know whether these adaptations directly improve or worsen the CRR to hypoglycaemia, they provide an interesting examination of the intrinsic responses generated by human astrocytes in response to acute or recurrent low glucose *in vitro*.

Chapter 4

Human astrocytes sustain normal calcium signalling in low glucose

Introduction

Calcium signalling is a ubiquitous mechanism in many living cells including astrocytes. Early work found calcium transients in astrocytes could be induced by mechanical stimulation (Charles et al. 1991). The increases to $[Ca^{2+}]_i$ could also travel through glial syncytium allowing for the propagation of long range signalling from an initial stimulus (Cornell-Bell et al. 1990, Charles et al. 1991, Cornell-Bell et al. 1991, Dani et al. 1992). The spread of calcium waves through astroglial syncytium has been investigated *in vitro* and *in situ* and is due to the intercellular diffusion of inositol triphosphate (IP_3) via gap-junctions (Verkhratsky et al. 2017). Calcium signalling is mediated by a complex interaction between plasma membrane and organelle ion channels, pumps and transporters, as well as buffering and sensing of cytosolic calcium through calcium binding proteins.

Gene transcription, metabolism and neurotransmission can all be regulated by calcium signalling (Verkhratsky et al. 2012). Accumulation of Ca^{2+} in the mitochondria is necessary for the activation of mitochondrial matrix dehydrogenases, including pyruvate dehydrogenase (Denton et al. 1972), isocitrate dehydrogenase (Denton et al. 1978), and α-ketoglutarate dehydrogenase (Lawlis et al. 1981). Ca^{2+} has also been shown to activate ATP synthase through the action of Ca^{2+}-binding proteins (Yamada et al. 1985, Hubbard et al. 1996, Territo et al. 2000). Therefore, astrocyte excitability and metabolism can be modulated by changes in cytosolic calcium. Additionally, CaMKK2, an AMPK kinase and activator, is regulated by calcium and changes cellular metabolic activity in hypothalamic neurons (Anderson et al. 2008). Interestingly, regionally specific control of metabolism, i.e. mitochondria, in micro domains can occur in the absence of somatic calcium signalling (Grosche et al. 1999). Maintaining ion balance via Na^+/K^+-ATPase is estimated to use approximately 20% of ATP produced by astrocytes (Silver et al. 1997). Similarly, plasma membrane Ca^{2+} ATPase (PMCA) and sarcoplasmic reticulum Ca^{2+} ATPase (SERCA) utilise ATP to maintain calcium homeostasis (Carafoli 1991, Yu et al. 1993). Therefore, calcium signalling is necessary for regulating metabolism but also has a metabolic cost in its maintenance. If uncontrolled, excessive calcium entry into the cell can result in oxidative stress and mitochondrial dysfunction (Peng Tsung et al. 2010, McElnea et al. 2011). Therefore, well controlled calcium homeostasis is essential for astrocytes to survive and react to various stimuli.

Ultimately, the exchange of ions between the extracellular space via transporters and channels, or from other cells (via gap junctions) couples external stimuli and astrocyte excitability leading to changes in gene transcription and metabolism (Verkhratsky et al. 2012). Changes in astrocyte calcium can be elicited by neurotransmitters, including: glutamate (Cornell-Bell et al. 1990), acetylcholine (Araque et al. 2002), serotonin (5HT) (Schipke et al. 2011), noradrenaline (NA) (McCarthy et al. 1991), GABA (Kang et al. 1998); as well as purines (Abbracchio et al. 2009), pH (Rose et al. 2005), as well as ligands of Gq or Gs-protein coupled receptors (Verkhratsky et al. 2017). Astrocytic integration of these inputs is necessary for long-term potentiation (LTP) in the hippocampus via the gliotransmitter D-serine, for example (Henneberger et al. 2010). ATP-evoked astrocyte Ca^{2+} transients can also promote neurotransmission via glutamate release and subsequent activation of glutamate receptors (Perea et al. 2007). Increased $[Ca^{2+}]_i$ in turn can release gliotransmitters including ATP (Guerra-Gomes et al. 2018). ATP release from astrocytes can be via diffusion through connexin hemi-channels (Stout et al. 2002), pannexin hemi-channels (Bao et al. 2004), P_2X_7 receptors (Suadicani et al. 2006), and direct exocytotic release (Zhang et al. 2007b). ATP release is also required for Ca^{2+} wave propagation in astrocytes (Guthrie et al. 1999, Cotrina et al. 2000). Once released, ATP binds to P_2X (ionotropic) and/or P_2Y (metabotropic) receptors to increase $[Ca^{2+}]_i$ via direct ion influx or release from intracellular stores (Abbracchio et al. 2009). ATP release can also decrease intracellular ATP:AMP ratios leading to AMPK activation, found in kidney epithelial and mesangial cells (Chi et al. 2014). Extracellular ATP is metabolised by ectonucleotidases to produce adenosine (Cunha et al. 1996). Adenosine can then suppress excitatory synapses (via A_1 receptors) (Dunwiddie et al. 2001), or augment activation of synapses (via A_{2A} receptors) (Cunha 2001).

ATP-evoked $[Ca^{2+}]_i$ increases also trigger glutamate release from hippocampal synapses (Perea et al. 2007). Glutamate is the predominant excitatory neurotransmitter in the brain with receptors on neurons and astrocytes (Meldrum 2000). Agonism of astrocyte glutamate receptors increases calcium flux (Pearce et al. 1986) and can mediate neuronal excitation (Huang et al. 2004). Interestingly, glutamate-induced increases in $[Ca^{2+}]_i$ can increase glucose uptake 2- to 3-fold within 10 seconds of exposure via transport of Glut-1 to the membrane (Loaiza et al.

2003), which couples glucose uptake to areas of high synaptic activity. In diseases like Alzheimer's disease, abnormally high extracellular glutamate levels can occur leading to excitotoxicity (Hynd et al. 2004). Astrocytes uptake glutamate by Na^+-dependent mechanisms, to decrease excitotoxicity (Anderson et al. 2000, Swanson et al. 2004). Astrocytic glutamate uptake requires co-transport of three Na^+ ions (Levy et al. 1998). To maintain $[Na^+]_i$ it is actively pumped from the cell by the Na^+/K^+-ATPase (Chatton et al. 2003a). Indeed, the metabolic cost associated with maintaining astrocyte Na^+/K^+-ATPase is estimated to be approximately 20% of ATP production (Silver et al. 1997). Interestingly, glutamate uptake stimulates aerobic glycolysis in astrocytes to account for the increased metabolic demand (Pellerin et al. 1994). SERCA and PMCA consume ATP to maintain calcium homeostasis by the reuptake of Ca^{2+} into the endoplasmic reticulum (ER) (Yu et al. 1993) and export from the cell (Carafoli 1991), respectively. NCX enables the influx of Na^+ in exchange for calcium being exported against a Ca^{2+} gradient (Blaustein 2010). The increase in $[Na^+]_i$ is exported from the cell by the Na^+/K^+-ATPase (Chatton et al. 2003a). Increased ATP usage will decrease the ratio of ATP:AMP which activates the intracellular nucleotide sensor and master energy regulator AMPK (Herzig et al. 2017). Activation of AMPK inhibits anabolism and increases catabolism to maintain $[ATP]_i$ (Herzig et al. 2017).

The mechanisms discussed here all have an energetic cost. In this thesis it was shown that total ATP and ATP:ADP ratios were maintained in low glucose but the effects on intracellular calcium remain unknown. It has previously been shown that glucose-oxygen deprivation increases glutamate accumulation which may be due to a failure of glutamate reuptake mechanisms (Goldberg et al. 1993). Furthermore, neurodegeneration is dependent on the presence of Ca^{2+} and its uptake (Goldberg et al. 1993). Both high and low extracellular glucose levels increased $[Ca^{2+}]_i$ *in vitro* in neurons (Moriyama et al. 2004). However, little is known about the effects of acute or recurrent low glucose on astrocyte $[Ca^{2+}]_i$. While astrocytic calcium signalling has been implicated in diabetes (Revsin et al. 2005, Lebed et al. 2008, Nagayach et al. 2014), inflammation (Hamby et al. 2012), Alzheimer's disease (Rossi et al. 2005), epilepsy (Carmignoto et al. 2012), and Huntington's disease (Lee et al. 2013), little is known about how calcium signalling itself is modulated by neuroglycopenia

Monoamines such as noradrenaline (NA) and serotonin (5-hydroxytryptamine; 5HT) are neurotransmitters that mediate a range of physiological processes. NA is also a catecholamine, like adrenaline. NA is released from locus coeruleus-noradrenergic (LC-NA) neurons which are associated with anxiety related behaviours including vigilance, attention, and arousal (Elam et al. 1986, Gorman et al. 1993, Dazzi et al. 2002, Kim et al. 2005, Lapiz et al. 2006). NA binds to α1 receptors which are G_q protein coupled and increase $[Ca^{2+}]_i$ via IP_3, which is associated with vasoconstriction, and glucose metabolism (Burcelin et al. 2004, Cotecchia 2010). NA also binds to α2 receptors which are G_i protein coupled and inhibits adenylyl cyclase activity thus inhibiting cAMP production; associated with inhibiting insulin release, stimulating glucagon release, and hepatic gluconeogenesis (Nakaki et al. 1980, Fagerholm et al. 2011). β1 and β2 receptors are G_s protein coupled receptors, activated by NA, which increase adenylyl cyclase raising $[cAMP]_i$ effecting heart function, smooth muscle relaxation, and stimulating gluconeogenesis and glycolysis (Danulat et al. 1990, Xiao et al. 1995, Fonseca 2010, Gibbs 2015).

If blood glucose falls below approximately 3.6-3.9 mM counterregulatory hormone release occurs, including glucagon and adrenaline (Sprague et al. 2011). NA is also released as a part of CRR and has been shown to act in the periphery on the liver via β-2 adrenergic receptors to increase glycogenolysis and gluconeogenesis (Exton 1987). Additionally, α-adrenergic receptor activation has been shown to increase hyperglycaemia *in vivo* (Metz et al. 1978, Nakadate et al. 1980, DiTullio et al. 1984, Angel et al. 1990). Glucoprivation within the hypothalamus induces NA, adrenaline, and glucagon secretion (Borg et al. 1995, Borg et al. 1997). Ingestion of caffeine has also been shown to increase anxiety related pathways which includes the activity of LC-NA neurons (Goldberg et al. 1982, Baldwin et al. 1989, Smith et al. 1999). Interestingly, coffee (containing caffeine), in a case study, improved hypoglycaemia awareness (Kerr et al. 2005). Hypoglycaemia activates LC-NA neurons to release NA which mediates hypoglycaemia-associated behavioural changes (Morilak et al. 1987, Flugge 2000, Yuan et al. 2002). During hypoglycaemia in rats, NA is released into the VMN from LC-NA neurons (Beverly et al. 2001), which can be prevented by glucose perfusion into the VMN (de Vries et al. 2005). Agonising β_2-adrenergic receptors in the VMN also enhances CRR response to hypoglycaemia (Szepietowska et al. 2011). Furthermore, chronic NA infusion into the VMN induces

obesity, glucose intolerance and insulin resistance (Cincotta et al. 2000). NA, therefore, has an orexigenic function within the CNS.

Stress adaptation is a well-known phenomenon in animal models facilitated in part by β-adrenergic receptor desensitisation in the cortex (Nomura et al. 1981, Stone et al. 1982, Funk et al. 1996). It is possible that, the loss of behavioural changes in IHA may be partly due to impaired NA signalling. As hypoglycaemia increases NA release (Davis et al. 2000), RH may result in adrenergic receptor desentisation. If β-adrenergic receptor desensitisation occurs this would prevent the normal activation of the amygdala in response to hypoglycaemia and thus contribute to the behavioural deficits in IHA. LC-NA neurons project to the lateral orbitofrontal cortex (LOFC) to excite GABAergic neurons via β-adrenergic receptors (Cavada et al. 2000, Ramos et al. 2007). These GABAergic neurons inhibit the glutamatergic neurons in the LOFC (Ramos et al. 2007), therefore, reducing glutamatergic neurotransmission to the amygdala (Ramos et al. 2007), which normally activates GABAergic neurons resulting in reduced activity in the amygdala (Bishop 2007). Therefore, NA signalling disinhibits amygdala activity to increase anxiety associated behavioural responses. If β-adrenergic receptor desensitisation occurs this might prevent the normal activation of the amygdala in response to hypoglycaemia and thus contribute to the behavioural deficits in IHA. However, as receptor desensitisation is reversible it is plausible that normal adrenergic responses to hypoglycaemia can be regained given sufficient avoidance of their activation by strict glycaemic control. Indeed, hypoglycaemia awareness can be restored in humans with strict avoidance of hypoglycaemia (Fanelli et al. 1993, Cranston et al. 1994, Dagogo-Jack et al. 1994, Fritsche et al. 2001). Taken together this suggests β-adrenergic receptors on the GABAergic neurons in the LOFC may regain NA sensitivity allowing for the disinhibition of the amygdala during hypoglycaemia.

LC-NA neurons also release NA during sensory stimulation, arousal, and locomotion that stimulates a global rise in astrocyte $[Ca^{2+}]_i$ (Ding et al. 2013). This can be blocked by the inhibition of α-1 adrenoreceptors (Ding et al. 2013), indicating astrocytes as targets of NA function. Astrocytes also express β-adrenergic receptors (Salm et al. 1989, Salm et al. 1992, Shao et al. 1992). Interestingly, β-adrenergic agonism within the VMN, and peripherally in rats can enhance CRR (Szepietowska et al. 2011, Szepietowska et al. 2013). Furthermore, NA delivery to the VMN

increases blood glucose and CRR hormone levels (Chafetz et al. 1986, Steffens et al. 1988). NA stimulation of astrocytes results in glucose uptake (Catus et al. 2011) and glycogenolysis which produces glucose-6-phosphate which is further metabolised by glycolysis to produce ATP and pyruvate. In astrocytes, pyruvate is predominantly converted to lactate due to the presence of lactate dehydrogenase isomer 5 (LDH5) (Bittar et al. 1996). Interestingly, lactate perfusion into the VMN in the presence of systemic hypoglycaemia prevents CRR (Borg et al. 2003). Therefore, NA-induced glycogenolysis and subsequent lactate production by astrocytes may contribute to defective CRR. Alternatively, the lactate produced by the astrocytes in this context, may be required for maintaining energy supply to β-adrenergic neurons.

In summary, NA is released within the VMN in response to hypoglycaemia which stimulates adrenergic receptors (Chafetz et al. 1986, Steffens et al. 1988, Beverly et al. 2001, de Vries et al. 2005). While neuronal responses to NA stimulation have been somewhat characterised the role of astrocytic responses to NA have been understudied. In particular the following studies aimed to assess the effects of low glucose availability on NA signalling in human astrocytes.

5HT is a neurotransmitter found centrally and acts on sympathoadrenal and hypothalamic-pituitary-adrenal pathways (Lowry 2002). Low 5HT signalling is known for its role in depression (Mann et al. 1992, Eley et al. 2004). Selective serotonin reuptake inhibitors (SSRIs) are effective and commonly used anti-depressant medications, including fluoxetine (Amsterdam et al. 1994), sertraline (Glassman et al. 2002) and fluvoxamine (Grimsley et al. 1992), among others. However, two case studies in patients with T1DM and depression have shown a temporally sensitive correlation between SSRI use and IHA and increased hypoglycaemia incidence (Sawka et al. 2000, Sawka et al. 2001). In these case studies patients had T1DM and suffered from depression. As depression can be a result of diminished 5HT signalling (Eley et al. 2004) this could result in an altered baseline from which SSRIs may have a different effect on metabolism compared to otherwise healthy individuals with diabetes. Nevertheless, the two case studies incidence of hypoglycaemia increased with fluoxetine treatment and returned to normal with its discontinuation (Sawka et al. 2000, Sawka et al. 2001). These studies provide a correlation between the use of SSRIs and increased incidence of hypoglycaemia. Mechanistically, SSRIs

may increase 5HT signalling in astrocytes which is known to increase glycogenolysis in chick astrocytes, which is necessary for memory consolidation (Gibbs et al. 2014). As discussed previously, astrocytic glycogenolysis results in lactate production, and while lactate is neuroprotective (Pellerin et al. 2012) it can prevent CRR (Borg et al. 2003). Nevertheless, these case studies are the only incidences reported of hypoglycaemia correlating with SSRI usage. While the incidence of hypoglycaemia was temporally correlated with the usage of SSRIs in the patients in the case studies, it does not prove causation.

To clarify whether SSRIs increase the risk of hypoglycaemia and the effects they have on CRR, three studies were done in humans and rats. Conversely to the case studies, these showed fluoxetine and sertraline improved CRR in healthy people (Briscoe et al. 2008b), healthy rats (Sanders et al. 2008), and patients with T1DM (Briscoe et al. 2008a). Pre-treatment with sertraline increased glucagon, adrenaline and noradrenaline CRR to a single hypoglycaemic exposure indicating increased hypothalamic-pituitary-adrenal axis and sympathetic tone in rats (Sanders et al. 2008). Furthermore, sertraline was able to prevent blunting of the adrenaline and NA responses to RH. After 5 years of T1DM and in long standing T2DM glucagon secretion is lost or diminished resulting in decreased endogenous glucose production (Gerich et al. 1973). Therefore, the enhanced sympathetic activity induced by sertraline, including increased glucagon, would help maintain glucagon secretion in T1DM. Similarly, in healthy human volunteers given fluoxetine which showed improved adrenaline and NA responses to hypoglycaemia (Briscoe et al. 2008b). Briscoe *et*. *al*., also showed enhanced lipolysis, glycogenolysis, and ketogenesis which are important catabolic processes fuelling the body (Briscoe et al. 2008b). However, it is important to note that these studies were carried out on otherwise healthy rats and humans respectively, with no diabetes or depression which may impact the action of SSRIs. To address this in an additional study Briscoe *et*. *al*., investigated the impact of fluoxetine on patients with T1DM and their CRR to hypoglycaemia (Briscoe et al. 2008a). Even in the presence of T1DM, adrenaline and NA responses were improved as well as increased lipolysis; indicating increased sympathetic nervous system activity and improved endogenous glucose production (Briscoe et al. 2008a). While the effects of fluoxetine were broadly similar between healthy volunteers and patients with T1DM, there was no increase in glycogenolysis

or ketogenesis in patients with T1DM. Therefore, the effects of SSRIs on hypoglycaemia counterregulation are altered by T1DM.

Mechanistically, it is unclear how SSRIs, 5HT or other serotonergic agonists alter CRR. Serotonergic and chatecholaminergic activity is present in the hypothalamus and hindbrain nuclei that are important for energy homeostasis and regulation of the autonomic response to hypoglycaemia (Blardi et al. 2005). Indeed, fluoxetine increases adrenaline and NA which are important for a functional CRR (Bymaster et al. 2002). Moreover, third-ventricle injections of fluoxetine in rats causes hyperglycaemia in the absence of hyperinsulinaemia (Carvalho et al. 2004).

Despite the contrasting literature suggesting that SSRIs alter the CRR to hypoglycaemia in diabetes, little is known about how astrocytes modulate these CRR pathways. In the context of depression, however, a recent study has shown fluoxetine exerts its therapeutic effect via astrocytic-dependent ATP release increasing brain-derived neurotrophic factor (BDNF) (Kinoshita et al. 2018). ATP and its metabolite adenosine have metabolic regulatory functions as discussed previously. Astrocytes also have serotonergic receptors (Schipke et al. 2011). Given that the mechanisms by which 5HT modulates the CRR are not fully understood this study aimed to perform some basic characterisation of the effects of 5HT on isolated human astrocytes and neurons *in vitro* during exposure to euglycaemia-like and hypoglycaemic-like glucose levels.

Astrocytic calcium signalling can modulate whole-body energy metabolism (Chen et al. 2016) In rodents it has been shown that activation of neurons in *ex vivo* slice of the NTS rely on functional astrocytes and that astrocytes respond to glucoprivation before neurons (Rogers et al. 2018). While astrocytes are recently being investigated in more detail, the effects of low glucose on isolated human astrocytes has not been studied in detail. Calcium signalling also has a metabolic cost through the function of ATP dependent ion pumps, e.g. SERCA (Yu et al. 1993), and Na^+/K^+-ATPase (Morth et al. 2007). As such, it was hypothesised that basal $[Ca^{2+}]_i$ would increase as a result of calcium dysregulation. The studies presented here expand on works by Rogers *et*. *al*., (Rogers et al. 2018) McDougal *et*. *al*., (McDougal et al. 2011) Marty *et*. *al*., (Marty et al. 2005) and Chen *et*. *al*., (Chen et al. 2016) by characterising the calcium responses of isolated human astrocytes to low glucose using the ratiometric

calcium sensitive dye fura-2. To characterise the calcium response to purinergic stimuli ATP and ADP, and NA, the cell-permeable calcium binding dye fluo-4 was used. Lastly, lactate release was measured to test whether monoamine, NA or 5HT, modulation of metabolism was affected by low glucose. Briefly, these studies show that human astrocytes sustain calcium homeostasis during low glucose-induced metabolic stress.

Overall aim and objectives

Rodent astrocytes have been shown to respond by changes in $[Ca^{2+}]_i$ to low glucose stimuli and mediate changes in neuronal activity. Given that calcium signalling metabolically taxing, it was hypothesised that the metabolic alterations seen in chapter 3 may affect it. Therefore, the principle aim of this chapter was to investigate if calcium signalling, either innate or induced, could be altered by acute or recurrent low glucose. Specifically the following questions were addressed:

- Does acute or recurrent low glucose induce changes to $[Ca^{2+}]_i$ as seen previously?
- Are astrocyte responses to calcium signalling activators, i.e. purines, NA and 5HT, altered by acute or recurrent low glucose?

Results

4.1 Low glucose increases basal intracellular Ca^{2+} in HPA

Unlike neurons, astrocytes are non-electrically excitable and rely changes in $[Ca^{2+}]_i$ to propagate signals, regulate their metabolism and release of gliotransmitters (Verkhratsky et al. 2012). Astrocytes are known to be activated by glucoprivation (McDougal et al. 2011), fasting (Daumas-Meyer et al. 2018), and obesity (Horvath et al. 2010, Thaler et al. 2012), but the intrinsic calcium response to low glucose in human astrocytes (0.1mM) has not been characterised. Therefore, HPA cells were exposed to three hours of either 2.5 or 0.1 mM glucose and free calcium measured during ratiometric imaging. $[Ca^{2+}]_i$ was significantly elevated in 0.1 mM glucose compared to control (2.5 mM glucose) (figure 4.1A,B).

4.2 During measurement of intracellular calcium for 90 minutes, intracellular calcium increases in HPAs regardless of RLG

Given $[Ca^{2+}]_i$ was increased in HPA by low glucose, a time course of the astrocytic response to low glucose was measured using fura-2 and the use of a microscope, rather than a plate reader. Figure 4.2A-D shows the raw traces of averaged readings from cells from an individual coverslip from control, acute low glucose, antecedent RLG, or RLG. A baseline measurement was taken for 5 minutes in 2.5 mM glucose, before being perfused with 2.5 or 0.1 mM glucose for 90 minutes. Interestingly, all groups after 90 minutes showed between a 5-10% increase in unstimulated $[Ca^{2+}]_i$ compared to their respective baseline, regardless of glucose concentration. The effect of this increase reached significance in cells treated with control conditions prior to the day of study (figure 4.2E). The RLG treated cells did increase more than the control treated cells but did not reach significance due to large variation between coverslips (figure 4.2E). Taken together this data shows that HPA cells do not respond to low glucose by increasing $[Ca^{2+}]_i$.

4.3 ATP increases intracellular Ca^{2+} in either 2.5 or 0.1 mM glucose in HPA

To further test whether basal calcium in HPAs was affected by low glucose and to establish the sensitivity of HPAs to ATP, they were cultured in 2.5 or 0.1 mM glucose for 3 hours and stimulated with 100 μM ATP. There was no significant difference in baseline, non-ATP stimulated calcium (figure 4.3A,B). Additionally, there was no significant difference in the maximum fold-change of $[Ca^{2+}]_i$ (figure 4.3A). However,

shortly after the peak response was reached, the ATP-induced response of 2.5 mM glucose treated cells was significantly lower than that of 0.1 mM glucose. But, this was quickly matched again by the low glucose treated group.

4.4 The effect of ATP treatment on isolated human neural cells

While there was conflicting data on whether the $[Ca^{2+}]_i$ of HPA cells was increased by low glucose it was not the robust response seen by Rogers *et*. *al*., (Rogers et al. 2018). Therefore, perhaps inputs from other cell types are necessary for strong astrocytic calcium responses to low glucose. It has been shown that P2 antagonism prevents increases in neuronal calcium in response to low glucose (Rogers et al. 2018), therefore purinergic signalling may be an important factor in mediating astrocytic responses to low glucose. Additionally, ATP is necessary for Ca^{2+} wave propagation in astrocytes (Guthrie et al. 1999, Cotrina et al. 2000), and stimulates increased $[Ca^{2+}]_i$ purinergic signalling (Abbracchio et al. 2009).

Glucose excited cells, such as GT1-7 glucose-excited neuroblastomas, are hyperpolarised by low glucose reducing their firing rates (Beall et al. 2012b). Therefore, these cells were used as a positive control to show that cells known to be inhibited by low glucose had altered calcium responses to ATP stimulation. The extra challenge of an ATP treatment in low glucose may result in an altered calcium response due to the metabolic demands of ion channel activity (Carafoli 1991, Yu et al. 1993).

4.4.1 ATP increases intracellular Ca^{2+} in HPA and U373 astrocytoma cells in either 2.5 or 0.1 mM glucose

HPA and U373 cells were stimulated with ATP after 3 hours of either 2.5 or 0.1 mM glucose. In both cell types, 20 (figure 4.4.1A,B), 50 (figure 4.4.1C,D) and 100 µM ATP (figure 4.4.1E,F) significantly increased calcium in both 2.5 and 0.1 mM glucose compared to vehicle. However, the maximal fold-change in calcium was unaffected by glucose concentration used in either cell type (figure 4.4.1G,H). HPA had the greatest increase in $[Ca^{2+}]_i$ reaching approximately a 2-fold change with 100 µM ATP (figure 4.4.1A,G), this compares to a circa 1.2-fold change in U373 cells (figure 4.4.1F,H).

4.4.2 ATP-induced increases in intracellular Ca^{2+} are attenuated by low glucose in GT-1 glucose excited neuroblastoma cells

GT1-7 cells were treated with 20 (figure 4.4.2A), 50 (figure 4.4.2B), and 100 µM ATP (figure 4.4.2C) in either 2.5 or 0.1 mM glucose. ATP treatment significantly increased the peak response compared to vehicle treated cells in 2.5 mM glucose at all concentrations (figure 4.4.2D). However, only 100 µM ATP induced a significant increase in 0.1 mM glucose (figure 4.4.2D). Furthermore, at both 50 and 100 µM ATP the peak response was significantly lower in 0.1 compared to 2.5 mM glucose treated cells. Together, this shows that ATP-induced calcium responses are attenuated by low glucose in GT1-7 glucose-excited neuroblastoma cells.

4.5 Low concentrations of ATP increase HPA and U373 astrocytoma intracellular Ca^{2+}

Given that the EC50 for different purinergic receptors is different (Liu et al. 2001, Roberts et al. 2006) and 20 µM ATP induced a significant increase in intracellular calcium a lower range of ATP concentrations were used to test for a differential response. The HPA and U373 cells were treated with 5 (figure 4.5A,B), 10 (figure 4.5C,D), and 20 µM ATP (figure 4.5E,F). The peak fold-change calcium response was significantly elevated in U373 cells at all concentrations compared to vehicle (figure 4.5H). However, in the HPA cells significance was only reached with 10 and 20 µM ATP. Nevertheless, no significant differences were found in either cell type between glucose treatments.

4.6 U373 astrocytoma intracellular Ca^{2+} response to ADP

ATP is broken down both intra- and extracellularly to adenosine diphosphate (ADP), then adenosine monophosphate (AMP) and adenosine, which can act as separate signalling molecules (Eltzschig et al. 2012). Extracellularly ATP can be converted to ADP, AMP and/or adenosine by ectonucleotidases: ectonucleotide pyrophosphatase/ phosphodiesterase (E-NPP), ecto-nucleoside triphosphate diphosphohydrolase (E-NTDPase), and cluster of differentiation 73 (CD73) (Velasquez et al. 2014). Therefore, to test whether the rise in $[Ca^{2+}]_i$ was mediated by ADP, U373 cells were stimulated with 5, 10 and 20 µM ADP. ADP stimulation did not significantly alter $[Ca^{2+}]_i$ at any concentration used (figure 4.6A-D).

Figure 4.1

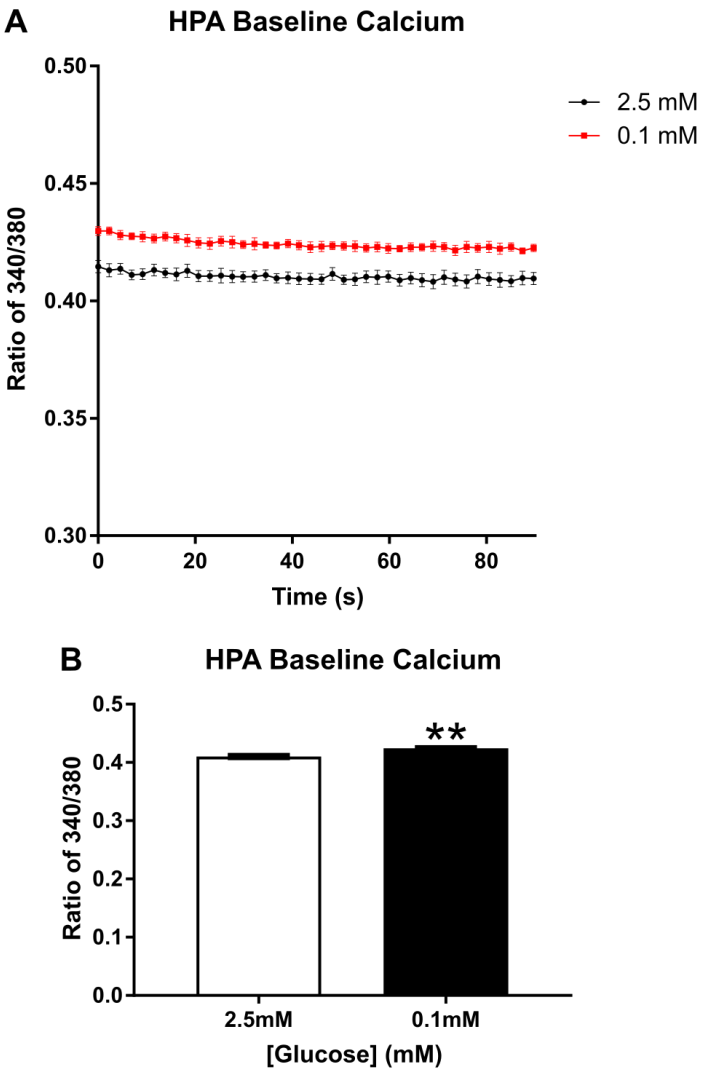

Figure 4.1. Acute low glucose increases basal calcium in human primary astrocyte (HPA)

HPA were exposed to 2.5 or 0.1 mM glucose for 3 hours and the ratio of bound/unbound calcium was measured using the cell permeable dye fura-2 (**A**). **B**. HPA basal calcium is increased by low glucose (n=5). **p<0.01 vs 2.5 mM glucose. Error bars represent standard error of the mean (SEM). Two-tailed unpaired student's t-test.

Figure 4.2

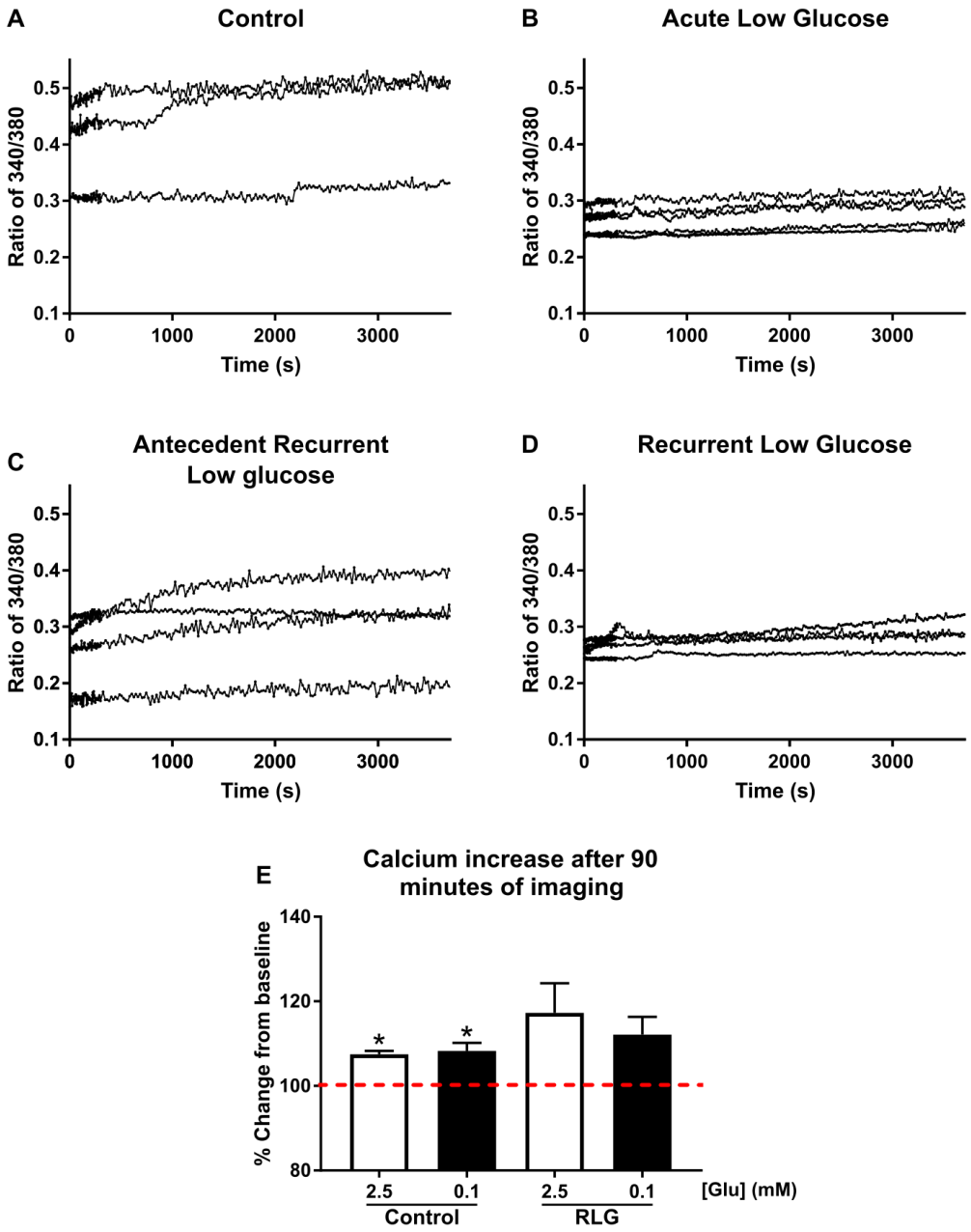

Figure 4.2. During measurement of intracellular calcium for 90 minutes, intracellular calcium increases in human primary astrocytes (HPA) regardless of recurrent low glucose (RLG)

HPA were exposed to control or RLG and loaded with fura-2. The ratio of bound and unbound calcium was measured using the cell permeable dye fura-2 while imaging media glucose concentrations were maintained in 2.5 or 0.1 mM glucose for 90 minutes. **A**. Control (n=3), (**B**) acute low glucose (n=5), (**C**) antecedent RLG (n=4), (**D**) RLG (n=4). E. All treatments increase basal calcium irrespectively of glucose concentration, significantly so in control and acute low glucose. *p<0.05 compared to baseline. Error bars represent standard error of the mean (SEM). One-sample t-test in comparison to baseline (100%, represented by the dashed red line).

Figure 4.3

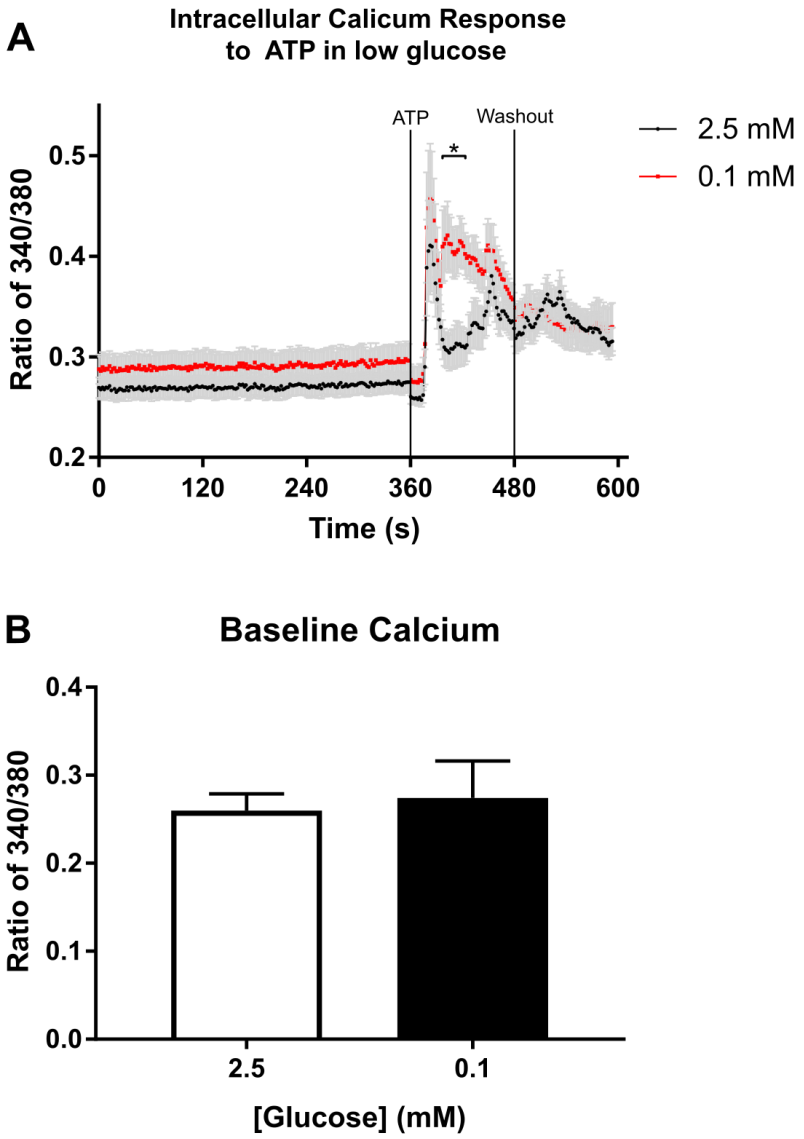

Figure 4.3. ATP stimulates increases intracellular calcium in human primary astrocytes (HPA) in either 2.5 or 0.1 mM glucose

HPA were exposed to 2.5 or 0.1 mM glucose for three hours and stimulated with 100 μM ATP, with the ratio of bound/unbound calcium measured using the cell permeable dye fura-2. **A**. raw trace of intracellular calcium in either 2.5 or 0.1 mM glucose with an ATP stimulation, the ATP response in 0.1 mM glucose was significantly different at some points, but the peak values were not significantly different. **B**. An average of basal intracellular calcium was unchanged by 2.5 (n=4 coverslips with 26 cells) or 0.1 mM (n=5 coverslips with 22 cells) glucose. Note there was no change to absolute peak Y value and the average intracellular calcium levels during ATP exposure were not different. *p<0.05 vs 2.5 mM glucose. Two-way ANOVA with post hoc Bonferroni multiple comparisons tests. Unpaired two-tailed student's t-test. Error bars represent standard error of the mean (SEM).

Figure 4.4.1

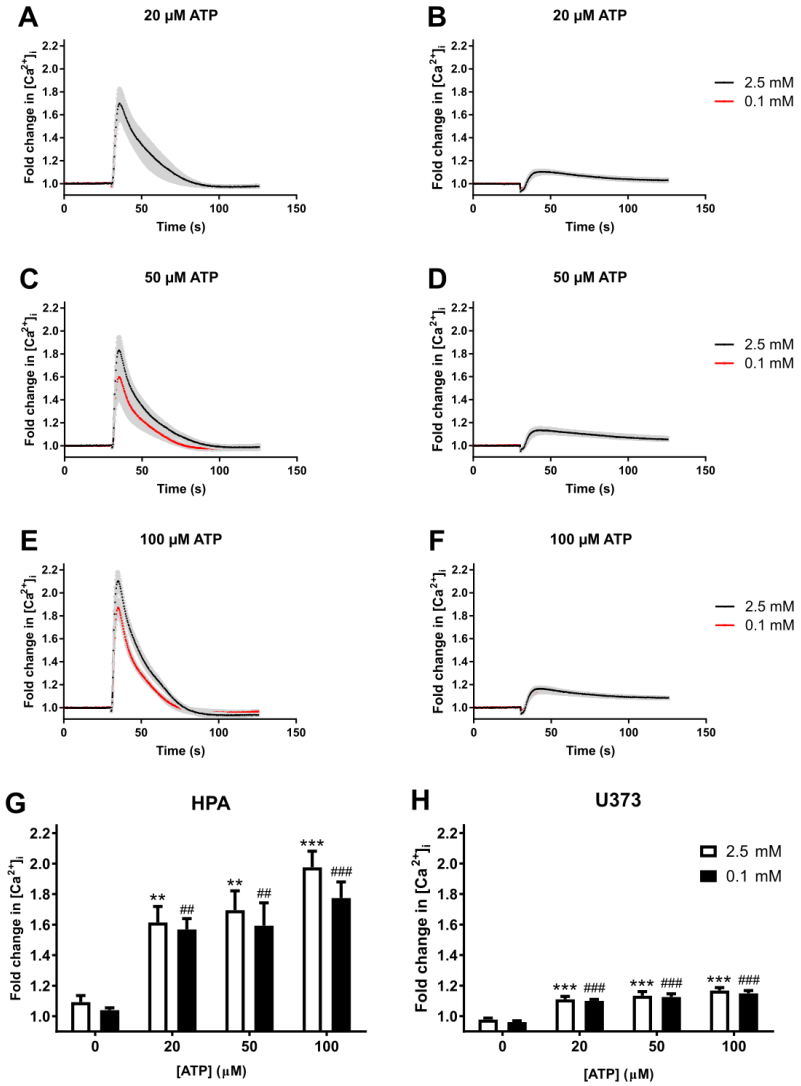

Figure 4.4.1 ATP stimulates increased intracellular calcium in human primary astrocyte (HPA) and U373 astrocytoma cells

HPA (n=6) and U373 (n=6) cells were exposed to 2.5 or 0.1 mM glucose for three hours before stimulation with 20, 50 or 100 µM ATP. Resulting changes to intracellular calcium were measured using the cell permeable, calcium sensitive dye Fluo-4. **A** and **B** show the responses of HPA and U373 cells to 20 µM ATP. **C** and **D**, show the responses of HPA and U373 cells to 50 µM ATP. **E** and **F** show the responses of HPA and U373 cells to 100 µM ATP. **G** and **H** show the peak response to each concentration of ATP in HPA and U373 cells respectively. "*" denotes significant differences of 2.5 mM glucose treated samples from 2.5 mM glucose vehicle *p<0.05, **p<0.01, ***p<0.001. "#" denotes significant differences between 0.1 mM glucose treated samples and the 0.1 mM vehicle ##p<0.01, ###p<0.001. One-way ANOVA with post hoc Bonferonni multiple comparison tests. Error bars represent standard error of the mean (SEM).

Figure 4.4.2

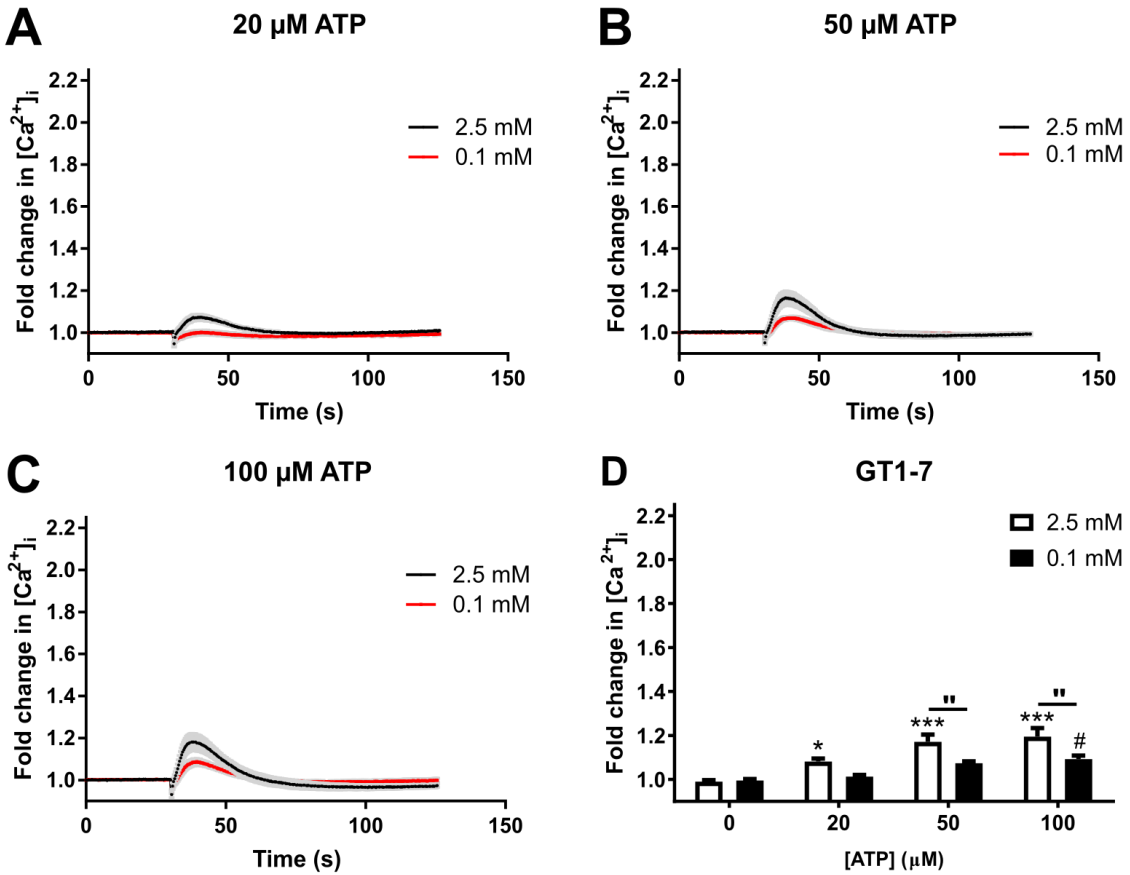

Figure 4.4.2 ATP stimulates increased intracellular calcium in GT1-7 glucose excited neurons

GT1-7 cells (n=7) were exposed to 2.5 or 0.1 mM glucose for three hours before stimulation with 20, 50 or 100 µM ATP. Resulting changes to intracellular calcium were measured using the cell permeable, calcium sensitive dye Fluo-4. **A**, **B** and **C** show the responses of GT1-7 cells to 20, 50 and 100 µM ATP. "*" denotes significant differences of 2.5 mM glucose treated samples from 2.5 mM glucose vehicle *p<0.05, ***p<0.001. "#" denotes significant differences between 0.1 mM glucose treated samples and the 0.1 mM vehicle #p<0.05. "p<0.05 between highlighted groups. One-way ANOVA with post hoc Bonferonni multiple comparison tests. Error bars represent standard error of the mean (SEM).

Figure 4.5

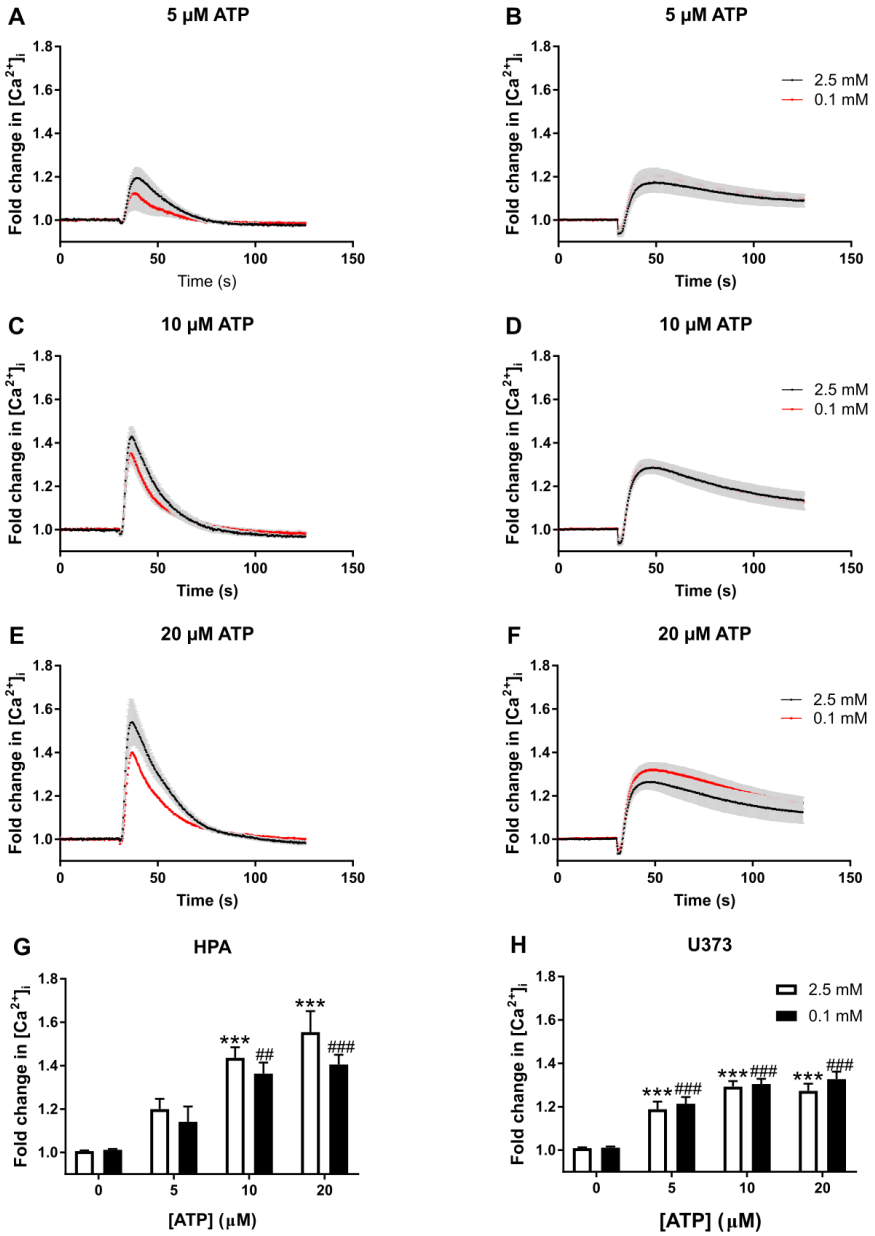

Figure 4.5. ATP increases intracellular calcium in human primary astrocyte (HPA) and U373 cells

HPA (n=4) and U373 (n=6) cells were exposed to three hours of 2.5 or 0.1 mM glucose, stimulated with 5, 10 and 20 µM ATP with intracellular calcium measured using the cell permeable calcium dye fluo-4. **A** and **B**, 5 µM increases intracellular calcium in HPA and U373 cells respectively. **C** and **D**, 10 µM increases intracellular calcium in HPA and U373 cells respectively. **E** and **F**, 20 µM increases intracellular calcium in HPA and U373 cells respectively. **G** and **H**, show the peak response to each ATP concentration used in HPA and U373 cells respectively. While there was a significant increase to intracellular calcium it did not differ between groups. ***p<0.001 significantly different from 2.5 mM glucose vehicle. ##p<0.01, ###p<0.001 significantly different from 0.1 mM glucose vehicle. Error bars represent standard error of the mean (SEM). One-way ANOVA with post hoc Bonferonni multiple comparison tests.

Figure 4.6

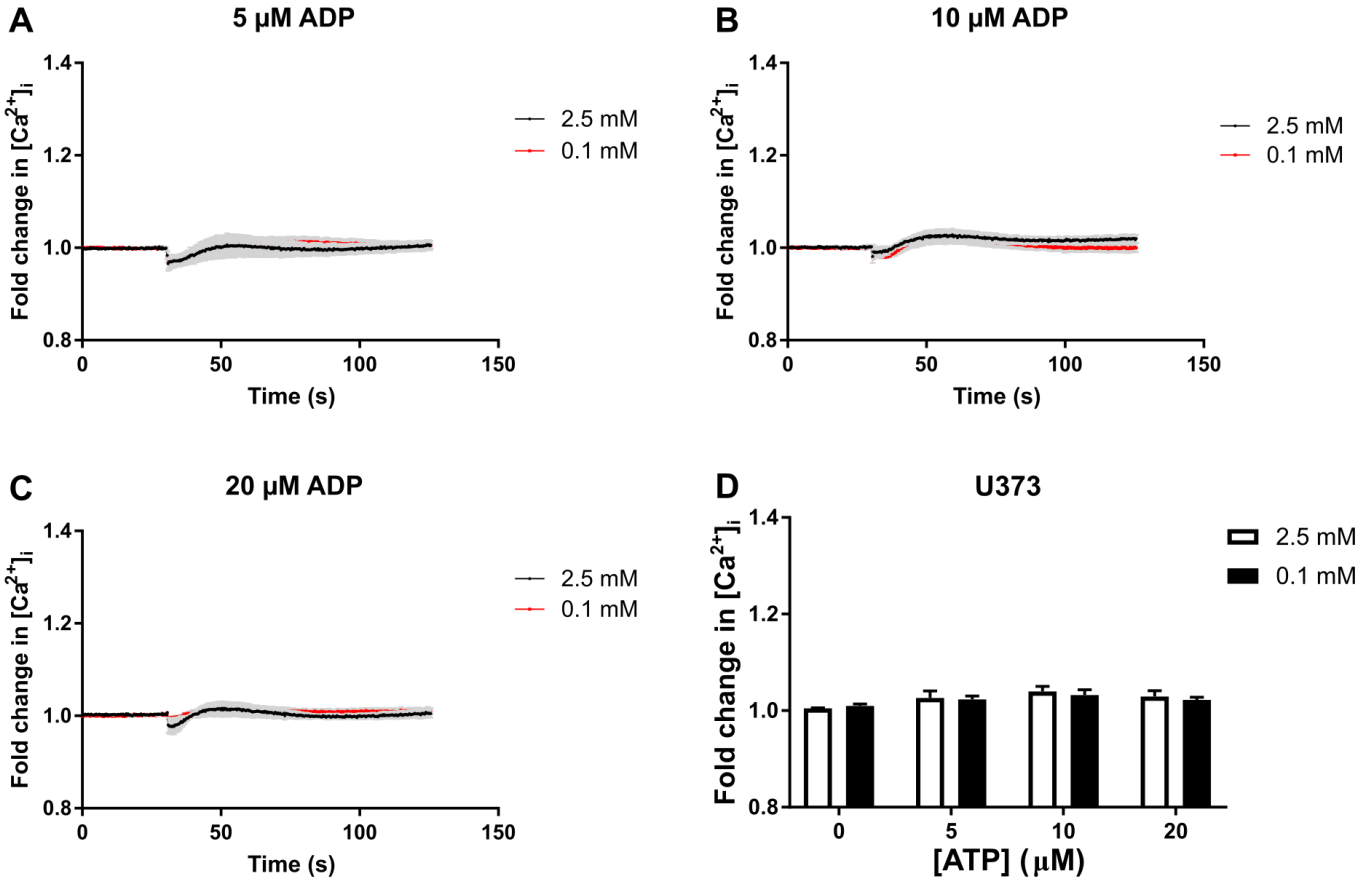

Figure 4.6. ADP does not significantly increase intracellular calcium in U373 astrocytoma cells

U373 (n=4) cells were cultured in 2.5 or 0.1 mM low glucose for 3 hours and stimulated with 5, 10 and 20 µM ADP. Changes to intracellular calcium were measured using the cell permeable calcium sensitive dye fluo-4. U373 intracellular calcium responses to 5 (**A**), 10 (**B**), and 20 µM (**C**) ADP. **D**. No significant differences were found in the peak responses to ADP at any concentration in comparison to vehicle. One-way ANOVA with post hoc Bonferroni multiple comparisons tests. Error bars represent standard error of the mean (SEM).

4.7 RLG does not modulate the intracellular Ca^{2+} response to ATP by HPA

As RLG significantly alters cellular metabolism, the $[Ca^{2+}]_i$ response to ATP was investigated. HPA cells were treated in control or RLG conditions with or without an additional exposure to medium containing 0.1 mM glucose on the final day. Cells were subsequently treated with 100 µM ATP. As seen previously, 100 µM ATP increased $[Ca^{2+}]_i$ but neither prior RLG nor low glucose exposure altered the response (figure 4.7A-D).

4.8 RLG U373 ATP dose responses

Given that purinergic receptors are differentially activated by different concentrations of agonist (Liu et al. 2001, Roberts et al. 2006) a lower range of ATP concentrations were used to stimulate U373 astrocytoma cells. As acute low glucose had no effect on ATP-induced calcium responses in these cells, they were assayed in 2.5 mM glucose after control or prior RLG.

4.8.1 RLG U373 higher ATP dose response

The following experiment was carried out by Julia Vlachaki Walker but included for completeness. U373 cells were treated with 20 (figure 4.8.1A), 50 (figure 4.8.1B), and 100 µM ATP (figure 4.8.1C). The peak ATP-induced response at each concentration was calculated and found to be significantly different compared to vehicle (figure 4.8.1D). Furthermore, prior exposure to RLG did not affect the calcium response of the U373 cells (figure 4.8.1D).

4.8.2 RLG does not modulate the intracellular Ca^{2+} response to ATP in U373 astrocytoma cells

To establish a more complete concentration curve, and to reveal any subtle differences, lower concentrations of ATP were used to stimulate U373 cells after control or prior RLG. U373 cells were treated with 5 (figure 4.8.2A), 10 (figure 4.8.2B), and 20 µM ATP (figure 4.8.2C). The peak fold-change in $[Ca^{2+}]_i$ was calculated and in control conditions, all ATP concentrations used stimulated a significant increase (figure 4.8.2D). However, with antecedent RLG while 10 and 20 µM ATP significantly increased $[Ca^{2+}]_i$ 5 µM did not (figure 4.8.2D). Nevertheless, there were no significant differences between control or antecedent RLG at any concentration used.

Figure 4.7

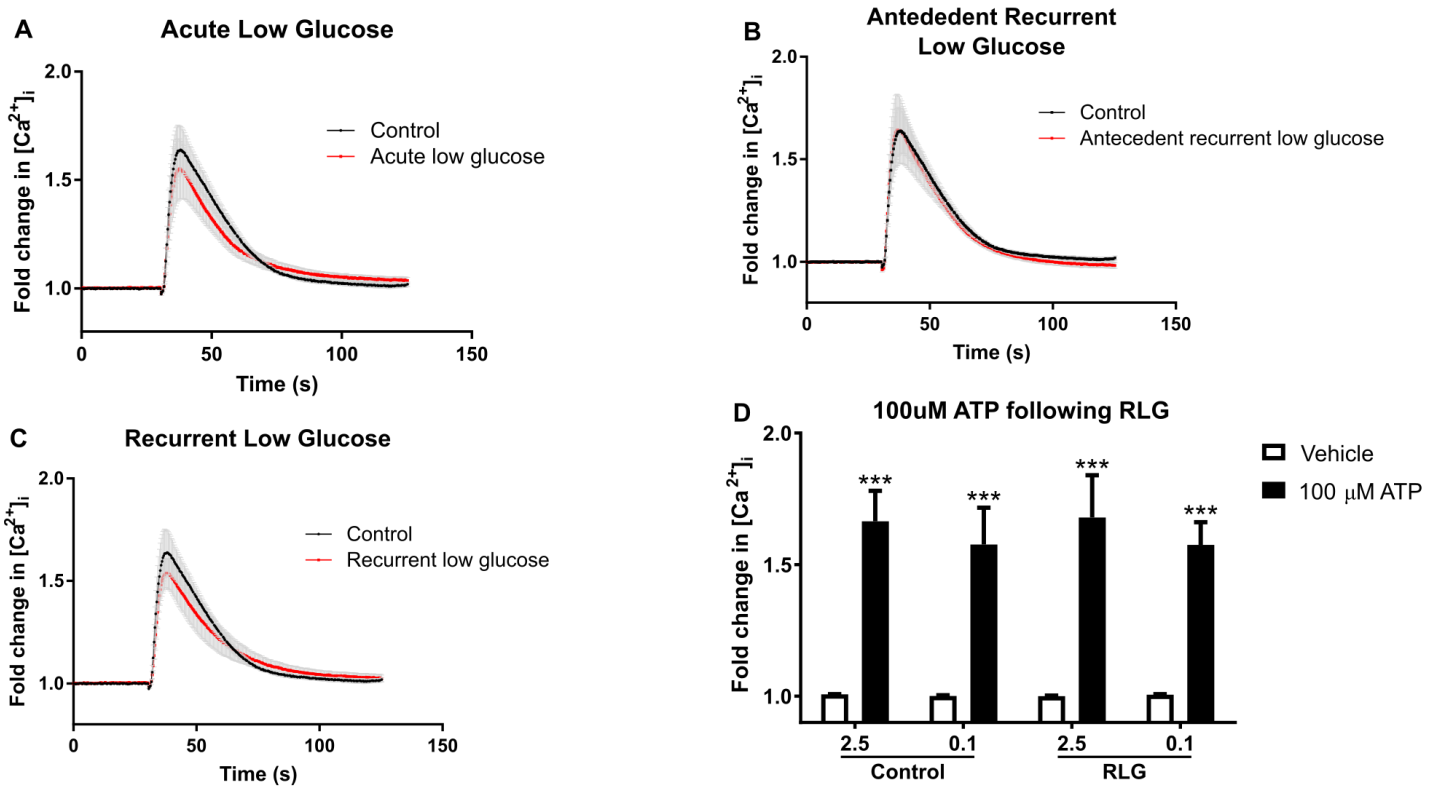

Figure 4.7. Recurrent low glucose (RLG) does not affect the ATP stimulated increase in intracellular calcium in human primary astrocytes (HPA)

HPA (n=5) were exposed to control or RLG and a further three hours of 2.5 or 0.1 mM and stimulated with 100 μM ATP. Changes to intracellular calcium were measured using the cell permeable, calcium sensitive dye fluo-4. **A**, **B** and **C**, show the fold change from baseline in intracellular calcium in acute low glucose, antecedent RLG, and RLG respectively. **D**. ATP caused intracellular calcium to significantly increase in comparison to vehicle, irrespectively of glucose concentration or pre-treatment. ***p<0.001 vs vehicle. One-way ANOVA with post hoc Bonferroni multiple comparisons tests. Error bars represent standard error of the mean (SEM).

Figure 4.8.1

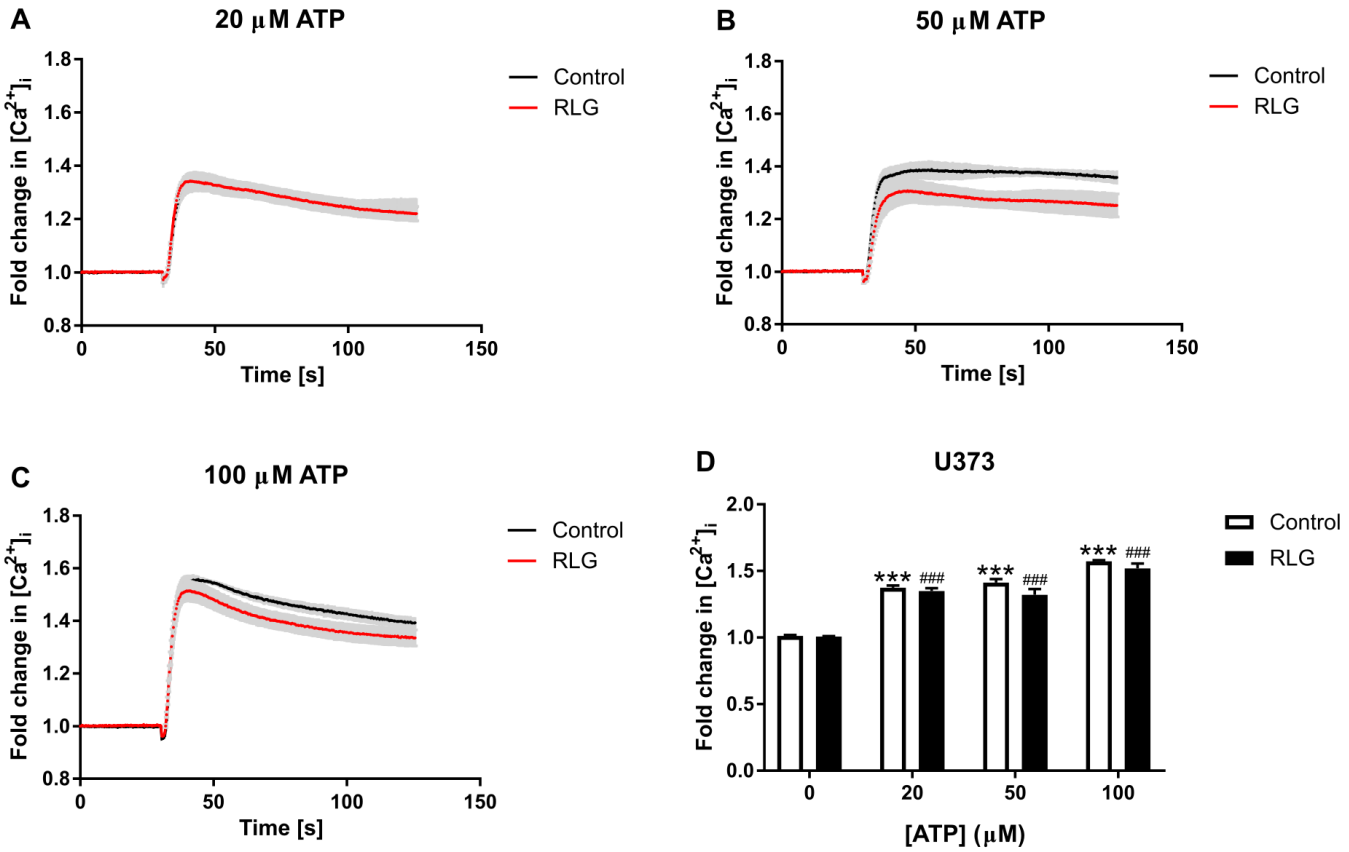

Figure 4.8.1. Recurrent low glucose (RLG) does not affect the ATP stimulated increase in intracellular calcium in U373 astrocytoma cells

U373 (n=4) were exposed to control or RLG and treated with vehicle, 20, 50 and 100 µM ATP in 2.5 mM glucose. Changes to intracellular calcium were measured using the cell permeable, calcium sensitive dye fluo-4. **A**, **B** and **C**, show the fold change from baseline in intracellular calcium in acute low glucose, antecedent RLG, and RLG respectively. **D**. ATP caused intracellular calcium to significantly increase in comparison to vehicle, irrespectively of pre-treatment. ***p<0.001 significantly different from control vehicle. ###p<0.001 significantly different from RLG vehicle. One-way ANOVA with post hoc Bonferroni multiple comparisons tests. Error bars represent standard error of the mean (SEM).

Figure 4.8.2

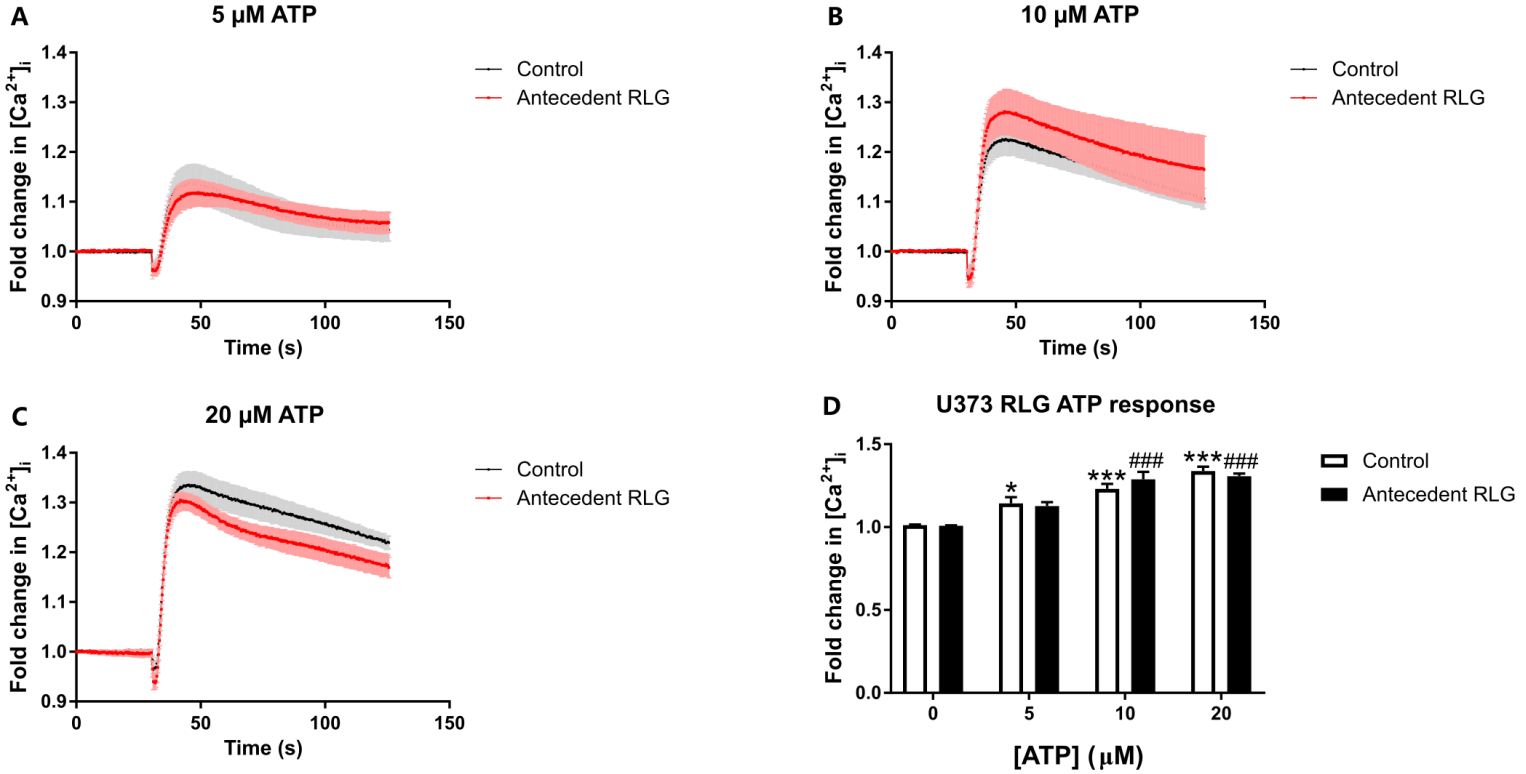

Figure 4.8.2. Prior recurrent low glucose (RLG) does not affect ATP stimulated increase in intracellular calcium in U373 astrocytoma cells

U373 cells were exposed to control or RLG and stimulated with 5 (n=5), 10 (n=5) or 20 (n=4) µM ATP in 2.5 mM glucose containing media. Changes to intracellular calcium were measured using the cell permeable, calcium sensitive dye fluo-4. **A**, **B** and **C**, show the fold change from baseline in intracellular calcium in response to 5, 10 and 20 µM ATP respectively. **D**. The peak response to any concentration did not differ between groups but was significantly elevated from vehicle, apart from 5 µM ATP in low glucose. "*" denotes significant differences between ATP treated controls and vehicle *p<0.05, ***p<0.001. "#" denotes significant differences between treated experimental groups and the experimental group treated with vehicle ###p<0.001. One-way ANOVA with post hoc Bonferroni multiple comparisons tests. Error bars represent standard error of the mean (SEM).

4.9 The broad spectrum P_2 antagonist, PPADS, but not the P_2X_7 antagonist, A438079, reduce HPA intracellular Ca^{2+} response to ATP

The P_2X_7 receptor has increased expression in diabetic rats' glomerulus (Vonend et al. 2004) and is associated with increased diabetic complications, particularly in the kidney (Platania et al. 2017). P_2X_7 receptors also modulate human astrocyte Ca2+ signalling and ATP release (Suadicani et al. 2006). Therefore, to test whether P_2X_7 mediates part of the calcium response to ATP treatment and whether this was altered by low glucose, HPA cells were treated with 100 µM ATP in combination with pyridoxalphosphate-6-azophenyl-2',4'-disulfonic acid (PPADS), a broad-spectrum P_2 receptor inhibitor, and 100 µM A438079 (A4) to block P_2X_7 receptor activity. PPADS significantly attenuated the ATP-induced increase in $[Ca^{2+}]_i$, only in acute low glucose conditions (figure 4.9A,B). A4 did not significantly alter the ATP-induced $[Ca^{2+}]_i$. Figure 4.9D shows the peak fold change in $[Ca^{2+}]_i$ of HPA cells treated with 100 µM and purinergic inhibitors.

4.10 Noradrenaline increases HPA and U373 astrocytoma intracellular Ca^{2+}

NA is released from locus coeruleus noradrenergic (LC-NA) neurons during hypoglycaemia (Morilak et al. 1987, Flugge 2000, Yuan et al. 2002). NA can stimulate glycogenolysis (Hutchinson et al. 2007, Gibbs et al. 2008a, Gibbs et al. 2008b, Gibbs 2015), leading to increased lactate release from astrocytes (Bittar et al. 1996). Importantly lactate perfusion into the VMN prevents full CRR to hypoglycaemia and increased lactate production may occur following RLG (Borg et al. 2003), which may occur by lactate induced GABA release (Chan et al. 2013). To determine whether HPA or U373 cells are sensitive to NA, they were treated with 10 (figure 4.10A,B), 50 (figure 4.10C,D) and 100 µM NA (figure 4.10E,F) in 2.5 or 0.1 mM glucose containing media. HPAs had approximately a 1.75-fold increase to $[Ca^{2+}]_i$ compared to 1.2-fold in U373 cells (figure 4.10G,H). There was no difference between 2.5 and 0.1 mM glucose treated cells at any concentration in either cell type (figure 4.10A-H). Preliminary experiments in SH-SY5Y neuroblastoma cells showed no sensitivity to NA (data not shown).

Figure 4.9

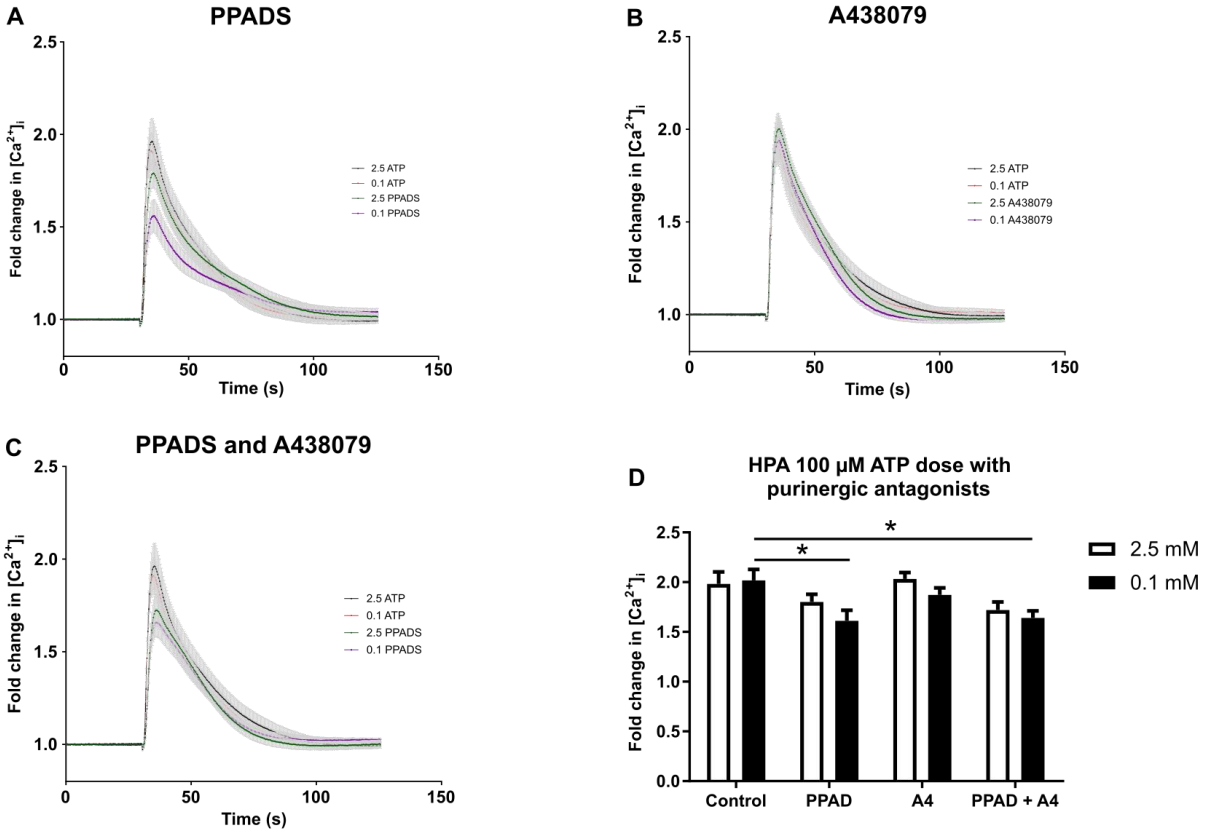

Figure 4.9. Pyridoxalphosphate-6-azophenyl-2',4'-disulfonic acid (PPADS) significantly reduces ATP-sensitive increase in intracellular calcium in human primary astrocytes (HPA)

HPA (n=8) were stimulated with 100 µM ATP after incubation in 2.5 or 0.1 mM media containing vehicle, PPADS, A438079 (A4), or PPADS and A4. PPAD is a broad spectrum P2 receptor antagonist whereas A4 is specific to the P2X7 receptor. **A**, **B** and **C**, show the fold change from baseline changes to intracellular calcium in response to 100 µM ATP in the presence of PPADS, A4, and PPADS with A4 respectively. **D**, the peak of ATP-sensitive calcium increase is significantly reduced by PPADs only in 0.1 mM glucose, whereas A4 did not affect the result. *p<0.05 between annotated groups. One-way ANOVA with post hoc Bonfeonni multiple comparisons tests. Error bars represent standard error of the mean (SEM).

Figure 4.10

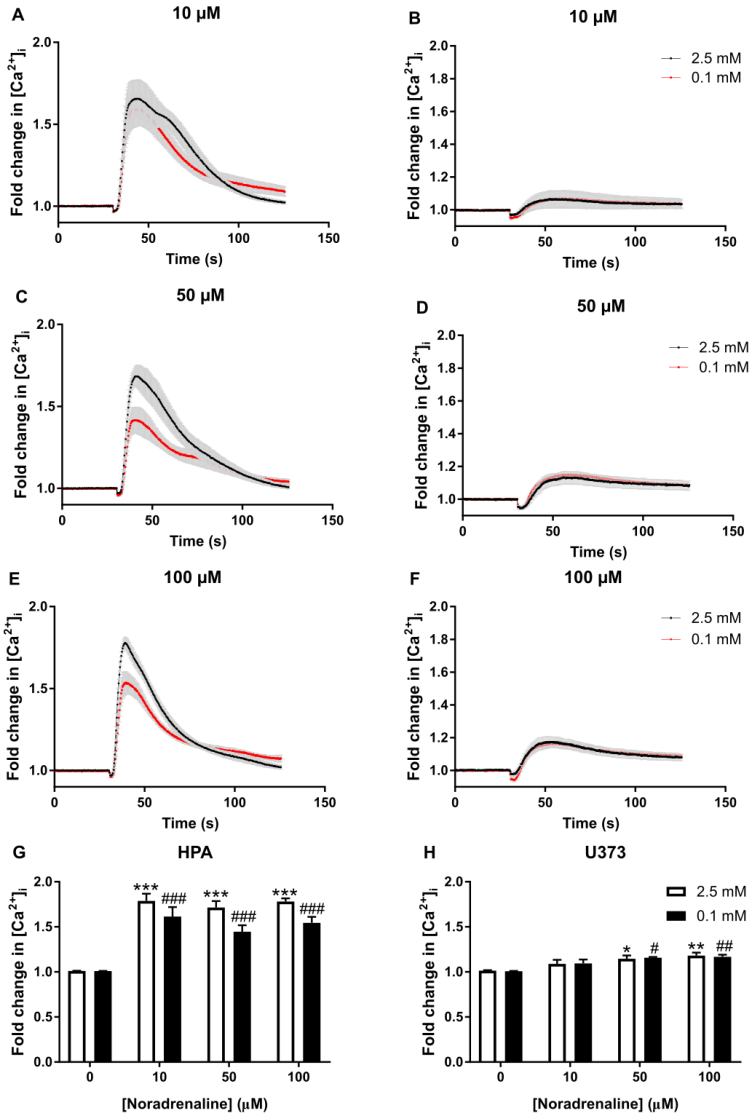

Figure 4.10. Noradrenaline (NA) increases intracellular calcium in human primary astrocytes (HPA) and U373 astrocytoma cells

HPA and U373 cells were cultured in 2.5 or 0.1 mM glucose for three hours and stimulated with NA at 10, 50 or 100 µM. Changes to intracellular calcium were measured using the cell permeable, calcium sensitive dye fluo-4. **A** and **B**, show the fold change from baseline of intracellular calcium in response to 10 µM NA in HPA and U373 respectively. This was significant in HPA but not at U373. **C** and **D**, show the significant fold change from baseline of intracellular calcium in response to 50 µM NA in HPA (n=5) and U373 (n=6) respectively. **E** and **F**, show the significant fold change from baseline of intracellular calcium in response to 100 µM NA in HPA and U373 respectively. **G** and **H**, show the peak change to intracellular calcium in response to NA at each concentration in HPA and U373 respectively. There were no significant differences between 2.5 and 0.1 mM glucose in any condition. "*" denotes significant differences of 2.5 mM glucose treated samples from 2.5mM glucose vehicle *p<0.05, **p<0.01, ***p<0.001. "#" denotes significant differences between 0.1 mM glucose treated samples and the 0.1 mM vehicle #p<0.05, ##p<0.01, ###p<0.001. One-way ANOVA with post hoc multiple comparisons tests. Error bars represent standard error of the mean (SEM).

4.11 Noradrenaline increases lactate release from HPA, U373 astrocytoma and SH-SY5Y

NA can stimulate glycogenolysis and increase lactate production (Bittar et al. 1996, Hutchinson et al. 2007, Gibbs et al. 2008a, Gibbs et al. 2008b, Gibbs 2015), which can negatively affect CRR to hypoglycaemia (Borg et al. 2003). Therefore, to test the effect of NA on both astrocytes and a neuronal cell line, lactate was measured in conditioned media from HPA, U373 and SH-SY5Y neuroblastoma cells exposed to 2.5 or 0.1 mM glucose conditions. While NA did not evoke a significant increase in $[Ca^{2+}]_i$ in SH-SY5Y cells NA may affect glycolytic pathways altering lactate release. NA significantly increased extracellular lactate concentrations by approximately 3-fold, 1.5-fold, and 2-fold for HPA, U373 and SH-SY5Y cells, respectively (figure 4.11A-C). The absolute amount of lactate present in the conditioned media was highest in the HPA (figure 4.11A). NA-stimulated lactate release from U373 cells was significantly lower in 0.1 mM glucose compared to control conditions (figure 4.11B). Furthermore, vehicle-treated cells cultured in 0.1 mM glucose also had significantly lower lactate levels in the extracellular medium (figure 4.11B).

4.12 Noradrenaline does not alter extracellular ATP in U373 astrocytoma and SH-SY5Y cells

ATP is co-released by sympathetic nerves (Burnstock 1990) and can modulate noradrenaline release in rat brain cortex (von Kügelgen et al. 1994). Furthermore, glutamate and adenosine stimulated release of ATP from astrocytes is dependent on glycogenolysis (Xu et al. 2013). However, whether or not this occurs with NA stimulation, known to induce glycogenolysis in astrocytes (Gibbs 2015), is unknown. To test whether this was the case, U373 and SH-SY5Y cells were treated with NA, and ATP content in conditioned media measured. Neither NA nor low glucose altered the eATP levels in conditioned media in either cell type (figure 4.12A,B). There was no detectable eATP in conditioned media from HPA cells under any conditions.

4.13 Serotonin increases extracellular lactate from U373 astrocytoma cells, but not HPA or SH-SY5Y cells

5HT has been implicated in modifying hypoglycaemia awareness (Sawka et al. 2000, Sawka et al. 2001, Briscoe et al. 2008a, Briscoe et al. 2008b, Sanders et al. 2008). Moreover, 5HT also mediates some of its effects on memory and learning in a

glycogenolysis-dependent manner (Gibbs 2015), which should also increase lactate release in astrocytes (Newman et al. 2011). To test whether lactate release was altered by 5HT, HPA, U373 and SH-SY5Y cells were stimulated with vehicle or 50 µM 5HT and lactate content of conditioned media quantified. There were no significant differences between 5HT and vehicle; regardless of glucose concentration in either HPA (figure 4.13A) or SH-SY5Y cells (figure 4.13B). However, 5HT did significantly increase lactate in the conditioned media of U373 cells (figure 4.13B) but this was unaffected by glucose concentration.

4.14 Serotonin does not alter extracellular ATP of U373 astrocytoma cells or SH-SY5Y cells.

To test whether 5HT altered release of ATP from SH-SY5Y (figure 4.14A) or U373 (figure 4.14B) cells, they were exposed to 30 minutes of 2.5 or 0.1 mM glucose with vehicle or 50 µM 5HT. The amount of ATP in the conditioned media was assayed and shown to be unaffected by 5HT in either cell type and unaltered by changes in glucose concentration.

Figure 4.11

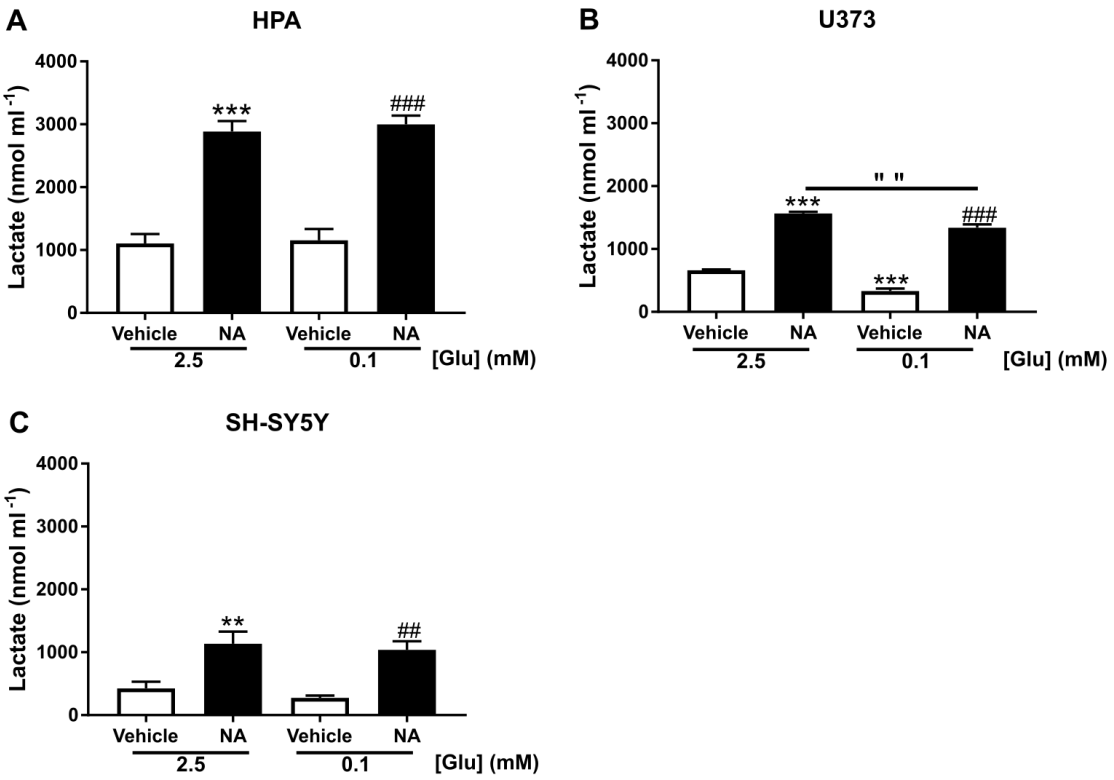

Figure 4.11. Noradrenaline (NA) increase lactate release in human primary astrocyte (HPA), U373 astrocytoma, and SH-SY5Y neuroblastoma cells

(n=4), U373 (n=3), and SH-SY5Y (n=6) cells were incubated in 2.5 or 0.1 mM low glucose for 30 minutes with vehicle or 50 μM NA. Lactate content within the conditioned media was quantified by fluorescence, plate based assay. **A**, **B** and **C**, NA significantly increases extracellular lactate in comparison to vehicle in HPA, U373, and SH-SY5Y cells respectively. Interestingly, in U373 cells low glucose significantly reduced both basal and NA stimulated lactate release compared to their respective controls. "*" denotes significant differences of 2.5mM glucose treated samples from 2.5mM glucose vehicle **p<0.01, ***p<0.001. "#" denotes significant differences between 0.1mM glucose treated samples and the 0.1mM vehicle ##p<0.01, ###p<0.001. ""p<0.1 denotes significance between annotated groups. One-way ANOVA with post hoc multiple comparisons tests. Error bars represent standard error of the mean (SEM).

Figure 4.12

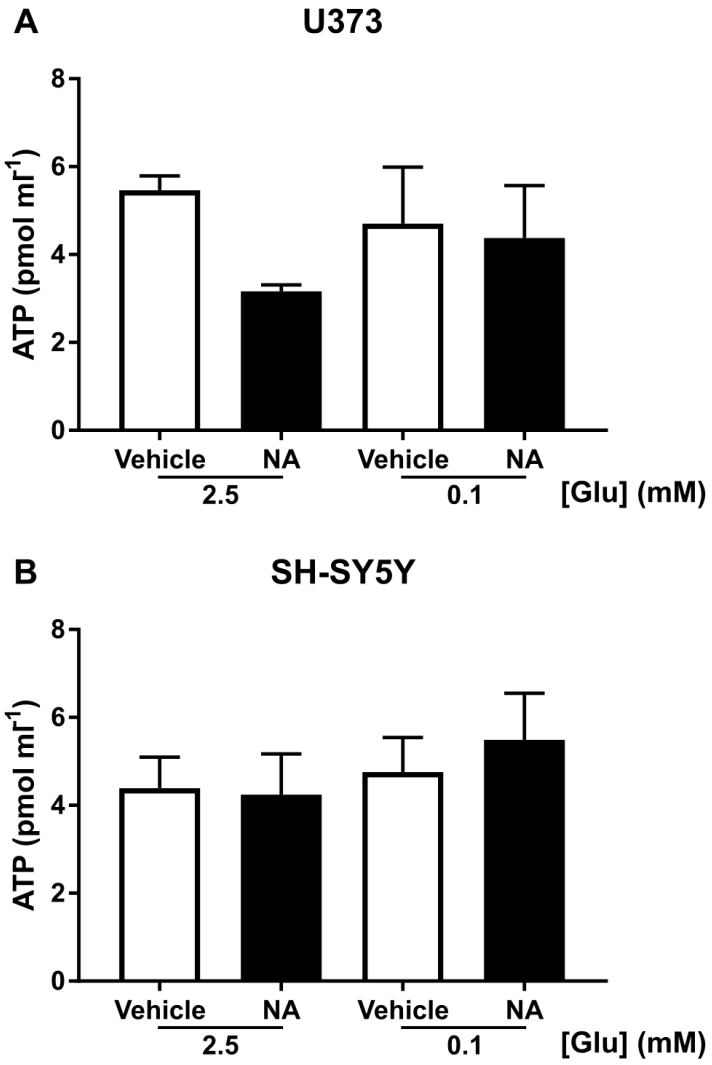

Figure 4.12. Noradrenaline (NA) does not significantly alter extracellular ATP (eATP) release from U373 and SH-SY5Y cells

U373 (n=3) and SH-SY5Y (n=6) were incubated in 2.5 or 0.1 mM low glucose for 30 minutes with vehicle or 50 μM NA. eATP content within the conditioned media was quantified by luminescence, plate based assay. **A** and **B**, NA does not increase eATP release from U373 or SH-SY5Y cells respectively. One-way ANOVA with post hoc multiple comparisons tests. Error bars represent standard error of the mean (SEM).

Figure 4.13

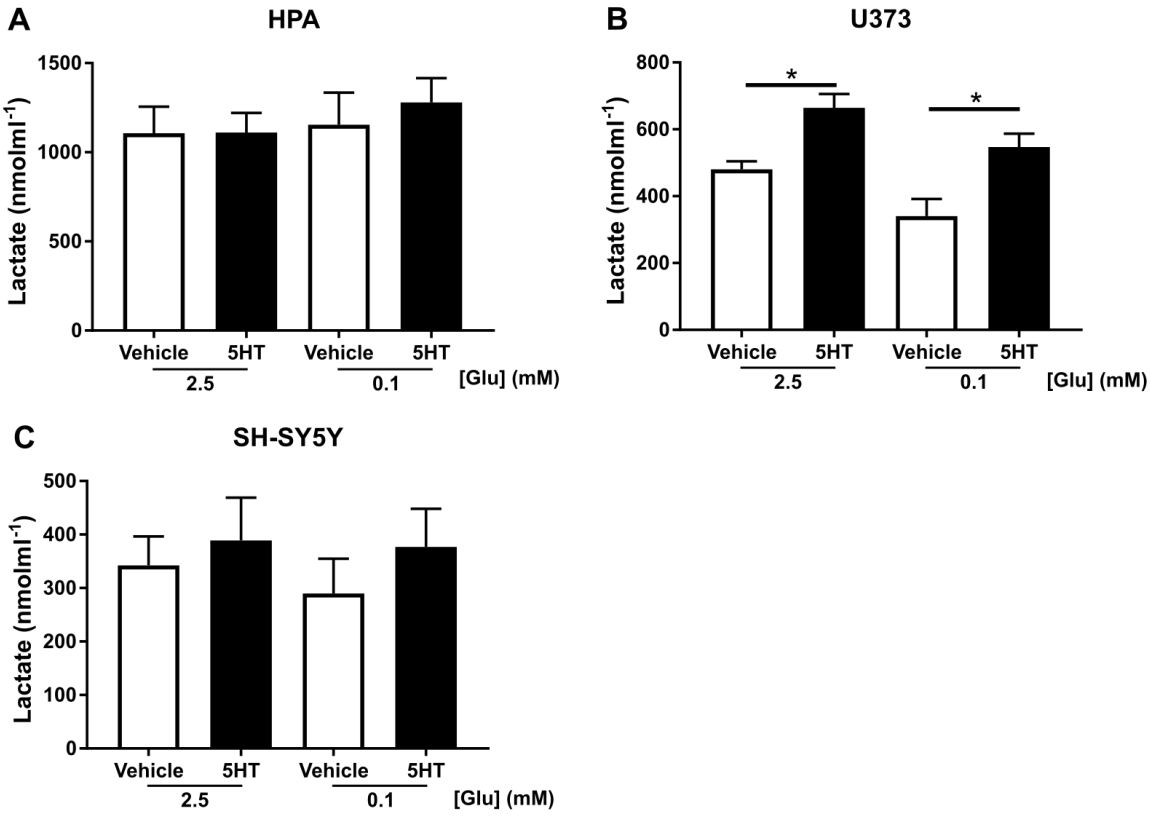

Figure 4.13. Serotonin (5HT) increases lactate release in U373 astrocytoma cells but not human primary astrocytes (HPA) or SH-SY5Y neuroblastoma cells

HPA (n=4) U373 (n=3) and SH-SY5Y (n=6) were incubated in 2.5 or 0.1 mM low glucose for 30 minutes with vehicle or 50 μM 5HT. Lactate content within the conditioned media was quantified by fluorescence, plate based assay. **A**, and **C**, 5HT did not increase intracellular lactate in HPA or SH-SY5Y cells respectively. **B**, 5HT significantly increased lactate content in conditioned media from U373 cells, but 2.5 or 0.1 mM glucose did not affect the result. *$p<0.05$ denotes significance between annotated groups. One-way ANOVA with post hoc multiple comparisons tests. Error bars represent standard error of the mean (SEM).

Figure 4.14

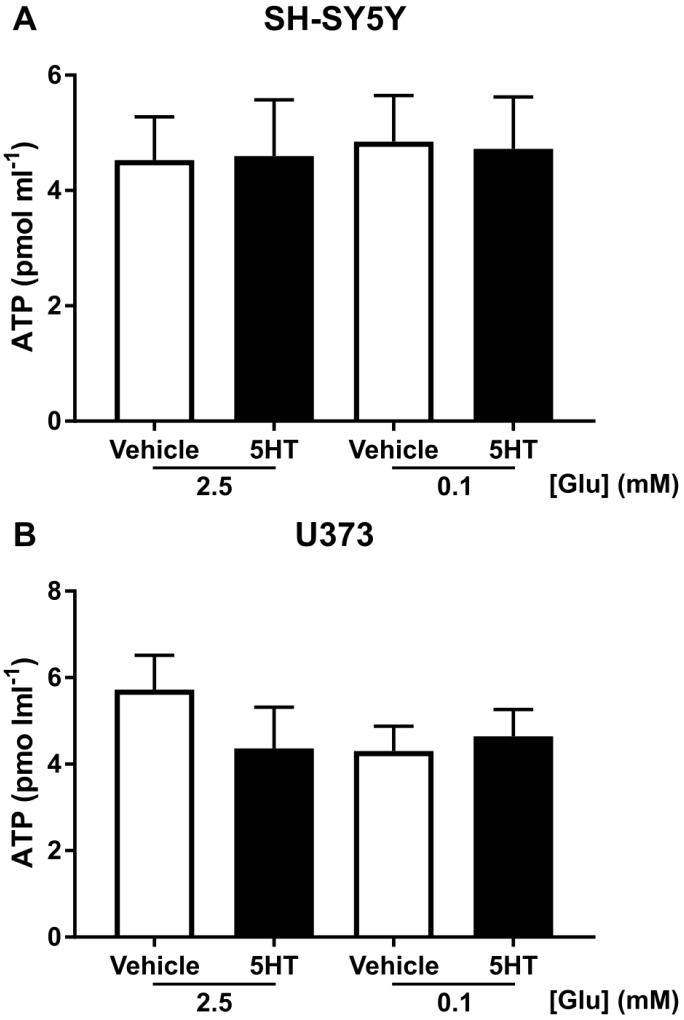

Figure 4.14. Serotonin (5HT) does not alter extracellular ATP (eATP) release from SH-SY5Y neuroblastoma U373 astrocytoma cells

SH-SY5Y (n=6), and U373 (n=3) were incubated in 2.5 or 0.1 mM low glucose for 30 minutes with vehicle or 50 μM 5HT. eATP content within the conditioned media was quantified by luminescence, plate based assay. **A** and **B**, 5HT does not increase eATP release from U373 or SH-SY5Y cells respectively. One-way ANOVA with post hoc multiple comparisons tests. Error bars represent standard error of the mean.

Discussion

Recurrent hypoglycaemia and diabetes are known to impair counterregulation (Heller et al. 1991, Segel et al. 2002). A complete understanding of glucose-sensing in the brain remains unknown and the aetiology of CRR blunting is poorly understood. Additionally, while the role of neurons as glucose-sensors has been known since 1953 (Mayer 1953), astrocytes have relatively recently come into the spotlight (Young et al. 2000, Ainscow et al. 2004, Guillod-Maximin et al. 2004, Lam et al. 2005b). Still, the effects of RLG on astrocytic calcium signalling remain poorly understood. Astrocytic signalling and activation is mediated by changes in $[Ca^{2+}]_i$ (Charles et al. 1991, Verkhratsky et al. 2012). Inter-astrocyte calcium signalling is also required for long range calcium wave propagation (Cornell-Bell et al. 1990, Cornell-Bell et al. 1991). Calcium signalling can modulate mitochondrial function by the activation of pyruvate, isocitrate, and α-ketoglutarate dehydrogenases and electron transport activity (Denton et al. 1972, Denton et al. 1978, Lawlis et al. 1981, Yamada et al. 1985, Hubbard et al. 1996, Territo et al. 2000). And in mouse neurons calcium signalling also increases AMPK activity via CaMKK2 (Anderson et al. 2008). While calcium can modulate mitochondria and therefore cellular metabolism (Denton et al. 1972, Denton et al. 1978, Lawlis et al. 1981, Yamada et al. 1985, Hubbard et al. 1996, Territo et al. 2000), calcium homeostasis requires a metabolic input; for example, the reuptake of calcium into the endoplasmic reticulum and its export through the plasma membrane by SERCA and PMCA respectively both require ATP (Carafoli 1991, Yu et al. 1993). Moreover, elevated resting $[Ca^{2+}]_i$ has been reported in neurons with concomitant mitochondrial dysfunction in mice with STZ-induced diabetes and db/db mice (Kostyuk et al. 1999). Furthermore, a low glucose (0.5 mM) or glucoprivic (5 mM 2-DG in 5 mM glucose) challenge increases $[Ca^{2+}]_i$ in a subset of NTS astrocytes (McDougal et al. 2011). Additionally, using DREADD (designer receptors exclusively activated by designer drugs) technology, Chen *et. al.*, demonstrated that increasing intracellular calcium in the GFAP expressing cells of the mouse arcuate nucleus increased food intake (Chen et al. 2016); demonstrating a role of astrocytes in regulating whole body energy homeostasis.

In the present study, 3 hours of low glucose exposure had conflicting outcomes depending on the methodology used to investigate the response. Using a plate reader there was a small increase in basal, unstimulated $[Ca^{2+}]_i$, however, using a

microscope to measure $[Ca^{2+}]_i$ imaging rig no significant difference was found. This may be due to a more prolonged imaging period with the microscope which could induce damage from the lasers used. Additionally, the cells studied with the plate reader had a higher confluency than those on glass coverslips used under the microscope. This may affect autocrine and paracrine signalling. For example, P2 signalling appears to be necessary for astrocyte-neuron signalling in reacting to glucoprivation or low glucose (McDougal et al. 2011). Given that RLG alters astrocyte metabolic phenotype (e.g. increased fatty acid oxidation and decreased coupling efficiency) and calcium homeostasis has a metabolic cost, it is plausible that calcium signalling may be affected by RLG. Over a 90-minute imaging period, HPA cell $[Ca^{2+}]_i$ significantly increased by about 10-20%, but this occurred in both 2.5 and 0.1 mM glucose and in control or RLG treated cells. Therefore, it is unlikely that prior RLG exposure or acute exposure to 0.1 mM glucose is having a large effect on HPA $[Ca^{2+}]_i$. The increase in $[Ca^{2+}]_i$ may be mediated by stress induced during the imaging period. For example, repeated light doses are known to be toxic to cells *in vitro* (Wang 1976, Tinevez et al. 2012). However, there may be an additional source of stress that is mediating this rise in calcium that remains unknown. Taken together, these studies contrast the findings by McDougal *et*. *al*. showing increased intracellular calcium in astrocytes in response to low glucose (McDougal et al. 2011). However, those studies used *ex vivo* slices from mice, whereas, the present studies were performed using human astrocytes without neuronal input. Furthermore, recent data suggests a large degree of heterogeneity in astrocytes within the brain (Verkhratsky et al. 2017). McDougal *et. al*. used brain slices containing the NTS, a region involved in regulating whole-body energy homeostasis (Grill et al. 1998, Marty et al. 2007), whereas, the HPA cells used in this study were from a generic sub-ventricular white matter region and have been cultured for up to 20 passages *in vitro*. Therefore, the HPA cells may no longer accurately represent their physiological setting, and/or input from other cell types is necessary for astrocytic glucose-sensing. Nevertheless, as shown previously, human astrocytes are able to defend intracellular ATP/ADP nucleotide ratios well after RLG and 3 hours of low glucose exposure. While these astrocytes suitably match ATP supply to demand they are not under the added pressure of recycling neurotransmitters, supporting neuronal function or being stimulated with additional astrocytic agonists.

Despite glucose not conclusively altering $[Ca^{2+}]_i$ in HPA cells, it was hypothesised that an additional challenge from ATP, a purinergic agonist, may have been altered by low glucose. ATP is also an important gliotransmitter (Guerra-Gomes et al. 2018) that can stimulate glutamate release from neurons (Perea et al. 2007), the principle neurotransmitter in the brain. ATP is also released from neurons *in vitro* in response to low glucose challenge (Zhang et al. 2007a). Interestingly, recent evidence shows astrocytic activation of chatecholaminergic neurons in mouse hindbrain is dependent on purinergic activity (Rogers et al. 2018). Nevertheless, ATP-induced increase in $[Ca^{2+}]_i$ in HPA and U373 cells were unaffected by low glucose. This shows that in addition to sustaining ATP production in low glucose, ATP-induced calcium signalling is maintained. The glucose excited GT1-7 cells were used as a positive control to show that ATP-induced increases in $[Ca^{2+}]_i$ can be attenuated by low glucose exposure, in a known glucose-sensing cell line (Beall et al. 2012b). This occurs as glucose excited cells via the K^+_{ATP} channel depolarise in high glucose and are hyperpolarised during low glucose (Beall et al. 2012a). Interestingly, ATP stimulated a 5-fold larger increase in $[Ca^{2+}]_i$ in HPA cells compared to U373 and GT1-7 cells. Purinergic receptor desensitisation can occur with repeated exposure to agonists (Kasakov et al. 1982). Therefore, the higher sensitivity found in HPA cells, may be due to the absence of detectable levels of ATP in HPA conditioned media resulting in no receptor desensitisation. Additionally, P_2 receptors may be more highly expressed in HPA cells than the U373 or GT1-7 cells.

ATP is metabolised extracellularly into ADP, AMP and adenosine by extracellular ectonucleotidases (E-NPP, E-NTDPase, and CD73) (Cunha et al. 1996, Velasquez et al. 2014). Adenosine can suppress (via A_1 receptors) (Dunwiddie et al. 2001) or augment (via A_{2A} receptors) (Cunha 2001) synapse excitation, therefore, modulating neurotransmission. Therefore, to determine whether the increase to $[Ca^{2+}]_i$ was due to ATP breakdown and to characterise the intracellular calcium response to other purinergic receptor modulators, U373 cells were stimulated with ADP, which had no significant effect. Therefore, the ATP-induced calcium transients were likely due to ATP itself and not its breakdown products. However, to rule out whether adenosine was acting on adenoreceptors receptors and increasing $[Ca^{2+}]_i$ adenosine should be used to treat the cells in a similar manner. Nevertheless, to confirm that ATP was binding to purinergic receptors and having a direct effect on $[Ca^{2+}]_i$, the broad

spectrum P2 inhibitor, PPADs, was used to block purinergic receptors. Interestingly, this only significantly reduced $[Ca^{2+}]_i$ in 0.1 mM glucose compared to vehicle. However, there was also no significant difference between 2.5 or 0.1 mM glucose treated cells also given PPADs. This suggests that while some of the ATP-induced increase in $[Ca^{2+}]_i$ is due to receptors blocked by PPADs, the majority is being mediated by those that are not, i.e. P_2X_4, P_2Y_1, P_2Y_{11}, P_2Y_{13}, or P_2Y_{14}. P_2X_7 is a receptor found in astrocytes and when sufficiently activated can result in release of excitatory amino acids (Duan et al. 2003), and ATP (Suadicani et al. 2006). A selective P_2X_7 antagonist, A4, did not significantly alter ATP-induced $[Ca^{2+}]_i$ responses, therefore P_2X_7 is not involved in the calcium response in HPA cells at the concentrations used in the current study. P_2X_7, is a heterotrimeric receptor that requires higher ATP concentrations to fully activate it (Syed et al. 2012). Therefore, to fully rule out P2X7 activity in HPA and U373 cells, a high concentration of ATP should be used.

During hypoglycaemia in rats, NA is released from LC-NA neurons into the VMN (de Vries et al. 2005). Additionally, this response was prevented by glucose perfusion into the VMN during systemic hypoglycaemia (de Vries et al. 2005). This provides compelling evidence that NA is a part of the CRR to hypoglycaemia. NA is known to have effects on metabolism, for example, α-adrenergic receptor activation has been shown to increase hyperglycaemia *in vivo* (Metz et al. 1978, Nakadate et al. 1980, DiTullio et al. 1984, Angel et al. 1990), and, β_2-adrenergic receptor agonism in the VMN improves CRR (Szepietowska et al. 2011). Repeated 2-DG-induced glucoprivation also blunts the NA response to further glucoprivation and glucoregulatory responses, including decreased activation of chatecholaminergic cells (Sanders et al. 2000).

NA binds to adrenergic receptors to increase $[Ca^{2+}]_i$, or to either increase or decrease $[cAMP]_i$ depending on the receptor. NA has been shown to increase glucose uptake and increase glycogenolysis specifically in astrocytes (Salm et al. 1989, Salm et al. 1992, Shao et al. 1992) (Catus et al. 2011). Activation of β-adrenergic receptors increases cAMP which activates protein kinase A which then activates glycogenolysis via activating glycogen phosphorylase (Mayes et al. 2003). By this process, glycolytic activity will increase within astrocytes and result in increased lactate production due to astrocytes expressing LDH5 (Bittar et al. 1996).

This lactate release could be detrimental to CRR (Borg et al. 2003). In the present study HPA, U373 and SH-SY5Y neuroblastoma cells had increased lactate levels in their conditioned media. SH-SY5Y cells were used as a comparator for differences in responses of human astrocytes and neurons to neurotransmitters. Interestingly, the lactate release from U373 cells was diminished in low glucose, but not HPA or SH-SY5Y cells. Interestingly, lactate uptake and utilisation triggers GABA release within the VMN which is normally suppressed during hypoglycaemia but enhanced following RH (Chan et al. 2013). In euglycaemia GABA suppresses the release of glucagon and adrenaline, whereas in hypoglcyaemia GABAergic tone is suppressed (Zhu et al. 2010). The decrease in lactate release from U373 cells during hypo would hypothetically correspond in less GABA release; however, no decrease is seen in HPA cells. In previous studies presented in this thesis (figure 3.17) RLG did not affect lactate release from either U373 or HPA cells. Still, if NA increases lactate release from human neural cells this could suppress glucagon and adrenaline release.

It is interesting that the SH-SY5Y cells had an increase in lactate production, albeit lower than the astrocytes, as mature neurons contain very little glycogen (Brown 2004). Therefore, it is unlikely that NA would be triggering significant glycogenolysis. NA could be stimulating glycolysis which would increase lactate production.

NA significantly increased $[Ca^{2+}]_i$ in both HPA and U373 cells, whereas, SH-SY5Y cells did not. Therefore, HPA and U373 cells likely contain α-adrenergic receptors that increase $[Ca^{2+}]_i$, whereas SH-SY5Y cells do not. Previously α-adrenergic receptors have been confirmed in rat and human astrocytes immunochemically *in situ* (Aoki et al. 1998, Milner et al. 1998, Glass et al. 2001). As NA did not increase $[Ca^{2+}]_i$ in SH-SY5Y cells, the increased lactate release is likely mediated by β-adrenergic receptors that use the secondary signalling molecule cAMP. Likewise, the HPA and U373 cells may also contain β-adrenergic receptors.

Neurons are able to use lactate as a metabolic substrate during energy deprivation or to fuel high levels of activity (Pellerin 2003). This may be important when LC-NA neurons become particularly active in response to stressors, like hypoglycaemia. On the other hand, lactate can be detrimental to CRR as exogenous lactate supply to the VMN prevents CRR to hypoglycaemia (Borg et al. 2003). Either way, the lactate

release caused by NA in HPA, U373 and SH-SY5Y cells was unaffected by the amount of glucose present. This data therefore shows that the action of NA on isolated astrocytes and neuronal cells is preserved during acute low glucose. Lastly, NA did not significantly alter any ATP release from U373 or SH-SY5Y cells, suggesting that NA mediates its effects in an ATP-independent manner. Taken together these data show that HPA, U373 and SH-SY5Y cells are sensitive to NA signalling by increasing $[Ca^{2+}]_i$, in HPA and U373 cells, or increasing lactate release in all cell types. Given that RH blunts NA signalling (Davis et al. 1997), it would be interesting to determine whether the NA response is altered by RLG.

5HT is a monoamine that modulates mood (Martinowich et al. 2008), memory formation (Gibbs 2015), and hypoglycaemia counterregulation (Briscoe et al. 2008a, Briscoe et al. 2008b, Sanders et al. 2008). SSRIs are used to treat depression by preventing reuptake of 5HT leading to increased seretonergic activity in hindbrain nuclei which are associated with mood control (Stahl 1998, Andrews et al. 2015). Additionally, while some evidence suggests SSRI usage worsens hypoglycaemia awareness and incidence (Sawka et al. 2000, Sawka et al. 2001), SSRIs have also been shown to improve the CRR (Briscoe et al. 2008a, Briscoe et al. 2008b, Sanders et al. 2008). Mechanistically, 5HT improved glucoregulatory hormone responses, autonomic drive, and increased lipolysis and hepatic glucose production that help defend against hypoglycaemia (Briscoe et al. 2008a, Briscoe et al. 2008b, Sanders et al. 2008).

5HT acts via serotonergic receptors $5HT_{1-7}$ which mainly act through modulating $[cAMP]_i$ (Nichols et al. 2008). Increased $[cAMP]_i$ can activated glycogenolysis via PKA activation of glycogen phosphorylase (Gibbs 2015) and therefore modulate lactate release from astrocytes (Bittar et al. 1996). While U373 cells increased lactate release when treated with 5HT, HPA and SH-SY5Y cells did not. This indicates that U373 cells likely express 5HT4, 6 and 7 receptors that are G_s-protein coupled and increase $[cAMP]_i$. Likewise, these receptors are unlikely to be present in HPA or SH-SY5Y cells. $5HT_2$ and $5HT_3$ receptors can increase $[Ca^{2+}]_i$ via calcium release from intracellular stores or influx of Ca^{2+} ions (Nichols et al. 2008). Future studies should investigate whether 5HT is increasing intracellular calcium in HPA, U373 or SH-SY5Y cells as this could alter their activation state.

Depending on the site of SSRI-induced lactate release it may have differential effects on CRR. For example, 5HT mediated lactate release could contribute to neuronal supply according to the astrocyte-neuron lactate shuttle hypothesis (Pellerin et al. 2012). This could then facilitate the activity of neurons that do not directly sense glucose, i.e. LC-NA neurons in the locus coeruleus. In this context SSRIs could contribute to CRR. Conversely, if SSRIs increase serotonergic activity resulting in lactate release in the VMN this would be detrimental to CRR (Borg et al. 1997).

The data presented in this chapter show that HPA do not increase $[Ca^{2+}]_i$ in response to acute or recurrent low glucose. Additionally, ATP and NA-induced $[Ca^{2+}]_i$ are unaffected by low glucose, while glucose excited GT1-7 cells are. While calcium homeostasis requires ATP (Carafoli 1991, Yu et al. 1993), astrocytes sustain calcium homeostasis during glucose restriction. These data are in conjunction with findings from chapter 3 where both HPA and U373 cells defend intracellular nucleotide ratios during acute and recurrent low glucose. These studies characterise for the first time the responses of isolated human astrocytes to low glucose with additional stimulation. However, a more replete model including the interaction of other cell types would likely alter the results. For example, rat and mouse hindbrain astrocytes can react to low glucose by increasing $[Ca^{2+}]_i$ when not in isolation (McDougal et al. 2011, Rogers et al. 2018). This suggests that other cellular inputs might trigger the astrocytic calcium response to low glucose that then mediates changes in neuronal activity.

Chapter 5

Glucose variation increases inflammation in human astrocytes

Introduction

All forms of diabetes are associated with pathological hyperglycaemia, which induces inflammation (Lin et al. 2005). The current medical practice is to restore euglycaemia with glucose-lowering agents, such as, sulfonylureas, metformin, and in those without endogenous insulin production, exogenous insulin is provided. The implementation of these glucose lowering medications must be measured as iatrogenic hypoglycaemia can be a common occurrence, particularly in those with T1DM undergoing intensive insulin therapy (Edridge et al. 2015). The occurrence of hypoglycaemia is the limiting factor in sustaining optimal glucose control (Cryer 2008). Indeed, as optimal glucose control is not achieved currently diabetes still causes a progressive deterioration of the central and peripheral nervous system (Di Mario et al. 1995, Jacobson et al. 2007, Little et al. 2007) as well as the vasculature (Duh et al. 1999).

Hypoglycaemia in healthy people, and those with diabetes, increases proinflammatory, prothrombotic and proatherogenic cytokines, including plasminogen activator inhibitor-1 (PAI-1), vascular endothelial growth factor (VEGF), vascular adhesion molecules, and interleukin-6 (IL-6) (Gogitidze Joy et al. 2010, Wright et al. 2010). The inflammatory response to hypoglycaemia is exacerbated by recovery immediately to hyperglycaemic conditions where oxidative stress and inflammation are further worsened (Ceriello et al. 2012). Interestingly, while RH blunts the CRR to further hypoglycaemia, it appears to exacerbate cytokine release (Joy et al. 2015) and prevent the normal rise in leukocytes, which are strongly correlated with the adrenaline response to hypoglycaemia (Ratter et al. 2017).

Inflammation is involved in many CNS diseases (Chavarria et al. 2004). Within the CNS microglia are the predominant immune cells, and are activated by RH in diabetic rats (Won et al. 2012). However, astrocytes are also sensitive to inflammatory stimuli (John et al. 2001, Murakami et al. 2003, Walter et al. 2004, Ballerini et al. 2005, Kucher et al. 2005, Narcisse et al. 2005) and can release a range of pro-inflammatory factors including tumour necrosis factor-α (TNF-α) (Beattie et al. 2002, Pribiag et al. 2013, Habbas et al. 2015), IL-1β (Choi et al. 2014) and IL-6 (Erta et al. 2015). Moreover, some studies show that astrocytes regulate the inflammatory response of microglia (Aloisi et al. 1997, Vincent et al. 1997, Pyo et al. 2003, Min et al. 2006, Kim et al. 2010). Diabetes is characterised by hyperglycaemia,

as such much work has focussed on the effects of high glucose exposure has on a range of cell types. Astrocytes exposed to high glucose increase cytokine expression, including: TNF-α, IL-6, IL-1B, IL-4, and VEGF (Wang et al. 2012). Interestingly, co-treatment with ROS scavengers and inhibition of NFκB prevented cytokine expression, indicating hyperglycaemic mediated CNS inflammation may be mediated by NFκB and oxidative stress. In glucose/oxygen deprivation, an ischaemia model, IL-1β, IL-6, and TNF-α expression increased as well as NFκB activation in astrocytes (Zhao et al. 2013).

Inflammatory signalling can modulate the activity of local neurons, for example central administration of IL-6 increases energy expenditure in mice and protects against diet induced obesity (Wallenius et al. 2002). Additionally, IL-6 activates the hypothalamic-pituitary-adrenal axis (van der Meer et al. 1996) and increases glucagon secretion in man (Tsigos et al. 1997). Within the CNS, astrocytes are the principle source of IL-6 (Van Wagoner et al. 1999) and therefore may directly modulate whole-body energy status through inflammatory signalling. Additionally, astrocyte specific inactivation of NFκB protected against high fat diet induced obesity in mice (Buckman et al. 2015, Douglass et al. 2017). Fasting also induces astrocyte expansion and activation (Daumas-Meyer et al. 2018), but the effects on inflammatory signalling remain unknown. The present study aimed to characterise the cytokines released by isolated human astrocytes in response to acute and recurrent low glucose treatment. Interesting targets were then validated and quantified. In brief these studies show that macrophage migration inhibitory factor specifically is upregulated by low glucose exposure. Secondly, U373 cells have upregulated PAI-1 release following RLG. Lastly, preliminary evidence suggests that general cytokine release is increased with low glucose and RLG in HPA cells.

Overall aim and objectives

Hypoglycaemia induces the increase of inflammatory markers in humans and these may be associated with acute and chronic consequences of T1DM. Furthermore, extremes in nutritional state induce changes in astrocyte inflammatory state. However, the study of human astrocytes during acute and recurrent low glucose has not thoroughly investigated changes to cytokine release. This chapter's primary aim was to uncover cytokines released by HPA cells during acute and recurrent low glucose. This was achieved by addressing the following research questions:

- What cytokines are released by HPA cells during acute and recurrent low glucose?
- How may these cytokines contribute to impaired hypoglycaemia counterregulation?

Results

5.1 Identification of cytokines differentially released by HPA exposed to glucose variation

Hypoglycaemia triggers cytokine release in both healthy people and those with diabetes (Gogitidze Joy et al. 2010, Wright et al. 2010), although typically those with diabetes have higher baseline cytokine levels than controls. However, the specific release of cytokines within the CNS in response to low glucose is less understood. Hyperglycaemia and high glucose triggers the release of cytokines from glial cells (Lin et al. 2005, Wang et al. 2012). And glucose/oxygen deprivation also releases cytokines from astrocytes. This study aimed to characterise the cytokines that are differentially released from HPA cells exposed to control, acute low glucose, antecedent low glucose or RLG. Using a human cytokine array panel more cytokines were detectable in the conditioned media from acute low glucose, antecedent low glucose and RLG treated HPA cells than control (figure 5.1A). The map of where each cytokine is detected is in figure 5.1B. IL-13, MIF and PAI-1 were strongly detected in the control samples and appeared to be differentially regulated by glucose treatments. To semi-quantitatively analyse the change densitometric analysis was performed. IL-13 appeared to be increased compared to control in all groups (figure 5.2A). MIF appeared to be elevated in all groups compared to control but especially so in low glucose (figure 5.2B). PAI-1 appeared to be elevated by low glucose (figure 5.2C). The additional densitometry of all detectable cytokines can be found in appendix B.

5.2 Interleukin-13 in the conditioned media of HPA and U373 astrocytoma cells is unaltered by RLG

IL-13 is a cytokine with similar activity to IL-4 (Minty et al. 1993). IL-13 is an anti-inflammatory cytokine that is necessary for the suppression of post-prandial hepatic glucose production (Stanya et al. 2013). IL-13 KO in mice induces insulin resistance, weight gain and metabolic syndrome, implicating IL-13 as an important metabolic regulator (Stanya et al. 2013). However, despite an apparent increase in IL-13 release by RLG in the cytokine array panel, there was no significant difference found in HPA or U373 cells using targeted ELISA (figure 5.2A,B).

5.3 Plasminogen activator inhibitor-1 in the conditioned media of HPA and U373 astrocytoma cells is unaltered by RLG

PAI-1 is a serine protease inhibitor which prevents plasmin from degrading extracellular matrix proteins involved in the clotting response (Ghosh et al. 2011). In T2DM PAI-1 is elevated and implicated in insulin resistance (Potter van Loon et al. 1993, Juhan-Vague et al. 2003), and therefore also correlates with development of T2DM (Festa et al. 2002). Furthermore, PAI-1 is also detected in the cerebrospinal fluid of patients with AD (Sutton et al. 1994). Plasmin, inhibited by PAI-1, normally degrades Aβ, therefore PAI-1 may contribute to Aβ accumulation in AD (Kutz et al. 2012). However, despite there being an apparent increase in PAI-1 release from HPA in the cytokine array panel, there were no significant differences detected in HPA cells (figure 5.3A). Interestingly, U373 cells did significantly increase PAI-1 release when treated with RLG compared to control and acute low glucose treated cells (figure 5.3B). Antecedent RLG also increased from control but did not reach significance. It appears that PAI-1 may remain elevated even following a recovery period. Furthermore, the release of PAI-1 appears to be a dose dependent response, where each bout of low glucose increases PAI-1 expression.

5.4 Macrophage-migration inhibitory factor in the conditioned media of HPA or U373 astrocytoma cells is unaltered by RLG

MIF is an inflammatory cytokine that suppresses glucocorticoid function (Calandra et al. 1995), and triggers the release of other pro-inflammatory cytokines (Riedemann et al. 2003). MIF can also increase glucose uptake in skeletal muscle (Benigni et al. 2000) and cardiac (Liang et al. 2015) cells. Interestingly, it is upregulated in T1DM (Ismail et al. 2016), T2DM (Yabunaka et al. 2000, Herder et al. 2008, Stosic-Grujicic et al. 2008) and AD (Popp et al. 2009, Bacher et al. 2010). However, despite there being an apparent increase in MIF release from HPA in the cytokine array panel, there were no significant differences detected in HPA or U373 cells following control or recurrent low glucose treatment (figure 5.4A,B).

5.5 Macrophage-migration inhibitory factor release from U373 human astrocytoma cells is increased by 24 hours of low glucose treatment

Given that modest increases in MIF were seen over the 3-hour treatment period, a 24 hour incubation period was used to provide sufficient time for MIF to accumulate in the conditioned media allowing for more pronounced differences between groups.

During this time, U373 cells were treated with 5, 2.5, 1 and 0.1 mM glucose. By 24 hours, the conditioned media of cells treated with 0.1 mM glucose had significantly higher MIF concentrations than the other groups (figure 5.5A). No other glucose concentrations significantly differed. This work was completed by Julia Vlachaki Walker and included here for completeness.

Figure 5.1

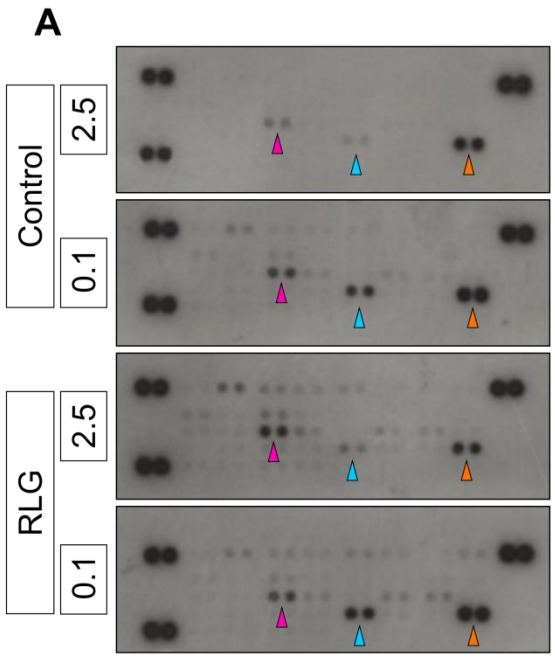

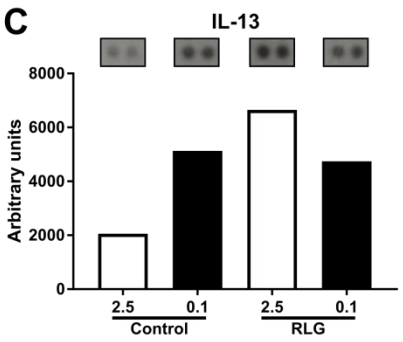

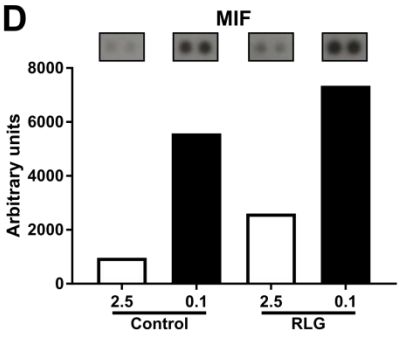

B

	1,2	3,4	5,6	7,8	9,10	11,12	13,14	15,16	17,18	19,20
A	Positive control	C5	CD40L	G-CSF	GM-CSF	GROz	I-309	sICAM-1	IFN-γ	Positive control
B		IL-1a	IL-1B	IL-1ra	IL-2	IL-4	IL-5	IL-6	IL-8	
C		IL-10	IL-12 p70	IL-13	IL-16	IL-17	IL-17E	IL-23	IL-27	
D		IL-32a	IP-10	I-TAC	MCP-1	MIF	MIP-1a	MIP-1B	PAI1	
E	Positive control	RANTES	SDF-1	TNF-a	sTREM-1					Negative control

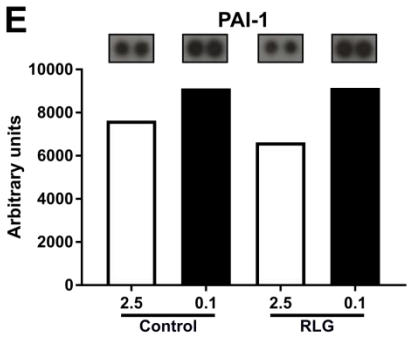

Figure 5.1. Human primary astrocyte (HPA) cytokine release after recurrent low glucose (RLG)

Conditioned media from HPA cells exposed to control or RLG and a further 2.5 or 0.1 mM glucose exposure was incubated on a cytokine array panel. **A**. Image of the cytokine array panel. Each couplet of dots represents the signal from one of 37 different cytokines. Pink arrows point to interleukin-13 (IL-13), cyan arrows point to macrophage-migration inhibitory factor (MIF), and orange arrows point to plasminogen activator inhibitor (PAI-1). **B**. A map of the cytokine panel showing the location of each cytokine measured. **C**,**D**,**E** individual densitometric analysis of IL-13, MIF and PAI-1 respectively. Only one n was used to generate this data so no statistical analysis can be performed.

Figure 5.2

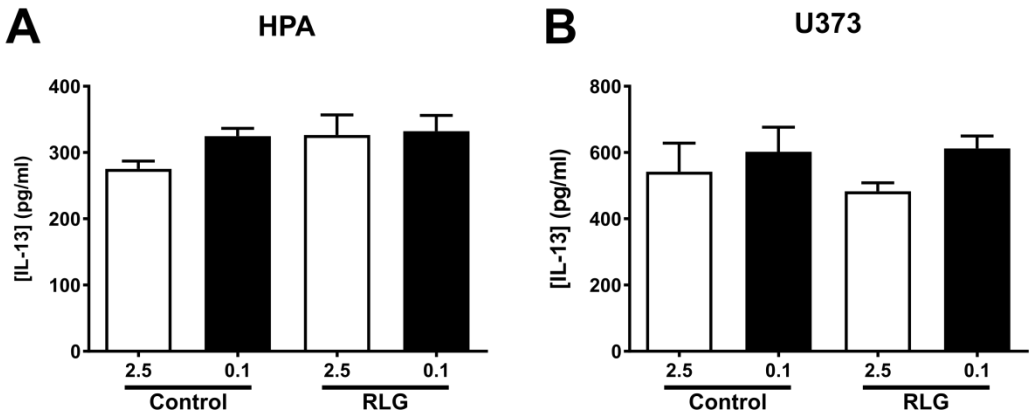

Figure 5.2. Interleukin-13 (IL-13) quantification in conditioned media from human primary astrocytes (HPA) and U373 astrocytoma cells exposed to control or recurrent low glucose (RLG)

IL-13 content in conditioned media from human astrocytes exposed to RLG was quantified using a targeted ELISA. **A**. There were no significant differences between any treatment groups in HPA cells (n=3). **B**. There were no significant differences between any treatment groups in U373 cells (n=3-4). One-way ANOVA with post hoc Bonferroni multiple comparisons tests. Error bars represent standard error of the mean (SEM).

Figure 5.3

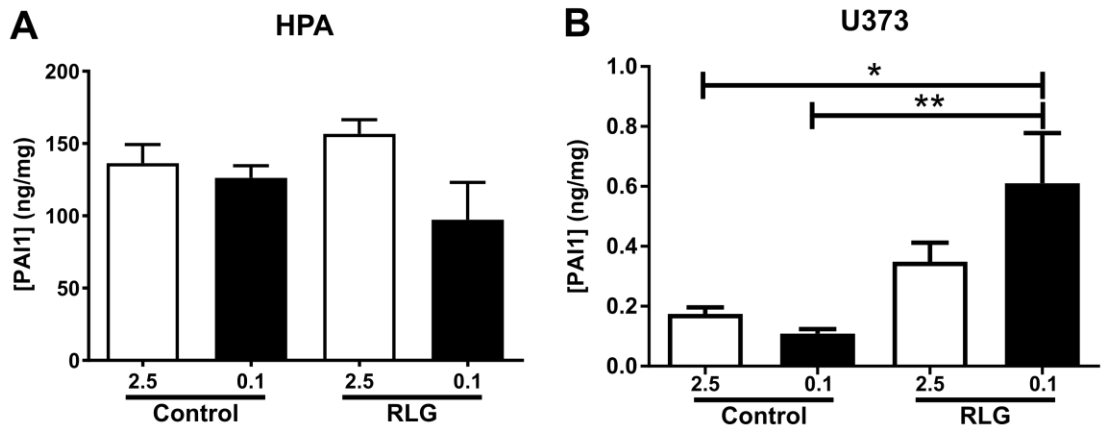

Figure 5.3. Plasminogen activator inhibitor-1 (PAI-1) quantification in conditioned media from human primary astrocytes (HPA) exposed to control or recurrent low glucose (RLG)

PAI-1 content in conditioned media from HPA (n=3-4) and U373 (n=5) cells exposed to RLG was quantified using a targeted ELISA. **A**. There were no significant differences between any treatment groups (n=3-4) in HPA cells. **B**. RLG cells treated to further low glucose had significantly higher PAI-1 than control treated cells. *p<0.05, **p<0.01 between annotated groups. One-way ANOVA with post hoc Bonferroni multiple comparisons tests. Error bars represent standard error of the mean (SEM).

Figure 5.4

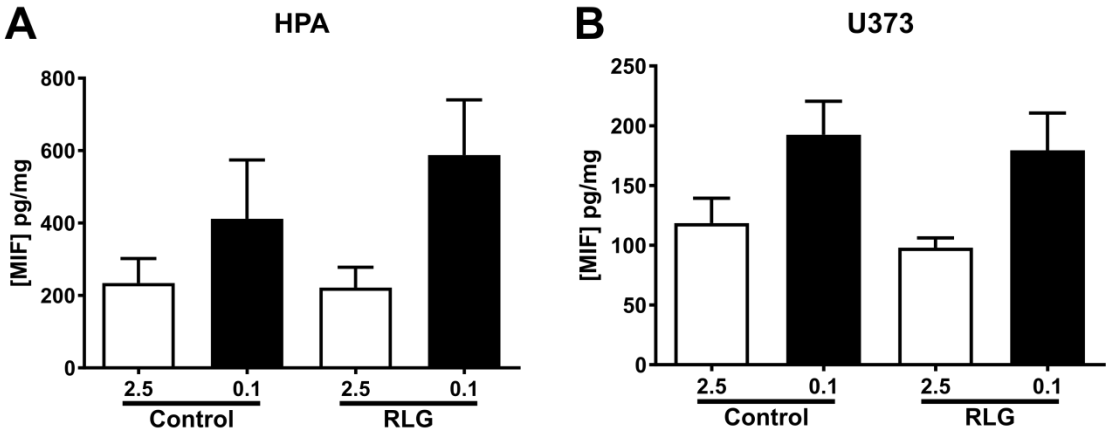

Figure 5.4. Macrophage-migration inhibitory factor (MIF) quantification in conditioned media from human primary astrocytes (HPA) and U373 astrocytoma cells exposed to control or recurrent low glucose (RLG)

MIF content in conditioned media from human astrocytes exposed to RLG was quantified using a targeted ELISA. **A**. There were no significant differences between any treatment groups in HPA cells (n=7-8). **B**. There were no significant differences between any treatment groups in U373 cells (n=6-7). One-way ANOVA with post hoc Bonferroni multiple comparisons tests. Error bars represent standard error of the mean (SEM).

Figure 5.5

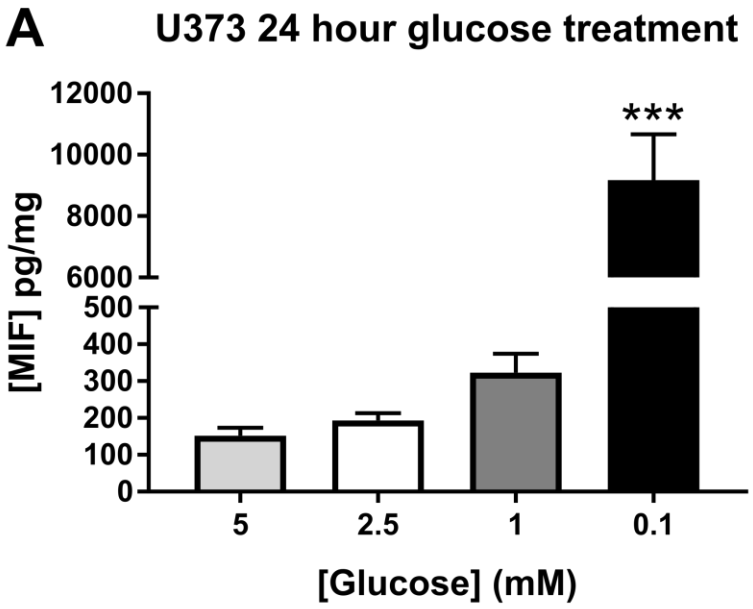

Figure 5.5. Macrophage migration inhibitory factor (MIF) release from U373 human astrocytoma cells is increased after 24 hours of low glucose exposure

MIF content of conditioned media from U373 cells treated with 5, 2.5, 1 and 0.1 mM glucose for 24 hours was measured using a targeted ELISA (n=4-6). **A**. Conditioned media from 0.1 mM glucose treated cells contained significantly more MIF compared to all other groups ($P<0.001$). There were no other groups that were significantly different. One-way ANOVA with post hoc Bonferroni multiple comparisons tests. Error bars represent standard error of the mean (SEM).

Discussion

Acutely inflammation is necessary for the resolution of injuries and beneficial. However, chronic low-grade inflammation is linked to the onset of pathologies, such as obesity and insulin resistance (Heilbronn et al. 2008). Indeed, metabolism and inflammation are intrinsically linked (O'Neill et al. 2016).

Both hyperglycaemia, in rat adipocytes and mouse astrocytes (Lin et al. 2005, Wang et al. 2012), and hypoglycaemia, in human plasma (Gogitidze Joy et al. 2010, Wright et al. 2010, O'Neill et al. 2016), trigger the release of PAI-1, VEGF, vascular adhesion molecules, and IL-6 (Gogitidze Joy et al. 2010, Wright et al. 2010). Additionally, cytokines can act within the brain to modulate whole body energy homeostasis via the hypothalamic-pituitary-adrenal axis (van der Meer et al. 1996). Microglia are the principle immune cells of the brain (Won et al. 2012), however astrocytes are also sensitive to inflammatory stimuli, such as ATP or cytokines like TNF-α or IL-1β and release cytokines in response (John et al. 2001, Beattie et al. 2002, Murakami et al. 2003, Walter et al. 2004, Ballerini et al. 2005, Kucher et al. 2005, Narcisse et al. 2005, Pribiag et al. 2013, Choi et al. 2014, Erta et al. 2015, Habbas et al. 2015) The inflammatory responses of astrocytes can modulate whole-body energy homeostasis, as an astrocyte specific NFκB KO reduced diet induced obesity in mice (Buckman et al. 2015, Douglass et al. 2017). While some evidence using a glucose/oxygen deprivation model in rats shows astrocytic cytokine release and NFκB activation (Zhao et al. 2013), the effects of repeated glucose variation (5.5, 2.5 and 0.1 mM glucose) has not been well studied on isolated human astrocytes. This data presented here characterises the release of cytokines from human astrocytes *in vitro* when treated with low glucose.

The cytokine array panel was used as a screening tool to identify cytokines that were differentially released from astrocytes by RLG. Only one set of biological replicates was used for this screen meaning no statistical significance could be determined. However, several cytokines appeared to be altered by RLG. Generally, there were more cytokines detectable in the experimental groups, including acute low glucose, antecedent RLG and RLG, in comparison to control. Interestingly, the highest detection of cytokines was in the antecedent RLG group. These data corroborate findings that recovery from low glucose to high glucose can exacerbate inflammatory response (Ceriello et al. 2012), and RH appears to exacerbate cytokine release (Joy

et al. 2015). This could mean that people with T1DM would have elevated basal cytokine levels, resulting in chronic inflammatory signalling. Indeed, people with T1DM had higher baselines cytokine levels compared to healthy controls (Wright et al. 2010). Additionally, unlike, the CRR to hypoglycaemia being blunted by hypoglycaemia, the inflammatory response remains equal to if not greater than controls (Joy et al. 2015). Therefore, inflammatory signalling may contribute to blunting the CRR by modulating metabolism. For example, MIF has been shown to increase glucose uptake and AMPK activation, and disrupt mitochondrial function (Benigni et al. 2000, Miller et al. 2008, Preau et al. 2013).

To validate some of the top hits from the cytokine screen, IL-13, PAI-1 and MIF were quantified following the same treatment using ELISAs. Interestingly, no significant differences were found in IL-13 and MIF in HPA or U373 cells, or PAI-1 in HPA cells from a 3-hour treatment period. Despite the cytokine array panel allowing for the simultaneous semi-quantitative assessment of 37 cytokines, array panel is optimised for all the cytokines. Therefore, the array panel will not be optimised for the detection each cytokine individually. Moreover, this may result in a non-linear relationship between amount of signal and cytokine present, making quantification unreliable. Therefore, ELISAs were used to fully quantify and validate prospective targets.

PAI-1, however, was significantly elevated in the U373 cells by RLG, compared to acute low glucose and control treated cells, unlike the HPAs where no significant differences were found. Inflammatory signalling is an integral part of cancer progression (Coussens et al. 2002), and cytokine signalling can be different between primary and immortalised cell lines, in human respiratory cells, for example (Ferreira Lopes et al. 2017). Nevertheless, as PAI-1 inhibits plasmin and prevents the degradation of clots it increases risk of atherothrombosis (Vaughan 2005). Furthermore, plasmin also degrades Aβ, the key component of amyloid plaques in Alzheimer's disease, therefore, elevated PAI-1 may increase the predispose a person to increased risk of dementia (Kutz et al. 2012). Indeed, PAI-1 levels are elevated in the cerebrospinal fluid of people with Alzheimer's disease (Sutton et al. 1994).

While MIF did not reach statistical significance in short-term low glucose exposure, there was a consistent trend seen between the cytokine array panel and the ELISAs

including two different cell lines, HPA and U373 cells. Over a 24-hour period, MIF was significantly released from U373 cells compared to controls. MIF release has previously been shown to be induced by prolonged hypoglycaemia in a human glioblastoma cell line (LN18) (Bacher et al. 2003). Interestingly, MIF is constitutively produced and packaged into intracellular stores (Lue et al. 2002) which are also strongly influenced by circadian rhythms (Petrovsky et al. 2003). The generation of samples for these studies was carried out at different times in the day which may have influenced the sensitivity of the astrocytes to release MIF. Therefore, future experiments could be optimised to account for circadian rhythms.

MIF can activate AMPK (Miller et al. 2008) and promote glucose uptake in skeletal muscle (Benigni et al. 2000), cardiac (Liang et al. 2015), therefore, astrocytic MIF release may also affect glucose uptake within the CNS. This hypothesis could be tested by injecting rats with MIF and measuring changes in cerebral glucose concentration using microdialysis complemented with glucose transporter gene expression analysis. Interestingly, MIF is elevated in T1DM (Ismail et al. 2016), T2DM (Yabunaka et al. 2000, Herder et al. 2008, Stosic-Grujicic et al. 2008) and AD (Popp et al. 2009, Bacher et al. 2010) implicating it in the relationship between CNS metabolic stress and neurodegeneration. Neurofibrillary tangles are associated with multiple neurodegenerative disorders, known as tauopathies, including AD, Pick disease, and frontotemporal dementia (Iqbal et al. 2010). Interestingly, a MIF KO model protected against the hyperphosphorylation of tau protein and thus reducing its aggregation (Li et al. 2015). If the inverse is true, and MIF release can trigger tau phosphorylation, this provides a novel link between hypoglycaemia and the neuron-toxic accumulation of NFTs. Tau is a cytoskeletal component found in neurons, however, MIF is proposed to modulate macrophage migration by remodelling the cytoskeleton (McCarthy et al. 1979, Pick et al. 1979). Disruption of mitochondrial-cytoskeletal interaction impairs mitochondrial function in human heart (Saks et al. 2012) which MIF can mediate (Preau et al. 2013). MIF also activates AMPK and promotes glucose uptake. Taken together MIF is a hub for metabolic and immune interaction which may be altered RLG in human astrocytes.

While preliminary these findings represent an interesting therapeutic target that warrants further investigation. Further, quantitative, analysis of cytokines released from astrocytes in response to acute and recurrent low glucose could be investigated

using cytokine multiplex techniques. This method enables the simultaneous detection of multiple cytokines in a quantitative manner (Burkert et al. 2012) unlike the cytokine array panel used in the work presented above. Additionally, as previously established in chapter 3, RLG alters human astrocyte metabolic function. A question remaining is whether the metabolic dysfunction is affected by or affects the changes in inflammatory signalling discussed in this chapter. To test this, the same RLG model could be used whilst inhibiting or exacerbating inflammatory signalling and measuring the effect on metabolism using mitochondrial stress tests as outlined in chapter 3.

Chapter 6

Glucose variation alters human primary astrocyte mRNA expression

Introduction

With the advent of next generation sequencing technologies, the changes to gene expression can be characterised and tested for novel targets in an unbiased manner. In the studies presented here RNA-sequencing was used to identify differentially expressed genes in human primary astrocytes (HPA) exposed to control, acute low glucose, antecedent recurrent low glucose, or RLG.

Previously, microarray and reverse transcriptase PCR (RT-PCR) techniques have been used to investigate how fasting and low glucose treatment affects the expression of metabolic genes in rat hypothalamic and cortical tissues (Poplawski et al. 2010). Interestingly, 48-hour fasting increased altered metabolic gene expression profiles that would indicate increased fatty acid oxidation and decreased mitochondrial glucose metabolism (Poplawski et al. 2010), which partly corroborates data from chapter 3 of this thesis. Differences in results may be due to the use of rat brain tissue extracts containing multiple cell types rather than isolated HPA cells, indicating different cell-type-dependent responses to low glucose and nutritional restriction. Additionally, the changes in glycolytic gene expression were primarily seen in the hypothalamic tissue extracts and not in the cortex (Poplawski et al. 2010), and the HPA cells used in this thesis were not hypothalamic. Nevertheless, this thesis expands on previous studies by using RNA-seq instead of microarrays and RT-PCR. While microarrays have a good dynamic range and are relatively high throughput, compared to RT-PCR, RNA-seq has a higher dynamic range. Furthermore, RNA-seq also improves on microarrays as it does not require *a priori* knowledge of sequences of interest (Hoheisel 2006). Additionally, the unbiased approach of RNA-seq allows for the detection of the full combinatorial splicing pattern of a transcript and repeat elements (Kratz et al. 2014). In comparison to quantitative-PCR (q-PCR) and RT-PCR, RNA-seq is much higher throughput; q-PCR and RT-PCR can measure tens of targets in parallel compared to tens of thousands in RNA-seq. Lastly, RNA-seq gives an increasingly accurate assessment of the entire transcriptome which can provide a powerful tool to elucidate changes in gene expression between different groups of interest (Kukurba et al. 2015).

To the author's knowledge this is the first characterisation of the transcriptome of human primary astrocytes exposed to RLG used to replicate the chronic glucose variation seen in T1DM. A more in-depth description of the means by which RNA-

seq is carried out can be found in chapter 2 of this thesis. Briefly, once RNA has been extracted from cells the RNA underwent poly-A selection to enrich mRNAs. The transcripts were fragmented and converted to complimentary DNA (cDNA). Sequencing primers were added and sequencing performed using Illumina HiSeq 2500 sequencer. Raw read data underwent FastQC quality control. Reads were mapped to the human reference genome GRCh38 using the read-aligning software STAR (Dobin et al. 2013, Dobin et al. 2015). Gene abundance was calculated with featureCounts software (Liao et al. 2014). Differential gene expression was calculated by a series of contrasts between groups of interest using DESeq2 (Love et al. 2014). Lastly, gene set enrichment was calculated using the web-based Enrichr software (Chen et al. 2013, Kuleshov et al. 2016).

Overall aim and objectives

Very few studies have attempted to measure changes in gene expression of astrocytes during acute and recurrent glucose. The studies that have been completed used rodent models and mircoarrays to investigate genes of interest. Acute and recurrent low glucose-induced gene expression changes have not been investigated in human astrocytes. Therefore, the aim of this chapter was to identify novel genes of interest that were significantly altered by glucose variation. To investigate this, the following research questions were explored:

- Does acute or recurrent low glucose induce changes in differential gene expression?
- If so, what gene ontologies are they associated with?

Results

6.1 Quality control following RNAseq

The Phred quality score briefly is a measure of how accurate the determination of each base is during the RNA sequencing (Ewing et al. 1998a, Ewing et al. 1998b). The Phred score is logarithmically linked to error probabilities meaning a quality score of 10 has a 90% base call accuracy, a score of 20 has a 99% base call accuracy, and so on (Ewing et al. 1998a). The Phred score was calculated by the Exeter Sequencing Service and shows good quality read accuracy with Phred scores >30 giving a base call accuracy of >99.9% (Fig 6.1A).

6.2 STAR read mapping

The output data from RNA-sequencing was mapped to the human reference genome GRCh38 using STAR software (Dobin et al. 2013). All the reads generated by RNA-sequencing from each sample are attempted to be aligned to the reference genome in a two-part process; firstly, seed searching, and secondly, clustering, stitching and scoring. The number of uniquely mapped reads is a percentage of the total number of reads generated from each sample that were successfully mapped to the reference genome (Dobin et al. 2015). All of the samples had a score of >80% which is regarded as good (Dobin et al. 2015) (table 6.1).

Figure 6.1

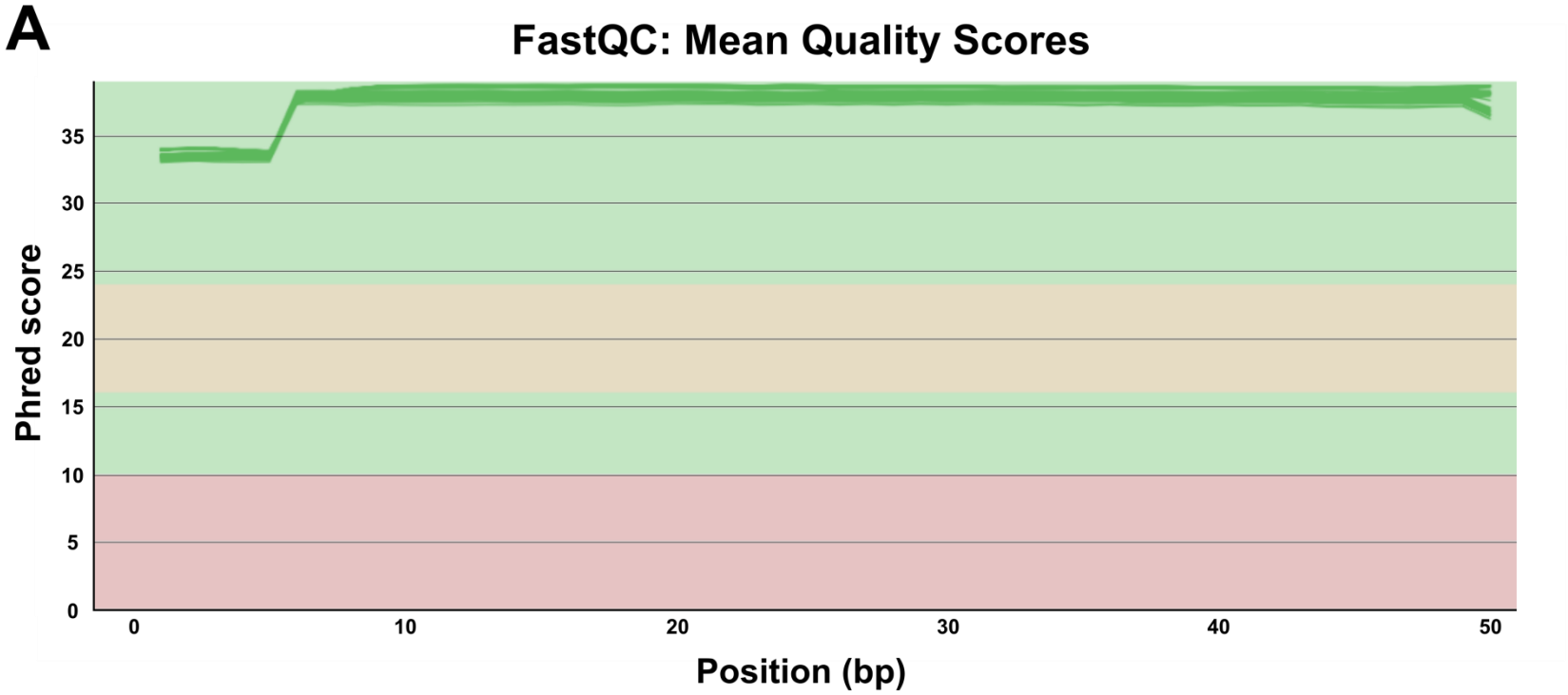

Figure 6.1. RNA sequencing read quality was high in all samples

A. The mean quality value across each base position in the read. In all samples, the accuracy for calling each base was good, represented by a high phred score (>30; >99.9% base call accuracy).

Table 6.1. Read mapping using STAR had a high percentage of uniquely mapped reads

Sample	Biological replicate number	Uniquely Mapped Reads (%)
Control	1	92.26
Control	2	92.06
Control	3	91.67
Control	4	92.24
Control	5	91.48
Low glucose	1	92.06
Low glucose	2	92.09
Low glucose	3	92.70
Low glucose	4	92.34
Low glucose	5	92.63
Antecedent RLG	1	92.01
Antecedent RLG	2	92.23
Antecedent RLG	3	91.75
Antecedent RLG	4	92.23
Antecedent RLG	5	91.54
RLG	1	91.96
RLG	2	91.49
RLG	3	92.21
RLG	4	91.55
RLG	5	86.00

Table 6.1 shows the uniquely mapped reads as a percentage for each sample that underwent RNA sequencing and read mapping using STAR. This is a metric which is defined as the proportion of input reads that are uniquely mapped. A score of >80% is considered good.

6.3 Differential gene expression results

Differential gene expression analysis was performed using DESeq2 through a series of contrasts between groups of interest. The contrast is a determination of whether

the log_2 fold change of two groups, or levels, is significantly different from zero. False discovery rates (FDR) were corrected for using Benjamini-Hochberg corrections. The resulting data was then represented as a volcano plot which depicts the significance (log^{10} adjusted-P value) versus effect size (fold-change; log^2) on the y- and x-axes respectively. Any genes that were significantly different following FDR correction ($\alpha<0.05$) and had an effect size >0.5 log2 were highlighted in red.

6.3.1 Low glucose exposure on the last day of treatment differentially regulates gene expression unlike prior exposure to RLG

A contrast of groups treated to 2.5 or 0.1 mM low glucose on the last day (control and antecedent RLG versus low glucose and RLG) had the largest number (74) of differentially expressed genes (figure 6.2.1A). A complete list of differentially expressed genes can be seen in appendix D, supplementary table 1. A contrast of cells exposed to control or RLG prior to the day of collection (control and low glucose versus antecedent low glucose and RLG) showed no significantly differentially expressed genes.

6.3.2 Low glucose, but not antecedent RLG or RLG, differentially regulates gene expression

Acute low glucose significantly altered the expression of 60 genes compared to control samples with the highest significance and largest effect size genes depicted in figure 6.2.2A. A complete list of differentially expressed genes can be seen in appendix D, supplementary table 2. Conversely, antecedent RLG and RLG did not significantly alter gene expression compared to control (figure 6.2.2BC).

6.3.3 Antecedent RLG significantly altered gene expression compared to low glucose and RLG but low glucose and RLG did not differ

Antecedent RLG significantly altered the expression of 16 genes compared to low glucose (figure 6.2.3A; see the appendix D, supplementary table 3 for a complete list). Furthermore, RLG significantly altered the expression of one gene *TMEM116*, compared to antecedent RLG. However, RLG did not significantly differentially regulate gene expression compared to acute low glucose.

6.4 Enrichr gene ontology data

Genes that were determined to be differentially expressed by DESeq2 were exported and uploaded as an unweighted crisp data set for gene ontology enrichment

assessment by fisher-exact tests and pathway analysis using the web-based program Enrichr (Chen et al. 2013, Kuleshov et al. 2016). The gene sets were compared against models of biological systems generated by the gene ontology (GO) consortium (The Gene Ontology et al. 2000, The Gene Ontology Consortium 2017). Additionally, the gene sets were compared against KEGG pathways which are pathway maps representing the current understanding of the interactions between proteins (Kanehisa et al. 2000, Kanehisa et al. 2016, Kanehisa et al. 2017). Significance was determined if there was a significant overlap, or enrichment, of DEGs identified in the GO or KEGG gene sets, using fisher-exact tests. Multiple correction testing adjustment was included using the Benjamini-Hochberg method.

Only the groups with more than one differentially expressed gene were included in this analysis. Therefore, the comparisons analysed here were 2.5 versus 0.1 mM glucose, control versus low glucose, and low glucose versus RLG. The tables below (6.2.1. 6.2.2, 6.2.3, 6.3.1, 6.3.2, 6.4.1, 6.4.2 and 6.5) contain the pathways that were determined to be significantly enriched ($\alpha<0.05$) after p-value adjustment. The genes that made a pathway significantly enriched, and the pathways are also included. Of interest, a number of endoplasmic reticulum (ER), mitochondrial and inflammatory pathways were identified as being significantly enriched by the different treatments.

6.4.1 Biological process enrichment analysis

Biological process gene ontologies are defined the contribution of a gene or gene product to a specific objective, for example mitochondrial electron transport, NADH to ubiquinone (GO:0006120) (The Gene Ontology et al. 2000). This is usually comprised of multiple molecular functions which combine to perform higher level, for example cell proliferation or apoptosis, or lower level and more specific functions. The differentially expressed gene sets were compared against biological process gene sets to search for enrichment (tables 6.2.1, 6.2.2, and 6.2.3).

6.4.1.1 Biological process enrichment: 2.5 versus 0.1 mM glucose treated cells

The 73 genes that were determined to be differentially regulated by 0.1 mM glucose treatment compared to 2.5 mM glucose were analysed by using Enrichr GO biological process 2018 program. The ten pathways are listed in table 6.2.1. Of these the top three pathways were associated with different aspects of mitochondrial function and shared the same three genes, *XBP1*, *HERPUD1* and *HSPA1A*.

Interestingly, *XBP1* has been previously identified in ER stress-mediated β-cell apoptosis (Laybutt et al. 2007). XBP1 is a key effector of the unfolded protein responses in mammals (Yoshida et al. 2001). Additionally, mitochondrial electron transport, between NADH and ubiquinone, was also significantly enriched which is associated with mitochondrial complex 1 (Janssen et al. 2006).

6.4.1.2 Biological process enrichment: control versus low glucose

The 60 genes that were differentially regulated by low glucose in comparison to control were analysed by using Enrichr GO biological process 2018 program. The top ten pathways are listed in table 6.2.2. For a complete list see appendix D, supplementary table 4. In this instance, the top results were nearly all associated with ER-stress, and negative regulation of the apoptotic signalling pathways. Three common genes were often upregulated as in the 2.5 versus 0.1 mM glucose comparison, *XBP1*, *HERPUD1* and *HSPA1A*.

Figure 6.2.1

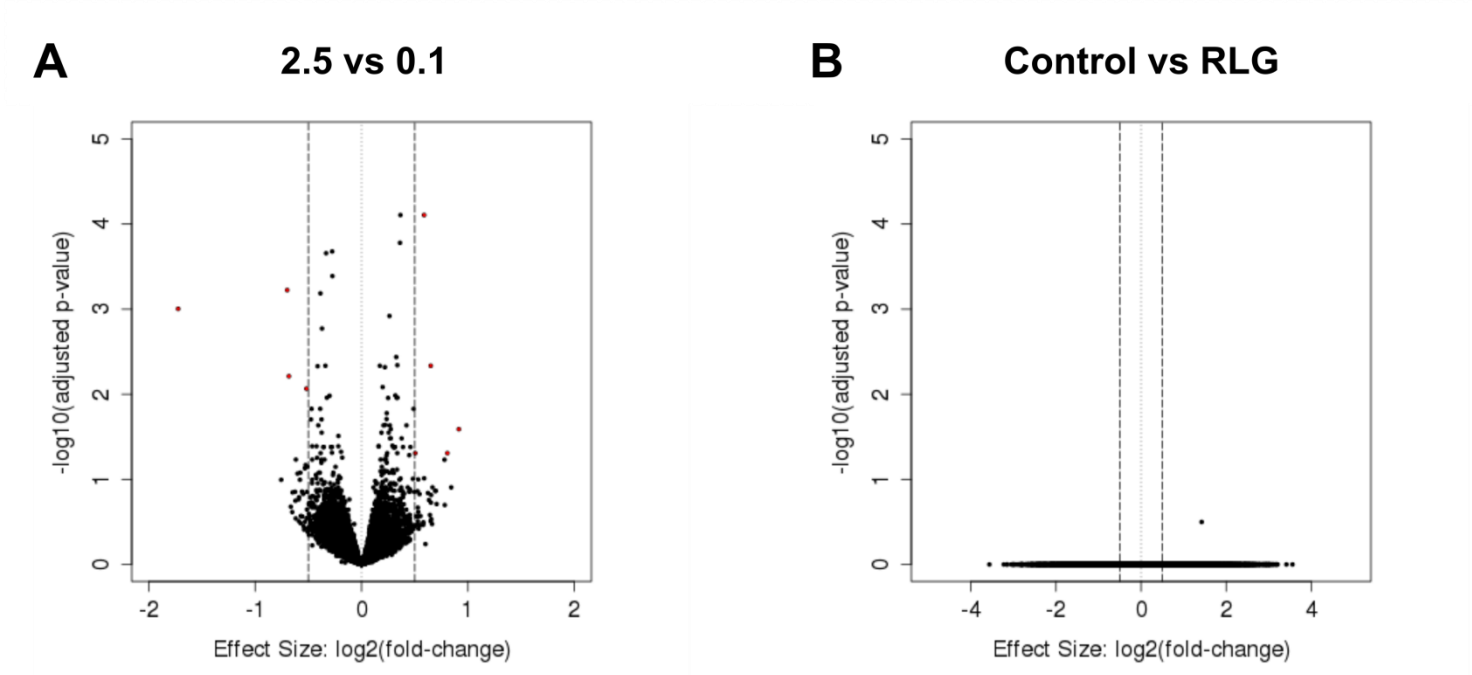

Figure 6.2.1. 2.5 and 0.1 mM glucose treated groups contain differentially expressed genes, whereas control versus recurrent low glucose (RLG) treated cells do not

Volcano plots summarising the distribution of differentially expressed based on their effect size and significance. Genes that had an effect size of >0.05 and significant ($p<0.05$) were highlighted in red. **A**. A comparison between 2.5 and 0.1 mM glucose treated cells. There were a number of significantly differentially expressed genes with high effect sizes both positively and negatively. **B**. A comparison of control and RLG treated cells. No significantly differential gene expression was detected.

Figure 6.2.2

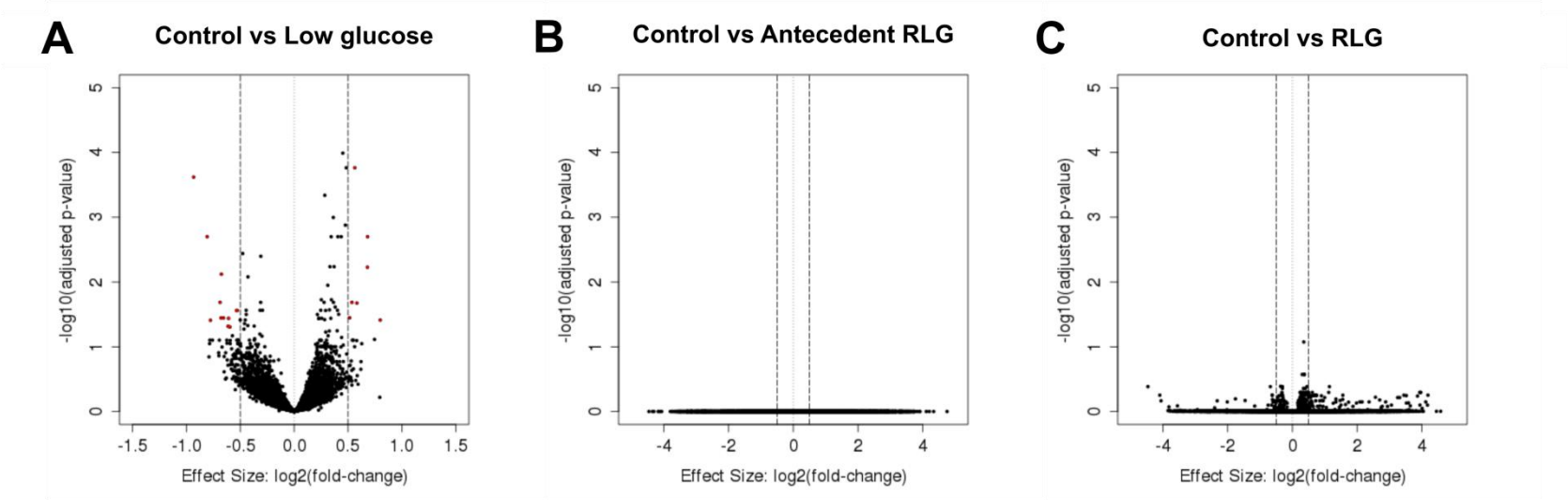

Figure 6.2.2. Low glucose significantly differentially regulates gene expression, whereas control versus antecedent recurrent low glucose (RLG), and control versus RLG does not

Volcano plots summarising the distribution of differentially expressed based on their effect size and significance. Genes that had an effect size of >0.05 and significant ($p<0.05$) were highlighted in red. **A**. A comparison between control and low glucose treated cells. There were a number of significantly differentially expressed genes with high effect sizes both positively and negatively. **B**. A comparison of control and antecedent RLG treated cells. No significantly differential gene expression was detected. **C**. A comparison of control and RLG treated cells. No significantly differential gene expression was detected.

Figure 6.2.3

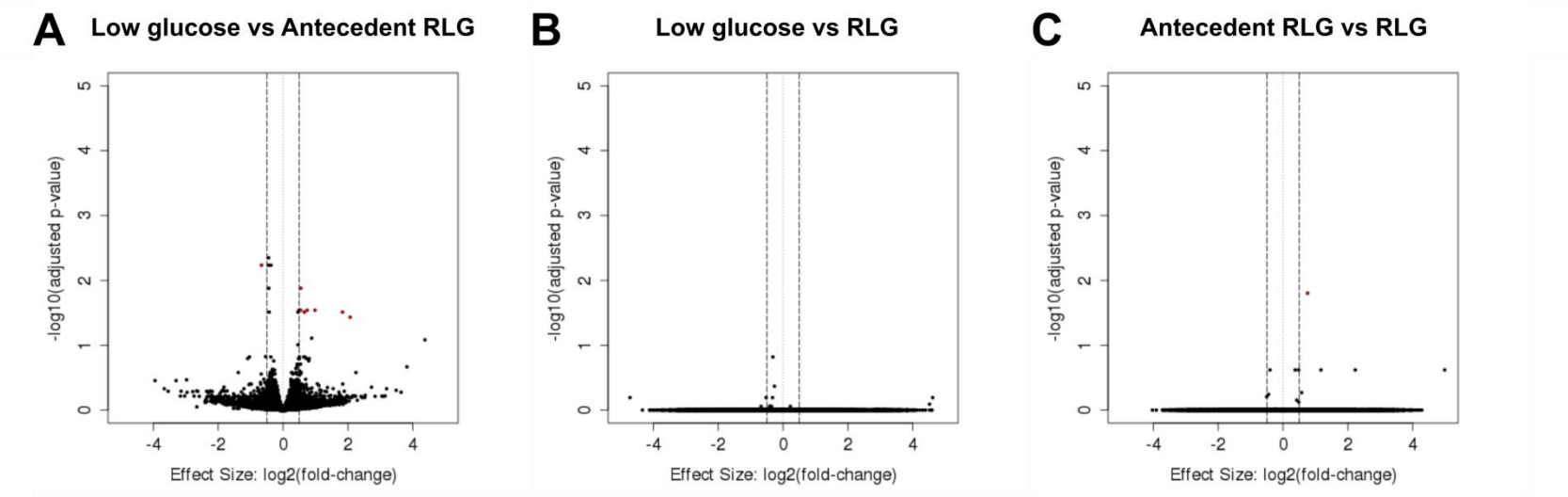

Figure 6.2.3. Low glucose and antecedent recurrent low glucose (RLG), and antecedent RLG versus RLG have significantly differentially regulated gene expression, whereas low glucose versus RLG does not

Volcano plots summarising the distribution of differentially expressed based on their effect size and significance. Genes that had an effect size of >0.05 and significant ($p<0.05$) were highlighted in red. **A**. A comparison between low glucose and antecedent RLG treated cells. There were a number of significantly differentially expressed genes with high effect sizes both positively and negatively. **B**. A comparison of low glucose and RLG treated cells. No significantly differential gene expression was detected. **C**. A comparison of antecedent RLG and RLG treated cells. No significantly differential gene expression was detected. There was one differentially expressed gene with a high effect size.

Table 6.2.1. Biological process pathway analysis of differentially expressed genes in 2.5 versus 0.1 mM glucose treated cells

Term	Adjusted P-value	Genes
negative regulation of endoplasmic reticulum stress-induced intrinsic apoptotic signaling pathway (GO:1902236)	0.017	*XBP1;HERPUD1; HSPA1A*
regulation of endoplasmic reticulum stress-induced intrinsic apoptotic signaling pathway (GO:1902235)	0.022	*XBP1;HERPUD1; HSPA1A*
negative regulation of response to endoplasmic reticulum stress (GO:1903573)	0.022	*XBP1;HERPUD1; HSPA1A*
mitochondrial electron transport, NADH to ubiquinone (GO:0006120)	0.050	*MT-ND4L;MT-ND4;MT-ND2*
negative regulation of transcription from RNA polymerase II promoter in response to stress (GO:0097201)	0.050	*BAG3;HSPA1A*
regulation of DNA endoreduplication (GO:0032875)	0.050	*FBXW7;E2F7*
regulation of amyloid-beta clearance (GO:1900221)	0.050	*SRF;LDLR*
positive regulation of cytokine-mediated signaling pathway (GO:0001961)	0.050	*MAVS;TSLP;HSPA1A*
positive regulation of actin filament bundle assembly (GO:0032233)	0.050	*FHOD1;ABL1;SYNPO*
regulation of mitotic cell cycle phase transition (GO:1901990)	0.050	*CDC20;TUBA1A; HECW2;TUBB4B; TUBA4A*

Table 6.2.2. Biological process pathway analysis of differentially expressed genes in control versus low glucose treated cells

Term	Adjusted P-value	Genes
negative regulation of intrinsic apoptotic signaling	0.00002	DNAJA1;XBP1;M

pathway (GO:2001243)		DM2;HSPB1;HERPUD1;HSPA1A
response to unfolded protein (GO:0006986)	0.00007	DNAJA1;HSPA5;HSPB1;HERPUD1;HSPA1A
negative regulation of programmed cell death (GO:0043069)	0.001	DNAJA1;XBP1;HSPA5;TSLP;HSPB1;FMN2;CD44;EPHB4;HSPA1A
negative regulation of endoplasmic reticulum stress-induced intrinsic apoptotic signaling pathway (GO:1902236)	0.002	XBP1;HERPUD1;HSPA1A
negative regulation of apoptotic process (GO:0043066)	0.002	DNAJA1;XBP1;HSPA5;TSLP;HSPB1;FMN2;CD44;EPHB4;HSPA1A
IRE1-mediated unfolded protein response (GO:0036498)	0.003	XBP1;HSPA5;CXXC1;EXTL3
regulation of endoplasmic reticulum stress-induced intrinsic apoptotic signaling pathway (GO:1902235)	0.003	XBP1;HERPUD1;HSPA1A
negative regulation of response to endoplasmic reticulum stress (GO:1903573)	0.004	XBP1;HERPUD1;HSPA1A
positive regulation of ubiquitin-protein transferase activity (GO:0051443)	0.010	ARRDC4;CDC20;FBXW7
regulation of apoptotic process (GO:0042981)	0.010	DNAJA1;XBP1;HSPA5;TSLP;HSPB1;FMN2;INHBA;CD44;EPHB4;HSPA1A

6.4.1.3 Biological process enrichment: antecedent RLG versus low glucose

The 16 genes that were differentially regulated by antecedent RLG compared to low glucose were analysed by using Enrichr GO biological process 2018 program. This comparison shows the recovery from prior low glucose treatments. Indeed, glucose

reperfusion following hypoglycaemia is a contributor to neuronal death (Suh et al. 2007). The top ten pathways are listed in table 6.2.3. For a complete list see appendix D, supplementary table 5. Interestingly, some of the upregulated processes involved the upregulation of the inflammatory cytokine IL-6, and more generic immune responses. Similarly to the previous comparisons, ER-stress related processes were also upregulated.

Table 6.2.3. Biological process pathway analysis of differentially expressed genes in low glucose versus antecedent recurrent low glucose (RLG) treated cells

Term	Adjusted P-value	Genes
positive regulation of interleukin-6 production (GO:0032755)	$1.7x10^{-3}$	XBP1;TSLP;EREG
positive regulation of multicellular organismal process (GO:0051240)	$2.6x10^{-3}$	XBP1;LDLR;EREG;BCL9L
negative regulation of cell activation (GO:0050866)	$3.4x10^{-3}$	THBD;LDLR
positive regulation of immune response (GO:0050778)	0.0380	XBP1;EREG
cholesterol homeostasis (GO:0042632)	0.0380	XBP1;LDLR
IRE1-mediated unfolded protein response (GO:0036498)	0.0380	XBP1;EXTL3
keratinocyte differentiation (GO:0030216)	0.0380	TXNIP;EREG
sterol homeostasis (GO:0055092)	0.0380	XBP1;LDLR
regulation of DNA replication (GO:0006275)	0.0380	ESCO2;EREG
epidermal cell differentiation (GO:0009913)	0.0411	TXNIP;EREG

6.4.2 Molecular function enrichment analysis

A molecular function is defined as the biochemical activity of gene products, for example enzyme, NADH dehydrogenase (ubiquinone) activity (GO:0008137) (The Gene Ontology et al. 2000). The molecular function shows the functional capability rather than whether it is being completed. Furthermore, molecular functions are not

tied to a specific cellular localisation. The differentially expressed gene sets were compared against molecular function gene sets to search for enrichment.

6.4.2.1 Molecular function enrichment: 2.5 versus 0.1 mM glucose treated cells

The 73 genes that were differentially regulated by 0.1 mM glucose compared to 2.5 mM glucose treated cells were analysed by using Enrichr GO molecular function 2018 program. The top ten pathways are listed in table 6.3.1. For a complete list see appendix D, supplementary table 6. Of interest, electron transport chain functions were significantly altered by 0.1 mM glucose, centering on the differential expression of *MT-ND4L*, *MT-ND4* and *MT-ND2*. Also, the gene *RELA* was involved in three of the top ten molecular functions. The gene product of *RELA* also is commonly known as p65 and is a part the NF-κB, an immune master-regulator transcription factor (Brasier 2006).

Table 6.3.1. Molecular function pathway analysis of differentially expressed genes in 2.5 versus 0.1 mM glucose treated cells

Term	Adjusted P-value	Genes
phosphate ion binding (GO:0042301)	0.011	*MTHFD2;RELA*
purine ribonucleoside triphosphate binding (GO:0035639)	0.011	*TUBA1A;ABL1;TUBE1;PEX1;TUBB4B;RND3;TUBA4A;HSPA1A*
guanyl ribonucleotide binding (GO:0032561)	0.011	*TUBA1A;TUBE1;TUBB4B;RND3;TUBA4A*
NADH dehydrogenase (ubiquinone) activity (GO:0008137)	0.011	*MT-ND4L;MT-ND4;MT-ND2*
NADH dehydrogenase (quinone) activity (GO:0050136)	0.011	*MT-ND4L;MT-ND4;MT-ND2*
GTP binding (GO:0005525)	0.011	*TUBA1A;TUBE1;TUBB4B;RND3;TUBA4A*
purine ribonucleoside binding (GO:0032550)	0.011	*TUBA1A;TUBE1;T*

		UBB4B;RND3;TUBA4A
cadherin binding (GO:0045296)	0.017	*EHD1;EIF5;BAG3;PLIN3;DBN1;HSPA1A*
transcriptional activator activity, RNA polymerase II distal enhancer sequence-specific binding (GO:0001205)	0.033	*SRF;RELA*
transcription factor activity, RNA polymerase II core promoter sequence-specific (GO:0000983)	0.036	*SRF;RELA*

6.4.2.2 Molecular function enrichment: control versus low glucose

The 60 genes that were differentially regulated by low glucose compared to control were analysed by using Enrichr GO molecular function 2018 program. The 4 enriched pathways are listed in table 6.3.2. The four pathways involved protein binding functions and DEGs that produce heat-shock family proteins.

Table 6.3.2. Molecular function pathway analysis of differentially expressed genes in control versus low glucose treated cells

Term	**Adjusted P-value**	**Genes**
C3HC4-type RING finger domain binding (GO:0055131)	0.008	*DNAJA1;HSPA1A*
cadherin binding (GO:0045296)	0.005	*EIF5;HSPA5;CDC42EP1;PLIN3;CORO1B;DBN1;HSPA1A*
ubiquitin-like protein ligase binding (GO:0044389)	0.008	*DNAJA1;HSPA5;FBXW7;MDM2;TXNIP;HSPA1A*
ubiquitin protein ligase binding (GO:0031625)	0.008	*DNAJA1;HSPA5;FBXW7;MDM2;TXNIP;HSPA1A*

6.4.2.3 Molecular function enrichment: antecedent RLG versus low glucose

The 16 genes that were differentially regulated by antecedent RLG versus low glucose treatment were analysed by using Enrichr GO molecular function 2018 program. No molecular function gene ontologies were significantly enriched.

6.4.3 Cellular component enrichment analysis

The cellular component refers to where the action of a gene product takes place, for example, mitochondrial respiratory chain complex I (GO:0005747) (The Gene Ontology et al. 2000). The differentially expressed gene sets were compared against cellular component sets to search for enrichment.

6.4.3.1 Cellular component enrichment: 2.5 versus 0.1 mM glucose treated cells

The 73 genes that were differentially regulated by 0.1 mM glucose compared to 2.5 mM glucose treated cells were analysed by using Enrichr GO cellular component 2018 program. The 3 pathways are listed in table 6.4.1. The top hit, GO:0005747, corresponds to the previous identification of mitochondrial associated biological processes in table 6.2.1 and 6.3.1 and shares the same DEGs.

Table 6.4.1. Cellular component pathway analysis of differentially expressed genes in 2.5 versus 0.1 mM glucose treated cells

Term	Adjusted P-value	Genes
mitochondrial respiratory chain complex I (GO:0005747)	0.029	*MT-ND4L;MT-ND4;MT-ND2*
cytoskeleton (GO:0005856)	0.029	*TUBA1A;MAP7D1;ABL1;TARS;SYNPO;TUBB4B;DBN1;TUBA4A*
actomyosin (GO:0042641)	0.029	*FHOD1;SYNPO;DBN1*

6.4.3.2 Cellular component enrichment: control versus low glucose treated cells

The 60 genes that were differentially regulated by low glucose compared to control treated cells were analysed by using Enrichr GO cellular component 2018 program. The three significantly enriched components are listed in table 6.4.2. These three components involved a number of heat-shock family genes as well as cytoskeletal components which resulted in cellular structural elements being altered.

Table 6.4.2. Cellular component pathway analysis of differentially expressed genes in control versus low glucose treated cells

Term	Adjusted P-value	Genes
focal adhesion (GO:0005925)	$9x10^{-5}$	*HSPA5;RPS19;CDC42EP1;HSPB1;LPP;RND3;CD44;CORO1B;HSPA1A*
actomyosin (GO:0042641)	0.019	*FHOD1;CORO1B;DBN1*
cytoskeleton (GO:0005856)	0.027	*DNAJA1;TUBA1A;CDC42EP1;HSPB1;FMN2;TUBB4B;DBN1*

6.4.3.3 Cellular component enrichment: antecedent RLG versus low glucose

The 16 genes that were differentially regulated by antecedent RLG compared to low glucose treated cells were analysed by using Enrichr GO cellular component 2018 program. No cellular components were significantly enriched.

6.4.4 KEGG pathway

KEGG pathways are computerised cellular processes and molecular functions (Kanehisa et al. 2000). The differentially expressed gene lists were compared against the database of KEGG pathways to search for pathway enrichment.

6.4.4.1 KEGG pathway enrichment: 2.5 versus 0.1 mM glucose treated cells

The 73 genes that were differentially regulated by 0.1 mM glucose compared to 2.5 mM glucose were analysed by using Enrichr KEGG 2016 program. Only Pathogenic Escherichia coli infection_Homo sapiens_hsa05130 was significantly enriched. However, the DEGs involved in this pathway are cytoskeletal related and this may be a false positive, especially as these samples were cultured in aseptic conditions.

Table 6.5. KEGG pathway analysis of differentially expressed genes in 2.5 versus 0.1 mM glucose treated cells

Term	Adjusted P-value	Genes
Pathogenic Escherichia coli infection_Homo sapiens_hsa05130	0.004	*TUBA1A;ABL1;TUBB4B;TUBA4A*

6.4.4.2 KEGG pathway enrichment: 2.5 versus 0.1 mM glucose treated cells

The 60 genes that were differentially regulated by low glucose compared to control treated cells were analysed by using Enrichr KEGG 2016 program. No KEGG pathways were significantly enriched.

6.4.4.3 KEGG pathway enrichment: antecedent RLG versus low glucose treated cells

The 16 genes that were differentially regulated by antecedent RLG compared to low glucose treated cells were analysed by using Enrichr KEGG 2016 program. No KEGG pathways were significantly enriched.

Discussion

In chapter 3 of this thesis RLG treatment significantly altered mitochondrial function in both HPA and U373 cells. Interestingly, low glucose differentially regulated the expression of several mitochondrial encoded genes that are enriched in gene sets associated with mitochondrial respiration (tables 6.2.1, 6.2.2, 6.3.1, and 6.4.1). In particular, four genes, *MT-ND4L, MT-ND4*, *MT-ND2, and MT-ATP6* had increased gene expression (0.33, 0.25, 0.16 and 0.19 respectively) and are all part of mitochondrial respiratory complex I (Andrews et al. 2013) which is reflected with the enrichment of mitochondrial respiratory chain complex 1 (GO:0005747). Complex I translocates protons into the intramitochondrial membrane space by transferring electrons from NADH to coenzyme Q10 (Janssen et al. 2006). Despite enrichment of genes in complex I, this does not provide any information on how the proton pumping function of complex I is altered. To assess changes in complex I function its activity can be assessed in isolated mitochondria by following the conversion of NADH to NAD^+ and the simultaneous alteration a colourimetric electron acceptor dye such as nitrotetrazolium blue chloride (NBT) which can be measured by changes in optical density as described previously (Li et al. 2010). If complex I is inhibited this decreases ATP synthesis and can increase ROS production leading to apoptosis (Loeffen et al. 1998, Li et al. 2003).

Earlier in this thesis the expression levels of glycolytic enzyme hexokinase 2 (HK2) were measured to test whether it was contributing to RLG-induced altered glycolytic activity. There was no change to protein content in the HPA cells. However, following RNA-seq and DGE analysis *HK2* was a differentially expressed gene with an increased $\log^2$ fold-change of 0.36. Interestingly, this did not result in detectable changes in protein expression. However, mRNA expression does not always strongly correlate with steady state protein levels (Tian et al. 2004). This can be due to changes in post-transcriptional regulatory processes, protein half-life, and error in quantifying both mRNA and protein levels (Greenbaum et al. 2003).

The endoplasmic reticulum (ER) consists of a network of membranes that coordinates the tertiary folding and maturations of proteins (Braakman et al. 2011). Some GO terms (tables 6.2.1 and 6.2.2) that involve regulation of endoplasmic reticulum stress response are enriched. These centre on the detection of X-box binding protein 1 (*XBP1*), homocysteine inducible ER protein with ubiquitin like

domain 1 (*HERPUD1)*, and heat shock protein family A member 1A (*HSPA1A*) as genes that are differentially expressed by low glucose exposure. The ER stress response is induced by glucose deprivation (Benavides et al. 2005, Ikesugi et al. 2006, de la Cadena et al. 2014), and altered redox state (Harding et al. 2003) and calcium dysregulation (Høyer-Hansen et al. 2007). This reduces protein folding and thus increases unfolded proteins which in turn further activates ER stress and triggers the unfolded protein response (Ron et al. 2007). Interestingly, this was reflected by low glucose upregulating GO terms involved in the unfolded protein response (GO:0006986, GO:1900101, and GO:0036500). Dysfunctional ER stress responses have been implicated in diabetes and obesity (Park et al. 2013, Jiang et al. 2015, Wu et al. 2015). A gene central to this is *XBP1*, a transcription factor that upregulates the unfolded protein response (Iwakoshi et al. 2003). In HPA cells low glucose significantly regulated *XBP1* expression with an increased $\log^2$ fold change of 0.28. Increased XBP1 expression is associated with the induction of immune plasma cells becoming “professional secretory cells” (Shaffer et al. 2004). Aside from upregulating ER function and protein folding, XBP1 binds to the promotor of genes associated with glycolysis, gluconeogenesis and lipid metabolism (Acosta-Alvear et al. 2007). Interestingly, *XBP1* haploinsufficiency creates severe insulin resistance and diabetes (Ozcan et al. 2004). Conversely, *XBP1* overexpression can improve glucose tolerance in *ob/ob* diabetic mice (Zhou et al. 2011). This may be due to its ability to increase glycolysis via changes in HK2 expression (Liu et al. 2016). Therefore, the increase in *XBP1* expression found by RNA-seq may be underlying some of the enhanced glycolytic activity seen in the HPA cells induced by RLG treatment discussed in chapter 3. Furthermore, the enrichment of GO terms associated with ER stress implicates modifications to ER stress induced by low glucose treatment in HPA cells. This supports a previous study demonstrating glucose and oxygen deprivation increases ER stress in astrocytes (Benavides et al. 2005).

In chapter 5, preliminary evidence suggests low glucose and RLG increase inflammatory cytokine release by HPA cells. Interestingly, RNA-seq and subsequent gene ontology analysis shows enrichment of GO terms associated with cytokine signalling and immune cell regulation (GO:0001961, GO:2000662, GO:0032755, GO:0043031, and GO:1903978). It is known that hypoglycaemia increases the

release of inflammatory cytokines, including interleukin-6 (IL-6) (Gogitidze Joy et al. 2010, Wright et al. 2010, O'Neill et al. 2016). Interestingly, the transcription factor XBP1, discussed earlier as a regulator of ER stress, can induce IL-6 expression in B cells (Iwakoshi et al. 2003). The enriched GO terms also include pathways involved in the regulation of macrophage and microglial cell activation. Taken together these data support the role for hypoglycaemia causing inflammation.

Some of the most significantly enriched cellular component GO terms were cytoskeletal related (GO:0015630, GO:0015629, GO:0001725, GO:0099513, GO:0005874 and GO:0005856). Astrogliosis is a marker of astrocyte activation that is characterised by a ramification of cell morphology (Pekny et al. 2005). This can be induced by nutritional changes (Horvath et al. 2010, Thaler et al. 2012, Daumas-Meyer et al. 2018), as well as in response to CNS pathologies and trauma (Pekny et al. 2005). While no significant changes to GFAP were found, the RNA-seq analysis suggests that microtubule proteins are differentially expressed by low glucose (*TUBA1A*, *TUBE1*, *TUBA4A* and *TUBB4B*). This indicates that changes in cytoskeletal networks are modified in HPA cells during low glucose treatment. While low glucose did not generally appear to change gross cellular morphology, it may be prudent to examine this more closely.

Taken together there are many interesting differentially expressed genes and enriched gene ontologies altered by low glucose treatment. But it remains unknown how these pathways are altered, and what functional outcome that would have. While low glucose appears to be the largest driving factor in regulating gene expression, RLG did not appear to impact gene expression greatly. This could indicate that normal gene expression changes induced by low glucose are blunted by RLG.

Despite the success in identifying multiple DEGs and enriched gene ontologies, there are still opportunities for more refined analysis. The DESeq2 analysis for differentially expressed genes was carried out using a series of contrasts. This could increase the FDR by doing multiple comparisons. However, this is a relatively small increase in FDR, eight contrasts, compared to the comparisons between approximately 20,000 genes in each sample. The false discovery rate was corrected for using Benjamini-Hochberg corrections within contrast comparisons, but this was

unable to be used for the multiple contrasts performed. FDR corrections can also eliminate true positives, reducing their power (Benjamini et al. 1995). Following abundance estimation, genes with low reads are often excluded as random changes in a sample can have a large impact on variance (Love et al. 2014). While DESeq2 software accounts for this in part, often genes with read counts below a manually set threshold are excluded from differential gene expression analysis. In this study genes with <5 reads across all samples were excluded from further analysis. However, a higher threshold could have been used which would have eliminated many lowly expressed genes that are unlikely to have a physiological impact and improved the power for detection of differentially expressed genes lost through FDR corrections. Additionally, the need for FDR corrections could be avoided through a multi-factor analysis design, with subsequent post-hoc analysis. Nevertheless, this first pass analysis gives a good indication that HPA gene expression is differentially regulated by low glucose exposure.

The differentially expressed gene sets derived from DESeq2 analysis were put into the web-based program Enrichr as a crisp data set with no membership weighting included. Crisp data sets are simple as membership to a classifying factor, or gene ontology in this case, is binary, i.e. yes or no, 0 or 1 (Kuleshov et al. 2016). A fuzzy data set is one in which membership can be partial, i.e. a value between 0 and 1. However, fuzzy data sets only marginally improve enrichment analysis (Kuleshov et al. 2016), therefore the crisp data sets used here are still valid. Nonetheless, gene enrichment analysis could be improved using GOseq which takes into account gene length (Young et al. 2010). Genes with a longer sequence are often overrepresented by abundance estimation which means they are more likely to be detected as being differentially expressed and therefore the contribution to GO enrichment is overestimated (Young et al. 2010). Before this data analysis is prepared for peer-reviewed publication read length should be considered during GO analysis and, therefore, GOseq should be used as an alternative to Enrichr. A flaw of gene enrichment analysis is that it assumes each gene contributes an equal weight to the functional gene set it is compared to (Subramanian et al. 2005). Therefore, weighted gene co-expression network analysis (WGCNA) could be utilised to look for relationships between highly correlated gene clusters or modules that takes into account the weighting of gene interactions (Langfelder et al. 2008). This provides

more information into network connectivity rather than simple membership enrichment (Alexeyenko et al. 2012). The identification of hub genes would allow for potentially novel targets to be found and their functional significance could be confirmed experimentally.

Chapter 7

Conclusions

7.1 Research questions and novelty of the study

The purpose of this research was to characterise the effect of how hypoglycaemia-like, low glucose treatments affected human astrocytes in isolation. In this concluding chapter the author presents a recapitulation of the principle findings, and places them in the context of current understanding. Secondly, the limitations of the studies and suggested future research will be discussed. Lastly, a conclusion of the work is presented.

Briefly, the novel contribution of this work is that human astrocyte mitochondrial and glycolytic metabolism is fundamentally altered by acute and recurrent low glucose (RLG) which can be partially restored by recovery from RLG. Despite significant metabolic alterations to RLG astrocytic calcium signalling remained unaffected. But, release of cytokines, particularly macrophage-migration inhibitory factor (MIF) was increased by low glucose treatment. Lastly, for the first time low glucose-induced differentially expressed genes were identified in human primary astrocytes, which is also a resource for further data mining.

7.2 Key outcomes of the study

7.2.1 Chapter 3

Astrocytic sensitivity to changes in low glucose was measured by phosphorylation and activation of AMPK. AMPK is necessary for neuronal glucose sensing whole-body energy metabolism (Claret et al. 2007) and can upregulate astrocytic catabolic metabolism (Voss et al. 2015). HPA AMPK was activated by low glucose but, this was blunted by RLG, which is a novel finding in astrocytes. Moreover, RLG increased mitochondrial activity, which was at least in part through increased fatty acid dependency; while there was a concurrent decrease in coupling efficiency, likely mediated by increased proton leak. RLG also increased HPA glycolytic activity and augmented glucose reperfusion activation of glycolysis. Through these metabolic adaptations astrocytes can sustain both intracellular nucleotide content and ratios, as well as lactate release. Lastly, the metabolic adaptions by HPA cells induced by RLG could be restored by maintenance in euglycaemia-like glucose concentrations. This chapter also showed important differences in the metabolic phenotype between HPA and U373 astrocytoma cells. U373 cells were less dependent on fatty acid or pyruvate oxidation and had increased glutamine metabolic flexibility.

7.2.2 Chapter 4

Previous studies have shown activation of astrocytes to low glucose exposure, the ability to sense hypoglycaemia and roles in CRR (Marty et al. 2005, McDougal et al. 2013a, McDougal et al. 2013b, Chen et al. 2016, Rogers et al. 2016, Rogers et al. 2018). As calcium signalling incurs a significant metabolic cost, it was hypothesised that calcium signalling would be elevated by acute and dysregulated by RLG treatment. Conversely, it was found that astrocytes sustain basal intracellular calcium levels and maintain a normal $[Ca^{2+}]_i$ response to ATP and noradrenaline treatment in low glucose. Additionally, noradrenaline-induced lactate release was unaffected in HPA but significantly attenuated in U373 cells by low glucose.

7.2.3 Chapter 5

Modulation of astrocytic inflammatory signalling protects against diet induced obesity in mice (Buckman et al. 2015, Douglass et al. 2017). As astrocytes have an inflammatory function in the CNS, a cytokine screen was performed to identify cytokines in HPA conditioned media following RLG. Several targets of interest were identified and further validated using targeted ELISAs. MIF maintained a consistent but non-significant trend to be increased by RLG. To allow for further accumulation a 24 hour low glucose exposure was used which significantly increased MIF release from U373 cells. This is a novel finding and interesting as MIF is detrimental to diabetes and dementia.

7.2.4 Chapter 6

RNA-sequencing was used as an unbiased screen for RLG-induced differential gene expression in HPA cells. Whilst a preliminary analysis, further gene ontology investigation demonstrated several mitochondrial-associated genes which may underlie the changes to mitochondrial function seen in chapter 3. Additionally, endoplasmic reticulum-associated gene ontologies were significantly altered by RLG which is has not been shown to be associated with low glucose in astrocytes before. Interestingly, this may also underpin mitochondrial changes seen in chapter 3. ER stress increases mitochondrial respiration to improve cell survival (Knupp et al. 2018). Therefore, if the gene ontologies identified in ER stress do translate to actual protein misfolding then this may also contribute to the mitochondrial stress in chapter 3. This could be tested by inhibiting or activating ER stress and assessing whether mitochondrial disruption could be rescued or exacerbated during RLG. Lastly,

several inflammatory markers were also differentially expressed by glucose variation which corroborates data from chapter 5. Mitochondria that excessively produce ROS, which can be induced by fatty acid oxidation (St-Pierre et al. 2002), activate the NLRP3 inflammasome complex which leads to IL-1β production and increased cytokine signalling (Zhou et al. 2010). Perhaps ER stress-induced mitochondrial alterations may modulate the inflammatory response to low glucose.

7.3 Relationships to previous research

Since the turn of the millennium, the specific role of astrocytes sensing low glucose has been discovered (Marty et al. 2005, McDougal et al. 2013a, McDougal et al. 2013b, Chen et al. 2016, Rogers et al. 2016, Rogers et al. 2018). In chapter 3 it was shown that astrocytes react to low glucose by increasing AMPK phosphorylation and activity, a mechanism known in glucose-sensing neurons (Claret et al. 2007). McDougal *et al*, demonstrated that *in vitro* glucose deprivation of NTS astrocytes stimulates astrocytic Ca^{2+} signalling (McDougal et al. 2013a). Additionally, modulation of Ca^{2+} signalling in astrocytes can bi-directionally control food intake (Chen et al. 2016). While these authors have shown a change in $[Ca^{2+}]_i$ to be involved in calcium signalling, this was not seen in the HPA or U373 cells (see chapter 4). As the primary signalling modality of astrocytes is based on Ca^{2+} this was unexpected and contradicts the literature. Nevertheless, fluorocitrate-induced inhibition of glial metabolism is detrimental to the neuronal response to low glucose (McDougal et al. 2013b, Rogers et al. 2016, Rogers et al. 2018). For the first time, the studies presented in this thesis characterise the metabolic alterations of human astrocytes to acute and RLG. Astrocytes become more dependent on fatty acid metabolism to increase mitochondrial respiration. The increased mitochondrial metabolism and fuel switching may facilitate the protection of astrocytic intracellular nucleotide levels and delay the onset of low glucose sensing. There was also an increase in basal AMPK phosphorylation after RLG compared to control which could increase catabolic processes to maintain intracellular nucleotide levels, but also alter metabolic phenotype; AMPK activation disinhibits fatty acid oxidation (Minokoshi et al. 2002, Yamauchi et al. 2002), for example, and may be increasing the dependency on fatty acids seen in the HPA cells.

Hypoglycaemia increases inflammatory cytokine levels in humans (Gogitidze Joy et al. 2010, Wright et al. 2010). Cytokines, such as IL-6, can directly modulate neuronal

metabolism, altering the hypothalamic pituitary adrenal axis for example (Naitoh et al. 1988, Späth-Schwalbe et al. 1994). Additionally, disruption of astrocyte NFκB signalling protects against diet induced obesity (Buckman et al. 2015, Douglass et al. 2017). The studies presented in chapter 5 demonstrate astrocytic cytokine release in acute low glucose which was exacerbated by RLG, supporting data showing RH increases cytokine production in humans (Joy et al. 2015). Interestingly, in chapter 6, RNA-sequencing found differentially expressed genes involved with inflammatory signalling which also implicates astrocytes as inflammatory mediators of the response to hypoglycaemia. RNA-sequencing also corroborated findings from chapter 3 and demonstrated significant changes in mitochondrial associated gene ontologies.

7.4 Limitations the study

While specific limitations within each preceding chapter have been covered in the discussion, there are more general limitations of this experimental paradigm. These studies were a characterisation of astrocytes in isolation, *in vitro* which should be confirmed in more complete experimental models, i.e. *in vivo*. It is known the gene expression of astrocytes *in vitro* differs from *in vivo* (Passaquin et al. 1994). Astrocytes are a heterogeneous cell type (Wang et al. 2008) with significant differences in neurotransmitter sensitivity when astrocytes from different brain regions are cultured *in vitro* (Schousboe et al. 1979). Therefore, it would be important to study astrocytes from different brain regions, *in situ*, to account for astrocyte heterogeneity. Furthermore, these astrocytes were isolated from a sub-ventricular grey matter region of a 17-year old male. Therefore, it is unknown which region they are from and what impact this has on their morphology. Additionally, *in situ* astrocytes have many thousands of processes (Bushong et al. 2002) which cannot be replicated without the complex interaction with both other cell types and a three-dimensional (3D) extracellular matrix. Indeed, 3D cultures can greatly alter cellular behaviour (Weaver et al. 1997). As such, both the HPA and U373 cells had a relatively simple morphology. The input of signalling molecules from other cell types and the interstitial microenvironment is replaced in culture with supplementation with foetal bovine serum which differs from normal physiology (Foo et al. 2011). Furthermore, *in vitro* usage of animal and human derived products can differentially affect cell phenotype and expression profile (van der Valk et al. 2010). U373 cells

are an astrocytoma cell line, cancerous, and therefore have fundamentally different behaviour and metabolism (Warburg et al. 1936). Therefore, metabolic challenges of these cells would also not precisely replicate the physiological setting; but, this is why human primary astrocytes were used where possible.

Nevertheless, while no cell culture model can fully replicate their normal environment this experimental paradigm has some advantages. Firstly, the characterisation of isolated astrocytes enables a resolution of cellular behaviour that is not easily achieved *in vivo*. For example, measuring mitochondrial and glycolytic metabolism from just astrocytes *in vivo* would not be possible with the current technology available. Again, the separation of different brain cell types allows for distinct transcriptome and proteome profiling with subsequent comparisons between cell types (Cahoy et al. 2008). While these studies have their advantages further validation *in vivo* is required and future experiments should address this. For example, through the use of viral vector injections requiring the *GFAP* promotor could be used to modulate gene expression in astroglial cells specifically (Brenner et al. 1994). Mechanistic questions could be answered by inhibiting or enhancing expression of genes involved in a target process. One could test whether astrocytic fatty acid usage modulates the counterregulatory response. For example, if CPT1-a expression is reduced, does this improve the counterregulatory response?

7.5 Future directions

Ultimately, the aim of this thesis is to elucidate mechanisms by which astrocytes respond to acute and recurrent low glucose. This forms the fundamental research that can be expanded upon to improve hypoglycaemia detection in people with impaired hypoglycaemia awareness, and to better understand astrocytic roles in whole-body energy homeostasis.

Astrocytic support of neuronal cells relies on provision of metabolic support (Pellerin et al. 2012). Beyond direct energy substrate production astrocytes directly contribute to the metabolically costly glutamate-glutamine cycle (Silver et al. 1997), as mentioned in the discussion of chapter 3. Therefore, mitochondrial dysfunction may attenuate the required Na^+ homeostasis for glutamate signalling which would impair glutamate recycling. If this hypothesis is correct, there are two implications. Firstly, excess glutamate accumulation in the synaptic cleft, by insufficient astrocytic

glutamate uptake, could lead to excitotoxicity (Rothstein et al. 1996). However, after RH in rats glutamate levels are decreased in the VMH, which was due to neuronal-astrocyte glutamate-glutamine recycling dysfunction (Chowdhury et al. 2017). Decreased glutamate released, from neurons, could be due to a failure of astrocytes to recycle the glutamate to glutamine and provide it to neurons. Strategies that restore glutamate-glutamine cycle functionality may therefore improve the normal hypoglycaemia-induced glutamate release in the VMH. One such method would be to enhance system N amino acid transporter 3 (SNAT3) activity as it is the primary glutamine exporter in astrocytes (Boulland et al. 2002, McKenna 2007). Hypothetically, increased SNAT3 expression would increase glutamine release from astrocytes and supply neurons with more glutamine to increase glutamate synthesis. Interestingly, knocking out SNAT3 results in hypoglycaemia in mice (Chan et al. 2016). Moreover, a mouse Nuclear factor-erythroid 2-related factor 2 (Nrf2) KO model decreases SNAT3 expression (Lister et al. 2018) and worsens RH-associated brain damage in mice too (McNeilly et al. 2016). Therefore, if the inverse is true, an NRF2 activator, such as dimethyl fumarate (commercially available as Tecfidera, and safe for human consumption) (Linker et al. 2011), could increase SNAT3 expression in astrocytes and improve glutamate-glutamine recycling.

The mechanism by which this mitochondrial dysfunction occurs is not fully elucidated yet. One driver in the metabolic phenotype change may be due to inflammatory signalling. Changes in mitochondrial function, for example increased ROS production, can increase inflammatory signalling (Zhou et al. 2010). Additionally, if ER stress is increased by low glucose as indicated by RNA-seq in chapter 6, unfolded proteins may occur triggering the unfolded protein response (UPR) and increasing ER stress. In itself, this can lead to increased mitochondrial respiration (Knupp et al. 2018). Interestingly, MIF, a cytokine released in response to low glucose from U373 cells, as shown in chapter 5, causes mitochondrial dysfunction in cardiac cells by disrupting cytoskeletal components (Preau et al. 2013). Therefore, low glucose-induced MIF release may contribute to the mitochondrial changes seen in chapter 3. To test the hypothesis that the inhibition of MIF action would prevent or reduce mitochondrial dysfunction, cells could be treated with RLG, or rats with RH with or without an inhibitor of MIF, for example ISO-1 (Al-Abed et al. 2011). If ISO-1 reduces RLG induced mitochondrial dysfunction the subsequent effects on the CRR

could be measured by measuring glucose infusion rates or counterregulatory hormone release during an acute hyperinsulinaemic-hypoglycaemic clamp.

It is known that strict glycaemic control and avoidance of hypoglycaemia can lead to a restoration of hypoglycaemia awareness (Fritsche et al. 2001). Similarly, the mitochondrial adaptations induced by RLG could be partially restored *in vitro* by stopping low glucose treatments and maintenance in 2.5 mM glucose or stock media. However, whether or not these changes are completely reverted given sufficient time should be investigated with a longer time period, as the effects of a single hypoglycaemic episode can last for up to a week in humans (Chow et al. 2014b). An issue with longer duration treatments *in vitro* is that cell division occurs which may affect the outcome of treatment. This could be addressed by using dibutyryl cAMP which matures the astrocyte phenotype and reduces division rates (Wang et al. 2008, Paco et al. 2016).

The adaptation of the astrocytes to increase fatty acid dependency could cause increased ROS production (St-Pierre et al. 2002). This coincides with elevated proton leak, a mitochondrial defence against ROS (Skulachev 1998, Tonkonogi et al. 2000). Therefore, oxidative stress may be increasing within the cell or specifically in the mitochondrial compartment, which could damage mitochondrial function (Kowaltowski et al. 1999). This could be investigated using intracellular ROS fluorescent probes or using electron paramagnetic resonance techniques. Additionally, the increased fatty acid dependency may allow for astrocytic nucleotide levels to be maintained even in low glucose. Therefore, increased fatty acid dependency may prevent the appropriate astrocytic response to low glucose and inhibit normal CRR. This could be investigated by modulating fatty acid activity *in vivo* by overexpressing CPT1-a in glial cells using a *Gfap* promotor, or constitutively activating AMPK to disinhibit fatty acid uptake. Subsequently, the effect of this change in fatty acid metabolism on CRR could be tested using an acute hyperinsulinaemic-hypoglycaemic clamp and measuring the counterregulatory hormone production. The hypothesis being that increased glial fatty acid dependency inhibits CRR.

Lastly, the RNA-sequencing data provides a resource for further data mining. Whilst in the short-term multi-factor analysis and improved fuzzy GO analysis should be

completed, validation and functional characterisation of differentially expressed genes should be investigated. Furthermore, how acute and RLG affects the epigenetic methylation of DNA will be performed. In combination with the RNA-seq data this will be the first comprehensive assessment of the low glucose-induced changes to HPA epigenome and transcriptome.

Table 7.1 Key targets for future research. The table below presents a list of key targets and mechanisms revealed during this thesis that would be a priority for future research.

Target	Evidence	Future research questions
Glutamate-glutamine cycle	RLG-induced mitochondrial dysfunction in HPA cells may be exacerbated when challenged with additional glutamate signalling which may lead to impaired glutamate-glutamine recycling.	Does modulating neuron-astrocyte glutamate-glutamine recycling improve the counterregulatory response to hypoglycaemia?
SNAT3	A SNAT3 KO mouse model results in hypoglycaemia and Nrf2 KO decreases SNAT3 expression, therefore increasing Nrf2 activity may enhance SNAT3 expression and increase glutamine export from astrocytes to improve glutamate-glutamine recycling.	Does dimethyl fumarate, an Nrf2 activator, increase SNAT3 expression in astrocytes and improve glutamate-glutamine recycling by increasing astrocytic glutamine export?
MIF	MIF causes mitochondrial dysfunction in cardiac muscle cells and is released from U373 and HPA cells. MIF release is increased by low glucose and may contribute to astrocytic RLG-induced mitochondrial dysfunction.	Does blocking MIF signalling protect mitochondria from RLG-induced mitochondrial dysfunction?
Mitochondrial ROS	Fatty acid oxidation increases ROS in mitochondria. Both fatty acid oxidation and proton leak were increased by RLG in HPA cells indicating ROS may be increased by RLG.	Does preventing ROS in astrocytes inhibit RLG-induced mitochondrial dysfunction?
CPT1-a	Fatty acid oxidation increases in HPA after RLG. This may be enabling astrocytes to maintain intracellular nucleotide levels	Does increased fatty acid oxidation impair the counterregulatory response *in vivo*?

	and ratios during low glucose.	
AMPK	AMPK inactivation has previously been implicated in blunting CRR. In HPA cells RLG induced an elevated phosphorylation of AMPK in 2.5 mM glucose compared to control treated cells. Chronic AMPK activation may be increasing fatty acid oxidation by disinhibiting CPT1-a.	Does chronic AMPK activation increased fatty acid oxidation and thus worsens the CRR *in vivo*?
Unfolded protein response pathway	RNA-seq has shown HPA cells have differentially regulated gene expression in pathways associated with the endoplasmic reticulum stress response and unfolded protein response pathway. This may increase ROS within the cell and increase cellular stress.	How does ER-stress affect the astrocytic response to low glucose and does it impact hypoglycaemia CRR?

7.5 Final conclusion

In conclusion, this thesis is a characterisation of the intrinsic responses of human astrocytes in response to acute and recurrent low glucose. This includes the novel findings that astrocytes react to low glucose and metabolism is both altered by RLG and recovered following RLG avoidance. While it is unlikely these changes exactly replicate those induced by RH in astrocytes *in situ*, these adaptations could be a protective response, or contribute to hypoglycaemia-induced CRR blunting.

Appendix A

Characterisation of HPA cells morphology and GFAP expression in cell culture

Introduction

Due to cell culture-induced selective pressures and genetic drift cells may have no longer closely represent their original phenotype (Hughes et al. 2007). Furthermore, immortalised or cancerous cells have altered metabolic phenotypes (Warburg et al. 1936). Indeed, U373 cells had several differences from HPA cells, discussed in chapter 3. Long-term cell culture and successive sub-culturing leads to genetic drift and divergent phenotypes (Chang-Liu et al. 1997, Sambuy et al. 2005). Furthermore, contamination of cell cultures with undesired cell types is common (Markovic et al. 1998).

Long term cell culture of HPA cells changes cellular morphology

As a broad measure of phenotypic drift cellular morphology was assessed by staining for GFAP, a key marker of astrocyte phenotype (Bignami et al. 1972). A comparison was made between passage 11 and 18 cells (supplementary figure 1A and B). Note, these passage numbers encompassed the differences between which most experiments were carried out in this thesis. Firstly, all cells observed stained positive for GFAP indicating an astrocyte pure culture. Corrected total cell fluorescence (CTCF), a measure of staining intensity, was unchanged between young and old cells (supplementary figure 1C). Using built in components of the image analysis software FIJI (Fiji is just image J; v1.52a) shape descriptors were calculated and compared. Perimeter to area ratio was significantly decreased in passage 18 cells (supplementary figure 1D) compared to passage 11, indicating a decrease in morphological complexity. Roundness was not different between groups (supplementary figure 1E). Solidity and circularity trended ($p<0.1$) to be higher in older cells (supplementary figure 1F and H). Aspect ratio trended ($p<0.1$) to be lower in passage 18 compared to passage 11 cells. This data shows passage 18 cells have some morphological differences to passage 11 cells.

Supplementary figure 1

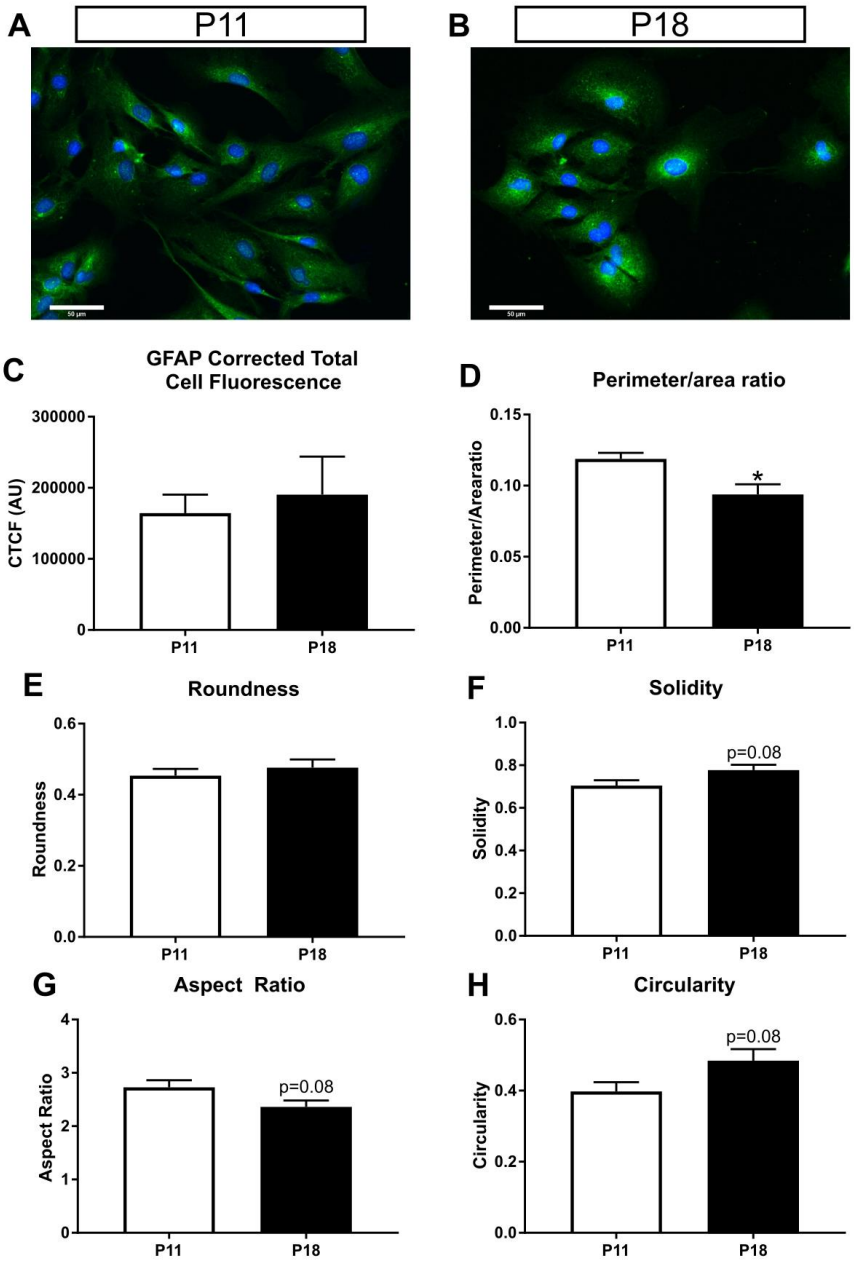

Supplementary figure 1. A comparison of low and high passage human primary astrocytic morphology.

A, **B**. Representative images of human primary astrocytes (HPA; n=4) stained with a glial fibrillary acid protein (GFAP; green) antibody and DAPI to identify nuclei (blue) in young (passage 11) and old (passage 18) cells respectively. Scale bar: 50 μm **C**. Corrected total cell fluorescence (CTCF) of GFAP. **D**. Perimeter to area ratio, a measure of how compact cells are. **E**. Roundness, indicating how round a cell is. **F**. Solidity, demonstrating cellular complexity. **G**. Aspect ratio, indicating how elongated a cell is. **H**. Circularity. *P<0.05. Unpaired two-tailed t-tests. Error bars represent standard error of the mean (SEM).

Discussion

Phenotypic drift of cells occurs during long term cell culture (Hughes et al. 2007). Therefore, using cells within a narrow range of passage numbers will improve variability between experiments and improve reproducibility (Hughes et al. 2007). It is also important to ensure cell type is as expected due to large amounts of cell line contamination occurring in the scientific community (Markovic et al. 1998, Buehring et al. 2004). Therefore, HPA cells used in experimentation were used between passages 10-20 to minimise these problems. However, some cellular morphological differences were detected between passage 11 and 18 cells, indicating some phenotypic drift had occurred. The HPA cells did stain positive for GFAP suggesting they are astrocytes and as there were no cells which did not stain negative for GFAP it also indicates there is no contamination with another cell line.

To determine whether any phenotypic drift that had occurred impacted the functions assessed in this study, comparisons could have been made between passage 10 and 20 cells, the maximum difference in passage number, to test for significant differences. Additionally, to further validate cell type and possible cross contamination, DNA profiling could be used or markers for likely cell contaminators like microglia (CD11b; (Ford et al. 1995)) or neurons (NeuN; (Gusel'nikova et al. 2015)), for example.

Appendix B

Additional detection of cytokines from human primary astrocyte conditioned media

Introduction

Inflammation is a physiological response to noxious stimuli, however it can contribute to pathogenesis in many diseases (Heilbronn et al. 2008). Hypoglycaemia has previously been shown to stimulate the release of cytokines in man (Gogitidze Joy et al. 2010, Wright et al. 2010). However, the release of cytokines from isolated human astrocytes has not been investigated well. Therefore, a cytokine array panel was used to screen for cytokines that may be differentially released from astrocytes following RLG.

Result

Detection of cytokines in conditioned media from human primary astrocytes (HPA) exposed to recurrent low glucose (RLG)

Cytokine release from HPA cells appears to be altered RLG. The following cytokines were detected in the cytokine array panel: C5/C5a, CD40L, G-CSF, GM-CSF, CXCL1, I-309, sICAM-1, IFN-γ (figure 7.2.1A,B,C,D,E,F,G,H), IL-1a, IL-1β, IL-1ra, IL-2, IL-4, IL-5, IL-6, IL-8 (figure 7.2.2A,B,C,D,E,F,G,H), IL-10, IL-12-p70, IL-16, IL-17, IL-17E, IL-23, IL-27, IL-32a (figure 7.2.3A,B,C,D,E,F,G,H), IP10, I-TAC, sTREM-1, MCP-1, MIP-1A, RANTES, MIP-1B, TNF-α, and SDF-1 (figure 7.2.4A,B,C,D,E,F,G,H,I). The expression of cytokines in the control cells was relatively low, with many cytokines below detection level. Comparatively, the expression of cytokines appeared most prevalent cells treated with antecedent RLG.

Supplementary figure 2.1

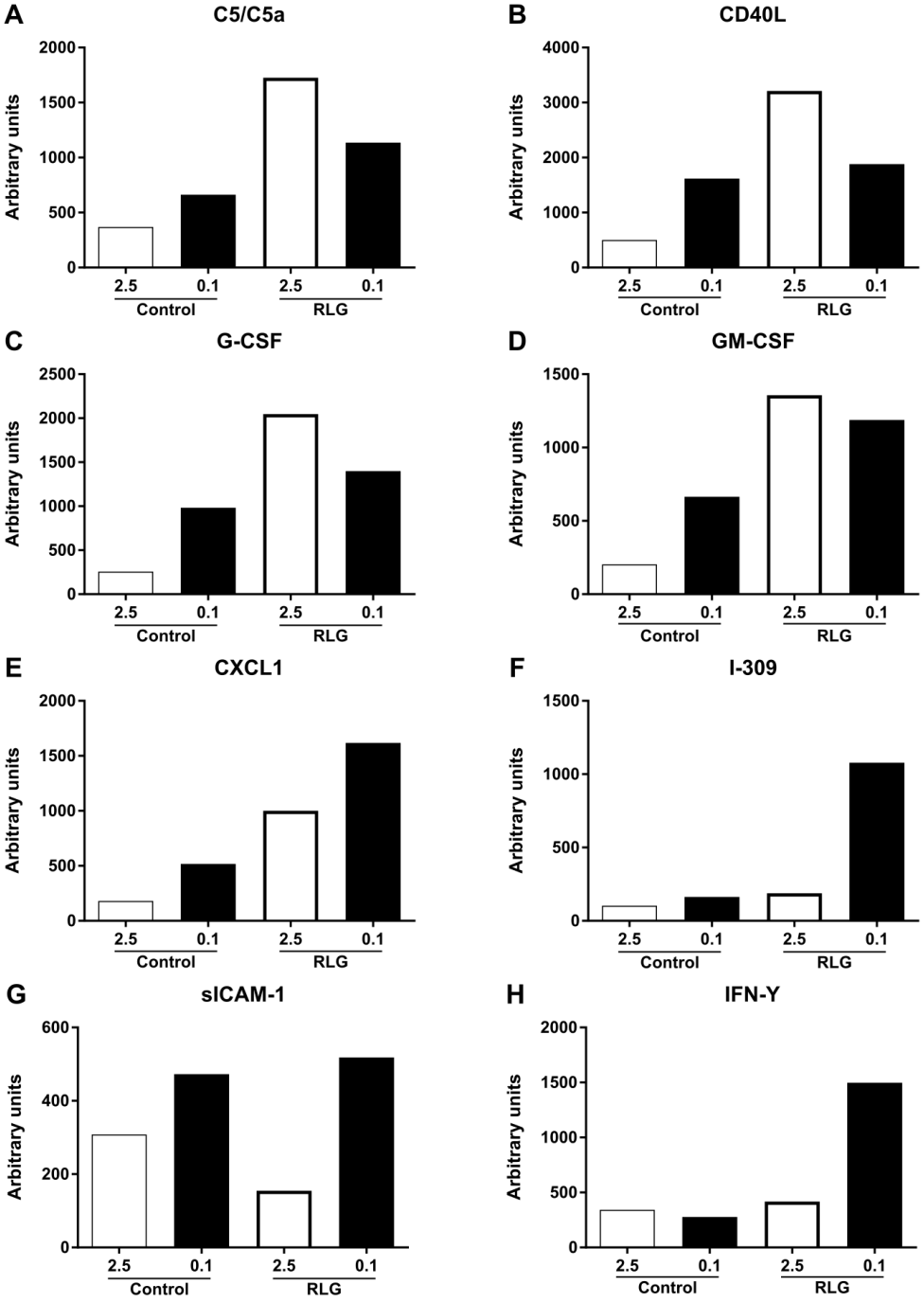

Supplementary figure 2.1 Cytokine release from human primary astrocytes (HPA) exposed to recurrent low glucose (RLG)

The following cytokines were detected in the conditioned media of HPA cells exposed to RLG: **A**. Complement component 5a (C5/C5a). **B**. CD40-ligand (CD40L). **C**. Granulocyte-colony stimulating factor (G-CSF). **D**. Granulocyte-macrophage colony-stimulating factor (GM-CSF). **E**. C-X-C motif chemokine ligand 1 (CXCL1). **F**. I-309. **G**. Soluble intracellular adhesion molecule-1 (sICAM-1). **H**. Interferon-ϒ (IFN-ϒ).

Supplementary figure 2.2

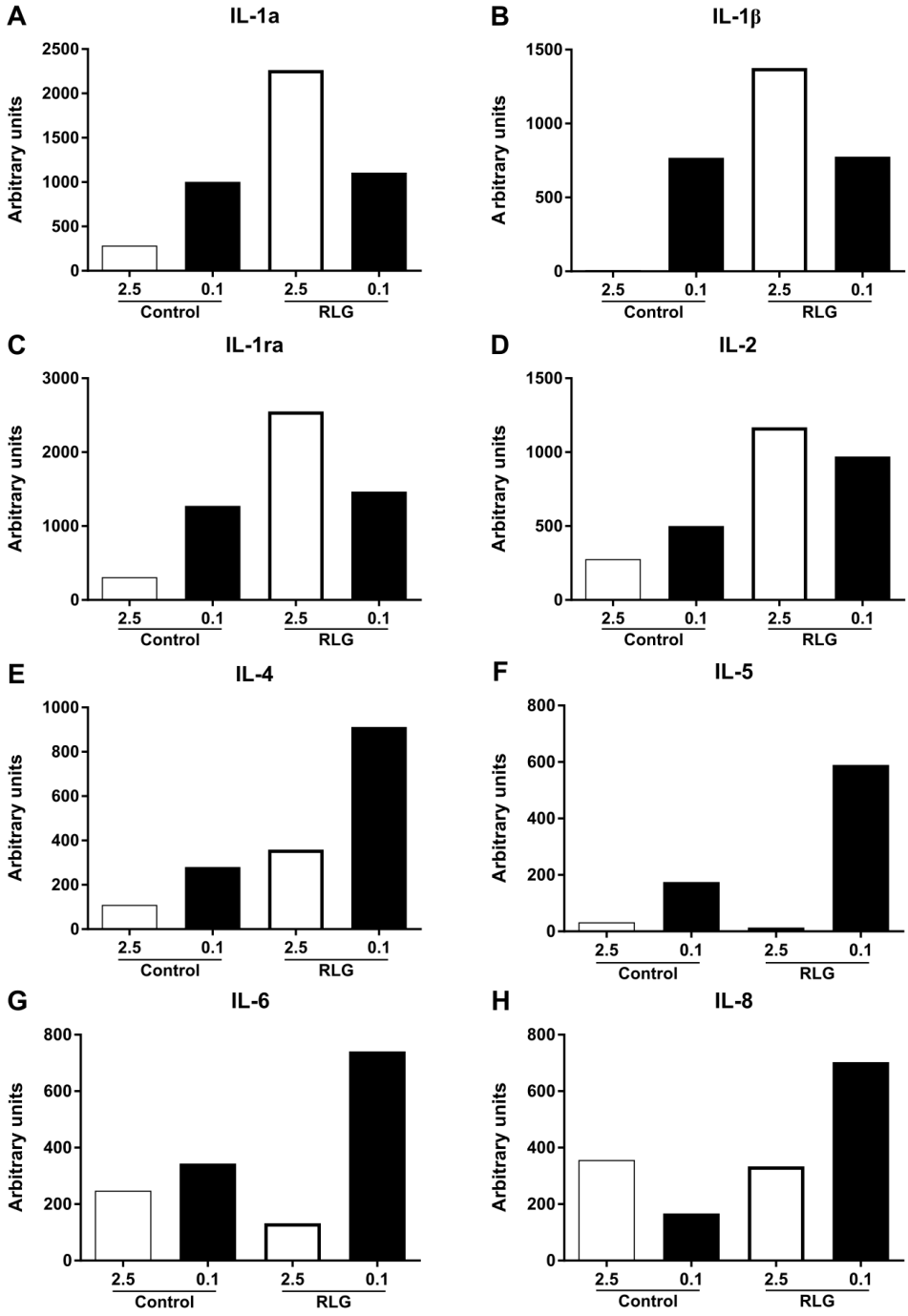

Supplementary figure 2.2 Cytokine release from human primary astrocytes (HPA) exposed to recurrent low glucose (RLG)

The following cytokines were detected in the conditioned media of HPA cells exposed to RLG: **A**. Interleukin-1a (IL-1a). **B**. IL-1β. **C**. IL-1ra. **D**. IL-2. **E**. IL-4. **F**. IL-5. **G**. IL-6. **H**. IL-8.

Supplementary figure 2.3

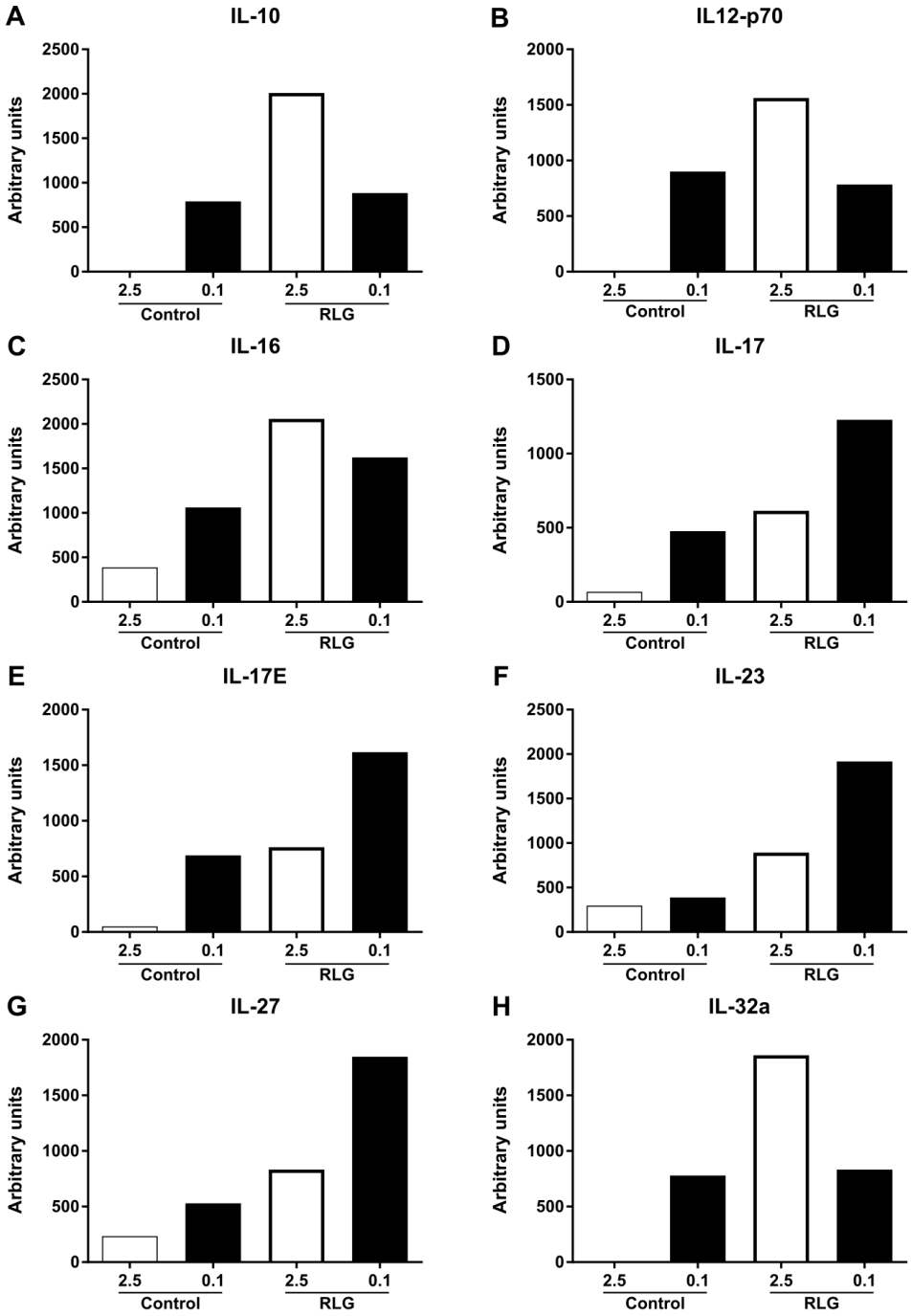

Supplementary figure 2.3 Cytokine release from human primary astrocytes (HPA) exposed to recurrent low glucose (RLG)

The following cytokines were detected in the conditioned media of HPA cells exposed to RLG: **A**. Interleukin-10 (IL-10). **B**. IL-12-p70. **C**. IL-16. D. IL-17. **E**. IL-17E. **F**. IL-23. **G**. IL-27. **H**. IL-32a.

Supplementary figure 2.4

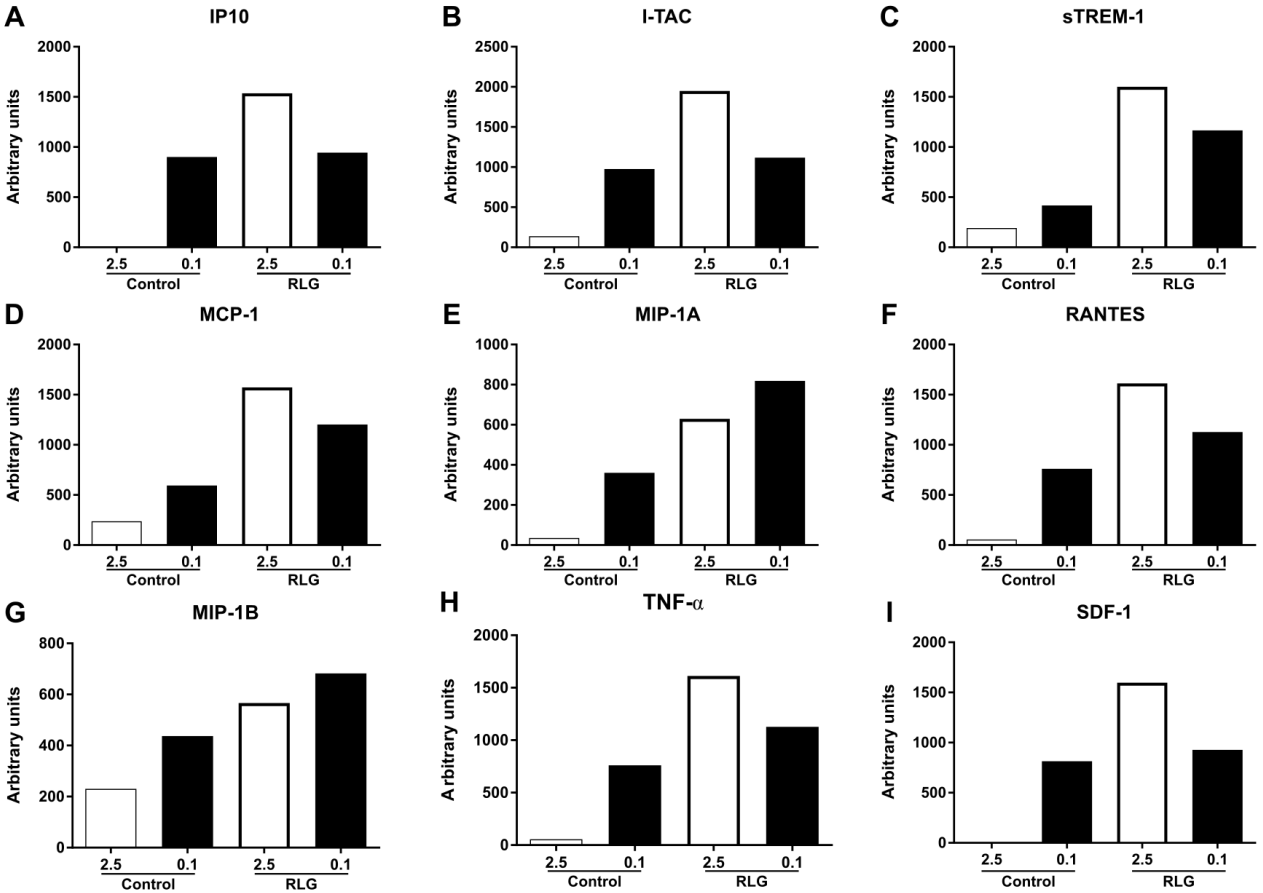

FSupplementary figure 2.4 Cytokine release from human primary astrocytes (HPA) exposed to recurrent low glucose (RLG)

The following cytokines were detected in the conditioned media of HPA cells exposed to RLG: **A**. C-X-C motif chemokine ligand 10 (IP-10). **B**. C-X-C motif chemokine ligand 11 (I-TAC). **C**. Soluble triggering receptor expressed on myeloid cells 1 (sTREM-1). **D**. Monocyte chemoattractant protein-1 (MCP-1). **E**. C-C motif chemokine ligand 3 (MIP-1A). **F**. C-C motif chemokine ligand 5 (RANTES). **G**. C-C motif chemokine ligand 4 (MIP-1B). **H**. Tumour necrosis factor-α (TNF-α). **I**. Stromal cell-derived factor 1 (SDF-1).

Discussion

While there are many cytokines detected by the cytokine array panel it is a semi-quantitative measure of each target. Therefore, validation with quantitative ELISAs is required to establish whether a cytokine is differentially regulated by low glucose exposure. Nevertheless, if inflammatory signalling is significantly altered by acute low glucose this could prove to be an exciting avenue of research to pursue.

Appendix C

Standard curves for enzyme-linked immunosorbent assays

Analysis of enzyme-linked immunosorbent assays

To analyse ELISA data raw optical density data was extracted and put into a web-based ELISA analysis software tool found on www.elisaanalysis.com. A 4-parameter logistic regression algorithm was used as recommended by manufacturers to generate a standard curve from samples of known concentration. The regression formula was as follows:

$$y = d + \frac{a - d}{1 + (\frac{x}{c})^b}$$

Where *y* = response value e.g. optical density, *x* = dose value e.g. concentration, *a* and *d* are the asymptotic ends, b controls the transition between the two asymptotes, and *c* is the transition point midway between the two asymptotes where the direction of the curve changes (Dunn et al. 2013).

For an example of standard curves for an IL-13 ELISA, a PAI1 ELISA, and a MIF ELISA see supplementary figure 3.1A, B and C respectively. The sensitivity ranges for each ELISA are as follows: IL-13 94-6000 pg/ml, PAI1 ELISA 102-25000 pg/ml, and MIF ELISA 8.23-6000 pg/ml.

Supplementary figure 3.1

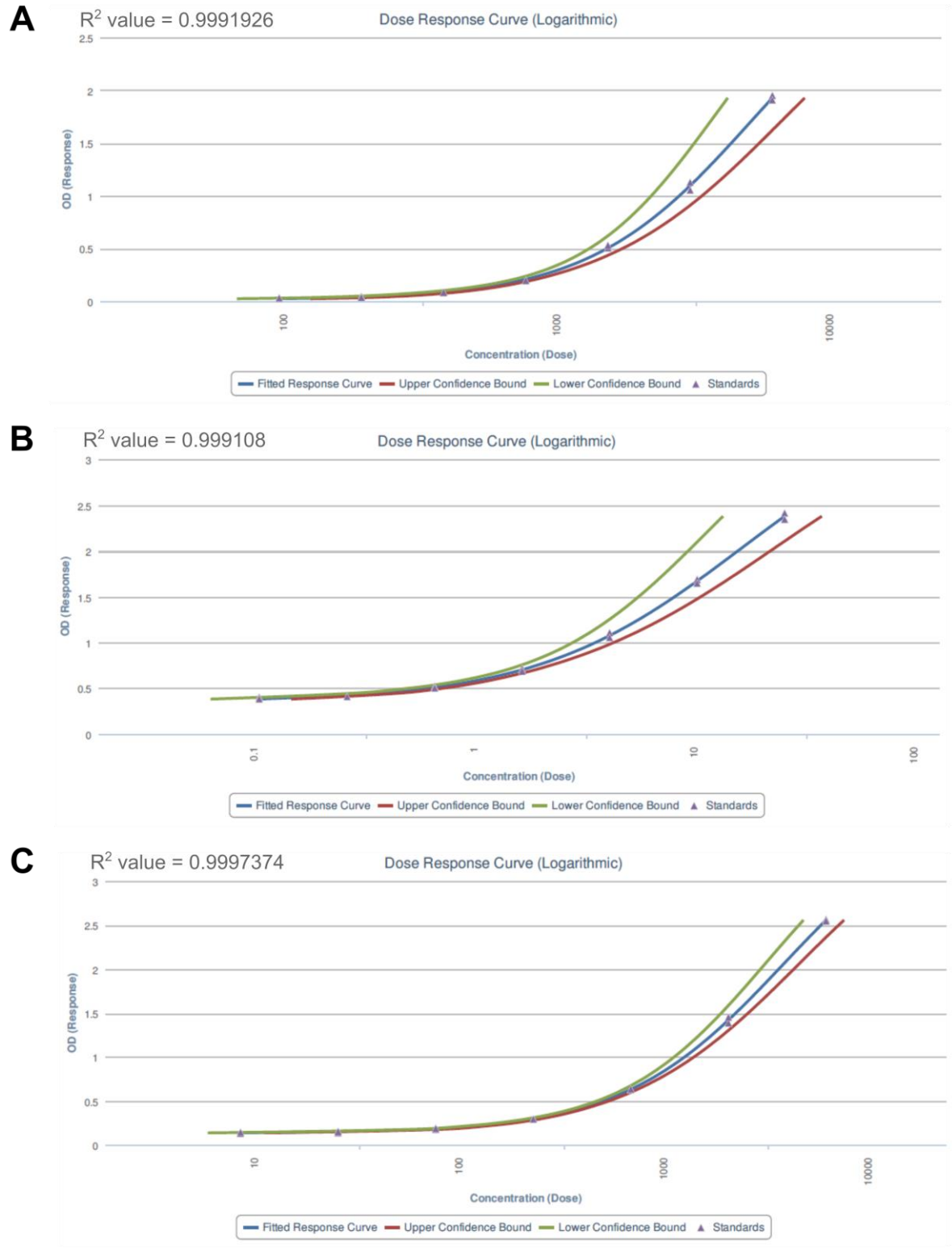

Supplementary figure 3.1. Ensyme-linked immunosorbent assays (ELISAs) were analysed using standard curves generated from samples of known concentration. The line of best fit was determined using 4-parameter logistic regression. **A**. an example of an interleukin-13 ELISA standard curve. **B**. an example of a plasminogen activator inhibitor-1 (PAI-1) ELISA standard curve. **C**. an example of a macrophgae migration inhibitory factor (MIF) ELISA standard curve.

Appendix D

Supplementary tables for RNA-sequencing

Supplementary table 1. Differentially expressed genes induced by 0.1 mM glucose compared to 2.5 mM glucose treated cells

Gene	ENSEMBL ID	Base Mean	log2 Fold-Change	lfcSE	padj
MANF	ENSG00000145050	599.575	0.365	0.063	7.84E-05
TSLP	ENSG00000145777	435.295	0.588	0.104	7.84E-05
IVNS1ABP	ENSG00000116679	1033.816	0.362	0.066	1.66E-04
UBTF	ENSG00000108312	646.619	-0.276	0.051	2.10E-04
BAG3	ENSG00000151929	457.971	-0.333	0.062	2.20E-04
TUBA1A	ENSG00000167552	2943.742	-0.274	0.053	4.08E-04
HSPA1A	ENSG00000204389	125.121	-0.699	0.137	5.97E-04
SRF	ENSG00000112658	235.965	-0.387	0.077	6.51E-04
TXNIP	ENSG00000265972	752.547	-1.724	0.349	9.90E-04
MINDY3	ENSG00000148481	477.137	0.262	0.054	1.20E-03
EXTL3	ENSG00000012232	328.437	-0.372	0.077	1.69E-03
MT-ND4L	ENSG00000212907	10950.516	0.326	0.070	3.65E-03
FBXW7	ENSG00000109670	573.778	0.337	0.074	4.55E-03
CLHC1	ENSG00000162994	59.805	0.650	0.144	4.63E-03
TARS	ENSG00000113407	1944.367	0.172	0.038	4.63E-03
IRF1	ENSG00000125347	273.315	-0.340	0.075	4.63E-03
TUBB4B	ENSG00000188229	1068.985	-0.413	0.092	4.68E-03
EIF5	ENSG00000100664	3079.852	0.219	0.049	4.80E-03
SYNPO	ENSG00000171992	59.493	-0.683	0.155	6.14E-03
IBTK	ENSG00000005700	1218.915	0.198	0.046	8.23E-03
BCL9L	ENSG00000186174	190.312	-0.518	0.120	8.60E-03
PEX1	ENSG00000127980	378.811	0.318	0.075	1.03E-02
PLIN3	ENSG00000105355	550.956	-0.300	0.071	1.04E-02
SGIP1	ENSG00000118473	873.826	0.330	0.078	1.10E-02
NAMPT	ENSG00000105835	477.162	0.337	0.080	1.10E-02
LDLR	ENSG00000130164	1074.790	-0.326	0.077	1.10E-02
MT-ND4	ENSG00000198886	132078.262	0.249	0.059	1.11E-02
ARL4C	ENSG00000188042	146.609	0.489	0.118	1.48E-02
MVK	ENSG00000110921	107.106	-0.470	0.114	1.48E-02
FHOD1	ENSG00000135723	378.504	-0.388	0.094	1.48E-02
XBP1	ENSG00000100219	983.400	0.237	0.058	1.67E-02
WDR36	ENSG00000134987	597.763	0.235	0.058	1.95E-02
CDC20	ENSG00000117399	314.827	-0.475	0.118	1.98E-02
EHD1	ENSG00000110047	253.753	-0.377	0.094	1.98E-02
SLC38A1	ENSG00000111371	443.976	0.223	0.056	2.29E-02

CD55	ENSG00000196352	436.637	0.266	0.067	2.32E-02
ZC3H6	ENSG00000188177	183.543	0.422	0.107	2.32E-02
CCDC25	ENSG00000147419	471.434	0.206	0.052	2.32E-02
NAB2	ENSG00000166886	160.546	-0.407	0.103	2.32E-02
LINC01050	ENSG00000271216	30.309	0.915	0.234	2.57E-02
HERPUD1	ENSG00000051108	1060.067	0.274	0.070	2.57E-02
CLSPN	ENSG00000092853	177.633	-0.375	0.097	2.83E-02
MTHFD2	ENSG00000065911	1050.437	0.255	0.066	2.83E-02
MT-ATP6	ENSG00000198899	59640.661	0.187	0.048	2.83E-02
PNMA1	ENSG00000176903	540.991	-0.217	0.056	3.09E-02
ZNF330	ENSG00000109445	323.717	0.274	0.072	3.28E-02
TUBE1	ENSG00000074935	144.558	0.377	0.099	3.30E-02
E2F7	ENSG00000165891	1122.375	0.268	0.070	3.30E-02
WSB1	ENSG00000109046	2277.164	0.290	0.077	4.02E-02
DCTN4	ENSG00000132912	1011.598	0.160	0.043	4.08E-02
CEP170B	ENSG00000099814	82.942	-0.464	0.124	4.08E-02
AJUBA	ENSG00000129474	704.902	-0.218	0.058	4.08E-02
CENPB	ENSG00000125817	279.448	-0.423	0.113	4.08E-02
MT-ND2	ENSG00000198763	29540.481	0.162	0.043	4.08E-02
MGAT1	ENSG00000131446	772.774	-0.280	0.075	4.16E-02
MAP7D1	ENSG00000116871	484.820	-0.282	0.076	4.17E-02
RND3	ENSG00000115963	2648.063	0.305	0.083	4.17E-02
NABP1	ENSG00000173559	344.282	0.310	0.084	4.17E-02
HECW2	ENSG00000138411	743.925	0.303	0.082	4.17E-02
TUBA4A	ENSG00000127824	314.455	-0.356	0.096	4.17E-02
PACRGL	ENSG00000163138	143.410	0.390	0.105	4.17E-02
DBN1	ENSG00000113758	366.902	-0.359	0.097	4.17E-02
ERMP1	ENSG00000099219	182.851	0.315	0.085	4.17E-02
ECM2	ENSG00000106823	422.926	0.300	0.081	4.17E-02
ABL1	ENSG00000097007	526.352	-0.287	0.078	4.17E-02
TMEM116	ENSG00000198270	107.819	0.460	0.124	4.17E-02
MAVS	ENSG00000088888	1823.207	-0.192	0.053	4.75E-02
RELA	ENSG00000173039	350.050	-0.278	0.077	4.86E-02
CROCCP3	ENSG00000080947	20.235	0.807	0.223	4.92E-02
WFS1	ENSG00000109501	165.696	-0.385	0.107	4.92E-02
MATR3	ENSG00000015479	72.708	0.504	0.140	4.92E-02
ZNF117	ENSG00000152926	197.044	0.336	0.093	4.92E-02
ZNF160	ENSG00000170949	463.337	0.241	0.067	4.92E-02

This table shows the genes that were calculated to be significantly ($p<0.05$) differentially regulated by the software DESeq2 during a contrast of 2.5 and 0.1 mM glucose treated HPA cells.

Supplementary table 2. Differentially expressed genes induced by low glucose compared to control treated cells

Gene	ENSEMBL ID	Base Mean	log2 Fold-Change	lfcSE	padj
TXNIP	ENSG00000265972	746.811	-2.161	0.233	1.59E-16
E2F7	ENSG00000165891	1165.980	0.451	0.081	1.02E-04
IVNS1ABP	ENSG00000116679	1094.735	0.483	0.090	1.72E-04
HECW2	ENSG00000138411	791.570	0.562	0.103	1.72E-04
HSPA1A	ENSG00000204389	129.631	-0.933	0.176	2.40E-04
ATP6	ENSG00000198899	61681.992	0.284	0.055	4.59E-04
THBD	ENSG00000178726	843.004	0.363	0.073	1.01E-03
ND4L	ENSG00000212907	11177.298	0.475	0.097	1.33E-03
RND3	ENSG00000115963	2866.415	0.436	0.093	2.00E-03
MANF	ENSG00000145050	631.756	0.405	0.086	2.00E-03
TSLP	ENSG00000145777	461.264	0.680	0.144	2.00E-03
HSPA5	ENSG00000044574	13380.727	0.343	0.072	2.00E-03
ARRDC4	ENSG00000140450	101.869	-0.807	0.171	2.00E-03
TUBB4B	ENSG00000188229	1065.602	-0.478	0.105	3.63E-03
TUBA1A	ENSG00000167552	3053.849	-0.310	0.069	4.00E-03
HERPUD1	ENSG00000051108	1117.074	0.332	0.075	5.80E-03
ND4	ENSG00000198886	133291.580	0.370	0.084	5.80E-03
ADAMTS6	ENSG00000049192	192.668	0.679	0.154	5.92E-03
BCL9L	ENSG00000186174	182.548	-0.675	0.156	7.58E-03
PLIN3	ENSG00000105355	572.449	-0.429	0.100	8.33E-03
KIAA1109	ENSG00000138688	1367.839	0.311	0.074	1.12E-02
TBC1D8	ENSG00000204634	824.931	0.345	0.085	1.88E-02
LPP	ENSG00000145012	2045.102	0.252	0.062	1.88E-02
HK2	ENSG00000159399	568.131	0.364	0.091	2.06E-02
ZC3H6	ENSG00000188177	192.734	0.535	0.133	2.06E-02
IBTK	ENSG00000005700	1239.309	0.277	0.069	2.06E-02
UBTF	ENSG00000108312	670.508	-0.310	0.077	2.06E-02
SYNGR2	ENSG00000108639	163.828	-0.687	0.171	2.06E-02

LINC00702	ENSG00000233117	190.571	0.581	0.145	2.12E-02
INHBA	ENSG00000122641	1177.565	0.380	0.096	2.44E-02
FMN2	ENSG00000155816	754.142	0.327	0.083	2.70E-02
RNF181	ENSG00000168894	697.084	-0.317	0.081	2.74E-02
FBXW7	ENSG00000109670	576.644	0.402	0.103	2.74E-02
DNAJA1	ENSG00000086061	2855.938	-0.294	0.076	2.74E-02
FHOD1	ENSG00000135723	376.249	-0.445	0.115	2.74E-02
ND2	ENSG00000198763	30185.58	0.246	0.063	2.74E-02
CDC20	ENSG00000117399	303.855	-0.535	0.139	2.76E-02
CD109	ENSG00000156535	1376.444	0.291	0.075	2.76E-02
CENPB	ENSG00000125817	286.676	-0.529	0.137	2.76E-02
DCAF16	ENSG00000163257	270.755	0.413	0.108	3.16E-02
CD44	ENSG00000026508	7605.176	0.215	0.056	3.17E-02
ZNF776	ENSG00000152443	244.777	-0.445	0.117	3.17E-02
NAALADL2	ENSG00000177694	246.646	0.514	0.136	3.57E-02
CORO1B	ENSG00000172725	194.292	-0.656	0.174	3.60E-02
RPS28	ENSG00000233927	141.310	-0.679	0.180	3.60E-02
VGLL3	ENSG00000206538	1238.122	0.340	0.091	3.64E-02
HSPB1	ENSG00000106211	506.869	-0.609	0.163	3.64E-02
EIF5	ENSG00000100664	3142.685	0.254	0.068	3.64E-02
TTC3	ENSG00000182670	4467.921	0.228	0.061	3.64E-02
MDM2	ENSG00000135679	1650.008	0.227	0.061	3.66E-02
XBP1	ENSG00000100219	1057.580	0.282	0.076	3.81E-02
EPHB4	ENSG00000196411	173.693	-0.500	0.135	3.86E-02
RPS19	ENSG00000105372	1289.627	-0.454	0.123	3.86E-02
CLHC1	ENSG00000162994	61.687	0.798	0.216	3.88E-02
CTSD	ENSG00000117984	207.745	-0.777	0.210	3.90E-02
DBN1	ENSG00000113758	368.581	-0.460	0.126	4.39E-02
EXTL3	ENSG00000012232	327.473	-0.431	0.119	4.71E-02
LDLR	ENSG00000130164	1038.284	-0.371	0.102	4.80E-02
CDC42EP1	ENSG00000128283	276.332	-0.613	0.169	4.83E-02
CXXC1	ENSG00000154832	96.564	-0.596	0.165	4.95E-02

This table shows the genes that were calculated to be significantly ($p<0.05$) differentially regulated by the software DESeq2 during a contrast of control and low glucose treated HPA cells.

Supplementary table 3. Differentially expressed genes induced by antecedent RLG compared to low glucose treated cells

Gene	ENSEMBL ID	baseMean	log2FoldChange	lfcSE	padj
THBD	ENSG00000178726	840.365	-0.496	0.071	5.82E-08
RND3	ENSG00000115963	2962.663	-0.446	0.089	4.48E-03
MANF	ENSG00000145050	647.956	-0.439	0.092	5.83E-03
TSLP	ENSG00000145777	480.599	-0.666	0.139	5.83E-03
XBP1	ENSG00000100219	1066.535	-0.371	0.078	5.83E-03
IVNS1ABP	ENSG00000116679	1150.191	-0.438	0.096	1.32E-02
DEPP1	ENSG00000165507	424.987	0.547	0.121	1.32E-02
SYNPO	ENSG00000171992	63.930	0.986	0.230	2.89E-02
ESCO2	ENSG00000171320	169.325	0.542	0.127	2.89E-02
BCL9L	ENSG00000186174	194.479	0.740	0.173	2.89E-02
LDLR	ENSG00000130164	1132.249	0.497	0.115	2.89E-02
CDC20	ENSG00000117399	330.960	0.657	0.157	3.08E-02
EREG	ENSG00000124882	3885.744	-0.430	0.103	3.08E-02
EXTL3	ENSG00000012232	343.269	0.458	0.109	3.08E-02
SMOX	ENSG00000088826	14.605	1.834	0.437	3.08E-02
TXNIP	ENSG00000265972	736.275	2.072	0.502	3.70E-02

This table shows the genes that were calculated to be significantly ($p<0.05$) differentially regulated by the software DESeq2 during a contrast of low glucose and antecedent RLG treated HPA cells.

Supplementary table 4. Significantly affected biological process gene ontologies caused by acute low glucose treatment compared to control

Term	**Adjusted P-value**	**Genes**
negative regulation of intrinsic apoptotic signaling pathway (GO:2001243)	0.00002	DNAJA1;XBP1;MDM2;HSPB1;HERPUD1;HSPA1A
response to unfolded protein (GO:0006986)	0.00007	DNAJA1;HSPA5;HSPB1;HERPUD1;HSPA1A
negative regulation of programmed cell death (GO:0043069)	0.001	DNAJA1;XBP1;HSPA5;TSLP;HSPB1;FMN2;CD44;EPHB4;HSPA1A
negative regulation of endoplasmic reticulum stress-induced intrinsic apoptotic signaling pathway (GO:1902236)	0.002	XBP1;HERPUD1;HSPA1A
negative regulation of apoptotic process (GO:0043066)	0.002	DNAJA1;XBP1;HSPA5;TSLP;HSPB1;FMN2;CD44;EPHB4;HSPA1A
IRE1-mediated unfolded protein response (GO:0036498)	0.003	XBP1;HSPA5;CXXC1;EXTL3
regulation of endoplasmic reticulum stress-	0.003	XBP1;HERPUD1;HSP

induced intrinsic apoptotic signaling pathway (GO:1902235)		A1A
negative regulation of response to endoplasmic reticulum stress (GO:1903573)	0.004	XBP1;HERPUD1;HSPA1A
positive regulation of ubiquitin-protein transferase activity (GO:0051443)	0.010	ARRDC4;CDC20;FBXW7
regulation of apoptotic process (GO:0042981)	0.010	DNAJA1;XBP1;HSPA5;TSLP;HSPB1;FMN2;INHBA;CD44;EPHB4;HSPA1A
regulation of DNA endoreduplication (GO:0032875)	0.015	FBXW7;E2F7
proteasome-mediated ubiquitin-dependent protein catabolic process (GO:0043161)	0.015	CDC20;HSPA5;FBXW7;HECW2;MDM2;RNF181
regulation of endoplasmic reticulum unfolded protein response (GO:1900101)	0.019	XBP1;HSPA5
ATF6-mediated unfolded protein response (GO:0036500)	0.019	XBP1;HSPA5
positive regulation of multicellular organismal process (GO:0051240)	0.019	XBP1;RPS19;INHBA;LDLR;BCL9L
negative regulation of cell activation (GO:0050866)	0.020	THBD;LDLR
protein localization to mitochondrion (GO:0070585)	0.020	DNAJA1;HK2
negative regulation of cell division (GO:0051782)	0.020	TXNIP;E2F7
regulation of lamellipodium morphogenesis (GO:2000392)	0.020	CD44;CORO1B
negative regulation of cellular response to transforming growth factor beta stimulus (GO:1903845)	0.020	CD109;BCL9L;HSPA1A
ubiquitin-dependent protein catabolic process (GO:0006511)	0.020	CDC20;XBP1;HECW2;TTC3;MDM2;RNF181
negative regulation of DNA damage response, signal transduction by p53 class mediator (GO:0043518)	0.021	MDM2;CD44
PERK-mediated unfolded protein response (GO:0036499)	0.021	HSPA5;HERPUD1
negative regulation of transforming growth factor beta receptor signaling pathway (GO:0030512)	0.021	CD109;BCL9L;HSPA1A
regulation of triglyceride biosynthetic process (GO:0010866)	0.023	FBXW7;LDLR
negative regulation of intrinsic apoptotic signaling pathway by p53 class mediator (GO:1902254)	0.026	MDM2;CD44
negative regulation of signal transduction by p53 class mediator (GO:1901797)	0.027	MDM2;CD44

regulation of B cell differentiation (GO:0045577)	0.027	XBP1;INHBA
positive regulation of proteasomal ubiquitin-dependent protein catabolic process (GO:0032436)	0.032	MDM2;HERPUD1;HSPA1A
maintenance of protein localization in organelle (GO:0072595)	0.035	HSPA5;HK2
positive regulation of proteasomal protein catabolic process (GO:1901800)	0.035	FBXW7;MDM2;HSPA1A
ribosomal small subunit assembly (GO:0000028)	0.037	RPS28;RPS19
negative regulation of transmembrane receptor protein serine/threonine kinase signaling pathway (GO:0090101)	0.037	CD109;BCL9L;HSPA1A
regulation of transforming growth factor beta receptor signaling pathway (GO:0017015)	0.039	CD109;BCL9L;HSPA1A
negative regulation of cell cycle process (GO:0010948)	0.040	FBXW7;MDM2;E2F7
cellular response to unfolded protein (GO:0034620)	0.043	HSPA5;HSPA1A
positive regulation of erythrocyte differentiation (GO:0045648)	0.043	INHBA;HSPA1A
regulation of mitotic cell cycle phase transition (GO:1901990)	0.044	CDC20;TUBA1A;HECW2;TUBB4B
positive regulation of immune effector process (GO:0002699)	0.046	XBP1;RPS19
chaperone mediated protein folding requiring cofactor (GO:0051085)	0.046	HSPA5;HSPA1A
regulation of DNA damage response, signal transduction by p53 class mediator (GO:0043516)	0.047	MDM2;CD44
negative regulation of wound healing (GO:0061045)	0.047	THBD;CD109
regulation of protein catabolic process (GO:0042176)	0.047	HECW2;MDM2;FMN2

This table shows the biological process gene ontologies that were calculated to be significantly ($p<0.05$) differentially regulated by the software EnrichR from a list of gene differentially regulated by 0.1 mM glucose compared to 2.5 mM glucose HPA cells.

Supplementary table 5. Significantly affected biological process gene ontologies caused by antecedent RLG treatment compared to acute low glucose

Term	Adjusted P-value	Genes
positive regulation of interleukin-6 production (GO:0032755)	0.0017	XBP1;TSLP;EREG
positive regulation of multicellular organismal process (GO:0051240)	0.0026	XBP1;LDLR;EREG;BCL9L
negative regulation of cell activation (GO:0050866)	0.0034	THBD;LDLR
positive regulation of immune response (GO:0050778)	0.0380	XBP1;EREG
cholesterol homeostasis (GO:0042632)	0.0380	XBP1;LDLR
IRE1-mediated unfolded protein response (GO:0036498)	0.0380	XBP1;EXTL3
keratinocyte differentiation (GO:0030216)	0.0380	TXNIP;EREG
sterol homeostasis (GO:0055092)	0.0380	XBP1;LDLR
regulation of DNA replication (GO:0006275)	0.0380	ESCO2;EREG
epidermal cell differentiation (GO:0009913)	0.0411	TXNIP;EREG
positive regulation of defense response (GO:0031349)	0.0416	TSLP;EREG
positive regulation of cytokine secretion (GO:0050715)	0.0416	XBP1;TSLP
regulation of interleukin-5 secretion (GO:2000662)	0.0418	TSLP
regulation of smooth muscle cell differentiation (GO:0051150)	0.0418	EREG
negative regulation of macrophage activation (GO:0043031)	0.0418	LDLR
regulation of microglial cell activation (GO:1903978)	0.0418	LDLR
sterol import (GO:0035376)	0.0418	LDLR
positive regulation of B cell differentiation (GO:0045579)	0.0418	XBP1
cholesterol import (GO:0070508)	0.0418	LDLR
polyamine biosynthetic process (GO:0006596)	0.0418	SMOX
negative regulation of smooth muscle cell differentiation (GO:0051151)	0.0418	EREG
regulation of lysosomal protein catabolic process (GO:1905165)	0.0418	LDLR
regulation of interleukin-13 production (GO:0032656)	0.0418	TSLP
positive regulation of amyloid-beta clearance (GO:1900223)	0.0418	LDLR
regulation of endoplasmic reticulum unfolded protein response (GO:1900101)	0.0418	XBP1
intestinal lipid absorption (GO:0098856)	0.0418	LDLR
positive regulation of triglyceride biosynthetic process (GO:0010867)	0.0418	LDLR
cellular biogenic amine catabolic process	0.0418	SMOX

(GO:0042402)		
positive regulation of production of molecular mediator of immune response (GO:0002702)	0.0418	XBP1
cellular triglyceride homeostasis (GO:0035356)	0.0418	XBP1
regulation of MHC class II biosynthetic process (GO:0045346)	0.0418	XBP1
regulation of immunoglobulin production (GO:0002637)	0.0418	XBP1
response to interleukin-4 (GO:0070670)	0.0418	XBP1
negative regulation of nitrogen compound metabolic process (GO:0051172)	0.0418	LDLR
regulation of nitrogen compound metabolic process (GO:0051171)	0.0418	LDLR
positive regulation of synapse maturation (GO:0090129)	0.0418	CDC20
regulation of immunoglobulin secretion (GO:0051023)	0.0418	XBP1
chylomicron remnant clearance (GO:0034382)	0.0418	LDLR
regulation of synapse maturation (GO:0090128)	0.0418	CDC20
negative regulation of fibrinolysis (GO:0051918)	0.0418	THBD
adipose tissue development (GO:0060612)	0.0418	XBP1
intestinal cholesterol absorption (GO:0030299)	0.0418	LDLR
regulation of mast cell activation (GO:0033003)	0.0418	TSLP
positive regulation of immunoglobulin secretion (GO:0051024)	0.0418	XBP1
ATF6-mediated unfolded protein response (GO:0036500)	0.0418	XBP1
fatty acid homeostasis (GO:0055089)	0.0418	XBP1
regulation of amyloid-beta clearance (GO:1900221)	0.0418	LDLR
transcription, DNA-templated (GO:0006351)	0.0418	IVNS1ABP;XBP1;EREG
intracellular cholesterol transport (GO:0032367)	0.0418	LDLR
positive regulation of epidermal growth factor-activated receptor activity (GO:0045741)	0.0418	EREG
regulation of interleukin-6 biosynthetic process (GO:0045408)	0.0418	EREG
positive regulation of interleukin-5 production (GO:0032754)	0.0418	TSLP
regulation of cell motility (GO:2000145)	0.0418	RND3;EREG
positive regulation of cellular biosynthetic process (GO:0031328)	0.0418	LDLR;EREG
cellular response to interleukin-4	0.0418	XBP1

(GO:0071353)		
neuron differentiation (GO:0030182)	0.0418	XBP1;MANF
regulation of amyloid fibril formation (GO:1905906)	0.0418	LDLR
positive regulation of cell proliferation (GO:0008284)	0.0418	XBP1;TSLP;EREG
positive regulation of interleukin-13 production (GO:0032736)	0.0418	TSLP
skin development (GO:0043588)	0.0418	TXNIP;EREG
positive regulation of response to external stimulus (GO:0032103)	0.0418	THBD;TSLP
positive regulation of macromolecule biosynthetic process (GO:0010557)	0.0418	XBP1;EREG
positive regulation of cellular component organization (GO:0051130)	0.0418	CDC20;LDLR
positive regulation of cellular process (GO:0048522)	0.0418	XBP1;TSLP;EREG
neuron development (GO:0048666)	0.0418	XBP1;MANF
negative regulation of cell division (GO:0051782)	0.0442	TXNIP
negative regulation of myotube differentiation (GO:0010832)	0.0442	XBP1
positive regulation of endoplasmic reticulum unfolded protein response (GO:1900103)	0.0453	XBP1
regulation of cytokine biosynthetic process (GO:0042035)	0.0453	EREG
polyamine metabolic process (GO:0006595)	0.0453	SMOX
positive regulation of cell differentiation (GO:0045597)	0.0453	XBP1;BCL9L
negative regulation of muscle cell differentiation (GO:0051148)	0.0456	EREG
negative regulation of hemostasis (GO:1900047)	0.0456	THBD
cellular response to low-density lipoprotein particle stimulus (GO:0071404)	0.0456	LDLR
positive regulation of triglyceride metabolic process (GO:0090208)	0.0456	LDLR
positive regulation of leukocyte activation (GO:0002696)	0.0456	TSLP
regulation of triglyceride biosynthetic process (GO:0010866)	0.0456	LDLR
negative regulation of endoplasmic reticulum stress-induced intrinsic apoptotic signaling pathway (GO:1902236)	0.0456	XBP1
regulation of B cell differentiation (GO:0045577)	0.0456	XBP1
regulation of fibrinolysis (GO:0051917)	0.0456	THBD
negative regulation of coagulation (GO:0050819)	0.0456	THBD

positive regulation of response to endoplasmic reticulum stress (GO:1905898)	0.0456	XBP1
positive regulation of response to cytokine stimulus (GO:0060760)	0.0456	TSLP
negative regulation of platelet activation (GO:0010544)	0.0456	THBD
positive regulation of lymphocyte differentiation (GO:0045621)	0.0456	XBP1
positive regulation of secretion (GO:0051047)	0.0456	XBP1
heparan sulfate proteoglycan biosynthetic process (GO:0015012)	0.0456	EXTL3
establishment or maintenance of actin cytoskeleton polarity (GO:0030950)	0.0456	RND3
cellular biogenic amine biosynthetic process (GO:0042401)	0.0456	SMOX
negative regulation of striated muscle cell differentiation (GO:0051154)	0.0456	XBP1
positive regulation of cytokine production (GO:0001819)	0.0456	TSLP;EREG
positive regulation of signal transduction (GO:0009967)	0.0456	XBP1;TSLP
long-term memory (GO:0007616)	0.0472	LDLR
positive regulation of interleukin-6 secretion (GO:2000778)	0.0472	XBP1
positive regulation of STAT cascade (GO:1904894)	0.0478	TSLP
positive regulation of immunoglobulin production (GO:0002639)	0.0478	XBP1
regulation of chemokine production (GO:0032642)	0.0478	TSLP
regulation of myotube differentiation (GO:0010830)	0.0478	XBP1
anion homeostasis (GO:0055081)	0.0478	XBP1
regulation of platelet activation (GO:0010543)	0.0478	THBD
cellular response to interleukin-7 (GO:0098761)	0.0478	TSLP
positive regulation of blood coagulation (GO:0030194)	0.0478	THBD
interleukin-7-mediated signaling pathway (GO:0038111)	0.0478	TSLP
dopaminergic neuron differentiation (GO:0071542)	0.0488	MANF
regulation of endoplasmic reticulum stress-induced intrinsic apoptotic signaling pathway (GO:1902235)	0.0488	XBP1
heparan sulfate proteoglycan metabolic process (GO:0030201)	0.0488	EXTL3
mRNA transcription (GO:0009299)	0.0488	EREG
positive regulation of transcription from RNA	0.0488	XBP1

polymerase II promoter involved in cellular response to chemical stimulus (GO:1901522)		
hepaticobiliary system development (GO:0061008)	0.0488	XBP1
sterol transport (GO:0015918)	0.0488	LDLR
cellular response to hexose stimulus (GO:0071331)	0.0488	XBP1
positive regulation of interleukin-10 production (GO:0032733)	0.0496	TSLP
regulation of ERBB signaling pathway (GO:1901184)	0.0496	EREG
negative regulation of response to endoplasmic reticulum stress (GO:1903573)	0.0496	XBP1

This table shows the biological process gene ontologies that were calculated to be significantly ($p<0.05$) differentially regulated by the software EnrichR from a list of gene differentially regulated by antecedent RLG compared to acute low glucose treatment.

Supplementary table 6. Significantly affected molecular function gene ontologies caused by 0.1 mM glucose treatment compared to 2.5 mM glucose

Term	Adjusted P-value	Genes
phosphate ion binding (GO:0042301)	0.011	MTHFD2;RELA
purine ribonucleoside triphosphate binding (GO:0035639)	0.011	TUBA1A;ABL1;TUBE1; PEX1;TUBB4B;RND3; TUBA4A;HSPA1A
guanyl ribonucleotide binding (GO:0032561)	0.011	TUBA1A;TUBE1;TUBB 4B;RND3;TUBA4A
NADH dehydrogenase (ubiquinone) activity (GO:0008137)	0.011	MT-ND4L;MT-ND4;MT-ND2
NADH dehydrogenase (quinone) activity (GO:0050136)	0.011	MT-ND4L;MT-ND4;MT-ND2
GTP binding (GO:0005525)	0.011	TUBA1A;TUBE1;TUBB 4B;RND3;TUBA4A
purine ribonucleoside binding (GO:0032550)	0.011	TUBA1A;TUBE1;TUBB 4B;RND3;TUBA4A
cadherin binding (GO:0045296)	0.017	EHD1;EIF5;BAG3;PLIN 3;DBN1;HSPA1A
transcriptional activator activity, RNA polymerase II distal enhancer sequence-specific binding (GO:0001205)	0.033	SRF;RELA
transcription factor activity, RNA polymerase II core promoter sequence-specific	0.036	SRF;RELA

(GO:0000983)		
ubiquitin protein ligase binding (GO:0031625)	0.044	FBXW7;WFS1;TXNIP; RELA;HSPA1A
histone deacetylase binding (GO:0042826)	0.044	SRF;RELA;HSPA1A
ubiquitin-like protein ligase binding (GO:0044389)	0.049	FBXW7;WFS1;TXNIP; RELA;HSPA1A

This table shows the molecular function gene ontologies that were calculated to be significantly ($p<0.05$) differentially regulated by the software EnrichR from a list of gene differentially regulated by 0.1 mM glucose compared to 2.5 mM glucose HPA cells.

Bibliography

Abbracchio, M. P., Burnstock, G., Verkhratsky, A. and Zimmermann, H. (2009). "Purinergic signalling in the nervous system: an overview." Trends in Neurosciences **32**(1): 19-29.

Abi-Saab, W. M., Maggs, D. G., Jones, T., Jacob, R., Srihari, V., Thompson, J., Kerr, D., Leone, P., Krystal, J. H., Spencer, D. D., During, M. J. and Sherwin, R. S. (2002). "Striking Differences in Glucose and Lactate Levels between Brain Extracellular Fluid and Plasma in Conscious Human Subjects: Effects of Hyperglycemia and Hypoglycemia." Journal of Cerebral Blood Flow & Metabolism **22**(3): 271-279.

Abraira, C., Colwell, J. A., Nuttall, F. Q., Sawin, C. T., Nagel, N. J., Comstock, J. P., Emanuele, N. V., Levin, S. R., Henderson, W. and Lee, H. S. (1995). "Veterans Affairs Cooperative Study on Glycemic Control and Complications in Type II Diabetes (VA CSDM): Results of the feasibility trial." Diabetes Care **18**(8): 1113-1123.

Acosta-Alvear, D., Zhou, Y., Blais, A., Tsikitis, M., Lents, N. H., Arias, C., Lennon, C. J., Kluger, Y. and Dynlacht, B. D. (2007). "XBP1 controls diverse cell type- and condition-specific transcriptional regulatory networks." Mol Cell **27**(1): 53-66.

ADA (2014). "Diagnosis and Classification of Diabetes Mellitus." Diabetes Care **37**(Supplement 1): S81-S90.

Adachi, A., Shimizu, N., Oomura, Y. and Kobashi, M. (1984). "Convergence of hepatoportal glucose-sensitive afferent signals to glucose-sensitive units within the nucleus of the solitary tract." Neurosci Lett **46**(2): 215-218.

Ainscow, E. K., Mirshamsi, S., Tang, T., Ashford, M. L. J. and Rutter, G. A. (2004). "Dynamic imaging of free cytosolic ATP concentration during fuel sensing by rat hypothalamic neurones: evidence for ATP-independent control of ATP-sensitive K+ channels." The Journal of Physiology **544**(2): 429-445.

Akabayashi, A., Levin, N., Paez, X., Alexander, J. T. and Leibowitz, S. F. (1994). "Hypothalamic neuropeptide Y and its gene expression: relation to light/dark cycle and circulating corticosterone." Mol Cell Neurosci **5**(3): 210-218.

Akabayashi, A., Zaia, C. T., Silva, I., Chae, H. J. and Leibowitz, S. F. (1993). "Neuropeptide Y in the arcuate nucleus is modulated by alterations in glucose utilization." Brain Res **621**(2): 343-348.

Al-Abed, Y. and VanPatten, S. (2011). "MIF as a disease target: ISO-1 as a proof-of-concept therapeutic." Future medicinal chemistry **3**(1): 45-63.

Alberti, K. G. and Zimmet, P. Z. (1998). "Definition, diagnosis and classification of diabetes mellitus and its complications. Part 1: diagnosis and classification of diabetes mellitus provisional report of a WHO consultation." Diabet Med **15**(7): 539-553.

Alexeyenko, A., Lee, W., Pernemalm, M., Guegan, J., Dessen, P., Lazar, V., Lehtiö, J. and Pawitan, Y. (2012). "Network enrichment analysis: extension of gene-set enrichment analysis to gene networks." BMC Bioinformatics **13**(1): 226.

Allaman, I., Gavillet, M., Bélanger, M., Laroche, T., Viertl, D., Lashuel, H. A. and Magistretti, P. J. (2010). "Amyloid-β Aggregates Cause Alterations of Astrocytic Metabolic Phenotype: Impact on Neuronal Viability." The Journal of Neuroscience **30**(9): 3326-3338.

Almeida, A., Moncada, S. and Bolanos, J. P. (2004). "Nitric oxide switches on glycolysis through the AMP protein kinase and 6-phosphofructo-2-kinase pathway." Nat Cell Biol **6**(1): 45-51.

Aloisi, F., Penna, G., Cerase, J., Iglesias, B. M. and Adorini, L. (1997). "IL-12 production by central nervous system microglia is inhibited by astrocytes." The Journal of Immunology **159**(4): 1604-1612.

Alquier, T., Kawashima, J., Tsuji, Y. and Kahn, B. B. (2007). "Role of hypothalamic adenosine 5'-monophosphate-activated protein kinase in the impaired counterregulatory response induced by repetitive neuroglucopenia." Endocrinology **148**(3): 1367-1375.

Amaral, A. I., Teixeira, A. P., Martens, S., Bernal, V., Sousa, M. F. and Alves, P. M. (2010). "Metabolic alterations induced by ischemia in primary cultures of astrocytes: merging 13C NMR spectroscopy and metabolic flux analysis." J Neurochem **113**(3): 735-748.

Amsterdam, J. D., Maislin, G. and Potter, L. (1994). "Fluoxetine efficacy in treatment resistant depression." Progress in Neuro-Psychopharmacology and Biological Psychiatry **18**(2): 243-261.

An, Y., Varma, V. R., Varma, S., Casanova, R., Dammer, E., Pletnikova, O., Chia, C. W., Egan, J. M., Ferrucci, L., Troncoso, J., Levey, A. I., Lah, J., Seyfried, N. T., Legido-Quigley, C., O'Brien, R. and Thambisetty, M. (2018). "Evidence for brain

glucose dysregulation in Alzheimer's disease." Alzheimer's & Dementia **14**(3): 318-329.

Anderson, C. M. and Swanson, R. A. (2000). "Astrocyte glutamate transport: review of properties, regulation, and physiological functions." Glia **32**(1): 1-14.

Anderson, K. A., Ribar, T. J., Lin, F., Noeldner, P. K., Green, M. F., Muehlbauer, M. J., Witters, L. A., Kemp, B. E. and Means, A. R. (2008). "Hypothalamic CaMKK2 contributes to the regulation of energy balance." Cell Metab **7**(5): 377-388.

Andrew, S. F., Dinh, T. T. and Ritter, S. (2007). "Localized glucoprivation of hindbrain sites elicits corticosterone and glucagon secretion." Am J Physiol Regul Integr Comp Physiol **292**(5): R1792-1798.

Andrews, B., Carroll, J., Ding, S., Fearnley, I. M. and Walker, J. E. (2013). "Assembly factors for the membrane arm of human complex I." Proceedings of the National Academy of Sciences **110**(47): 18934-18939.

Andrews, P. W., Bharwani, A., Lee, K. R., Fox, M. and Thomson, J. A. (2015). "Is serotonin an upper or a downer? The evolution of the serotonergic system and its role in depression and the antidepressant response." Neuroscience & Biobehavioral Reviews **51**: 164-188.

Angel, I., Niddam, R. and Langer, S. Z. (1990). "Involvement of alpha-2 adrenergic receptor subtypes in hyperglycemia." Journal of Pharmacology and Experimental Therapeutics **254**(3): 877-882.

Angelova, P. R., Kasymov, V., Christie, I., Sheikhbahaei, S., Turovsky, E., Marina, N., Korsak, A., Zwicker, J., Teschemacher, A. G. and Ackland, G. L. (2015). "Functional oxygen sensitivity of astrocytes." Journal of Neuroscience **35**(29): 10460-10473.

Ankarcrona, M., Dypbukt, J. M., Bonfoco, E., Zhivotovsky, B., Orrenius, S., Lipton, S. A. and Nicotera, P. (1995). "Glutamate-induced neuronal death: a succession of necrosis or apoptosis depending on mitochondrial function." Neuron **15**(4): 961-973.

Aoki, C., Venkatesan, C. and Kurose, H. (1998). "Noradrenergic modulation of the prefrontal cortex as revealed by electron microscopic immunocytochemistry." Adv Pharmacol **42**: 777-780.

Aponte, Y., Atasoy, D. and Sternson, S. M. (2011). "AGRP neurons are sufficient to orchestrate feeding behavior rapidly and without training." Nat Neurosci **14**(3): 351-355.

Araque, A., Carmignoto, G. and Haydon, P. G. (2001). "Dynamic signaling between astrocytes and neurons." Annual review of physiology **63**(1): 795-813.

Araque, A., Li, N., Doyle, R. T. and Haydon, P. G. (2000). "SNARE protein-dependent glutamate release from astrocytes." Journal of Neuroscience **20**(2): 666-673.

Araque, A., Martín, E. D., Perea, G., Arellano, J. I. and Buño, W. (2002). "Synaptically released acetylcholine evokes Ca2+ elevations in astrocytes in hippocampal slices." Journal of Neuroscience **22**(7): 2443-2450.

Araque, A., Parpura, V., Sanzgiri, R. P. and Haydon, P. G. (1998a). "Glutamate-dependent astrocyte modulation of synaptic transmission between cultured hippocampal neurons." European Journal of Neuroscience **10**(6): 2129-2142.

Araque, A., Parpura, V., Sanzgiri, R. P. and Haydon, P. G. (1999). "Tripartite synapses: glia, the unacknowledged partner." Trends in Neurosciences **22**(5): 208-215.

Araque, A., Sanzgiri, R. P., Parpura, V. and Haydon, P. G. (1998b). "Calcium elevation in astrocytes causes an NMDA receptor-dependent increase in the frequency of miniature synaptic currents in cultured hippocampal neurons." Journal of Neuroscience **18**(17): 6822-6829.

Arzoine, L., Zilberberg, N., Ben-Romano, R. and Shoshan-Barmatz, V. (2009). "Voltage-dependent Anion Channel 1-based Peptides Interact with Hexokinase to Prevent Its Anti-apoptotic Activity." Journal of Biological Chemistry **284**(6): 3946-3955.

Ashcroft, F. M. (1996). "Mechanisms of the glycaemic effects of sulfonylureas." Hormone and metabolic research **28**(09): 456-463.

Assimacopoulos-Jeannet, F., Brichard, S., Rencurel, F., Cusin, I. and Jeanrenaud, B. (1995). "In vivo effects of hyperinsulinemia on lipogenic enzymes and glucose transporter expression in rat liver and adipose tissues." Metabolism **44**(2): 228-233.

Association, A. D. (2012). "Diagnosis and classification of diabetes mellitus." Diabetes Care **35**((suppl 1)): 64-71.

Atkinson, M. A. and Eisenbarth, G. S. (2001). "Type 1 diabetes: new perspectives on disease pathogenesis and treatment." The Lancet **358**(9277): 221-229.

Attwell, D. and Laughlin, S. B. (2001). "An energy budget for signaling in the grey matter of the brain." Journal of Cerebral Blood Flow & Metabolism **21**(10): 1133-1145.

Aveseh, M., Nikooie, R., Sheibani, V. and Esmaeili-Mahani, S. (2014). "Endurance training increases brain lactate uptake during hypoglycemia by up regulation of brain lactate transporters." Mol Cell Endocrinol **394**(1-2): 29-36.

Bacher, M., Deuster, O., Aljabari, B., Egensperger, R., Neff, F., Jessen, F., Popp, J., Noelker, C., Reese, J. P. and Al-Abed, Y. (2010). "The role of macrophage migration inhibitory factor in Alzheimer's disease." Mol Med **16**(3-4): 116-121.

Bacher, M., Schrader, J., Thompson, N., Kuschela, K., Gemsa, D., Waeber, G. and Schlegel, J. (2003). "Up-Regulation of Macrophage Migration Inhibitory Factor Gene and Protein Expression in Glial Tumor Cells during Hypoxic and Hypoglycemic Stress Indicates a Critical Role for Angiogenesis in Glioblastoma Multiforme." The American Journal of Pathology **162**(1): 11-17.

Bajaj, M., Suraamornkul, S., Pratipanawatr, T., Hardies, L. J., Pratipanawatr, W., Glass, L., Cersosimo, E., Miyazaki, Y. and DeFronzo, R. A. (2003). "Pioglitazone Reduces Hepatic Fat Content and Augments Splanchnic Glucose Uptake in Patients With Type 2 Diabetes." Diabetes **52**(6): 1364-1370.

Baldwin, H. A. and File, S. E. (1989). "Caffeine-induced anxiogenesis: The role of adenosine, benzodiazepine and noradrenergic receptors." Pharmacology Biochemistry and Behavior **32**(1): 181-186.

Balfour, R. H., Hansen, A. M. and Trapp, S. (2006). "Neuronal responses to transient hypoglycaemia in the dorsal vagal complex of the rat brainstem." J Physiol **570**(Pt 3): 469-484.

Ballerini, P., Ciccarellf, R., Caciagli, F., Rathbone, M. P., Werstiuk, E. S., Traversa, U., Buccella, S., Giuliani, P., Jiang, S., Nargi, E., Visini, D., Santavenere, C. and Di Iorio, P. (2005). "P2X7 Receptor Activation in Rat Brain Cultured Astrocytes Increases the Biosynthetic Release of Cysteinyl Leukotrienes." International Journal of Immunopathology and Pharmacology **18**(3): 417-430.

Banks, W. A. (2004). "The source of cerebral insulin." European Journal of Pharmacology **490**(1): 5-12.

Bao, L., Locovei, S. and Dahl, G. (2004). "Pannexin membrane channels are mechanosensitive conduits for ATP." FEBS letters **572**(1-3): 65-68.

Bartnik, B. L., Sutton, R. L., Fukushima, M., Harris, N. G., Hovda, D. A. and Lee, S. M. (2005). "Upregulation of pentose phosphate pathway and preservation of tricarboxylic acid cycle flux after experimental brain injury." J Neurotrauma **22**(10): 1052-1065.

Baskin, D. G., Breininger, J. F. and Schwartz, M. W. (1999). "Leptin receptor mRNA identifies a subpopulation of neuropeptide Y neurons activated by fasting in rat hypothalamus." Diabetes **48**(4): 828-833.

Baskin, D. G., Porte, J. D., Guest, K. and Dorsa, D. M. (1983). "Regional Concentrations of Insulin in the Rat Brain*." Endocrinology **112**(3): 898-903.

Bastard, J.-P., Maachi, M., Lagathu, C., Kim, M. J., Caron, M., Vidal, H., Capeau, J. and Feve, B. (2006). "Recent advances in the relationship between obesity, inflammation, and insulin resistance." European cytokine network **17**(1): 4-12.

Baura, G. D., Foster, D. M., Porte, D., Kahn, S. E., Bergman, R. N., Cobelli, C. and Schwartz, M. W. (1993). "Saturable transport of insulin from plasma into the central nervous system of dogs in vivo. A mechanism for regulated insulin delivery to the brain." The Journal of clinical investigation **92**(4): 1824-1830.

Beall, C., Ashford, M. L. and McCrimmon, R. J. (2012a). "The physiology and pathophysiology of the neural control of the counterregulatory response." American Journal of Physiology-Regulatory, Integrative and Comparative Physiology **302**(2): R215-R223.

Beall, C., Hamilton, D. L., Gallagher, J., Logie, L., Wright, K., Soutar, M. P., Dadak, S., Ashford, F. B., Haythorne, E., Du, Q., Jovanović, A., McCrimmon, R. J. and Ashford, M. L. J. (2012b). "Mouse hypothalamic GT1-7 cells demonstrate AMPK-dependent intrinsic glucose-sensing behaviour." Diabetologia **55**(9): 2432-2444.

Beattie, E. C., Stellwagen, D., Morishita, W., Bresnahan, J. C., Ha, B. K., Von Zastrow, M., Beattie, M. S. and Malenka, R. C. (2002). "Control of Synaptic Strength by Glial TNFα." Science **295**(5563): 2282-2285.

Bélanger, M., Allaman, I. and Magistretti, Pierre J. (2011). "Brain Energy Metabolism: Focus on Astrocyte-Neuron Metabolic Cooperation." Cell Metabolism **14**(6): 724-738.

Bellinger, L. L. and Bernardis, L. L. (2002). "The dorsomedial hypothalamic nucleus and its role in ingestive behavior and body weight regulation: lessons learned from lesioning studies." Physiol Behav **76**(3): 431-442.

Benarroch, E. E. (2014). "Brain glucose transporters." Implications for neurologic disease **82**(15): 1374-1379.

Benavides, A., Pastor, D., Santos, P., Tranque, P. and Calvo, S. (2005). "CHOP plays a pivotal role in the astrocyte death induced by oxygen and glucose deprivation." Glia **52**(4): 261-275.

Benigni, F., Atsumi, T., Calandra, T., Metz, C., Echtenacher, B., Peng, T. and Bucala, R. (2000). "The proinflammatory mediator macrophage migration inhibitory factor induces glucose catabolism in muscle." J Clin Invest **106**(10): 1291-1300.

Benjamini, Y. and Hochberg, Y. (1995). "Controlling the false discovery rate: a practical and powerful approach to multiple testing." Journal of the royal statistical society. Series B (Methodological): 289-300.

Benneyworth, M. A., Li, Y., Basu, A. C., Bolshakov, V. Y. and Coyle, J. T. (2012). "Cell Selective Conditional Null Mutations of Serine Racemase Demonstrate a Predominate Localization in Cortical Glutamatergic Neurons." Cellular and Molecular Neurobiology **32**(4): 613-624.

Bergersen, L. H. (2007). "Is lactate food for neurons? Comparison of monocarboxylate transporter subtypes in brain and muscle." Neuroscience **145**(1): 11-19.

Berridge, M. J. (2006). "Calcium microdomains: organization and function." Cell Calcium **40**(5-6): 405-412.

Beverly, J. L., de Vries, M. G., Beverly, M. F. and Arseneau, L. M. (2000). "Norepinephrine mediates glucoprivic-induced increase in GABA in the ventromedial hypothalamus of rats." Am J Physiol Regul Integr Comp Physiol **279**(3): R990-996.

Beverly, J. L., De Vries, M. G., Bouman, S. D. and Arseneau, L. M. (2001). "Noradrenergic and GABAergic systems in the medial hypothalamus are activated during hypoglycemia." Am J Physiol Regul Integr Comp Physiol **280**(2): R563-569.

Bignami, A., Eng, L. F., Dahl, D. and Uyeda, C. T. (1972). "Localization of the glial fibrillary acidic protein in astrocytes by immunofluorescence." Brain Research **43**(2): 429-435.

Bishop, S. J. (2007). "Neurocognitive mechanisms of anxiety: an integrative account." Trends Cogn Sci **11**(7): 307-316.

Bittar, P. G., Charnay, Y., Pellerin, L., Bouras, C. and Magistretti, P. J. (1996). "Selective distribution of lactate dehydrogenase isoenzymes in neurons and astrocytes of human brain." J Cereb Blood Flow Metab **16**(6): 1079-1089.

Blackburn, G. L. (2001). "Pasteur's Quadrant and malnutrition." Nature **409**(6818): 397-401.

Blardi, P., de Lalla, A., Auteri, A., Iapichino, S., Dell'Erba, A. and Castrogiovanni, P. (2005). "Plasma Catecholamine Levels after Fluoxetine Treatment in Depressive Patients." Neuropsychobiology **51**(2): 72-76.

Blaustein, M. P. (2010). Chapter 119 - Sodium/Calcium Exchange. Handbook of Cell Signaling (Second Edition). R. A. Bradshaw and E. A. Dennis. San Diego, Academic Press**:** 949-953.

Blevins, J. E. and Ho, J. M. (2013). "Role of oxytocin signaling in the regulation of body weight." Rev Endocr Metab Disord **14**(4): 311-329.

Blouin, M.-J., Zhao, Y., Zakikhani, M., Algire, C., Piura, E. and Pollak, M. (2010). "Loss of function of PTEN alters the relationship between glucose concentration and cell proliferation, increases glycolysis, and sensitizes cells to 2-deoxyglucose." Cancer Letters **289**(2): 246-253.

Boden, G. (1997). "Role of Fatty Acids in the Pathogenesis of Insulin Resistance and NIDDM." Diabetes **46**(1): 3-10.

Bohland, M., Matveyenko, A. V., Saberi, M., Khan, A. M., Watts, A. G. and Donovan, C. M. (2014). "Activation of hindbrain neurons is mediated by portal-mesenteric vein glucosensors during slow-onset hypoglycemia." Diabetes **63**(8): 2866-2875.

Boisvert, M. M., Erikson, G. A., Shokhirev, M. N. and Allen, N. J. (2018). "The Aging Astrocyte Transcriptome from Multiple Regions of the Mouse Brain." Cell reports **22**(1): 269-285.

Bolanos, J. P., Almeida, A., Stewart, V., Peuchen, S., Land, J. M., Clark, J. B. and Heales, S. J. (1997). "Nitric oxide-mediated mitochondrial damage in the brain: mechanisms and implications for neurodegenerative diseases." J Neurochem **68**(6): 2227-2240.

Bolli, G., de Feo, P., Compagnucci, P., Cartechini, M. G., Angeletti, G., Santeusanio, F., Brunetti, P. and Gerich, J. E. (1983). "Abnormal glucose counterregulation in insulin-dependent diabetes mellitus. Interaction of anti-insulin antibodies and impaired glucagon and epinephrine secretion." Diabetes **32**(2): 134-141.

Bonner-Weir, S., Deery, D., Leahy, J. L. and Weir, G. C. (1989). "Compensatory growth of pancreatic β-cells in adult rats after short-term glucose infusion." Diabetes **38**(1): 49-53.

Booth, H. D. E., Hirst, W. D. and Wade-Martins, R. (2017). "The Role of Astrocyte Dysfunction in Parkinson's Disease Pathogenesis." Trends in Neurosciences **40**(6): 358-370.

Borg, M. A., Sherwin, R. S., Borg, W. P., Tamborlane, W. V. and Shulman, G. I. (1997). "Local ventromedial hypothalamus glucose perfusion blocks

counterregulation during systemic hypoglycemia in awake rats." J Clin Invest **99**(2): 361-365.

Borg, M. A., Tamborlane, W. V., Shulman, G. I. and Sherwin, R. S. (2003). "Local lactate perfusion of the ventromedial hypothalamus suppresses hypoglycemic counterregulation." Diabetes **52**(3): 663-666.

Borg, W. P., Sherwin, R. S., During, M. J., Borg, M. A. and Shulman, G. I. (1995). "Local ventromedial hypothalamus glucopenia triggers counterregulatory hormone release." Diabetes **44**(2): 180-184.

Bornstein, S. R., Engeland, W. C., Ehrhart-Bornstein, M. and Herman, J. P. (2008). "Dissociation of ACTH and glucocorticoids." Trends in Endocrinology & Metabolism **19**(5): 175-180.

Boulland, J. L., Osen, K. K., Levy, L. M., Danbolt, N. C., Edwards, R. H., Storm-Mathisen, J. and Chaudhry, F. A. (2002). "Cell-specific expression of the glutamine transporter SN1 suggests differences in dependence on the glutamine cycle." Eur J Neurosci **15**(10): 1615-1631.

Bouzier-Sore, A. K., Voisin, P., Bouchaud, V., Bezancon, E., Franconi, J. M. and Pellerin, L. (2006). "Competition between glucose and lactate as oxidative energy substrates in both neurons and astrocytes: a comparative NMR study." European Journal of Neuroscience **24**(6): 1687-1694.

Boyle, P. J., Kempers, S. F., O'Connor, A. M. and Nagy, R. J. (1995). "Brain Glucose Uptake and Unawareness of Hypoglycemia in Patients with Insulin-Dependent Diabetes Mellitus." New England Journal of Medicine **333**(26): 1726-1732.

Boyle, P. J., Nagy, R. J., O'Connor, A. M., Kempers, S. F., Yeo, R. A. and Qualls, C. (1994). "Adaptation in brain glucose uptake following recurrent hypoglycemia." Proceedings of the National Academy of Sciences **91**(20): 9352-9356.

Braakman, I. and Bulleid, N. J. (2011). "Protein Folding and Modification in the Mammalian Endoplasmic Reticulum." Annual Review of Biochemistry **80**(1): 71-99.

Bradford, M. M. (1976). "A rapid and sensitive method for the quantitation of microgram quantities of protein utilizing the principle of protein-dye binding." Anal Biochem **72**: 248-254.

Braet, K., Cabooter, L., Paemeleire, K. and Leybaert, L. (2004). "Calcium signal communication in the central nervous system." Biology of the Cell **96**(1): 79-91.

Brasier, A. R. (2006). "The NF-κB regulatory network." Cardiovascular toxicology **6**(2): 111-130.

Brenner, M., Kisseberth, W. C., Su, Y., Besnard, F. and Messing, A. (1994). "GFAP promoter directs astrocyte-specific expression in transgenic mice." J Neurosci **14**(3 Pt 1): 1030-1037.

Briscoe, V. J., Ertl, A. C., Tate, D. B. and Davis, S. N. (2008a). "Effects of the Selective Serotonin Reuptake Inhibitor Fluoxetine on Counterregulatory Responses to Hypoglycemia in Individuals With Type 1 Diabetes." Diabetes **57**(12): 3315-3322.

Briscoe, V. J., Ertl, A. C., Tate, D. B., Dawling, S. and Davis, S. N. (2008b). "Effects of a Selective Serotonin Reuptake Inhibitor, Fluoxetine, on Counterregulatory Responses to Hypoglycemia in Healthy Individuals." Diabetes **57**(9): 2453-2460.

Broberger, C., De Lecea, L., Sutcliffe, J. G. and Hokfelt, T. (1998a). "Hypocretin/orexin- and melanin-concentrating hormone-expressing cells form distinct populations in the rodent lateral hypothalamus: relationship to the neuropeptide Y and agouti gene-related protein systems." J Comp Neurol **402**(4): 460-474.

Broberger, C., Johansen, J., Johansson, C., Schalling, M. and Hokfelt, T. (1998b). "The neuropeptide Y/agouti gene-related protein (AGRP) brain circuitry in normal, anorectic, and monosodium glutamate-treated mice." Proc Natl Acad Sci U S A **95**(25): 15043-15048.

Brown, A. M. (2004). "Brain glycogen re-awakened." Journal of Neurochemistry **89**(3): 537-552.

Brown, A. M., Sickmann, H. M., Fosgerau, K., Lund, T. M., Schousboe, A., Waagepetersen, H. S. and Ransom, B. R. (2005). "Astrocyte glycogen metabolism is required for neural activity during aglycemia or intense stimulation in mouse white matter." J Neurosci Res **79**(1-2): 74-80.

Brownlee, M. (2001). "Biochemistry and molecular cell biology of diabetic complications." Nature **414**: 813.

Brownlee, M. (2005). "The Pathobiology of Diabetic Complications." A Unifying Mechanism **54**(6): 1615-1625.

Brubaker, P. L. and Drucker, D. J. (2002). "Structure-function of the glucagon receptor family of G protein-coupled receptors: the glucagon, GIP, GLP-1, and GLP-2 receptors." Receptors Channels **8**(3-4): 179-188.

Brüning, J. C., Gautam, D., Burks, D. J., Gillette, J., Schubert, M., Orban, P. C., Klein, R., Krone, W., Müller-Wieland, D. and Kahn, C. R. (2000). "Role of Brain

Insulin Receptor in Control of Body Weight and Reproduction." Science **289**(5487): 2122-2125.

Buckman, L. B., Thompson, M. M., Lippert, R. N., Blackwell, T. S., Yull, F. E. and Ellacott, K. L. (2015). "Evidence for a novel functional role of astrocytes in the acute homeostatic response to high-fat diet intake in mice." Mol Metab **4**(1): 58-63.

Buehring, G. C., Eby, E. A. and Eby, M. J. (2004). "Cell line cross-contamination: how aware are Mammalian cell culturists of the problem and how to monitor it?" In Vitro Cellular & Developmental Biology-Animal **40**(7): 211-215.

Buijs, R. M., Chun, S. J., Niijima, A., Romijn, H. J. and Nagai, K. (2001). "Parasympathetic and sympathetic control of the pancreas: a role for the suprachiasmatic nucleus and other hypothalamic centers that are involved in the regulation of food intake." J Comp Neurol **431**(4): 405-423.

Buijs, R. M., Wortel, J., Van Heerikhuize, J. J., Feenstra, M. G., Ter Horst, G. J., Romijn, H. J. and Kalsbeek, A. (1999). "Anatomical and functional demonstration of a multisynaptic suprachiasmatic nucleus adrenal (cortex) pathway." European Journal of Neuroscience **11**(5): 1535-1544.

Burcelin, R., Printz, R. L., Kande, J., Assan, R., Granner, D. K. and Girard, J. (1993). "Regulation of glucose transporter and hexokinase II expression in tissues of diabetic rats." Am J Physiol **265**(3 Pt 1): E392-401.

Burcelin, R., Uldry, M., Foretz, M., Perrin, C., Dacosta, A., Nenniger-Tosato, M., Seydoux, J., Cotecchia, S. and Thorens, B. (2004). "Impaired glucose homeostasis in mice lacking the α1b-adrenergic receptor subtype." Journal of Biological Chemistry **279**(2): 1108-1115.

Burda, J. E., Bernstein, A. M. and Sofroniew, M. V. (2016). "Astrocyte roles in traumatic brain injury." Experimental Neurology **275**: 305-315.

Burda, J. E. and Sofroniew, M. V. (2014). "Reactive gliosis and the multicellular response to CNS damage and disease." Neuron **81**(2): 229-248.

Burdakov, D., Jensen, L. T., Alexopoulos, H., Williams, R. H., Fearon, I. M., O'Kelly, I., Gerasimenko, O., Fugger, L. and Verkhratsky, A. (2006). "Tandem-Pore K+ Channels Mediate Inhibition of Orexin Neurons by Glucose." Neuron **50**(5): 711-722.

Burkert, K., Moodley, K., Angel, C. E., Brooks, A. and Graham, E. S. (2012). "Detailed analysis of inflammatory and neuromodulatory cytokine secretion from human NT2 astrocytes using multiplex bead array." Neurochemistry International **60**(6): 573-580.

Burnstock, G. (1972). "Purinergic Nerves." Pharmacological Reviews **24**(3): 509-581.
Burnstock, G. (1990). "Noradrenaline and ATP as cotransmitters in sympathetic nerves." Neurochemistry international **17**(2): 357-368.
Burnstock, G. (2016). "An introduction to the roles of purinergic signalling in neurodegeneration, neuroprotection and neuroregeneration." Neuropharmacology **104**: 4-17.
Bushong, E. A., Martone, M. E., Jones, Y. Z. and Ellisman, M. H. (2002). "Protoplasmic astrocytes in CA1 stratum radiatum occupy separate anatomical domains." J Neurosci **22**(1): 183-192.
Bustamante, E. and Pedersen, P. L. (1977). "High aerobic glycolysis of rat hepatoma cells in culture: Role of mitochondrial hexokinase." Proceedings of the National Academy of Sciences **74**(9): 3735-3739.
Bymaster, F. P., Zhang, W., Carter, P. A., Shaw, J., Chernet, E., Phebus, L., Wong, D. T. and Perry, K. W. (2002). "Fluoxetine, but not other selective serotonin uptake inhibitors, increases norepinephrine and dopamine extracellular levels in prefrontal cortex." Psychopharmacology **160**(4): 353-361.
Cahoy, J. D., Emery, B., Kaushal, A., Foo, L. C., Zamanian, J. L., Christopherson, K. S., Xing, Y., Lubischer, J. L., Krieg, P. A., Krupenko, S. A., Thompson, W. J. and Barres, B. A. (2008). "A Transcriptome Database for Astrocytes, Neurons, and Oligodendrocytes: A New Resource for Understanding Brain Development and Function." The Journal of Neuroscience **28**(1): 264-278.
Cai, W., Xue, C., Sakaguchi, M., Konishi, M., Shirazian, A., Ferris, H. A., Li, M. E., Yu, R., Kleinridders, A., Pothos, E. N. and Kahn, C. R. (2018). "Insulin regulates astrocyte gliotransmission and modulates behavior." The Journal of Clinical Investigation **128**(7): 2914-2926.
Calandra, T., Bernhagen, J., Metz, C. N., Spiegel, L. A., Bacher, M., Donnelly, T., Cerami, A. and Bucala, R. (1995). "MIF as a glucocorticoid-induced modulator of cytokine production." Nature **377**(6544): 68-71.
Canabal, D. D., Song, Z., Potian, J. G., Beuve, A., McArdle, J. J. and Routh, V. H. (2007). "Glucose, insulin, and leptin signaling pathways modulate nitric oxide synthesis in glucose-inhibited neurons in the ventromedial hypothalamus." Am J Physiol Regul Integr Comp Physiol **292**(4): R1418-1428.

Canada, S. E., Weaver, S. A., Sharpe, S. N. and Pederson, B. A. (2011). "Brain glycogen supercompensation in the mouse after recovery from insulin-induced hypoglycemia." J Neurosci Res **89**(4): 585-591.

Canteras, N. S., Simerly, R. B. and Swanson, L. W. (1994). "Organization of projections from the ventromedial nucleus of the hypothalamus: a Phaseolus vulgaris-leucoagglutinin study in the rat." J Comp Neurol **348**(1): 41-79.

Cantorna, M. T. and Mahon, B. D. (2004). "Mounting Evidence for Vitamin D as an Environmental Factor Affecting Autoimmune Disease Prevalence." Experimental Biology and Medicine **229**(11): 1136-1142.

Carafoli, E. (1991). "Calcium pump of the plasma membrane." Physiol Rev **71**(1): 129-153.

Cardin, S., Jackson, P. A., Edgerton, D. S., Neal, D. W., Coffey, C. S. and Cherrington, A. D. (2001). "Effect of vagal cooling on the counterregulatory response to hypoglycemia induced by a low dose of insulin in the conscious dog." Diabetes **50**(3): 558-564.

Cardoso, S., Santos, R. X., Correia, S. C., Carvalho, C., Santos, M. S., Baldeiras, I., Oliveira, C. R. and Moreira, P. I. (2013). "Insulin-induced recurrent hypoglycemia exacerbates diabetic brain mitochondrial dysfunction and oxidative imbalance." Neurobiology of Disease **49**: 1-12.

Carmignoto, G. and Haydon, P. G. (2012). "Astrocyte calcium signaling and epilepsy." Glia **60**(8): 1227-1233.

Carvalho, F., Barros, D., Silva, J., Rezende, E., Soares, M., Fregoneze, J. and De Castro e Silva, E. (2004). "Hyperglycemia induced by acute central fluoxetine administration: role of the central CRH system and 5-HT3 receptors." Neuropeptides **38**(2): 98-105.

Castellano, C. A., Nugent, S., Paquet, N., Tremblay, S., Bocti, C., Lacombe, G., Imbeault, H., Turcotte, E., Fulop, T. and Cunnane, S. C. (2015). "Lower brain 18F-fluorodeoxyglucose uptake but normal 11C-acetoacetate metabolism in mild Alzheimer's disease dementia." J Alzheimers Dis **43**(4): 1343-1353.

Cataldo, A. M. and Broadwell, R. D. (1986). "Cytochemical identification of cerebral glycogen and glucose-6-phosphatase activity under normal and experimental conditions: I. Neurons and glia." Journal of Electron Microscopy Technique **3**(4): 413-437.

Catus, S. L., Gibbs, M. E., Sato, M., Summers, R. J. and Hutchinson, D. S. (2011). "Role of β-adrenoceptors in glucose uptake in astrocytes using β-adrenoceptor knockout mice." British Journal of Pharmacology **162**(8): 1700-1715.

Cavada, C., Company, T., Tejedor, J., Cruz-Rizzolo, R. J. and Reinoso-Suarez, F. (2000). "The anatomical connections of the macaque monkey orbitofrontal cortex. A review." Cereb Cortex **10**(3): 220-242.

Cechetto, D. F. and Saper, C. B. (1988). "Neurochemical organization of the hypothalamic projection to the spinal cord in the rat." J Comp Neurol **272**(4): 579-604.

Ceriello, A., Novials, A., Ortega, E., La Sala, L., Pujadas, G., Testa, R., Bonfigli, A. R., Esposito, K. and Giugliano, D. (2012). "Evidence that hyperglycemia after recovery from hypoglycemia worsens endothelial function and increases oxidative stress and inflammation in healthy control subjects and subjects with type 1 diabetes." Diabetes **61**(11): 2993-2997.

Chafetz, M. D., Parko, K., Diaz, S. and Leibowitz, S. F. (1986). "Relationships between medial hypothalamic alpha 2-receptor binding, norepinephrine, and circulating glucose." Brain Res **384**(2): 404-408.

Chan, K., Busque, S. M., Sailer, M., Stoeger, C., Bröer, S., Daniel, H., Rubio-Aliaga, I. and Wagner, C. A. (2016). "Loss of function mutation of the Slc38a3 glutamine transporter reveals its critical role for amino acid metabolism in the liver, brain, and kidney." Pflügers Archiv - European Journal of Physiology **468**(2): 213-227.

Chan, O., Cheng, H., Herzog, R., Czyzyk, D., Zhu, W., Wang, A., McCrimmon, R. J., Seashore, M. R. and Sherwin, R. S. (2008). "Increased GABAergic Tone in the Ventromedial Hypothalamus Contributes to Suppression of Counterregulatory Reponses After Antecedent Hypoglycemia." Diabetes **57**(5): 1363-1370.

Chan, O., Lawson, M., Zhu, W., Beverly, J. L. and Sherwin, R. S. (2007). "ATP-Sensitive K+ Channels Regulate the Release of GABA in the Ventromedial Hypothalamus During Hypoglycemia." Diabetes **56**(4): 1120-1126.

Chan, O., Paranjape, S. A., Horblitt, A., Zhu, W. and Sherwin, R. S. (2013). "Lactate-induced release of GABA in the ventromedial hypothalamus contributes to counterregulatory failure in recurrent hypoglycemia and diabetes." Diabetes **62**(12): 4239-4246.

Chan, O., Zhu, W., Ding, Y., McCrimmon, R. J. and Sherwin, R. S. (2006). "Blockade of GABA(A) receptors in the ventromedial hypothalamus further stimulates glucagon

and sympathoadrenal but not the hypothalamo-pituitary-adrenal response to hypoglycemia." Diabetes **55**(4): 1080-1087.

Chandra, R. K. (1996). "Nutrition, immunity and infection: from basic knowledge of dietary manipulation of immune responses to practical application of ameliorating suffering and improving survival." Proc Natl Acad Sci U S A **93**(25): 14304-14307.

Chang-Liu, C.-M. and Woloschak, G. E. (1997). "Effect of passage number on cellular response to DNA-damaging agents: cell survival and gene expression." Cancer letters **113**(1-2): 77-86.

Charles, A. C., Merrill, J. E., Dirksen, E. R. and Sandersont, M. J. (1991). "Intercellular signaling in glial cells: Calcium waves and oscillations in response to mechanical stimulation and glutamate." Neuron **6**(6): 983-992.

Chase, T. N., Foster, N. L., Fedio, P., Brooks, R., Mansi, L. and Di Chiro, G. (1984). "Regional cortical dysfunction in Alzheimer's disease as determined by positron emission tomography." Ann Neurol **15 Suppl**: S170-174.

Chatton, J.-Y., Pellerin, L. and Magistretti, P. J. (2003a). "GABA uptake into astrocytes is not associated with significant metabolic cost: Implications for brain imaging of inhibitory transmission." Proceedings of the National Academy of Sciences of the United States of America **100**(21): 12456-12461.

Chatton, J.-Y., Pellerin, L. and Magistretti, P. J. (2003b). "GABA uptake into astrocytes is not associated with significant metabolic cost: Implications for brain imaging of inhibitory transmission." Proceedings of the National Academy of Sciences **100**(21): 12456-12461.

Chavarria, A. and Alcocer-Varela, J. (2004). "Is damage in central nervous system due to inflammation?" Autoimmunity Reviews **3**(4): 251-260.

Chen, E. Y., Tan, C. M., Kou, Y., Duan, Q., Wang, Z., Meirelles, G. V., Clark, N. R. and Ma'ayan, A. (2013). "Enrichr: interactive and collaborative HTML5 gene list enrichment analysis tool." BMC Bioinformatics **14**: 128.

Chen, N., Sugihara, H., Kim, J., Fu, Z., Barak, B., Sur, M., Feng, G. and Han, W. (2016). "Direct modulation of GFAP-expressing glia in the arcuate nucleus bi-directionally regulates feeding." Elife **5**: e18716.

Cheunsuang, O. and Morris, R. (2005). "Astrocytes in the arcuate nucleus and median eminence that take up a fluorescent dye from the circulation express leptin receptors and neuropeptide Y Y1 receptors." Glia **52**(3): 228-233.

Chi, Y., Gao, K., Li, K., Nakajima, S., Kira, S., Takeda, M. and Yao, J. (2014). "Purinergic control of AMPK activation by ATP released through connexin 43 hemichannels - pivotal roles in hemichannel-mediated cell injury." J Cell Sci **127**(Pt 7): 1487-1499.

Chih, C.-P. and Roberts, E. L. (2003). "Energy Substrates for Neurons during Neural Activity: A Critical Review of the Astrocyte-Neuron Lactate Shuttle Hypothesis." Journal of Cerebral Blood Flow & Metabolism **23**(11): 1263-1281.

Choi, I. Y., Seaquist, E. R. and Gruetter, R. (2003). "Effect of hypoglycemia on brain glycogen metabolism in vivo." Journal of neuroscience research **72**(1): 25-32.

Choi, S. S., Lee, H. J., Lim, I., Satoh, J.-i. and Kim, S. U. (2014). "Human Astrocytes: Secretome Profiles of Cytokines and Chemokines." PLOS ONE **9**(4): e92325.

Cholet, N., Pellerin, L., Magistretti, P. J. and Hamel, E. (2002). "Similar perisynaptic glial localization for the Na+,K+-ATPase alpha 2 subunit and the glutamate transporters GLAST and GLT-1 in the rat somatosensory cortex." Cereb Cortex **12**(5): 515-525.

Chow, E., Bernjak, A., Williams, S., Fawdry, R. A., Hibbert, S., Freeman, J., Sheridan, P. J. and Heller, S. R. (2014a). "Risk of cardiac arrhythmias during hypoglycemia in patients with type 2 diabetes and cardiovascular risk." Diabetes **63**(5): 1738-1747.

Chow, E., Iqbal, A., Bernjak, A., Ajjan, R. and Heller, S. R. (2014b). "Effect of hypoglycaemia on thrombosis and inflammation in patients with type 2 diabetes." The Lancet **383**: S35.

Chowdhury, G. M. I., Wang, P., Ciardi, A., Mamillapalli, R., Johnson, J., Zhu, W., Eid, T., Behar, K. and Chan, O. (2017). "Impaired Glutamatergic Neurotransmission in the Ventromedial Hypothalamus May Contribute to Defective Counterregulation in Recurrently Hypoglycemic Rats." Diabetes **66**(7): 1979-1989.

Chowen, J. A., de Fonseca, F. R., Alvarez, E., Navarro, M., Garcia-Segura, L. M. and Blazquez, E. (1999). "Increased glucagon-like peptide-1 receptor expression in glia after mechanical lesion of the rat brain." Neuropeptides **33**(3): 212-215.

Chrousos, G. P. (1995). "The Hypothalamic–Pituitary–Adrenal Axis and Immune-Mediated Inflammation." New England Journal of Medicine **332**(20): 1351-1363.

Ciccarelli, R., Di Iorio, P., Giuliani, P., D'Alimonte, I., Ballerini, P., Caciagli, F. and Rathbone, M. P. (1999). "Rat cultured astrocytes release guanine-based purines in basal conditions and after hypoxia/hypoglycemia." Glia **25**(1): 93-98.

Cincotta, A. H., Luo, S., Zhang, Y., Liang, Y., Bina, K. G., Jetton, T. L. and Scislowski, P. W. D. (2000). "Chronic infusion of norepinephrine into the VMH of normal rats induces the obese glucose-intolerant state." American Journal of Physiology-Regulatory, Integrative and Comparative Physiology **278**(2): R435-R444.

Cirillo, D., Rachiglio, A. M., la Montagna, R., Giordano, A. and Normanno, N. (2008). "Leptin signaling in breast cancer: an overview." J Cell Biochem **105**(4): 956-964.

Ciudad, C., Camici, M., Ahmad, Z., Wang, Y., DePaoli-Roach, A. A. and Roach, P. J. (1984). "Control of glycogen synthase phosphorylation in isolated rat hepatocytes by epinephrine, vasopressin and glucagon." European journal of biochemistry **142**(3): 511-520.

Claret, M., Smith, M. A., Batterham, R. L., Selman, C., Choudhury, A. I., Fryer, L. G., Clements, M., Al-Qassab, H., Heffron, H., Xu, A. W., Speakman, J. R., Barsh, G. S., Viollet, B., Vaulont, S., Ashford, M. L., Carling, D. and Withers, D. J. (2007). "AMPK is essential for energy homeostasis regulation and glucose sensing by POMC and AgRP neurons." J Clin Invest **117**(8): 2325-2336.

Cloix, J.-F. and Hévor, T. (2009). "Epilepsy, regulation of brain energy metabolism and neurotransmission." Current medicinal chemistry **16**(7): 841-853.

Coll, A. P., Farooqi, I. S., Challis, B. G., Yeo, G. S. and O'Rahilly, S. (2004). "Proopiomelanocortin and energy balance: insights from human and murine genetics." J Clin Endocrinol Metab **89**(6): 2557-2562.

Concannon, P., Rich, S. S. and Nepom, G. T. (2009). "Genetics of type 1A diabetes." New England Journal of Medicine **360**(16): 1646-1654.

Considine, R. V., Sinha, M. K., Heiman, M. L., Kriauciunas, A., Stephens, T. W., Nyce, M. R., Ohannesian, J. P., Marco, C. C., McKee, L. J., Bauer, T. L. and et al. (1996). "Serum immunoreactive-leptin concentrations in normal-weight and obese humans." N Engl J Med **334**(5): 292-295.

Cornell-Bell, A., Finkbeiner, S., Cooper, M. and Smith, S. (1990). "Glutamate induces calcium waves in cultured astrocytes: long-range glial signaling." Science **247**(4941): 470-473.

Cornell-Bell, A. H. and Finkbeiner, S. M. (1991). "Ca2+ waves in astrocytes." Cell Calcium **12**(2): 185-204.

Cotecchia, S. (2010). "The α1-adrenergic receptors: diversity of signaling networks and regulation." Journal of Receptors and Signal Transduction **30**(6): 410-419.

Cotrina, M. L., Lin, J. H., Lopez-Garcia, J. C., Naus, C. C. and Nedergaard, M. (2000). "ATP-mediated glia signaling." J Neurosci **20**(8): 2835-2844.

Coussens, L. M. and Werb, Z. (2002). "Inflammation and cancer." Nature **420**(6917): 860-867.

Cowley, M. A., Smart, J. L., Rubinstein, M., Cerdán, M. G., Diano, S., Horvath, T. L., Cone, R. D. and Low, M. J. (2001). "Leptin activates anorexigenic POMC neurons through a neural network in the arcuate nucleus." Nature **411**: 480.

Craft, S., Asthana, S., Cook, D. G., Baker, L. D., Cherrier, M., Purganan, K., Wait, C., Petrova, A., Latendresse, S., Watson, G. S., Newcomer, J. W., Schellenberg, G. D. and Krohn, A. J. (2003). "Insulin dose-response effects on memory and plasma amyloid precursor protein in Alzheimer's disease: interactions with apolipoprotein E genotype." Psychoneuroendocrinology **28**(6): 809-822.

Craft, S., Asthana, S., Newcomer, J. W., Wilkinson, C. W., Matos, I. T., Baker, L. D., Cherrier, M., Lofgreen, C., Latendresse, S., Petrova, A., Plymate, S., Raskind, M., Grimwood, K. and Veith, R. C. (1999). "Enhancement of memory in Alzheimer disease with insulin and somatostatin, but not glucose." Arch Gen Psychiatry **56**(12): 1135-1140.

Cranston, I., Lomas, J., Amiel, S. A., Maran, A. and Macdonald, I. (1994). "Restoration of hypoglycaemia awareness in patients with long-duration insulin-dependent diabetes." The Lancet **344**(8918): 283-287.

Cranston, I., Reed, L. J., Marsden, P. K. and Amiel, S. A. (2001a). "Changes in regional brain (18)F-fluorodeoxyglucose uptake at hypoglycemia in type 1 diabetic men associated with hypoglycemia unawareness and counter-regulatory failure." Diabetes **50**(10): 2329-2336.

Cranston, I., Reed, L. J., Marsden, P. K. and Amiel, S. A. (2001b). "Changes in Regional Brain ¹⁸F-Fluorodeoxyglucose Uptake at Hypoglycemia in Type 1 Diabetic Men Associated With Hypoglycemia Unawareness and Counter-Regulatory Failure." Diabetes **50**(10): 2329-2366.

Criego, A. B., Tkac, I., Kumar, A., Thomas, W., Gruetter, R. and Seaquist, E. R. (2004). "Brain glucose concentrations in patients with type 1 diabetes and hypoglycemia unawareness." Journal of Neuroscience Research **79**(1-2): 42-47.

Cryer, P. E. (1994). "Banting Lecture. Hypoglycemia: the limiting factor in the management of IDDM." Diabetes **43**(11): 1378-1389.

Cryer, P. E. (1997a). "Hierarchy of physiological responses to hypoglycemia: relevance to clinical hypoglycemia in type I (insulin dependent) diabetes mellitus." Horm Metab Res **29**(3): 92-96.

Cryer, P. E. (1997b). Hypoglycemia: pathophysiology, diagnosis, and treatment, Oxford University Press, USA.

Cryer, P. E. (2004). "Diverse causes of hypoglycemia-associated autonomic failure in diabetes." New England Journal of Medicine **350**(22): 2272-2279.

Cryer, P. E. (2005). "Mechanisms of Hypoglycemia-Associated Autonomic Failure and Its Component Syndromes in Diabetes." Diabetes **54**(12): 3592-3601.

Cryer, P. E. (2008). "Hypoglycemia: still the limiting factor in the glycemic management of diabetes." Endocr Pract **14**(6): 750-756.

Cryer, P. E., Davis, S. N. and Shamoon, H. (2003). "Hypoglycemia in Diabetes." Diabetes Care **26**(6): 1902-1912.

Cunha, R. A. (2001). "Adenosine as a neuromodulator and as a homeostatic regulator in the nervous system: different roles, different sources and different receptors." Neurochemistry International **38**(2): 107-125.

Cunha, R. A., Vizi, E. S., Ribeiro, J. A. and Sebastião, A. M. (1996). "Preferential release of ATP and its extracellular catabolism as a source of adenosine upon high- but not low-frequency stimulation of rat hippocampal slices." Journal of neurochemistry **67**(5): 2180-2187.

D'Ascenzo, M., Podda, M. V. and Grassi, C. (2014). "The role of D-serine as co-agonist of NMDA receptors in the nucleus accumbens: relevance to cocaine addiction." Frontiers in Synaptic Neuroscience **6**: 16.

Dagogo-Jack, S., Fanelli, C., Paramore, D., Brothers, J. and Landt, M. (1996). "Plasma leptin and insulin relationships in obese and nonobese humans." Diabetes **45**(5): 695-698.

Dagogo-Jack, S., Rattarasarn, C. and Cryer, P. E. (1994). "Reversal of hypoglycemia unawareness, but not defective glucose counterregulation, in IDDM." Diabetes **43**(12): 1426-1434.

Danbolt, N. C. (2001). "Glutamate uptake." Progress in Neurobiology **65**(1): 1-105.

Danforth Jr, E. (2000). "Failure of adipocyte differentiation causes type II diabetes mellitus?" Nature Genetics **26**: 13.

Dani, J. W., Chernjavsky, A. and Smith, S. J. (1992). "Neuronal activity triggers calcium waves in hippocampal astrocyte networks." Neuron **8**(3): 429-440.

Danulat, E. and Mommsen, T. P. (1990). "Norepinephrine: a potent activator of glycogenolysis and gluconeogenesis in rockfish hepatocytes." Gen Comp Endocrinol **78**(1): 12-22.

Darlington, P. J., Podjaski, C., Horn, K. E., Costantino, S., Blain, M., Saikali, P., Chen, Z., Baker, K. A., Newcombe, J., Freedman, M., Wiseman, P. W., Bar-Or, A., Kennedy, T. E. and Antel, J. P. (2008). "Innate immune-mediated neuronal injury consequent to loss of astrocytes." J Neuropathol Exp Neurol **67**(6): 590-599.

Daumas-Meyer, V., Champeil-Potokar, G., Chaumontet, C., Dahirel, P., Papillon, C., Congar, P. and Denis, I. (2018). "Fasting induces astroglial plasticity in the olfactory bulb glomeruli of rats." Glia **66**(4): 762-776.

Daumas-Meyer, V., Champeil-Potokar, G., Chaumontet, C., Dahirel, P., Papillon, C., Congar, P. and Denis, I. (2018). "Fasting induces astroglial plasticity in the olfactory bulb glomeruli of rats." Glia **66**(4): 762-776.

Davalos, D., Grutzendler, J., Yang, G., Kim, J. V., Zuo, Y., Jung, S., Littman, D. R., Dustin, M. L. and Gan, W.-B. (2005). "ATP mediates rapid microglial response to local brain injury in vivo." Nature Neuroscience **8**: 752.

DAVIES, S. P., SIM, A. T. and HARDIE, D. G. (1990). "Location and function of three sites phosphorylated on rat acetyl-CoA carboxylase by the AMP-activated protein kinase." European journal of biochemistry **187**(1): 183-190.

Davis, S. N., Mann, S., Galassetti, P., Neill, R. A., Tate, D., Ertl, A. C. and Costa, F. (2000). "Effects of differing durations of antecedent hypoglycemia on counterregulatory responses to subsequent hypoglycemia in normal humans." Diabetes **49**(11): 1897-1903.

Davis, S. N., Shavers, C., Mosqueda-Garcia, R. and Costa, F. (1997). "Effects of Differing Antecedent Hypoglycemia on Subsequent Counterregulation in Normal Humans." Diabetes **46**(8): 1328-1335.

Dazzi, L., Ladu, S., Spiga, F., Vacca, G., Rivano, A., Pira, L. and Biggio, G. (2002). "Chronic treatment with imipramine or mirtazapine antagonizes stress- and FG7142-induced increase in cortical norepinephrine output in freely moving rats." Synapse **43**(1): 70-77.

De Feyter, H. M., Mason, G. F., Shulman, G. I., Rothman, D. L. and Petersen, K. F. (2013). "Increased brain lactate concentrations without increased lactate oxidation during hypoglycemia in type 1 diabetic individuals." Diabetes **62**(9): 3075-3080.

de Guia, R. M., Rose, A. J. and Herzig, S. (2014). "Glucocorticoid hormones and energy homeostasis." Horm Mol Biol Clin Investig **19**(2): 117-128.

de la Cadena, S. G., Hernandez-Fonseca, K., Camacho-Arroyo, I. and Massieu, L. (2014). "Glucose deprivation induces reticulum stress by the PERK pathway and caspase-7- and calpain-mediated caspase-12 activation." Apoptosis **19**(3): 414-427.

De Souza, C. T., Araujo, E. P., Bordin, S., Ashimine, R., Zollner, R. L., Boschero, A. C., Saad, M. J. and Velloso, L. A. (2005). "Consumption of a fat-rich diet activates a proinflammatory response and induces insulin resistance in the hypothalamus." Endocrinology **146**(10): 4192-4199.

de Vries, M. G., Lawson, M. A. and Beverly, J. L. (2005). "Hypoglycemia-induced noradrenergic activation in the VMH is a result of decreased ambient glucose." Am J Physiol Regul Integr Comp Physiol **289**(4): R977-981.

DeBerardinis, R. J. and Chandel, N. S. (2016). "Fundamentals of cancer metabolism." Science Advances **2**(5): e1600200.

Denton, R. M., Randle, P. J. and Martin, B. R. (1972). "Stimulation by calcium ions of pyruvate dehydrogenase phosphate phosphatase." Biochemical Journal **128**(1): 161-163.

Denton, R. M., Richards, D. A. and Chin, J. G. (1978). "Calcium ions and the regulation of NAD+-linked isocitrate dehydrogenase from the mitochondria of rat heart and other tissues." Biochemical Journal **176**(3): 899-906.

DeRosa, M. A. and Cryer, P. E. (2004). "Hypoglycemia and the sympathoadrenal system: neurogenic symptoms are largely the result of sympathetic neural, rather than adrenomedullary, activation." Am J Physiol Endocrinol Metab **287**(1): E32-41.

Dettmer, K., Vogl, F. C., Ritter, A. P., Zhu, W., Nürnberger, N., Kreutz, M., Oefner, P. J., Gronwald, W. and Gottfried, E. (2013). "Distinct metabolic differences between various human cancer and primary cells." ELECTROPHORESIS **34**(19): 2836-2847.

Devaskar, S. U., Giddings, S. J., Rajakumar, P. A., Carnaghi, L. R., Menon, R. K. and Zahm, D. S. (1994). "Insulin gene expression and insulin synthesis in mammalian neuronal cells." Journal of Biological Chemistry **269**(11): 8445-8454.

Di Castro, M. A., Chuquet, J., Liaudet, N., Bhaukaurally, K., Santello, M., Bouvier, D., Tiret, P. and Volterra, A. (2011). "Local Ca2+ detection and modulation of synaptic release by astrocytes." Nature Neuroscience **14**: 1276.

Di Mario, U., Morano, S., Valle, E. and Pozzessere, G. (1995). "Electrophysiological alterations of the central nervous system in diabetes mellitus." Diabetes/Metabolism Reviews **11**(3): 259-277.

Dickens, F. and Glock, G. (1951). "Direct oxidation of glucose-6-phosphate, 6-phosphogluconate and pentose-5-phosphates by enzymes of animal origin." Biochemical Journal **50**(1): 81.

Diehl-Schmid, J., Grimmer, T., Drzezga, A., Bornschein, S., Riemenschneider, M., Förstl, H., Schwaiger, M. and Kurz, A. (2007). "Decline of cerebral glucose metabolism in frontotemporal dementia: a longitudinal 18F-FDG-PET-study." Neurobiology of Aging **28**(1): 42-50.

Dienel, G. A. (2012). "Brain lactate metabolism: the discoveries and the controversies." Journal of Cerebral Blood Flow & Metabolism **32**(7): 1107-1138.

Ding, F., O'Donnell, J., Thrane, A. S., Zeppenfeld, D., Kang, H., Xie, L., Wang, F. and Nedergaard, M. (2013). "α1-Adrenergic receptors mediate coordinated Ca2+ signaling of cortical astrocytes in awake, behaving mice." Cell Calcium **54**(6): 387-394.

DiRocco, R. J. and Grill, H. J. (1979). "The forebrain is not essential for sympathoadrenal hyperglycemic response to glucoprivation." Science **204**(4397): 1112-1114.

DiTullio, N. W., Cieslinski, L., Matthews, W. D. and Storer, B. (1984). "Mechanisms involved in the hyperglycemic response induced by clonidine and other alpha-2 adrenoceptor agonists." J Pharmacol Exp Ther **228**(1): 168-173.

Divakaruni, A. S., Paradyse, A., Ferrick, D. A., Murphy, A. N. and Jastroch, M. (2014). Chapter Sixteen - Analysis and Interpretation of Microplate-Based Oxygen Consumption and pH Data. Methods in Enzymology. A. N. Murphy and D. C. Chan, Academic Press. **547:** 309-354.

Dobin, A., Davis, C. A., Schlesinger, F., Drenkow, J., Zaleski, C., Jha, S., Batut, P., Chaisson, M. and Gingeras, T. R. (2013). "STAR: ultrafast universal RNA-seq aligner." Bioinformatics **29**(1): 15-21.

Dobin, A. and Gingeras, T. R. (2015). "Mapping RNA-seq Reads with STAR." Current protocols in bioinformatics / editoral board, Andreas D. Baxevanis ... [et al.] **51**: 11.14.11-11.14.19.

Donnelly, L. A., Morris, A. D., Frier, B. M., Ellis, J. D., Donnan, P. T., Durrant, R., Band, M. M., Reekie, G. and Leese, G. P. (2005). "Frequency and predictors of

hypoglycaemia in Type 1 and insulin-treated Type 2 diabetes: a population-based study." Diabetic Medicine **22**(6): 749-755.

Dotson, S., Freeman, R., Failing, H. J. and Adler, G. K. (2008). "Hypoglycemia increases serum interleukin-6 levels in healthy men and women." Diabetes Care **31**(6): 1222-1223.

Douglass, J. D., Dorfman, M. D., Fasnacht, R., Shaffer, L. D. and Thaler, J. P. (2017). "Astrocyte IKKbeta/NF-kappaB signaling is required for diet-induced obesity and hypothalamic inflammation." Mol Metab **6**(4): 366-373.

Dringen, R., Gebhardt, R. and Hamprecht, B. (1993). "Glycogen in astrocytes: possible function as lactate supply for neighboring cells." Brain research **623**(2): 208-214.

Driscoll, K. A., Raymond, J., Naranjo, D. and Patton, S. R. (2016). "Fear of Hypoglycemia in Children and Adolescents and Their Parents with Type 1 Diabetes." Current diabetes reports **16**(8): 77-77.

Drucker, D. J. (2007). "The role of gut hormones in glucose homeostasis." The Journal of Clinical Investigation **117**(1): 24-32.

Drucker, D. J. and Nauck, M. A. (2006). "The incretin system: glucagon-like peptide-1 receptor agonists and dipeptidyl peptidase-4 inhibitors in type 2 diabetes." The Lancet **368**(9548): 1696-1705.

Duan, S., Anderson, C. M., Keung, E. C., Chen, Y., Chen, Y. and Swanson, R. A. (2003). "P2X₇ Receptor-Mediated Release of Excitatory Amino Acids from Astrocytes." The Journal of Neuroscience **23**(4): 1320-1328.

Duara, R., Grady, C., Haxby, J., Sundaram, M., Cutler, N. R., Heston, L., Moore, A., Schlageter, N., Larson, S. and Rapoport, S. I. (1986). "Positron emission tomography in Alzheimer's disease." Neurology **36**(7): 879-887.

Duh, E. and Aiello, L. P. (1999). "Vascular endothelial growth factor and diabetes: the agonist versus antagonist paradox." Diabetes **48**(10): 1899-1906.

Dunn, J. and Wild, D. (2013). Chapter 3.6 - Calibration Curve Fitting. The Immunoassay Handbook (Fourth Edition). D. Wild. Oxford, Elsevier**:** 323-336.

Dunn, J. T., Cranston, I., Marsden, P. K., Amiel, S. A. and Reed, L. J. (2007). "Attenuation of amydgala and frontal cortical responses to low blood glucose concentration in asymptomatic hypoglycemia in type 1 diabetes: a new player in hypoglycemia unawareness?" Diabetes **56**(11): 2766-2773.

Dunwiddie, T. V. and Masino, S. A. (2001). "The role and regulation of adenosine in the central nervous system." Annu Rev Neurosci **24**: 31-55.

Duran, J., Saez, I., Gruart, A., Guinovart, J. J. and Delgado-Garcia, J. M. (2013). "Impairment in long-term memory formation and learning-dependent synaptic plasticity in mice lacking glycogen synthase in the brain." J Cereb Blood Flow Metab **33**(4): 550-556.

Edridge, C. L., Dunkley, A. J., Bodicoat, D. H., Rose, T. C., Gray, L. J., Davies, M. J. and Khunti, K. (2015). "Prevalence and Incidence of Hypoglycaemia in 532,542 People with Type 2 Diabetes on Oral Therapies and Insulin: A Systematic Review and Meta-Analysis of Population Based Studies." PLoS ONE **10**(6): e0126427.

El Kadmiri, N., Slassi, I., El Moutawakil, B., Nadifi, S., Tadevosyan, A., Hachem, A. and Soukri, A. (2014). "Glyceraldehyde-3-phosphate dehydrogenase (GAPDH) and Alzheimer's disease." Pathologie Biologie **62**(6): 333-336.

Elam, M., Thoren, P. and Svensson, T. H. (1986). "Locus coeruleus neurons and sympathetic nerves: activation by visceral afferents." Brain Res **375**(1): 117-125.

Elbein, S. C., Wegner, K. and Kahn, S. E. (2000). "Reduced beta-cell compensation to the insulin resistance associated with obesity in members of caucasian familial type 2 diabetic kindreds." Diabetes care **23**(2): 221-227.

Eley, T. C., Sugden, K., Corsico, A., Gregory, A. M., Sham, P., McGuffin, P., Plomin, R. and Craig, I. W. (2004). "Gene–environment interaction analysis of serotonin system markers with adolescent depression." Molecular Psychiatry **9**: 908.

Elias, C. F., Aschkenasi, C., Lee, C., Kelly, J., Ahima, R. S., Bjorbaek, C., Flier, J. S., Saper, C. B. and Elmquist, J. K. (1999). "Leptin differentially regulates NPY and POMC neurons projecting to the lateral hypothalamic area." Neuron **23**(4): 775-786.

Elmquist, J. K. (2001). "Hypothalamic pathways underlying the endocrine, autonomic, and behavioral effects of leptin." Physiol Behav **74**(4-5): 703-708.

Elmquist, J. K., Elias, C. F. and Saper, C. B. (1999). "From lesions to leptin: hypothalamic control of food intake and body weight." Neuron **22**(2): 221-232.

Eltzschig, H. K., Sitkovsky, M. V. and Robson, S. C. (2012). "Purinergic Signaling during Inflammation." New England Journal of Medicine **367**(24): 2322-2333.

Enriori, P. J., Evans, A. E., Sinnayah, P., Jobst, E. E., Tonelli-Lemos, L., Billes, S. K., Glavas, M. M., Grayson, B. E., Perello, M., Nillni, E. A., Grove, K. L. and Cowley, M. A. (2007). "Diet-induced obesity causes severe but reversible leptin resistance in arcuate melanocortin neurons." Cell Metab **5**(3): 181-194.

Erta, M., Giralt, M., Esposito, F. L., Fernandez-Gayol, O. and Hidalgo, J. (2015). "Astrocytic IL-6 mediates locomotor activity, exploration, anxiety, learning and social behavior." Hormones and Behavior **73**: 64-74.

Evans, M. L., McCrimmon, R. J., Flanagan, D. E., Keshavarz, T., Fan, X., McNay, E. C., Jacob, R. J. and Sherwin, R. S. (2004a). "Hypothalamic ATP-sensitive K + channels play a key role in sensing hypoglycemia and triggering counterregulatory epinephrine and glucagon responses." Diabetes **53**(10): 2542-2551.

Evans, S. B., Wilkinson, C. W., Gronbeck, P., Bennett, J. L., Zavosh, A., Taborsky, G. J., Jr. and Figlewicz, D. P. (2004b). "Inactivation of the DMH selectively inhibits the ACTH and corticosterone responses to hypoglycemia." Am J Physiol Regul Integr Comp Physiol **286**(1): R123-128.

Ewing, B. and Green, P. (1998a). "Base-calling of automated sequencer traces using phred. II. Error probabilities." Genome Res **8**(3): 186-194.

Ewing, B., Hillier, L., Wendl, M. C. and Green, P. (1998b). "Base-calling of automated sequencer traces using phred. I. Accuracy assessment." Genome Res **8**(3): 175-185.

Exton, J. H. (1987). "Mechanisms of hormonal regulation of hepatic glucose metabolism." Diabetes Metab Rev **3**(1): 163-183.

Exton, J. H., Friedmann, N., Wong, E. H.-A., Brineaux, J. P., Corbin, J. D. and Park, C. R. (1972). "Interaction of glucocorticoids with glucagon and epinephrine in the control of gluconeogenesis and glycogenolysis in liver and of lipolysis in adipose tissue." Journal of Biological Chemistry **247**(11): 3579-3588.

Fagerholm, V., Haaparanta, M. and Scheinin, M. (2011). "α2-Adrenoceptor Regulation of Blood Glucose Homeostasis." Basic & clinical pharmacology & toxicology **108**(6): 365-370.

Fan, X., Ding, Y., Brown, S., Zhou, L., Shaw, M., Vella, M. C., Cheng, H., McNay, E. C., Sherwin, R. S. and McCrimmon, R. J. (2009). "Hypothalamic AMP-activated protein kinase activation with AICAR amplifies counterregulatory responses to hypoglycemia in a rodent model of type 1 diabetes." American Journal of Physiology-Regulatory, Integrative and Comparative Physiology **296**(6): R1702-R1708.

Fanelli, C. G., Epifano, L., Rambotti, A. M., Pampanelli, S., Di Vincenzo, A., Modarelli, F., Lepore, M., Annibale, B., Ciofetta, M., Bottini, P. and et al. (1993). "Meticulous prevention of hypoglycemia normalizes the glycemic thresholds and magnitude of most of neuroendocrine responses to, symptoms of, and cognitive

function during hypoglycemia in intensively treated patients with short-term IDDM." Diabetes **42**(11): 1683-1689.

Fekete, C., Legradi, G., Mihaly, E., Huang, Q. H., Tatro, J. B., Rand, W. M., Emerson, C. H. and Lechan, R. M. (2000). "alpha-Melanocyte-stimulating hormone is contained in nerve terminals innervating thyrotropin-releasing hormone-synthesizing neurons in the hypothalamic paraventricular nucleus and prevents fasting-induced suppression of prothyrotropin-releasing hormone gene expression." J Neurosci **20**(4): 1550-1558.

Ferreira Lopes, S., Vacher, G., Ciarlo, E., Savova-Bianchi, D., Roger, T. and Niculita-Hirzel, H. (2017). "Primary and Immortalized Human Respiratory Cells Display Different Patterns of Cytotoxicity and Cytokine Release upon Exposure to Deoxynivalenol, Nivalenol and Fusarenon-X." Toxins **9**(11): 337.

Festa, A., D'Agostino, R., Jr., Tracy, R. P. and Haffner, S. M. (2002). "Elevated levels of acute-phase proteins and plasminogen activator inhibitor-1 predict the development of type 2 diabetes: the insulin resistance atherosclerosis study." Diabetes **51**(4): 1131-1137.

Fiacco, T. A. and McCarthy, K. D. (2018). "Multiple Lines of Evidence Indicate That Gliotransmission Does Not Occur under Physiological Conditions." The Journal of Neuroscience **38**(1): 3-13.

Fields, R. D., Lee, P. R. and Cohen, J. E. (2005). "Temporal integration of intracellular Ca2+ signaling networks in regulating gene expression by action potentials." Cell Calcium **37**(5): 433-442.

Figley, C. R. (2011). "Lactate Transport and Metabolism in the Human Brain: Implications for the Astrocyte-Neuron Lactate Shuttle Hypothesis." The Journal of Neuroscience **31**(13): 4768-4770.

Filippi, B. M., Yang, C. S., Tang, C. and Lam, T. K. (2012). "Insulin activates Erk1/2 signaling in the dorsal vagal complex to inhibit glucose production." Cell metabolism **16**(4): 500-510.

Fisher, S. J., Bruning, J. C., Lannon, S. and Kahn, C. R. (2005). "Insulin signaling in the central nervous system is critical for the normal sympathoadrenal response to hypoglycemia." Diabetes **54**(5): 1447-1451.

Flier, J. S. (2004). "Obesity wars: molecular progress confronts an expanding epidemic." Cell **116**(2): 337-350.

Flugge, G. (2000). "Regulation of monoamine receptors in the brain: dynamic changes during stress." Int Rev Cytol **195**: 145-213.

Fonseca, V. A. (2010). "Effects of β-blockers on glucose and lipid metabolism." Current Medical Research and Opinion **26**(3): 615-629.

Foo, L. C., Allen, N. J., Bushong, E. A., Ventura, P. B., Chung, W. S., Zhou, L., Cahoy, J. D., Daneman, R., Zong, H., Ellisman, M. H. and Barres, B. A. (2011). "Development of a method for the purification and culture of rodent astrocytes." Neuron **71**(5): 799-811.

Forbes, J. M. and Cooper, M. E. (2013). "Mechanisms of Diabetic Complications." Physiological Reviews **93**(1): 137-188.

Ford, A. L., Goodsall, A. L., Hickey, W. F. and Sedgwick, J. D. (1995). "Normal adult ramified microglia separated from other central nervous system macrophages by flow cytometric sorting. Phenotypic differences defined and direct ex vivo antigen presentation to myelin basic protein-reactive CD4+ T cells compared." The Journal of Immunology **154**(9): 4309-4321.

Fraley, G. S. and Ritter, S. (2003). "Immunolesion of norepinephrine and epinephrine afferents to medial hypothalamus alters basal and 2-deoxy-D-glucose-induced neuropeptide Y and agouti gene-related protein messenger ribonucleic acid expression in the arcuate nucleus." Endocrinology **144**(1): 75-83.

Frasca, F., Pandini, G., Sciacca, L., Pezzino, V., Squatrito, S., Belfiore, A. and Vigneri, R. (2008). "The role of insulin receptors and IGF-I receptors in cancer and other diseases." Arch Physiol Biochem **114**(1): 23-37.

Fray, A. E., Forsyth, R. J., Boutelle, M. G. and Fillenz, M. (1996). "The mechanisms controlling physiologically stimulated changes in rat brain glucose and lactate: a microdialysis study." J Physiol **496 (Pt 1)**: 49-57.

Fritsche, A., Stefan, N., Häring, H., Gerich, J. and Stumvoll, M. (2001). "AVoidance of hypoglycemia restores hypoglycemia awareness by increasing β-adrenergic sensitivity in type 1 diabetes." Annals of Internal Medicine **134**(9_Part_1): 729-736.

Fu, W., Shi, D., Westaway, D. and Jhamandas, J. H. (2015). "Bioenergetic mechanisms in astrocytes may contribute to amyloid plaque deposition and toxicity." J Biol Chem **290**(20): 12504-12513.

Fujita, S. and Donovan, C. M. (2005). "Celiac-superior mesenteric ganglionectomy, but not vagotomy, suppresses the sympathoadrenal response to insulin-induced hypoglycemia." Diabetes **54**(11): 3258-3264.

Funahashi, M. and Adachi, A. (1993). "Glucose-responsive neurons exist within the area postrema of the rat: in vitro study on the isolated slice preparation." Brain Res Bull **32**(5): 531-535.

Funk, D. and Stewart, J. (1996). "Role of catecholamines in the frontal cortex in the modulation of basal and stress-induced autonomic output in rats." Brain Research **741**(1): 220-229.

Gadani, Sachin P., Walsh, James T., Lukens, John R. and Kipnis, J. (2015). "Dealing with Danger in the CNS: The Response of the Immune System to Injury." Neuron **87**(1): 47-62.

Galluzzi, L., López-Soto, A., Kumar, S. and Kroemer, G. (2016). "Caspases Connect Cell-Death Signaling to Organismal Homeostasis." Immunity **44**(2): 221-231.

García-Cáceres, C., Quarta, C., Varela, L., Gao, Y., Gruber, T., Legutko, B., Jastroch, M., Johansson, P., Ninkovic, J., Yi, C.-X., Le Thuc, O., Szigeti-Buck, K., Cai, W., Meyer, C. W., Pfluger, P. T., Fernandez, A. M., Luquet, S., Woods, S. C., Torres-Alemán, I., Kahn, C. R., Götz, M., Horvath, T. L. and Tschöp, M. H. (2016). "Astrocytic Insulin Signaling Couples Brain Glucose Uptake with Nutrient Availability." Cell **166**(4): 867-880.

Garraux, G., Salmon, E., Degueldre, C., Lemaire, C., Laureys, S. and Franck, G. (1999). "Comparison of Impaired Subcortico-Frontal Metabolic Networks in Normal Aging, Subcortico-Frontal Dementia, and Cortical Frontal Dementia." NeuroImage **10**(2): 149-162.

Geenen, V. (2012). "Thymus and type 1 diabetes: an update." Diabetes research and clinical practice **98**(1): 26-32.

Gerich, J. E., Langlois, M., Noacco, C., Karam, J. H. and Forsham, P. H. (1973). "Lack of Glucagon Response to Hypoglycemia in Diabetes: Evidence for an Intrinsic Pancreatic Alpha Cell Defect." Science **182**(4108): 171-173.

Gerozissis, K. (2003). "Brain Insulin: Regulation, Mechanisms of Action and Functions." Cellular and Molecular Neurobiology **23**(1): 1-25.

Gerozissis, K. (2008). "Brain insulin, energy and glucose homeostasis; genes, environment and metabolic pathologies." European Journal of Pharmacology **585**(1): 38-49.

Ghazarian, L., Diana, J., Simoni, Y., Beaudoin, L. and Lehuen, A. (2013). "Prevention or acceleration of type 1 diabetes by viruses." Cellular and Molecular Life Sciences **70**(2): 239-255.

Ghosh, A. K. and Vaughan, D. E. (2011). "PAI-1 in tissue fibrosis." Journal of Cellular Physiology **227**(2): 493-507.

Gibbs, M. and Hertz, L. (2014). "Serotonin mediation of early memory formation via 5-HT2B receptor-induced glycogenolysis in the day-old chick." Frontiers in Pharmacology **5**(54).

Gibbs, M. E. (2015). "Role of Glycogenolysis in Memory and Learning: Regulation by Noradrenaline, Serotonin and ATP." Frontiers in Integrative Neuroscience **9**: 70.

Gibbs, M. E., Bowser, D. N., Hutchinson, D. S., Loiacono, R. E. and Summers, R. J. (2008a). "Memory processing in the avian hippocampus involves interactions between beta-adrenoceptors, glutamate receptors, and metabolism." Neuropsychopharmacology **33**(12): 2831-2846.

Gibbs, M. E., Hutchinson, D. S. and Summers, R. J. (2008b). "Role of beta-adrenoceptors in memory consolidation: beta3-adrenoceptors act on glucose uptake and beta2-adrenoceptors on glycogenolysis." Neuropsychopharmacology **33**(10): 2384-2397.

Gibbs, M. E., Lloyd, H. G., Santa, T. and Hertz, L. (2007). "Glycogen is a preferred glutamate precursor during learning in 1-day-old chick: biochemical and behavioral evidence." J Neurosci Res **85**(15): 3326-3333.

Glaser, L. and Brown, D. H. (1955). "Purification and properties of D-glucose-6-phosphate dehydrogenase." J. biol. Chem **216**: 67-79.

Glass, M. J., Huang, J., Aicher, S. A., Milner, T. A. and Pickel, V. M. (2001). "Subcellular localization of α-2A-adrenergic receptors in the rat medial nucleus tractus solitarius: Regional targeting and relationship with catecholamine neurons." Journal of Comparative Neurology **433**(2): 193-207.

Glassman, A. H., O'Connor, C. M., Califf, R. M. and et al. (2002). "Sertraline treatment of major depression in patients with acute mi or unstable angina." JAMA **288**(6): 701-709.

Glick, Z. and Mayer, J. (1968). "Hyperphagia caused by cerebral ventricular infusion of phloridzin." Nature **219**(5161): 1374.

Glock, G. E. and McLean, P. (1953). "Further studies on the properties and assay of glucose 6-phosphate dehydrogenase and 6-phosphogluconate dehydrogenase of rat liver." Biochemical Journal **55**(3): 400-408.

Gogitidze Joy, N., Hedrington, M. S., Briscoe, V. J., Tate, D. B., Ertl, A. C. and Davis, S. N. (2010). "Effects of acute hypoglycemia on inflammatory and pro-

atherothrombotic biomarkers in individuals with type 1 diabetes and healthy individuals." Diabetes Care **33**(7): 1529-1535.

Goldberg, M. P. and Choi, D. W. (1993). "Combined oxygen and glucose deprivation in cortical cell culture: calcium-dependent and calcium-independent mechanisms of neuronal injury." Journal of Neuroscience **13**(8): 3510-3524.

Goldberg, M. R., Curatolo, P. W., Tung, C. S. and Robertson, D. (1982). "Caffeine down-regulates beta adrenoreceptors in rat forebrain." Neurosci Lett **31**(1): 47-52.

Gorman, A. L. and Dunn, A. J. (1993). "Beta-adrenergic receptors are involved in stress-related behavioral changes." Pharmacol Biochem Behav **45**(1): 1-7.

Greenbaum, D., Colangelo, C., Williams, K. and Gerstein, M. (2003). "Comparing protein abundance and mRNA expression levels on a genomic scale." Genome Biol **4**(9): 117.

Grill, H. J., Ginsberg, A. B., Seeley, R. J. and Kaplan, J. M. (1998). "Brainstem application of melanocortin receptor ligands produces long-lasting effects on feeding and body weight." J Neurosci **18**(23): 10128-10135.

Grill, Harvey J. and Hayes, Matthew R. (2012). "Hindbrain Neurons as an Essential Hub in the Neuroanatomically Distributed Control of Energy Balance." Cell Metabolism **16**(3): 296-309.

Grimmer, T., Diehl, J., Drzezga, A., Förstl, H. and Kurz, A. (2004). "Region-Specific Decline of Cerebral Glucose Metabolism in Patients with Frontotemporal Dementia: A Prospective ¹⁸F-FDG-PET Study." Dementia and Geriatric Cognitive Disorders **18**(1): 32-36.

Grimsley, S. and Jann, M. (1992). "Paroxetine, sertraline, and fluvoxamine: new selective serotonin reuptake inhibitors." Clinical Pharmacy **11**(11): 930-957.

Gropp, E., Shanabrough, M., Borok, E., Xu, A. W., Janoschek, R., Buch, T., Plum, L., Balthasar, N., Hampel, B., Waisman, A., Barsh, G. S., Horvath, T. L. and Bruning, J. C. (2005). "Agouti-related peptide-expressing neurons are mandatory for feeding." Nat Neurosci **8**(10): 1289-1291.

Grosche, J., Matyash, V., Möller, T., Verkhratsky, A., Reichenbach, A. and Kettenmann, H. (1999). "Microdomains for neuron–glia interaction: parallel fiber signaling to Bergmann glial cells." Nature Neuroscience **2**: 139.

Group, U. K. P. D. S. (1998). "Intensive blood-glucose control with sulphonylureas or insulin compared with conventional treatment and risk of complications in patients with type 2 diabetes (UKPDS 33)." The Lancet **352**(9131): 837-853.

Gruetter, R. (2003). "Glycogen: the forgotten cerebral energy store." Journal of neuroscience research **74**(2): 179-183.

Guerra-Gomes, S., Sousa, N., Pinto, L. and Oliveira, J. F. (2018). "Functional Roles of Astrocyte Calcium Elevations: From Synapses to Behavior." Frontiers in Cellular Neuroscience **11**(427).

Guillod-Maximin, E., Lorsignol, A., Alquier, T. and Penicaud, L. (2004). "Acute intracarotid glucose injection towards the brain induces specific c-fos activation in hypothalamic nuclei: involvement of astrocytes in cerebral glucose-sensing in rats." J Neuroendocrinol **16**(5): 464-471.

Gusel'nikova, V. V. and Korzhevskiy, D. E. (2015). "NeuN As a Neuronal Nuclear Antigen and Neuron Differentiation Marker." Acta Naturae **7**(2): 42-47.

Guthrie, P. B., Knappenberger, J., Segal, M., Bennett, M. V., Charles, A. C. and Kater, S. B. (1999). "ATP released from astrocytes mediates glial calcium waves." J Neurosci **19**(2): 520-528.

Habbas, S., Santello, M., Becker, D., Stubbe, H., Zappia, G., Liaudet, N., Klaus, Federica R., Kollias, G., Fontana, A., Pryce, Christopher R., Suter, T. and Volterra, A. (2015). "Neuroinflammatory TNFα Impairs Memory via Astrocyte Signaling." Cell **163**(7): 1730-1741.

Habib, S. L., Prihoda, T. J., Luna, M. and Werner, S. A. (2012). "Diabetes and risk of renal cell carcinoma." Journal of Cancer **3**: 42.

Halassa, M. M., Fellin, T. and Haydon, P. G. (2007). "The tripartite synapse: roles for gliotransmission in health and disease." Trends in Molecular Medicine **13**(2): 54-63.

Hamby, M. E., Coppola, G., Ao, Y., Geschwind, D. H., Khakh, B. S. and Sofroniew, M. V. (2012). "Inflammatory mediators alter the astrocyte transcriptome and calcium signaling elicited by multiple G-protein-coupled receptors." Journal of Neuroscience **32**(42): 14489-14510.

Hamilton, N., Vayro, S., Kirchhoff, F., Verkhratsky, A., Robbins, J., Gorecki, D. C. and Butt, A. M. (2008). "Mechanisms of ATP- and glutamate-mediated calcium signaling in white matter astrocytes." Glia **56**(7): 734-749.

Hansen, L. H., Abrahamsen, N. and Nishimura, E. (1995). "Glucagon receptor mRNA distribution in rat tissues." Peptides **16**(6): 1163-1166.

Harada, K., Kamiya, T. and Tsuboi, T. (2015). "Gliotransmitter Release from Astrocytes: Functional, Developmental, and Pathological Implications in the Brain." Front Neurosci **9**: 499.

Hardie, D. G., Ross, F. A. and Hawley, S. A. (2012). "AMPK: a nutrient and energy sensor that maintains energy homeostasis." Nature Reviews Molecular Cell Biology **13**: 251.

Harding, H. P., Zhang, Y., Zeng, H., Novoa, I., Lu, P. D., Calfon, M., Sadri, N., Yun, C., Popko, B., Paules, R., Stojdl, D. F., Bell, J. C., Hettmann, T., Leiden, J. M. and Ron, D. (2003). "An integrated stress response regulates amino acid metabolism and resistance to oxidative stress." Mol Cell **11**(3): 619-633.

Harley, G. (1866). Diabetes, its various forms and different treatments, Walton & Maberly.

Haskell-Luevano, C., Chen, P., Li, C., Chang, K., Smith, M. S., Cameron, J. L. and Cone, R. D. (1999). "Characterization of the neuroanatomical distribution of agouti-related protein immunoreactivity in the rhesus monkey and the rat." Endocrinology **140**(3): 1408-1415.

Hawley, S. A., Davison, M., Woods, A., Davies, S. P., Beri, R. K., Carling, D. and Hardie, D. G. (1996). "Characterization of the AMP-activated protein kinase kinase from rat liver and identification of threonine 172 as the major site at which it phosphorylates AMP-activated protein kinase." J Biol Chem **271**(44): 27879-27887.

Haydon, P. G. and Carmignoto, G. (2006). "Astrocyte Control of Synaptic Transmission and Neurovascular Coupling." Physiological Reviews **86**(3): 1009-1031.

Heilbronn, L. K. and Campbell, L. V. (2008). "Adipose tissue macrophages, low grade inflammation and insulin resistance in human obesity." Current pharmaceutical design **14**(12): 1225-1230.

Heller, S. R. and Cryer, P. E. (1991). "Reduced neuroendocrine and symptomatic responses to subsequent hypoglycemia after 1 episode of hypoglycemia in nondiabetic humans." Diabetes **40**(2): 223-226.

Henneberger, C., Papouin, T., Oliet, S. H. and Rusakov, D. A. (2010). "Long-term potentiation depends on release of D-serine from astrocytes." Nature **463**(7278): 232.

Herder, C., Klopp, N., Baumert, J., Müller, M., Khuseyinova, N., Meisinger, C., Martin, S., Illig, T., Koenig, W. and Thorand, B. (2008). "Effect of macrophage migration inhibitory factor (MIF) gene variants and MIF serum concentrations on the risk of type 2 diabetes: results from the MONICA/KORA Augsburg Case–Cohort Study, 1984–2002." Diabetologia **51**(2): 276-284.

Herrero-Mendez, A., Almeida, A., Fernández, E., Maestre, C., Moncada, S. and Bolaños, J. P. (2009). "The bioenergetic and antioxidant status of neurons is controlled by continuous degradation of a key glycolytic enzyme by APC/C–Cdh1." Nature Cell Biology **11**: 747.

Hertz, L., Dringen, R., Schousboe, A. and Robinson, S. R. (1999). "Astrocytes: Glutamate producers for neurons." Journal of Neuroscience Research **57**(4): 417-428.

Hertz, L., O'Dowd, B. S., Ng, K. T. and Gibbs, M. E. (2003). "Reciprocal changes in forebrain contents of glycogen and of glutamate/glutamine during early memory consolidation in the day-old chick." Brain Research **994**(2): 226-233.

Herzig, S., Long, F., Jhala, U. S., Hedrick, S., Quinn, R., Bauer, A., Rudolph, D., Schutz, G., Yoon, C. and Puigserver, P. (2001). "CREB regulates hepatic gluconeogenesis through the coactivator PGC-1." Nature **413**(6852): 179.

Herzig, S. and Shaw, R. J. (2017). "AMPK: guardian of metabolism and mitochondrial homeostasis." Nature Reviews Molecular Cell Biology **19**: 121.

Herzog, R. I., Chan, O., Yu, S., Dziura, J., McNay, E. C. and Sherwin, R. S. (2008). "Effect of Acute and Recurrent Hypoglycemia on Changes in Brain Glycogen Concentration." Endocrinology **149**(4): 1499-1504.

Hex, N., Bartlett, C., Wright, D., Taylor, M. and Varley, D. (2012). "Estimating the current and future costs of Type 1 and Type 2 diabetes in the UK, including direct health costs and indirect societal and productivity costs." Diabetic Medicine **29**(7): 855-862.

Hoang Do, O. and Thorn, P. (2015). "Insulin secretion from beta cells within intact islets: Location matters." Clinical and Experimental Pharmacology & Physiology **42**(4): 406-414.

Hoheisel, J. D. (2006). "Microarray technology: beyond transcript profiling and genotype analysis." Nature reviews genetics **7**(3): 200.

Holley, J. E., Gveric, D., Whatmore, J. L. and Gutowski, N. J. (2005). "Tenascin C induces a quiescent phenotype in cultured adult human astrocytes." Glia **52**(1): 53-58.

Holman, N., Young, B. and Gadsby, R. (2015). "Current prevalence of Type 1 and Type 2 diabetes in adults and children in the UK." Diabetic Medicine **32**(9): 1119-1120.

Horvath, T. L., Sarman, B., Garcia-Caceres, C., Enriori, P. J., Sotonyi, P., Shanabrough, M., Borok, E., Argente, J., Chowen, J. A., Perez-Tilve, D., Pfluger, P. T., Bronneke, H. S., Levin, B. E., Diano, S., Cowley, M. A. and Tschop, M. H. (2010). "Synaptic input organization of the melanocortin system predicts diet-induced hypothalamic reactive gliosis and obesity." Proc Natl Acad Sci U S A **107**(33): 14875-14880.

Hotamisligil, G. S., Arner, P., Caro, J. F., Atkinson, R. L. and Spiegelman, B. M. (1995). "Increased adipose tissue expression of tumor necrosis factor-alpha in human obesity and insulin resistance." J Clin Invest **95**(5): 2409-2415.

Hotamisligil, G. S., Shargill, N. S. and Spiegelman, B. M. (1993). "Adipose expression of tumor necrosis factor-alpha: direct role in obesity-linked insulin resistance." Science **259**(5091): 87-91.

Høyer-Hansen, M. and Jäättelä, M. (2007). "Connecting endoplasmic reticulum stress to autophagy by unfolded protein response and calcium." Cell Death And Differentiation **14**: 1576.

Huang, W.-J., Zhang, X. I. A. and Chen, W.-W. (2016). "Role of oxidative stress in Alzheimer's disease." Biomedical Reports **4**(5): 519-522.

Huang, Y. H., Sinha, S. R., Tanaka, K., Rothstein, J. D. and Bergles, D. E. (2004). "Astrocyte glutamate transporters regulate metabotropic glutamate receptor-mediated excitation of hippocampal interneurons." Journal of Neuroscience **24**(19): 4551-4559.

Hubbard, M. J. and McHugh, N. J. (1996). "Mitochondrial ATP synthase F1-β-subunit is a calcium-binding protein." FEBS Letters **391**(3): 323-329.

Hughes, P., Marshall, D., Reid, Y., Parkes, H. and Gelber, C. (2007). "The costs of using unauthenticated, over-passaged cell lines: how much more data do we need?" BioTechniques **43**(5): 575-586.

Hundal, R. S., Krssak, M., Dufour, S., Laurent, D., Lebon, V., Chandramouli, V., Inzucchi, S. E., Schumann, W. C., Petersen, K. F., Landau, B. R. and Shulman, G. I. (2000). "Mechanism by which metformin reduces glucose production in type 2 diabetes." Diabetes **49**(12): 2063-2069.

Husain, S. and Thrower, E. (2009). "Molecular and cellular regulation of pancreatic acinar cell function." Current Opinion in Gastroenterology **25**(5): 466-471.

Hutchinson, D. S., Summers, R. J. and Gibbs, M. E. (2007). "Beta2- and beta3-adrenoceptors activate glucose uptake in chick astrocytes by distinct mechanisms: a mechanism for memory enhancement?" J Neurochem **103**(3): 997-1008.

Hynd, M. R., Scott, H. L. and Dodd, P. R. (2004). "Glutamate-mediated excitotoxicity and neurodegeneration in Alzheimer's disease." Neurochemistry International **45**(5): 583-595.

Ibrahim, N., Bosch, M. A., Smart, J. L., Qiu, J., Rubinstein, M., Ronnekleiv, O. K., Low, M. J. and Kelly, M. J. (2003). "Hypothalamic proopiomelanocortin neurons are glucose responsive and express K(ATP) channels." Endocrinology **144**(4): 1331-1340.

Iglesias, J., Morales, L. and Barreto, G. E. (2017). "Metabolic and Inflammatory Adaptation of Reactive Astrocytes: Role of PPARs." Molecular Neurobiology **54**(4): 2518-2538.

Ikesugi, K., Mulhern, M. L., Madson, C. J., Hosoya, K.-i., Terasaki, T., Kador, P. F. and Shinohara, T. (2006). "Induction of Endoplasmic Reticulum Stress in Retinal Pericytes by Glucose Deprivation." Current Eye Research **31**(11): 947-953.

Innocenti, B., Parpura, V. and Haydon, P. G. (2000). "Imaging extracellular waves of glutamate during calcium signaling in cultured astrocytes." Journal of Neuroscience **20**(5): 1800-1808.

Iqbal, K., Liu, F., Gong, C.-X. and Grundke-Iqbal, I. (2010). "Tau in Alzheimer disease and related tauopathies." Current Alzheimer Research **7**(8): 656-664.

Ismail, N. A., Abd El Baky, A. N., Ragab, S., Hamed, M., Hashish, M. A. and Shehata, A. (2016). "Monocyte chemoattractant protein 1 and macrophage migration inhibitory factor in children with type 1 diabetes." J Pediatr Endocrinol Metab **29**(6): 641-645.

Iversen, L. L. and Neal, M. J. (1968). "The uptake of [3H]GABA by slices of rat cerebral cortex." J Neurochem **15**(10): 1141-1149.

Iwakoshi, N. N., Lee, A. H., Vallabhajosyula, P., Otipoby, K. L., Rajewsky, K. and Glimcher, L. H. (2003). "Plasma cell differentiation and the unfolded protein response intersect at the transcription factor XBP-1." Nat Immunol **4**(4): 321-329.

Jacobson, A. M., Musen, G., Ryan, C. M., Silvers, N., Cleary, P., Waberski, B., Burwood, A., Weinger, K., Bayless, M., Dahms, W. and Harth, J. (2007). "Long-term effect of diabetes and its treatment on cognitive function." N Engl J Med **356**(18): 1842-1852.

Jansen, A. S., Hoffman, J. L. and Loewy, A. D. (1997). "CNS sites involved in sympathetic and parasympathetic control of the pancreas: a viral tracing study." Brain Res **766**(1-2): 29-38.

Janssen, R. J., Nijtmans, L. G., Van Den Heuvel, L. P. and Smeitink, J. A. (2006). "Mitochondrial complex I: structure, function and pathology." Journal of inherited metabolic disease **29**(4): 499-515.

Jeftinija, S. D., Jeftinija, K. V., Stefanovic, G. and Liu, F. (1996). "Neuroligand-evoked calcium-dependent release of excitatory amino acids from cultured astrocytes." Journal of neurochemistry **66**(2): 676-684.

Jelluma, N., Yang, X., Stokoe, D., Evan, G. I., Dansen, T. B. and Haas-Kogan, D. A. (2006). "Glucose Withdrawal Induces Oxidative Stress followed by Apoptosis in Glioblastoma Cells but not in Normal Human Astrocytes." Molecular Cancer Research **4**(5): 319-330.

Jeremic, A., Jeftinija, K., Stevanovic, J., Glavaski, A. and Jeftinija, S. (2001). "ATP stimulates calcium-dependent glutamate release from cultured astrocytes." Journal of Neurochemistry **77**(2): 664-675.

Jerram, S. T. and Leslie, R. D. (2017). "The Genetic Architecture of Type 1 Diabetes." Genes **8**(8): 209.

Jiang, D., Niwa, M. and Koong, A. C. (2015). "Targeting the IRE1alpha-XBP1 branch of the unfolded protein response in human diseases." Semin Cancer Biol **33**: 48-56.

John, G. R., Simpson, J. E., Woodroofe, M. N., Lee, S. C. and Brosnan, C. F. (2001). "Extracellular nucleotides differentially regulate interleukin-1beta signaling in primary human astrocytes: implications for inflammatory gene expression." J Neurosci **21**(12): 4134-4142.

Johnson, L. N. (1997). From phosphorylase to phosphorylase kinase. Interacting Protein Domains, Springer**:** 9-14.

Jouvet, N. and Estall, J. L. (2017). "The pancreas: Bandmaster of glucose homeostasis." Experimental Cell Research **360**(1): 19-23.

Joy, N. G., Tate, D. B., Younk, L. M. and Davis, S. N. (2015). "Effects of Acute and Antecedent Hypoglycemia on Endothelial Function and Markers of Atherothrombotic Balance in Healthy Man." Diabetes.

Juhan-Vague, I., Alessi, M. C., Mavri, A. and Morange, P. E. (2003). "Plasminogen activator inhibitor-1, inflammation, obesity, insulin resistance and vascular risk." J Thromb Haemost **1**(7): 1575-1579.

Kanehisa, M., Furumichi, M., Tanabe, M., Sato, Y. and Morishima, K. (2017). "KEGG: new perspectives on genomes, pathways, diseases and drugs." Nucleic Acids Res **45**(D1): D353-d361.

Kanehisa, M. and Goto, S. (2000). "KEGG: kyoto encyclopedia of genes and genomes." Nucleic Acids Res **28**(1): 27-30.

Kanehisa, M., Sato, Y., Kawashima, M., Furumichi, M. and Tanabe, M. (2016). "KEGG as a reference resource for gene and protein annotation." Nucleic Acids Res **44**(D1): D457-462.

Kang, J., Jiang, L., Goldman, S. A. and Nedergaard, M. (1998). "Astrocyte-mediated potentiation of inhibitory synaptic transmission." Nature Neuroscience **1**: 683.

Kasakov, L. and Burnstock, G. (1982). "The use of the slowly degradable analog, α,β-methylene ATP, to produce desensitisation of the P2-purinoceptor: Effect on non-adrenergic, non-cholinergic responses of the guinea-pig urinary bladder." European Journal of Pharmacology **86**(2): 291-294.

Kataoka, A., Tozaki-Saitoh, H., Koga, Y., Tsuda, M. and Inoue, K. (2008). "Activation of P2X7 receptors induces CCL3 production in microglial cells through transcription factor NFAT." Journal of Neurochemistry **108**(1): 115-125.

Kawamori, D., Kurpad, A. J., Hu, J., Liew, C. W., Shih, J. L., Ford, E. L., Herrera, P. L., Polonsky, K. S., McGuinness, O. P. and Kulkarni, R. N. (2009). "Insulin Signaling in α Cells Modulates Glucagon Secretion In Vivo." Cell Metabolism **9**(4): 350-361.

Kenny, P. J. (2011). "Common cellular and molecular mechanisms in obesity and drug addiction." Nature Reviews Neuroscience **12**: 638.

Kerman, I. A., Akil, H. and Watson, S. J. (2006). "Rostral elements of sympatho-motor circuitry: a virally mediated transsynaptic tracing study." J Neurosci **26**(13): 3423-3433.

Kerman, I. A., Bernard, R., Rosenthal, D., Beals, J., Akil, H. and Watson, S. J. (2007). "Distinct populations of presympathetic-premotor neurons express orexin or melanin-concentrating hormone in the rat lateral hypothalamus." J Comp Neurol **505**(5): 586-601.

Kerman, I. A., Enquist, L. W., Watson, S. J. and Yates, B. J. (2003). "Brainstem substrates of sympatho-motor circuitry identified using trans-synaptic tracing with pseudorabies virus recombinants." J Neurosci **23**(11): 4657-4666.

Kerr, D. and Everett, J. (2005). "Coffee, diabetes and insulin sensitivity." Diabetologia **48**(7): 1418-1418.

Kety, S. S. and Schmidt, C. F. (1948). "The nitrous oxide method for the quantitative determination of cerebral blood flow in man: theory, procedure and normal values." The Journal of clinical investigation **27**(4): 476-483.

Khovidhunkit, W., Kim, M. S., Memon, R. A., Shigenaga, J. K., Moser, A. H., Feingold, K. R. and Grunfeld, C. (2004). "Effects of infection and inflammation on lipid and lipoprotein metabolism: mechanisms and consequences to the host." J Lipid Res **45**(7): 1169-1196.

Kim, J.-h., Min, K.-J., Seol, W., Jou, I. and Joe, E.-h. (2010). "Astrocytes in injury states rapidly produce anti-inflammatory factors and attenuate microglial inflammatory responses." Journal of Neurochemistry **115**(5): 1161-1171.

Kim, J. and Gorman, J. (2005). "The psychobiology of anxiety." Clinical Neuroscience Research **4**(5-6): 335-347.

Kinoshita, M., Hirayama, Y., Fujishita, K., Shibata, K., Shinozaki, Y., Shigetomi, E., Takeda, A., Le, H. P. N., Hayashi, H., Hiasa, M., Moriyama, Y., Ikenaka, K., Tanaka, K. F. and Koizumi, S. (2018). "Anti-Depressant Fluoxetine Reveals its Therapeutic Effect Via Astrocytes." EBioMedicine **32**: 72-83.

Kıray, H., Lindsay, S. L., Hosseinzadeh, S. and Barnett, S. C. (2016). "The multifaceted role of astrocytes in regulating myelination." Experimental Neurology **283**: 541-549.

Kirischuk, S., Héja, L., Kardos, J. and Billups, B. (2016). "Astrocyte sodium signaling and the regulation of neurotransmission." Glia **64**(10): 1655-1666.

Kiritsy-Roy, J. A., Appel, N. M., Bobbitt, F. G. and Van Loon, G. R. (1986). "Effects of mu-opioid receptor stimulation in the hypothalamic paraventricular nucleus on basal and stress-induced catecholamine secretion and cardiovascular responses." J Pharmacol Exp Ther **239**(3): 814-822.

Knip, M. and Simell, O. (2012). "Environmental triggers of type 1 diabetes." Cold Spring Harbor perspectives in medicine: a007690.

Knupp, J., Arvan, P. and Chang, A. (2018). "Increased mitochondrial respiration promotes survival from endoplasmic reticulum stress." Cell Death & Differentiation.

Kojima, S., Ueno, N., Asakawa, A., Sagiyama, K., Naruo, T., Mizuno, S. and Inui, A. (2007). "A role for pancreatic polypeptide in feeding and body weight regulation." Peptides **28**(2): 459-463.

Komatsu, M., Takei, M., Ishii, H. and Sato, Y. (2013). "Glucose-stimulated insulin secretion: A newer perspective." Journal of Diabetes Investigation **4**(6): 511-516.

Koopmans, S. J., Frolich, M., Gribnau, E. H., Westendorp, R. G. and DeFronzo, R. A. (1998). "Effect of hyperinsulinemia on plasma leptin concentrations and food intake in rats." American Journal of Physiology-Endocrinology And Metabolism **274**(6): E998-E1001.

Kostyuk, E., Svichar, N., Shishkin, V. and Kostyuk, P. (1999). "Role of mitochondrial dysfunction in calcium signalling alterations in dorsal root ganglion neurons of mice with experimentally-induced diabetes." Neuroscience **90**(2): 535-541.

Kowaltowski, A. J. and Vercesi, A. E. (1999). "Mitochondrial damage induced by conditions of oxidative stress." Free Radical Biology and Medicine **26**(3-4): 463-471.

Krashes, M. J., Koda, S., Ye, C., Rogan, S. C., Adams, A. C., Cusher, D. S., Maratos-Flier, E., Roth, B. L. and Lowell, B. B. (2011). "Rapid, reversible activation of AgRP neurons drives feeding behavior in mice." J Clin Invest **121**(4): 1424-1428.

Krashes, Michael J., Shah, Bhavik P., Koda, S. and Lowell, Bradford B. (2013). "Rapid versus Delayed Stimulation of Feeding by the Endogenously Released AgRP Neuron Mediators GABA, NPY, and AgRP." Cell Metabolism **18**(4): 588-595.

Kratz, A. and Carninci, P. (2014). "The devil in the details of RNA-seq." Nature Biotechnology **32**: 882.

Kruger, N. J. and von Schaewen, A. (2003). "The oxidative pentose phosphate pathway: structure and organisation." Current Opinion in Plant Biology **6**(3): 236-246.

Kucher, B. M. and Neary, J. T. (2005). "Bi-functional effects of ATP/P2 receptor activation on tumor necrosis factor-alpha release in lipopolysaccharide-stimulated astrocytes." Journal of Neurochemistry **92**(3): 525-535.

Kuhl, D. E., Metter, E. J. and Riege, W. H. (1984). "Patterns of local cerebral glucose utilization determined in Parkinson's disease by the [18F]fluorodeoxyglucose method." Ann Neurol **15**(5): 419-424.

Kukurba, K. R. and Montgomery, S. B. (2015). "RNA Sequencing and Analysis." Cold Spring Harbor protocols **2015**(11): 951-969.

Kuleshov, M. V., Jones, M. R., Rouillard, A. D., Fernandez, N. F., Duan, Q., Wang, Z., Koplev, S., Jenkins, S. L., Jagodnik, K. M., Lachmann, A., McDermott, M. G., Monteiro, C. D., Gundersen, G. W. and Ma'ayan, A. (2016). "Enrichr: a comprehensive gene set enrichment analysis web server 2016 update." Nucleic Acids Res **44**(W1): W90-97.

Kumagai, A. K., Kang, Y.-S., Boado, R. J. and Pardridge, W. M. (1995). "Upregulation of Blood-Brain Barrier GLUT1 Glucose Transporter Protein and mRNA in Experimental Chronic Hypoglycemia." Diabetes **44**(12): 1399-1404.

Kutz, S. M., Higgins, C. E. and Higgins, P. J. (2012). "Novel Combinatorial Therapeutic Targeting of PAI-1 (SERPINE1) Gene Expression in Alzheimer's Disease." Molecular Medicine & Therapeutics **1**(2): 106.

Laing, S. P., Swerdlow, A. J., Slater, S. D., Botha, J. L., Burden, A. C., Waugh, N. R., Smith, A. W. M., Hill, R. D., Bingley, P. J., Patterson, C. C., Qiao, Z. and Keen, H. (1999). "The British Diabetic Association Cohort Study, II: cause-specific mortality in patients with insulin-treated diabetes mellitus." Diabetic Medicine **16**(6): 466-471.

Lam, T. K., Schwartz, G. J. and Rossetti, L. (2005a). "Hypothalamic sensing of fatty acids." Nature neuroscience **8**(5): 579.

Lam, T. K. T., Gutierrez-Juarez, R., Pocai, A. and Rossetti, L. (2005b). "Regulation of Blood Glucose by Hypothalamic Pyruvate Metabolism." Science **309**(5736): 943-947.

Lane, M. D., Flores-Riveros, J. R., Hresko, R. C., Kaestner, K. H., Liao, K., Janicot, M., Hoffman, R. D., McLenithan, J. C., Kastelic, T. and Christy, R. J. (1990). "Insulin-Receptor Tyrosine Kinase and Glucose Transport." Diabetes Care **13**(6): 565-575.

Langfelder, P. and Horvath, S. (2008). "WGCNA: an R package for weighted correlation network analysis." BMC Bioinformatics **9**(1): 559.

Lapiz, M. D. and Morilak, D. A. (2006). "Noradrenergic modulation of cognitive function in rat medial prefrontal cortex as measured by attentional set shifting capability." Neuroscience **137**(3): 1039-1049.

Laughlin, S. B., de Ruyter van Steveninck, R. R. and Anderson, J. C. (1998). "The metabolic cost of neural information." Nature Neuroscience **1**: 36.

Lawlis, V. B. and Roche, T. E. (1981). "Regulation of bovine kidney. alpha.-ketoglutarate dehydrogenase complex by calcium ion and adenine nucleotides. Effects on S0. 5 for. alpha.-ketoglutarate." Biochemistry **20**(9): 2512-2518.

Laybutt, D., Preston, A., Åkerfeldt, M., Kench, J., Busch, A., Biankin, A. and Biden, T. (2007). "Endoplasmic reticulum stress contributes to beta cell apoptosis in type 2 diabetes." Diabetologia **50**(4): 752-763.

Lebed, Y. V., Orlovsky, M. A., Nikonenko, A. G., Ushakova, G. A. and Skibo, G. G. (2008). "Early reaction of astroglial cells in rat hippocampus to streptozotocin-induced diabetes." Neuroscience Letters **444**(2): 181-185.

Lee, W., Reyes, R. C., Gottipati, M. K., Lewis, K., Lesort, M., Parpura, V. and Gray, M. (2013). "Enhanced Ca 2+-dependent glutamate release from astrocytes of the BACHD Huntington's disease mouse model." Neurobiology of disease **58**: 192-199.

Leibowitz, S. F., Sladek, C., Spencer, L. and Tempel, D. (1988). "Neuropeptide Y, epinephrine and norepinephrine in the paraventricular nucleus: stimulation of feeding and the release of corticosterone, vasopressin and glucose." Brain Res Bull **21**(6): 905-912.

Leloup, C., Allard, C., Carneiro, L., Fioramonti, X., Collins, S. and Pénicaud, L. (2016). "Glucose and hypothalamic astrocytes: More than a fueling role?" Neuroscience **323**: 110-120.

Levin, B. E., Becker, T. C., Eiki, J.-i., Zhang, B. B. and Dunn-Meynell, A. A. (2008). "Ventromedial hypothalamic glucokinase is an important mediator of the counterregulatory response to insulin-induced hypoglycemia." Diabetes.

Levin, B. E., Routh, V. H., Kang, L., Sanders, N. M. and Dunn-Meynell, A. A. (2004). "Neuronal glucosensing: what do we know after 50 years?" Diabetes **53**(10): 2521-2528.

Levy, L. M., Warr, O. and Attwell, D. (1998). "Stoichiometry of the glial glutamate transporter GLT-1 expressed inducibly in a Chinese hamster ovary cell line selected for low endogenous Na+-dependent glutamate uptake." J Neurosci **18**(23): 9620-9628.

Lewis, L. D., Ljunggren, B., Norberg, K. and Siesjö, B. K. (1974). "Changes in carbohydrate substrates, amino acids, and ammonia in the brain during insulin-induced hypoglycemia." Journal of Neurochemistry **23**(4): 659-671.

Leybaert, L. (2005). "Neurobarrier coupling in the brain: a partner of neurovascular and neurometabolic coupling?" Journal of Cerebral Blood Flow & Metabolism **25**(1): 2-16.

Leybaert, L., Cabooter, L. and Braet, K. (2004). "Calcium signal communication between glial and vascular brain cells." Acta neurologica belgica **104**: 51-56.

Li, A. J. and Ritter, S. (2004). "Glucoprivation increases expression of neuropeptide Y mRNA in hindbrain neurons that innervate the hypothalamus." Eur J Neurosci **19**(8): 2147-2154.

Li, A. J., Wang, Q. and Ritter, S. (2006). "Differential responsiveness of dopamine-beta-hydroxylase gene expression to glucoprivation in different catecholamine cell groups." Endocrinology **147**(7): 3428-3434.

Li, N., Ragheb, K., Lawler, G., Sturgis, J., Rajwa, B., Melendez, J. A. and Robinson, J. P. (2003). "Mitochondrial Complex I Inhibitor Rotenone Induces Apoptosis through Enhancing Mitochondrial Reactive Oxygen Species Production." Journal of Biological Chemistry **278**(10): 8516-8525.

Li, Q., Vande Velde, C., Israelson, A., Xie, J., Bailey, A. O., Dong, M.-Q., Chun, S.-J., Roy, T., Winer, L., Yates, J. R., Capaldi, R. A., Cleveland, D. W. and Miller, T. M. (2010). "ALS-linked mutant superoxide dismutase 1 (SOD1) alters mitochondrial protein composition and decreases protein import." Proceedings of the National Academy of Sciences of the United States of America **107**(49): 21146-21151.

Li, S.-Q., Yu, Y., Han, J.-Z., Wang, D., Liu, J., Qian, F., Fan, G.-H., Bucala, R. and Ye, R. D. (2015). "Deficiency of macrophage migration inhibitory factor attenuates tau hyperphosphorylation in mouse models of Alzheimer's disease." Journal of Neuroinflammation **12**: 177.

Liang, Y., Yuan, W., Zhu, W., Zhu, J., Lin, Q., Zou, X., Deng, C., Fu, Y., Zheng, X., Yang, M., Wu, S., Yu, X. and Shan, Z. (2015). "Macrophage migration inhibitory factor promotes expression of GLUT4 glucose transporter through MEF2 and Zac1 in cardiomyocytes." Metabolism **64**(12): 1682-1693.

Liao, Y., Smyth, G. K. and Shi, W. (2014). "featureCounts: an efficient general purpose program for assigning sequence reads to genomic features." Bioinformatics **30**(7): 923-930.

Liberti, M. V. and Locasale, J. W. (2016). "The Warburg Effect: How Does it Benefit Cancer Cells?" Trends in biochemical sciences **41**(3): 211-218.

Lin, M. T. and Beal, M. F. (2006). "Mitochondrial dysfunction and oxidative stress in neurodegenerative diseases." Nature **443**: 787.

Lin, Y., Berg, A. H., Iyengar, P., Lam, T. K. T., Giacca, A., Combs, T. P., Rajala, M. W., Du, X., Rollman, B., Li, W., Hawkins, M., Barzilai, N., Rhodes, C. J., Fantus, I. G., Brownlee, M. and Scherer, P. E. (2005). "The Hyperglycemia-induced Inflammatory Response in Adipocytes: THE ROLE OF REACTIVE OXYGEN SPECIES." Journal of Biological Chemistry **280**(6): 4617-4626.

Linker, R. A., Lee, D.-H., Ryan, S., van Dam, A. M., Conrad, R., Bista, P., Zeng, W., Hronowsky, X., Buko, A., Chollate, S., Ellrichmann, G., Brück, W., Dawson, K., Goelz, S., Wiese, S., Scannevin, R. H., Lukashev, M. and Gold, R. (2011). "Fumaric acid esters exert neuroprotective effects in neuroinflammation via activation of the Nrf2 antioxidant pathway." Brain **134**(3): 678-692.

Lister, A., Bourgeois, S., Silva, P. H. I., Rubio-Aliaga, I., Marbet, P., Walsh, J., Shelton, L. M., Keller, B., Verrey, F. and Devuyst, O. (2018). "NRF2 regulates the glutamine transporter Slc38a3 (SNAT3) in kidney in response to metabolic acidosis." Scientific reports **8**(1): 5629.

Little, A. A., Edwards, J. L. and Feldman, E. L. (2007). "Diabetic neuropathies." Practical Neurology **7**(2): 82-92.

Liu, M., King, B. F., Dunn, P. M., Rong, W., Townsend-Nicholson, A. and Burnstock, G. (2001). "Coexpression of P2X3 and P2X2 Receptor Subunits in Varying Amounts Generates Heterogeneous Populations of P2X Receptors That Evoke a Spectrum of Agonist Responses Comparable to That Seen in Sensory Neurons." Journal of Pharmacology and Experimental Therapeutics **296**(3): 1043-1050.

Liu, X., Zhang, Z., Guo, W., Burnstock, G., He, C. and Xiang, Z. (2013). "The superficial glia limitans of mouse and monkey brain and spinal cord." Anat Rec (Hoboken) **296**(7): 995-1007.

Liu, Y., Hou, X., Liu, M., Yang, Z., Bi, Y., Zou, H., Wu, J., Che, H., Li, C., Wang, X., Wang, K., Zhong, C., Zhang, J., Yu, T., Bian, Q., Chai, S., Liu, H., Ai, J. and Zhao, S. (2016). "XBP1 silencing decreases glioma cell viability and glycolysis possibly by inhibiting HK2 expression." J Neurooncol **126**(3): 455-462.

Ljubicic, V., Miura, P., Burt, M., Boudreault, L., Khogali, S., Lunde, J. A., Renaud, J. M. and Jasmin, B. J. (2011). "Chronic AMPK activation evokes the slow, oxidative myogenic program and triggers beneficial adaptations in mdx mouse skeletal muscle." Hum Mol Genet **20**(17): 3478-3493.

Loaiza, A., Porras, O. H. and Barros, L. F. (2003). "Glutamate triggers rapid glucose transport stimulation in astrocytes as evidenced by real-time confocal microscopy." J Neurosci **23**(19): 7337-7342.

Lochhead, P. A., Coghlan, M., Rice, S. Q. J. and Sutherland, C. (2001). "Inhibition of GSK-3 Selectively Reduces Glucose-6-Phosphatase and Phosphoenolpyruvate Carboxykinase Gene Expression." Diabetes **50**(5): 937-946.

Loeffen, J., Smeitink, J., Triepels, R., Smeets, R., Schuelke, M., Sengers, R., Trijbels, F., Hamel, B., Mullaart, R. and van den Heuvel, L. (1998). "The first nuclear-encoded complex I mutation in a patient with Leigh syndrome." The American Journal of Human Genetics **63**(6): 1598-1608.

Loewy, A. D. (1991). "Forebrain nuclei involved in autonomic control." Prog Brain Res **87**: 253-268.

Louveau, A., Harris, T. H. and Kipnis, J. (2015). "Revisiting the Mechanisms of CNS Immune Privilege." Trends in Immunology **36**(10): 569-577.

Lovatt, D., Sonnewald, U., Waagepetersen, H. S., Schousboe, A., He, W., Lin, J. H., Han, X., Takano, T., Wang, S., Sim, F. J., Goldman, S. A. and Nedergaard, M. (2007). "The transcriptome and metabolic gene signature of protoplasmic astrocytes in the adult murine cortex." J Neurosci **27**(45): 12255-12266.

Love, M. I., Huber, W. and Anders, S. (2014). "Moderated estimation of fold change and dispersion for RNA-seq data with DESeq2." Genome Biology **15**(12): 550.

Lowry, C. A. (2002). "Functional Subsets of Serotonergic Neurones: Implications for Control of the Hypothalamic-Pituitary-Adrenal Axis." Journal of Neuroendocrinology **14**(11): 911-923.

Lu, Y. and Rowland, N. E. (1993). "Increased feeding after treatment with fructose, but not glucose, antimetabolites in rats with dopamine-depleting brain lesions." Brain Res **617**(1): 120-122.

Lue, H., Kleemann, R., Calandra, T., Roger, T. and Bernhagen, J. (2002). "Macrophage migration inhibitory factor (MIF): mechanisms of action and role in disease." Microbes Infect **4**(4): 449-460.

Lynch, R. M., Tompkins, L. S., Brooks, H. L., Dunn-Meynell, A. A. and Levin, B. E. (2000). "Localization of glucokinase gene expression in the rat brain." Diabetes **49**(5): 693-700.

MacDonald Patrick, E., Joseph Jamie, W. and Rorsman, P. (2005). "Glucose-sensing mechanisms in pancreatic β-cells." Philosophical Transactions of the Royal Society B: Biological Sciences **360**(1464): 2211-2225.

Machann, J., Häring, H., Schick, F. and Stumvoll, M. (2004). "Intramyocellular lipids and insulin resistance." Diabetes, Obesity and Metabolism **6**(4): 239-248.

MacLeod, K. M., Hepburn, D. A. and Frier, B. M. (1993). "Frequency and Morbidity of Severe Hypoglycaemia in Insulin-treated Diabetic Patients." Diabetic Medicine **10**(3): 238-245.

Madison, L. L., Combes, B., Unger, R. H. and Kaplan, N. (1959). "The relationship between the mechanism of action of the sulfonylureas and the secretion of insulin into the portal circulation." Annals of the New York Academy of Sciences **74**(3): 548-556.

Magistretti, P. J., Sorg, O., Yu, N., Martin, J. L. and Pellerin, L. (1993). "Neurotransmitters regulate energy metabolism in astrocytes: implications for the metabolic trafficking between neural cells." Dev Neurosci **15**(3-5): 306-312.

Malmstrom, R., Taskinen, M. R., Karonen, S. L. and Yki-Jarvinen, H. (1996). "Insulin increases plasma leptin concentrations in normal subjects and patients with NIDDM." Diabetologia **39**(8): 993-996.

Mancardi, G. L., Liwnicz, B. H. and Mandybur, T. I. (1983). "Fibrous astrocytes in Alzheimer's disease and senile dementia of Alzheimer's type." Acta Neuropathol **61**(1): 76-80.

Mancini, A. D. and Poitout, V. (2013). "The fatty acid receptor FFA1/GPR40 a decade later: how much do we know?" Trends in Endocrinology & Metabolism **24**(8): 398-407.

Mandal, S. K., Shrestha, P. K., Alenazi, F. S. H., Shakya, M., Alhamami, H. and Briski, K. P. (2017). "Role of hindbrain adenosine 5'-monophosphate-activated protein kinase (AMPK) in hypothalamic AMPK and metabolic neuropeptide adaptation to recurring insulin-induced hypoglycemia in the male rat." Neuropeptides **66**: 25-35.

Mangia, S., Simpson, I. A., Vannucci, S. J. and Carruthers, A. (2009). "The in vivo neuron-to-astrocyte lactate shuttle in human brain: evidence from modeling of measured lactate levels during visual stimulation." Journal of Neurochemistry **109**(s1): 55-62.

Mangia, S., Tesfaye, N., De Martino, F., Kumar, A. F., Kollasch, P., Moheet, A. A., Eberly, L. E. and Seaquist, E. R. (2012). "Hypoglycemia-induced increases in thalamic cerebral blood flow are blunted in subjects with type 1 diabetes and hypoglycemia unawareness." J Cereb Blood Flow Metab **32**(11): 2084-2090.

Mann, J. J., McBride, P. A., Anderson, G. M. and Mieczkowski, T. A. (1992). "Platelet and whole blood serotonin content in depressed inpatients: correlations with acute and life-time psychopathology." Biol Psychiatry **32**(3): 243-257.

Markovic, O. and Markovic, N. (1998). "Cell cross-contamination in cell cultures: the silent and neglected danger." In Vitro Cellular & Developmental Biology-Animal **34**(1): 1-8.

Martinowich, K. and Lu, B. (2008). "Interaction between BDNF and serotonin: role in mood disorders." Neuropsychopharmacology **33**(1): 73.

Marty, N., Dallaporta, M., Foretz, M., Emery, M., Tarussio, D., Bady, I., Binnert, C., Beermann, F. and Thorens, B. (2005). "Regulation of glucagon secretion by glucose transporter type 2 (glut2) and astrocyte-dependent glucose sensors." J Clin Invest **115**(12): 3545-3553.

Marty, N., Dallaporta, M. and Thorens, B. (2007). "Brain Glucose Sensing, Counterregulation, and Energy Homeostasis." Physiology **22**(4): 241-251.

Mason, G. F., Petersen, K. F., Lebon, V., Rothman, D. L. and Shulman, G. I. (2006). "Increased Brain Monocarboxylic Acid Transport and Utilization in Type 1 Diabetes." Diabetes **55**(4): 929-934.

Mastorakos, G., Chrousos, G. P. and Weber, J. S. (1993). "Recombinant interleukin-6 activates the hypothalamic-pituitary-adrenal axis in humans." The Journal of Clinical Endocrinology & Metabolism **77**(6): 1690-1694.

Matthias, K., Kirchhoff, F., Seifert, G., Huttmann, K., Matyash, M., Kettenmann, H. and Steinhauser, C. (2003). "Segregated expression of AMPA-type glutamate receptors and glutamate transporters defines distinct astrocyte populations in the mouse hippocampus." J Neurosci **23**(5): 1750-1758.

Maxwell, D. S. and Kruger, L. (1965). "The fine structure of astrocytes in the cerebral cortex and their response to focal injury produced by heavy ionizing particles." The Journal of Cell Biology **25**(2): 141-157.

Maxwell, K., Berliner, J. A. and Cancilla, P. A. (1989). "Stimulation of glucose analogue uptake by cerebral microvessel endothelial cells by a product released by astrocytes." J Neuropathol Exp Neurol **48**(1): 69-80.

Mayer, J. (1953). "Glucostatic Mechanism of Regulation of Food Intake." New England Journal of Medicine **249**(1): 13-16.

Mayes, P. A. and Bender, D. A. (2003). "Metabolism of glycogen." Harper's Illustrated Biochemistry: 145.

Mazzola, J. L. and Sirover, M. A. (2001). "Reduction of glyceraldehyde-3-phosphate dehydrogenase activity in Alzheimer's disease and in Huntington's disease fibroblasts." J Neurochem **76**(2): 442-449.

McCall, A. L., Fixman, L. B., Fleming, N., Tornheim, K., Chick, W. and Ruderman, N. B. (1986). "Chronic hypoglycemia increases brain glucose transport." American Journal of Physiology-Endocrinology and Metabolism **251**(4): E442-E447.

McCarthy, K. and Salm, A. (1991). "Pharmacologically-distinct subsets of astroglia can be identified by their calcium response to neuroligands." Neuroscience **41**(2-3): 325-333.
McCarthy, K. D. and de Vellis, J. (1980). "Preparation of separate astroglial and oligodendroglial cell cultures from rat cerebral tissue." J Cell Biol **85**(3): 890-902.
McCarthy, P. L., Shaw, J. E. and Remold, H. G. (1979). "The role of microtubules in the response of macrophages to MIF." Cell Immunol **46**(2): 409-415.
McCorry, L. K. (2007). "Physiology of the Autonomic Nervous System." American Journal of Pharmaceutical Education **71**(4): 78.
McCrimmon, R. (2008). "The mechanisms that underlie glucose sensing during hypoglycaemia in diabetes." Diabet Med **25**(5): 513-522.
McCrimmon, R. J., Evans, M. L., Fan, X., McNay, E. C., Chan, O., Ding, Y., Zhu, W., Gram, D. X. and Sherwin, R. S. (2005). "Activation of ATP-sensitive K+ channels in the ventromedial hypothalamus amplifies counterregulatory hormone responses to hypoglycemia in normal and recurrently hypoglycemic rats." Diabetes **54**(11): 3169-3174.
McCrimmon, R. J., Fan, X., Cheng, H., McNay, E., Chan, O., Shaw, M., Ding, Y., Zhu, W. and Sherwin, R. S. (2006a). "Activation of AMP-activated protein kinase within the ventromedial hypothalamus amplifies counterregulatory hormone responses in rats with defective counterregulation." Diabetes **55**(6): 1755-1760.
McCrimmon, R. J., Fan, X., Ding, Y., Zhu, W., Jacob, R. J. and Sherwin, R. S. (2004). "Potential Role for AMP-Activated Protein Kinase in Hypoglycemia Sensing in the Ventromedial Hypothalamus." Diabetes **53**(8): 1953-1958.
McCrimmon, R. J., Ryan, C. M. and Frier, B. M. (2012). "Diabetes and cognitive dysfunction." The Lancet **379**(9833): 2291-2299.
McCrimmon, R. J., Shaw, M., Fan, X., Cheng, H., Ding, Y., Vella, M. C., Zhou, L., McNay, E. C. and Sherwin, R. S. (2008). "Key role for AMP-activated protein kinase in the ventromedial hypothalamus in regulating counterregulatory hormone responses to acute hypoglycemia." Diabetes **57**(2): 444-450.
Mccrimmon, R. J., Shaw, M., Fan, X., Cheng, H., Ding, Y., Wang, A. and Sherwin, R. S. (2006b). "AMP-activated protein kinase (AMPK): a key mediator of hypoglycemia-sensing in the ventromedial hypothalamus (VMH)." Diabetes **55**: A15.
McCulloch, L. J., van de Bunt, M., Braun, M., Frayn, K. N., Clark, A. and Gloyn, A. L. (2011). "GLUT2 (SLC2A2) is not the principal glucose transporter in human

pancreatic beta cells: Implications for understanding genetic association signals at this locus." Molecular Genetics and Metabolism **104**(4): 648-653.

McDougal, D., Hermann, G. and Rogers, R. (2013a). "Astrocytes in the nucleus of the solitary tract are activated by low glucose or glucoprivation: evidence for glial involvement in glucose homeostasis." Frontiers in Neuroscience **7**(249).

McDougal, D. H., Rogers, R. C. and Hermann, G. E. (2011). "Astrocytes in rat nucleus of the solitary tract are activated by low glucose or glucoprivic challenges." Autonomic Neuroscience **163**(1): 76.

McDougal, D. H., Viard, E., Hermann, G. E. and Rogers, R. C. (2013b). "Astrocytes in the hindbrain detect glucoprivation and regulate gastric motility." Autonomic Neuroscience **175**(1-2): 61-69.

McElnea, E. M., Quill, B., Docherty, N. G., Irnaten, M., Siah, W. F., Clark, A. F., O'Brien, C. J. and Wallace, D. M. (2011). "Oxidative stress, mitochondrial dysfunction and calcium overload in human lamina cribrosa cells from glaucoma donors." Molecular Vision **17**: 1182-1191.

McEwan, P., Larsen Thorsted, B., Wolden, M., Jacobsen, J. and Evans, M. (2015). "Healthcare resource implications of hypoglycemia-related hospital admissions and inpatient hypoglycemia: retrospective record-linked cohort studies in England." BMJ Open Diabetes Research & Care **3**(1).

McGeer, P. L., Kamo, H., Harrop, R., Li, D. K., Tuokko, H., McGeer, E. G., Adam, M. J., Ammann, W., Beattie, B. L. and Calne, D. B. (1986). "Positron emission tomography in patients with clinically diagnosed Alzheimer's disease." CMAJ: Canadian Medical Association Journal **134**(6): 597-607.

McGowan, J. E., Chen, L., Gao, D., Trush, M. and Wei, C. (2006). "Increased mitochondrial reactive oxygen species production in newborn brain during hypoglycemia." Neuroscience Letters **399**(1–2): 111-114.

McKenna, M. C. (2007). "The glutamate-glutamine cycle is not stoichiometric: fates of glutamate in brain." J Neurosci Res **85**(15): 3347-3358.

McNeilly, A. D., Gallagher, J. R., Dinkova-Kostova, A. T., Hayes, J. D., Sharkey, J., Ashford, M. L. J. and McCrimmon, R. J. (2016). "Nrf2-mediated neuroprotection against recurrent hypoglycemia is insufficient to prevent cognitive impairment in a rodent model of type 1 diabetes." Diabetes.

Mehers, K. L. and Gillespie, K. M. (2008). "The genetic basis for type 1 diabetes." Br Med Bull **88**(1): 115-129.

Meier, J. J., Gallwitz, B., Siepmann, N., Holst, J. J., Deacon, C. F., Schmidt, W. E. and Nauck, M. A. (2003). "Gastric inhibitory polypeptide (GIP) dose-dependently stimulates glucagon secretion in healthy human subjects at euglycaemia." Diabetologia **46**(6): 798-801.

Meier, J. J. and Nauck, M. A. (2005). "Glucagon-like peptide 1(GLP-1) in biology and pathology." Diabetes/Metabolism Research and Reviews **21**(2): 91-117.

Meldrum, B. S. (2000). "Glutamate as a neurotransmitter in the brain: review of physiology and pathology." J Nutr **130**(4S Suppl): 1007s-1015s.

Merrill, G., Kurth, E., Hardie, D. and Winder, W. (1997). "AICA riboside increases AMP-activated protein kinase, fatty acid oxidation, and glucose uptake in rat muscle." American Journal of Physiology-Endocrinology And Metabolism **273**(6): E1107-E1112.

Metcalfe, K. A., Hitman, G. A., Rowe, R. E., Hawa, M., Huang, X., Stewart, T. and Leslie, R. D. (2001). "Concordance for type 1 diabetes in identical twins is affected by insulin genotype." Diabetes Care **24**(5): 838-842.

Metz, S. A., Halter, J. B. and Robertson, R. P. (1978). "Induction of defective insulin secretion and impaired glucose tolerance by clonidine. Selective stimulation of metabolic alpha-adrenergic pathways." Diabetes **27**(5): 554-562.

Miller, E. J., Li, J., Leng, L., McDonald, C., Atsumi, T., Bucala, R. and Young, L. H. (2008). "Macrophage migration inhibitory factor stimulates AMP-activated protein kinase in the ischaemic heart." Nature **451**(7178): 578-582.

Millhouse, O. E. (1973). "The organization of the ventromedial hypothalamic nucleus." Brain Res **55**(1): 71-87.

Milner, T. A., Lee, A., Aicher, S. A. and Rosin, D. L. (1998). "Hippocampal α2A-adrenergic receptors are located predominantly presynaptically but are also found postsynaptically and in selective astrocytes." Journal of Comparative Neurology **395**(3): 310-327.

Min, K.-J., Yang, M.-s., Kim, S.-U., Jou, I. and Joe, E.-h. (2006). "Astrocytes Induce Hemeoxygenase-1 Expression in Microglia: A Feasible Mechanism for Preventing Excessive Brain Inflammation." The Journal of Neuroscience **26**(6): 1880-1887.

Minokoshi, Y., Kim, Y.-B., Peroni, O. D., Fryer, L. G., Müller, C., Carling, D. and Kahn, B. B. (2002). "Leptin stimulates fatty-acid oxidation by activating AMP-activated protein kinase." Nature **415**(6869): 339.

Minor, T. R., Rowe, M. K., Soames Job, R. F. and Ferguson, E. C. (2001). "Escape deficits induced by inescapable shock and metabolic stress are reversed by adenosine receptor antagonists." Behav Brain Res **120**(2): 203-212.

Minty, A., Chalon, P., Derocq, J. M., Dumont, X., Guillemot, J. C., Kaghad, M., Labit, C., Leplatois, P., Liauzun, P., Miloux, B., Minty, C., Casellas, P., Loison, G., Lupker, J., Shire, D., Ferrara, P. and Caput, D. (1993). "Interleukin-13 is a new human lymphokine regulating inflammatory and immune responses." Nature **362**: 248.

Miya, K., Inoue, R., Takata, Y., Abe, M., Natsume, R., Sakimura, K., Hongou, K., Miyawaki, T. and Mori, H. (2008). "Serine racemase is predominantly localized in neurons in mouse brain." Journal of Comparative Neurology **510**(6): 641-654.

Mizuno, Y. and Oomura, Y. (1984). "Glucose responding neurons in the nucleus tractus solitarius of the rat: in vitro study." Brain Res **307**(1-2): 109-116.

Moghetti, P., Castello, R., Negri, C., Tosi, F., Perrone, F., Caputo, M., Zanolin, E. and Muggeo, M. (2000). "Metformin Effects on Clinical Features, Endocrine and Metabolic Profiles, and Insulin Sensitivity in Polycystic Ovary Syndrome: A Randomized, Double-Blind, Placebo-Controlled 6-Month Trial, followed by Open, Long-Term Clinical Evaluation1." The Journal of Clinical Endocrinology & Metabolism **85**(1): 139-146.

Montana, V., Malarkey, E. B., Verderio, C., Matteoli, M. and Parpura, V. (2006). "Vesicular transmitter release from astrocytes." Glia **54**(7): 700-715.

Mookerjee, S. A. and Brand, M. D. (2015). "Measurement and Analysis of Extracellular Acid Production to Determine Glycolytic Rate." Journal of Visualized Experiments : JoVE(106): 53464.

Morilak, D. A., Fornal, C. A. and Jacobs, B. L. (1987). "Effects of physiological manipulations on locus coeruleus neuronal activity in freely moving cats. III. Glucoregulatory challenge." Brain Res **422**(1): 32-39.

Moriyama, R., Tsukamura, H., Kinoshita, M., Okazaki, H., Kato, Y. and Maeda, K. (2004). "In vitro increase in intracellular calcium concentrations induced by low or high extracellular glucose levels in ependymocytes and serotonergic neurons of the rat lower brainstem." Endocrinology **145**(5): 2507-2515.

Morth, J. P., Pedersen, B. P., Toustrup-Jensen, M. S., Sørensen, T. L. M., Petersen, J., Andersen, J. P., Vilsen, B. and Nissen, P. (2007). "Crystal structure of the sodium–potassium pump." Nature **450**: 1043.

Morton, G. J., Cummings, D. E., Baskin, D. G., Barsh, G. S. and Schwartz, M. W. (2006). "Central nervous system control of food intake and body weight." Nature **443**: 289.

Motawei, K., Pyner, S., Ranson, R. N., Kamel, M. and Coote, J. H. (1999). "Terminals of paraventricular spinal neurones are closely associated with adrenal medullary sympathetic preganglionic neurones: immunocytochemical evidence for vasopressin as a possible neurotransmitter in this pathway." Exp Brain Res **126**(1): 68-76.

Mothet, J.-P., Pollegioni, L., Ouanounou, G., Martineau, M., Fossier, P. and Baux, G. (2005). "Glutamate receptor activation triggers a calcium-dependent and SNARE protein-dependent release of the gliotransmitter D-serine." Proceedings of the National Academy of Sciences of the United States of America **102**(15): 5606-5611.

Mountjoy, P. D., Bailey, S. J. and Rutter, G. A. (2007). "Inhibition by glucose or leptin of hypothalamic neurons expressing neuropeptide Y requires changes in AMP-activated protein kinase activity." Diabetologia **50**(1): 168-177.

Muhič, M., Vardjan, N., Chowdhury, H. H., Zorec, R. and Kreft, M. (2015). "Insulin and Insulin-like Growth Factor 1 (IGF-1) Modulate Cytoplasmic Glucose and Glycogen Levels but Not Glucose Transport across the Membrane in Astrocytes." The Journal of Biological Chemistry **290**(17): 11167-11176.

Muller, E. E., Cocchi, D. and Mantegazza, P. (1972). "Brain adrenergic system in the feeding response induced by 2-deoxy-D-glucose." American Journal of Physiology-Legacy Content **223**(4): 945-950.

Munck, A. (1971). "Glucocorticoid inhibition of glucose uptake by peripheral tissues: old and new evidence, molecular mechanisms, and physiological significance." Perspectives in Biology and Medicine **14**(2): 265-289.

Murakami, K., Nakamura, Y. and Yoneda, Y. (2003). "Potentiation by ATP of lipopolysaccharide-stimulated nitric oxide production in cultured astrocytes." Neuroscience **117**(1): 37-42.

Murphy, B. A., Fakira, K. A., Song, Z., Beuve, A. and Routh, V. H. (2009). "AMP-activated protein kinase and nitric oxide regulate the glucose sensitivity of ventromedial hypothalamic glucose-inhibited neurons." American Journal of Physiology - Cell Physiology **297**(3): C750-C758.

Murphy, Michael P. (2009). "How mitochondria produce reactive oxygen species." Biochemical Journal **417**(Pt 1): 1-13.

Nagayach, A., Patro, N. and Patro, I. (2014). "Astrocytic and microglial response in experimentally induced diabetic rat brain." Metabolic Brain Disease **29**(3): 747-761.

Naitoh, Y., Fukata, J., Tominaga, T., Nakai, Y., Tamai, S., Mori, K. and Imura, H. (1988). "Interleukin-6 stimulates the secretion of adrenocorticotropic hormone in conscious, freely-moving rats." Biochemical and biophysical research communications **155**(3): 1459-1463.

Nakadate, T., Muraki, T. and Kato, R. (1980). "Effects of alpha- and beta-adrenergic blockers on chlorpromazine-induced elevation of plasma glucose and cyclic AMP in fed mice." Jpn J Pharmacol **30**(2): 199-206.

Nakae, J. and Accili, D. (1999). "The mechanism of insulin action." Journal of pediatric endocrinology & metabolism: JPEM **12**: 721.

Nakaki, T., Nakadate, T. and Kato, R. (1980). "α 2-Adrenoceptors modulating insulin release from isolated pancreatic islets." Naunyn-Schmiedeberg's archives of pharmacology **313**(2): 151-153.

Narcisse, L., Scemes, E., Zhao, Y., Lee, S. C. and Brosnan, C. F. (2005). "The cytokine IL-1β transiently enhances P2X7 receptor expression and function in human astrocytes." Glia **49**(2): 245-258.

Nath, R., Probert, A., McGinnis, K. M. and Wang, K. K. W. (2002). "Evidence for Activation of Caspase-3-Like Protease in Excitotoxin- and Hypoxia/Hypoglycemia-Injured Neurons." Journal of Neurochemistry **71**(1): 186-195.

Newman, L. A., Korol, D. L. and Gold, P. E. (2011). "Lactate Produced by Glycogenolysis in Astrocytes Regulates Memory Processing." PLOS ONE **6**(12): e28427.

Newsholme, P., Brennan, L. and Bender, K. (2006). "Amino Acid Metabolism, β-Cell Function, and Diabetes." Diabetes **55**(Supplement 2): S39-S47.

Newsholme, P., Cruzat, V., Arfuso, F. and Keane, K. (2014). "Nutrient regulation of insulin secretion and action." **221**(3): R105.

Nichols, D. E. and Nichols, C. D. (2008). "Serotonin Receptors." Chemical Reviews **108**(5): 1614-1641.

Niijima, A. (1989). "Nervous regulation of metabolism." Prog Neurobiol **33**(2): 135-147.

Noble, M., Fok-Seang, J. and Cohen, J. (1984a). "Glia are a unique substrate for the in vitro growth of central nervous system neurons." J Neurosci **4**(7): 1892-1903.

Noble, M. and Murray, K. (1984b). "Purified astrocytes promote the in vitro division of a bipotential glial progenitor cell." Embo j **3**(10): 2243-2247.

Nomura, S., Watanabe, M., Ukei, N. and Nakazawa, T. (1981). "Stress and β-adrenergic receptor binding in the rat's brain." Brain Research **224**(1): 199-203.

Nordlie, R. C., Foster, J. D. and Lange, A. J. (1999). "Regulation of glucose production by the liver." Annual review of nutrition **19**(1): 379-406.

Norenberg, M. D. and Martinez-Hernandez, A. (1979). "Fine structural localization of glutamine synthetase in astrocytes of rat brain." Brain Research **161**(2): 303-310.

O'Neill, L. A. J., Kishton, R. J. and Rathmell, J. (2016). "A guide to immunometabolism for immunologists." Nature Reviews Immunology **16**: 553.

Obici, S., Feng, Z., Morgan, K., Stein, D., Karkanias, G. and Rossetti, L. (2002a). "Central administration of oleic acid inhibits glucose production and food intake." Diabetes **51**(2): 271-275.

Obici, S., Zhang, B. B., Karkanias, G. and Rossetti, L. (2002b). "Hypothalamic insulin signaling is required for inhibition of glucose production." Nature Medicine **8**: 1376.

Oe, Y., Baba, O., Ashida, H., Nakamura Kouichi, C. and Hirase, H. (2016). "Glycogen distribution in the microwave-fixed mouse brain reveals heterogeneous astrocytic patterns." Glia **64**(9): 1532-1545.

Ogurtsova, K., da Rocha Fernandes, J. D., Huang, Y., Linnenkamp, U., Guariguata, L., Cho, N. H., Cavan, D., Shaw, J. E. and Makaroff, L. E. (2017). "IDF Diabetes Atlas: Global estimates for the prevalence of diabetes for 2015 and 2040." Diabetes Research and Clinical Practice **128**: 40-50.

Okar, D. A. and Lange, A. J. (1999). "Fructose-2, 6-bisphosphate and control of carbohydrate metabolism in eukaryotes." Biofactors **10**(1): 1-14.

Oliet, S. H., Piet, R. and Poulain, D. A. (2001). "Control of glutamate clearance and synaptic efficacy by glial coverage of neurons." Science **292**(5518): 923-926.

Oomura, Y., Kimura, K., Ooyama, H., Maeno, T., Iki, M. and Kuniyoshi, M. (1964). "Reciprocal Activities of the Ventromedial and Lateral Hypothalamic Areas of Cats." Science **143**(3605): 484-485.

Oomura, Y., Ono, T., Ooyama, H. and Wayner, M. (1969). "Glucose and osmosensitive neurones of the rat hypothalamus." Nature **222**(5190): 282-284.

Orci, L., Amherdt, M., Malaisse-Lagae, F., Rouiller, C. and Renold, A. E. (1973). "Insulin Release by Emiocytosis: Demonstration with Freeze-Etching Technique." Science **179**(4068): 82-84.

Ouyang, Y.-B., He, Q.-P., Li, P.-A., Janelidze, S., Wang, G.-X. and Siesjö, B. K. (2000). "Is Neuronal Injury Caused by Hypoglycemic Coma of the Necrotic or Apoptotic Type?" Neurochemical Research **25**(5): 661-667.

Oz, G., Kumar, A., Rao, J. P., Kodl, C. T., Chow, L., Eberly, L. E. and Seaquist, E. R. (2009). "Human brain glycogen metabolism during and after hypoglycemia." Diabetes **58**(9): 1978-1985.

Öz, G., Tesfaye, N., Kumar, A., Deelchand, D. K., Eberly, L. E. and Seaquist, E. R. (2012). "Brain glycogen content and metabolism in subjects with type 1 diabetes and hypoglycemia unawareness." Journal of Cerebral Blood Flow & Metabolism **32**(2): 256-263.

Ozcan, U., Cao, Q., Yilmaz, E., Lee, A. H., Iwakoshi, N. N., Ozdelen, E., Tuncman, G., Gorgun, C., Glimcher, L. H. and Hotamisligil, G. S. (2004). "Endoplasmic reticulum stress links obesity, insulin action, and type 2 diabetes." Science **306**(5695): 457-461.

Paco, S., Hummel, M., Plá, V., Sumoy, L. and Aguado, F. (2016). "Cyclic AMP signaling restricts activation and promotes maturation and antioxidant defenses in astrocytes." BMC genomics **17**: 304-304.

Panday, A., Sahoo, M. K., Osorio, D. and Batra, S. (2014). "NADPH oxidases: an overview from structure to innate immunity-associated pathologies." Cellular And Molecular Immunology **12**: 5.

Panenka, W., Jijon, H., Herx, L. M., Armstrong, J. N., Feighan, D., Wei, T., Yong, V. W., Ransohoff, R. M. and MacVicar, B. A. (2001). "P2X7-like receptor activation in astrocytes increases chemokine monocyte chemoattractant protein-1 expression via mitogen-activated protein kinase." Journal of Neuroscience **21**(18): 7135-7142.

Papouin, T., Dunphy, J., Tolman, M., Foley, J. C. and Haydon, P. G. (2017). "Astrocytic control of synaptic function." Philosophical Transactions of the Royal Society B: Biological Sciences **372**(1715): 20160154.

Parekh, B. (2009). "Mechanisms of the blunting of the sympatho-adrenal response: a theory." Current diabetes reviews **5**(2): 79-91.

Park, E. J., Lee, J. H., Yu, G.-Y., He, G., Ali, S. R., Holzer, R. G., Österreicher, C. H., Takahashi, H. and Karin, M. (2010). "Dietary and genetic obesity promote liver inflammation and tumorigenesis by enhancing IL-6 and TNF expression." Cell **140**(2): 197-208.

Park, S. W. and Ozcan, U. (2013). "Potential for therapeutic manipulation of the UPR in disease." Seminars in Immunopathology **35**(3): 351-373.

Parpura, V., Basarsky, T. A., Liu, F., Jeftinija, K., Jeftinija, S. and Haydon, P. G. (1994). "Glutamate-mediated astrocyte–neuron signalling." Nature **369**(6483): 744.

Parpura, V. and Haydon, P. G. (2000). "Physiological astrocytic calcium levels stimulate glutamate release to modulate adjacent neurons." Proceedings of the National Academy of Sciences **97**(15): 8629-8634.

Parpura, V., Liu, F., Brethorst, S., Jeftinija, K., Jeftinija, S. and Haydon, P. G. (1995). "α-Latrotoxin stimulates glutamate release from cortical astrocytes in cell culture." FEBS letters **360**(3): 266-270.

Parton, L. E., Ye, C. P., Coppari, R., Enriori, P. J., Choi, B., Zhang, C.-Y., Xu, C., Vianna, C. R., Balthasar, N., Lee, C. E., Elmquist, J. K., Cowley, M. A. and Lowell, B. B. (2007). "Glucose sensing by POMC neurons regulates glucose homeostasis and is impaired in obesity." Nature **449**: 228.

Passaquin, A. C., Schreier, W. A. and de Vellis, J. (1994). "Gene expression in astrocytes is affected by subculture." Int J Dev Neurosci **12**(4): 363-372.

Paul, P. and de Belleroche, J. (2014). "The role of D-serine and glycine as co-agonists of NMDA receptors in motor neuron degeneration and amyotrophic lateral sclerosis (ALS)." Frontiers in Synaptic Neuroscience **6**: 10.

Pearce, B., Albrecht, J., Morrow, C. and Murphy, S. (1986). "Astrocyte glutamate receptor activation promotes inositol phospholipid turnover and calcium flux." Neuroscience letters **72**(3): 335-340.

Pekny, M. and Nilsson, M. (2005). "Astrocyte activation and reactive gliosis." Glia **50**(4): 427-434.

Pekny, M. and Pekna, M. (2016). "Reactive gliosis in the pathogenesis of CNS diseases." Biochimica et Biophysica Acta (BBA) - Molecular Basis of Disease **1862**(3): 483-491.

Pellerin, L. (2003). "Lactate as a pivotal element in neuron–glia metabolic cooperation." Neurochemistry International **43**(4–5): 331-338.

Pellerin, L. and Magistretti, P. J. (1994). "Glutamate uptake into astrocytes stimulates aerobic glycolysis: a mechanism coupling neuronal activity to glucose utilization." Proc Natl Acad Sci U S A **91**(22): 10625-10629.

Pellerin, L. and Magistretti, P. J. (2012). "Sweet sixteen for ANLS." J Cereb Blood Flow Metab **32**(7): 1152-1166.

Pellerin, L., Pellegri, G., Bittar, P. G., Charnay, Y., Bouras, C., Martin, J. L., Stella, N. and Magistretti, P. J. (1998). "Evidence Supporting the Existence of an Activity-Dependent Astrocyte-Neuron Lactate Shuttle." Developmental Neuroscience **20**(4-5): 291-299.

Peng, L., Zhang, X. and Hertz, L. (1994). "High extracellular potassium concentrations stimulate oxidative metabolism in a glutamatergic neuronal culture and glycolysis in cultured astrocytes but have no stimulatory effect in a GABAergic neuronal culture." Brain Res **663**(1): 168-172.

Peng Tsung, I. and Jou, M.-J. (2010). "Oxidative stress caused by mitochondrial calcium overload." Annals of the New York Academy of Sciences **1201**(1): 183-188.

Peppard, R. F., Martin, W. R., Clark, C. M., Carr, G. D., McGeer, P. L. and Calne, D. B. (1990). "Cortical glucose metabolism in Parkinson's and Alzheimer's disease." J Neurosci Res **27**(4): 561-568.

Perea, G. and Araque, A. (2007). "Astrocytes potentiate transmitter release at single hippocampal synapses." Science **317**(5841): 1083-1086.

Perrin, C., Knauf, C. and Burcelin, R. m. (2004). "Intracerebroventricular Infusion of Glucose, Insulin, and the Adenosine Monophosphate-Activated Kinase Activator, 5-Aminoimidazole-4-Carboxamide-1-β-d-Ribofuranoside, Controls Muscle Glycogen Synthesis." Endocrinology **145**(9): 4025-4033.

Pertsch, M., Duncan, G. E., Stumpf, W. E. and Pilgrim, C. (1988). "A histochemical study of the regional distribution in the rat brain of enzymatic activity hydrolyzing glucose- and 2-deoxyglucose-6-phosphate." Histochemistry **88**(3-6): 257-262.

Petrovsky, N., Socha, L., Silva, D., Grossman, A. B., Metz, C. and Bucala, R. (2003). "Macrophage migration inhibitory factor exhibits a pronounced circadian rhythm relevant to its role as a glucocorticoid counter-regulator." Immunol Cell Biol **81**(2): 137-143.

Pick, E., Honig, S. and Griffel, B. (1979). "The mechanism of action of soluble lymphocyte mediators. VI. Effect of migration inhibitory factor (MIF) on macrophage microtubules." Int Arch Allergy Appl Immunol **58**(2): 149-159.

Pihoker, C., Gilliam, L. K., Hampe, C. S. and Lernmark, Å. (2005). "Autoantibodies in diabetes." Diabetes **54**(suppl 2): S52-S61.

Pilkis, S. and Claus, T. (1991). "Hepatic gluconeogenesis/glycolysis: regulation and structure/function relationships of substrate cycle enzymes." Annual review of nutrition **11**(1): 465-515.

Platania, C. B. M., Giurdanella, G., Di Paola, L., Leggio, G. M., Drago, F., Salomone, S. and Bucolo, C. (2017). "P2X7 receptor antagonism: Implications in diabetic retinopathy." Biochemical Pharmacology **138**: 130-139.

Plum, L., Ma, X., Hampel, B., Balthasar, N., Coppari, R., Munzberg, H., Shanabrough, M., Burdakov, D., Rother, E., Janoschek, R., Alber, J., Belgardt, B. F., Koch, L., Seibler, J., Schwenk, F., Fekete, C., Suzuki, A., Mak, T. W., Krone, W., Horvath, T. L., Ashcroft, F. M. and Bruning, J. C. (2006). "Enhanced PIP3 signaling in POMC neurons causes KATP channel activation and leads to diet-sensitive obesity." J Clin Invest **116**(7): 1886-1901.

Poplawski, M. M., Mastaitis, J. W. and Mobbs, C. V. (2011). "Naloxone, but Not Valsartan, Preserves Responses to Hypoglycemia After Antecedent Hypoglycemia: Role of Metabolic Reprogramming in Counterregulatory Failure." Diabetes **60**(1): 39-46.

Poplawski, M. M., Mastaitis, J. W., Yang, X.-J. and Mobbs, C. V. (2010). "Hypothalamic responses to fasting indicate metabolic reprogramming away from glycolysis toward lipid oxidation." Endocrinology **151**(11): 5206-5217.

Popp, J., Bacher, M., Kolsch, H., Noelker, C., Deuster, O., Dodel, R. and Jessen, F. (2009). "Macrophage migration inhibitory factor in mild cognitive impairment and Alzheimer's disease." J Psychiatr Res **43**(8): 749-753.

Potapenko, E. S., Biancardi, V. C., Zhou, Y. and Stern, J. E. (2012). "Altered astrocyte glutamate transporter regulation of hypothalamic neurosecretory neurons in heart failure rats." Am J Physiol Regul Integr Comp Physiol **303**(3): R291-300.

Potter van Loon, B. J., Kluft, C., Radder, J. K., Blankenstein, M. A. and Meinders, A. E. (1993). "The cardiovascular risk factor plasminogen activator inhibitor type 1 is related to insulin resistance." Metabolism - Clinical and Experimental **42**(8): 945-949.

Pradhan, G., Samson, S. L. and Sun, Y. (2013). "Ghrelin: much more than a hunger hormone." Current opinion in clinical nutrition and metabolic care **16**(6): 619-624.

Preau, S., Montaigne, D., Modine, T., Fayad, G., Koussa, M., Tardivel, M., Durocher, A., Saulnier, F., Marechal, X. and Neviere, R. (2013). "Macrophage migration inhibitory factor induces contractile and mitochondria dysfunction by altering cytoskeleton network in the human heart." Crit Care Med **41**(7): e125-133.

Prentki, M., Matschinsky, Franz M. and Madiraju, S. R. M. (2013). "Metabolic Signaling in Fuel-Induced Insulin Secretion." Cell Metabolism **18**(2): 162-185.

Pribiag, H. and Stellwagen, D. (2013). "TNF-α Downregulates Inhibitory Neurotransmission through Protein Phosphatase 1-Dependent Trafficking of GABA_A Receptors." The Journal of Neuroscience **33**(40): 15879-15893.

Prodi, E. and Obici, S. (2006). "Minireview: The Brain as a Molecular Target for Diabetic Therapy." Endocrinology **147**(6): 2664-2669.

Pyo, H., Yang, M.-S., Jou, I. and Joe, E.-h. (2003). "Wortmannin enhances lipopolysaccharide-induced inducible nitric oxide synthase expression in microglia in the presence of astrocytes in rats." Neuroscience Letters **346**(3): 141-144.

Qiu, J., Zhang, C., Borgquist, A., Nestor, C. C., Smith, A. W., Bosch, M. A., Ku, S., Wagner, E. J., Ronnekleiv, O. K. and Kelly, M. J. (2014). "Insulin excites anorexigenic proopiomelanocortin neurons via activation of canonical transient receptor potential channels." Cell Metab **19**(4): 682-693.

Ramos, B. P. and Arnsten, A. F. T. (2007). "Adrenergic Pharmacology and Cognition: Focus on the Prefrontal Cortex." Pharmacology & therapeutics **113**(3): 523-536.

Ratter, J. M., Rooijackers, H. M. M., Tack, C. J., Hijmans, A. G. M., Netea, M. G., de Galan, B. E. and Stienstra, R. (2017). "Pro-inflammatory Effects of Hypoglycemia in Humans with or without Diabetes." Diabetes.

Régina, A., Morchoisne, S., Borson, N. D., McCall, A. L., Drewes, L. R. and Roux, F. (2001). "Factor(s) released by glucose-deprived astrocytes enhance glucose transporter expression and activity in rat brain endothelial cells." Biochimica et Biophysica Acta (BBA) - Molecular Cell Research **1540**(3): 233-242.

Reichard, P., Berglund, B., Britz, A., Cars, I., Nilsson, B. Y. and Rosenqvist, U. (1991). "Intensified conventional insulin treatment retards the microvascular complications of insulin-dependent diabetes mellitus (IDDM): the Stockholm Diabetes Intervention Study (SDIS) after 5 years." Journal of Internal Medicine **230**(2): 101-108.

Renkawek, K., Stege, G. J. and Bosman, G. J. (1999). "Dementia, gliosis and expression of the small heat shock proteins hsp27 and alpha B-crystallin in Parkinson's disease." Neuroreport **10**(11): 2273-2276.

Revsin, Y., Saravia, F., Roig, P., Lima, A., de Kloet, E. R., Homo-Delarche, F. and De Nicola, A. F. (2005). "Neuronal and astroglial alterations in the hippocampus of a mouse model for type 1 diabetes." Brain Research **1038**(1): 22-31.

Richardson, S. J., Willcox, A., Bone, A., Foulis, A. K. and Morgan, N. G. (2009). "The prevalence of enteroviral capsid protein vp1 immunostaining in pancreatic islets in human type 1 diabetes." Diabetologia **52**(6): 1143-1151.

Riedemann, N. C., Guo, R. F. and Ward, P. A. (2003). "Novel strategies for the treatment of sepsis." Nat Med **9**(5): 517-524.

Ritter, S., Li, A.-J., Wang, Q. and Dinh, T. T. (2011). "Minireview: The Value of Looking Backward: The Essential Role of the Hindbrain in Counterregulatory Responses to Glucose Deficit." Endocrinology **152**(11): 4019-4032.

Ritter, S., Watts, A. G., Dinh, T. T., Sanchez-Watts, G. and Pedrow, C. (2003). "Immunotoxin lesion of hypothalamically projecting norepinephrine and epinephrine neurons differentially affects circadian and stressor-stimulated corticosterone secretion." Endocrinology **144**(4): 1357-1367.

Roach, P. J. (1990). "Control of glycogen synthase by hierarchal protein phosphorylation." The FASEB Journal **4**(12): 2961-2968.

Roberts, J. A., Vial, C., Digby, H. R., Agboh, K. C., Wen, H., Atterbury-Thomas, A. and Evans, R. J. (2006). "Molecular properties of P2X receptors." Pflügers Archiv **452**(5): 486-500.

Robinson, R. T., Harris, N. D., Ireland, R. H., Macdonald, I. A. and Heller, S. R. (2004). "Changes in cardiac repolarization during clinical episodes of nocturnal hypoglycaemia in adults with Type 1 diabetes." Diabetologia **47**(2): 312-315.

Roden, M., Price, T. B., Perseghin, G., Petersen, K. F., Rothman, D. L., Cline, G. W. and Shulman, G. I. (1996). "Mechanism of free fatty acid-induced insulin resistance in humans." The Journal of Clinical Investigation **97**(12): 2859-2865.

Rodriguez, E. M., Blazquez, J. L. and Guerra, M. (2010). "The design of barriers in the hypothalamus allows the median eminence and the arcuate nucleus to enjoy private milieus: the former opens to the portal blood and the latter to the cerebrospinal fluid." Peptides **31**(4): 757-776.

Rogers, R. C., McDougal, D. H., Ritter, S., Qualls-Creekmore, E. and Hermann, G. E. (2018). "Response of catecholaminergic neurons in the mouse hindbrain to glucoprivic stimuli is astrocyte dependent." American Journal of Physiology-Regulatory, Integrative and Comparative Physiology **315**(1): R153-R164.

Rogers, R. C., Ritter, S. and Hermann, G. E. (2016). "Hindbrain cytoglucopenia-induced increases in systemic blood glucose levels by 2-deoxyglucose depend on

intact astrocytes and adenosine release." American Journal of Physiology-Regulatory, Integrative and Comparative Physiology **310**(11): R1102-R1108.

Rolfe, D. F. and Brown, G. C. (1997). "Cellular energy utilization and molecular origin of standard metabolic rate in mammals." Physiol Rev **77**(3): 731-758.

Romanyukha, A. A., Rudnev, S. G. and Sidorov, I. A. (2006). "Energy cost of infection burden: An approach to understanding the dynamics of host–pathogen interactions." Journal of theoretical biology **241**(1): 1-13.

Ron, D. and Walter, P. (2007). "Signal integration in the endoplasmic reticulum unfolded protein response." Nature reviews Molecular cell biology **8**(7): 519.

Ronnett, G. V., Ramamurthy, S., Kleman, A. M., Landree, L. E. and Aja, S. (2009). "AMPK in the Brain: Its Roles in Energy Balance and Neuroprotection." Journal of neurochemistry **109**(Suppl 1): 17-23.

Rose, C., Kresse, W. and Kettenmann, H. (2005). "Acute insult of ammonia leads to calcium-dependent glutamate release from cultured astrocytes, an effect of pH." Journal of biological chemistry **280**(22): 20937-20944.

Rose, C. R., Waxman, S. G. and Ransom, B. R. (1998). "Effects of Glucose Deprivation, Chemical Hypoxia, and Simulated Ischemia on Na+ Homeostasis in Rat Spinal Cord Astrocytes." The Journal of Neuroscience **18**(10): 3554-3562.

Rosen, E. D. and Spiegelman, B. M. (2006). "Adipocytes as regulators of energy balance and glucose homeostasis." Nature **444**(7121): 847.

Rossi, D., Brambilla, L., Valori, C. F., Crugnola, A., Giaccone, G., Capobianco, R., Mangieri, M., Kingston, A. E., Bloc, A. and Bezzi, P. (2005). "Defective tumor necrosis factor-α-dependent control of astrocyte glutamate release in a transgenic mouse model of Alzheimer disease." Journal of Biological Chemistry **280**(51): 42088-42096.

Roth, T. L., Nayak, D., Atanasijevic, T., Koretsky, A. P., Latour, L. L. and McGavern, D. B. (2013). "Transcranial amelioration of inflammation and cell death after brain injury." Nature **505**: 223.

Rothstein, J. D., Dykes-Hoberg, M., Pardo, C. A., Bristol, L. A., Jin, L., Kuncl, R. W., Kanai, Y., Hediger, M. A., Wang, Y., Schielke, J. P. and Welty, D. F. (1996). "Knockout of glutamate transporters reveals a major role for astroglial transport in excitotoxicity and clearance of glutamate." Neuron **16**(3): 675-686.

Routh, V. H. (2002). "Glucose-sensing neurons: are they physiologically relevant?" Physiol Behav **76**(3): 403-413.

Routh, V. H., Hao, L., Santiago, A. M., Sheng, Z. and Zhou, C. (2014). "Hypothalamic glucose sensing: making ends meet." Frontiers in Systems Neuroscience **8**: 236.

Rudy, C. C., Hunsberger, H. C., Weitzner, D. S. and Reed, M. N. (2015). "The role of the tripartite glutamatergic synapse in the pathophysiology of Alzheimer's disease." Aging Dis **6**(2): 131-148.

Saad, M. F., Khan, A., Sharma, A., Michael, R., Riad-Gabriel, M. G., Boyadjian, R., Jinagouda, S. D., Steil, G. M. and Kamdar, V. (1998). "Physiological insulinemia acutely modulates plasma leptin." Diabetes **47**(4): 544-549.

Saberi, M., Bohland, M. and Donovan, C. M. (2008). "The locus for hypoglycemic detection shifts with the rate of fall in glycemia: the role of portal-superior mesenteric vein glucose sensing." Diabetes **57**(5): 1380-1386.

Sacks, H., Waligora, K., Matthews, J. and Pimstone, B. (1977). "Inhibition by somatostatin of glucagon-induced glucose release from the isolated perfused rat liver." Endocrinology **101**(6): 1751-1759.

Saghizadeh, M., Ong, J. M., Garvey, W. T., Henry, R. R. and Kern, P. A. (1996). "The expression of TNF alpha by human muscle. Relationship to insulin resistance." J Clin Invest **97**(4): 1111-1116.

Sakamaki, J.-I., Fu, A., Reeks, C., Baird, S., Depatie, C., Al Azzabi, M., Bardeesy, N., Gingras, A.-C., Yee, S.-P. and Screaton, R. A. (2014). "Role of the SIK2–p35–PJA2 complex in pancreatic β-cell functional compensation." Nature Cell Biology **16**: 234.

Saks, V., Kuznetsov, A. V., Gonzalez-Granillo, M., Tepp, K., Timohhina, N., Karu-Varikmaa, M., Kaambre, T., Santos, P. D., Boucher, F. and Guzun, R. (2012). "Intracellular Energetic Units regulate metabolism in cardiac cells." Journal of Molecular and Cellular Cardiology **52**(2): 419-436.

Salm, A. K. and McCarthy, K. D. (1989). "Expression of beta-adrenergic receptors by astrocytes isolated from adult rat cortex." Glia **2**(5): 346-352.

Salm, A. K. and McCarthy, K. D. (1992). "The evidence for astrocytes as a target for central noradrenergic activity: Expression of adrenergic receptors." Brain Research Bulletin **29**(3): 265-275.

Sambuy, Y., De Angelis, I., Ranaldi, G., Scarino, M., Stammati, A. and Zucco, F. (2005). "The Caco-2 cell line as a model of the intestinal barrier: influence of cell and

culture-related factors on Caco-2 cell functional characteristics." Cell biology and toxicology **21**(1): 1-26.

Sanders, N. M. and Ritter, S. (2000). "Repeated 2-deoxy-D-glucose-induced glucoprivation attenuates Fos expression and glucoregulatory responses during subsequent glucoprivation." Diabetes **49**(11): 1865-1874.

Sanders, N. M., Wilkinson, C. W., Taborsky, G. J., Al-Noori, S., Daumen, W., Zavosh, A. and Figlewicz, D. P. (2008). "The selective serotonin reuptake inhibitor sertraline enhances counterregulatory responses to hypoglycemia." American journal of physiology. Endocrinology and metabolism **294**(5): E853-E860.

Saper, C. B. (2002). "The central autonomic nervous system: conscious visceral perception and autonomic pattern generation." Annu Rev Neurosci **25**: 433-469.

Saper, C. B., Loewy, A. D., Swanson, L. W. and Cowan, W. M. (1976). "Direct hypothalamo-autonomic connections." Brain Res **117**(2): 305-312.

Saudek, C. D., Duckworth, W. C., Giobbie-Hurder, A., Henderson, W. G., Henry, R. R., Kelley, D. E., Edelman, S. V., Zieve, F. J., Adler, R. A. and Anderson, J. W. (1996). "Implantable Insulin Pump vs Multiple-Dose Insulin for Non—Insulin-Dependent Diabetes Mellitus: A Randomized Clinical Trial." Jama **276**(16): 1322-1327.

Savtchouk, I. and Volterra, A. (2018). "Gliotransmission: Beyond Black-and-White." The Journal of Neuroscience **38**(1): 14-25.

Sawchenko, P. E. and Swanson, L. W. (1983). "The organization of forebrain afferents to the paraventricular and supraoptic nuclei of the rat." J Comp Neurol **218**(2): 121-144.

Sawka, A. M., Burgart, V. and Zimmerman, D. (2000). "Loss of hypoglycemia awareness in an adolescent with type 1 diabetes mellitus during treatment with fluoxetine hydrochloride." J Pediatr **136**(3): 394-396.

Sawka, A. M., Burgart, V. and Zimmerman, D. (2001). "Loss of awareness of hypoglycemia temporally associated with selective serotonin reuptake inhibitors." Diabetes Care **24**(10): 1845-1846.

Scemes, E. and Giaume, C. (2006). "Astrocyte calcium waves: what they are and what they do." Glia **54**(7): 716-725.

Schechter, R., Beju, D., Gaffney, T., Schaefer, F. and Whetsell, L. (1996). "Preproinsulin I and II mRNAs and insulin electron microscopic immunoreaction are present within the rat fetal nervous system." Brain Research **736**(1): 16-27.

Schipke, C. G., Heuser, I. and Peters, O. (2011). "Antidepressants act on glial cells: SSRIs and serotonin elicit astrocyte calcium signaling in the mouse prefrontal cortex." Journal of Psychiatric Research **45**(2): 242-248.

Schousboe, A. (2018). "Metabolic signaling in the brain and the role of astrocytes in control of glutamate and GABA neurotransmission." Neurosci Lett.

Schousboe, A., Bak, L. and Waagepetersen, H. (2013). "Astrocytic Control of Biosynthesis and Turnover of the Neurotransmitters Glutamate and GABA." Frontiers in Endocrinology **4**(102).

Schousboe, A. and Divac, I. (1979). "Differences in glutamate uptake in astrocytes cultured from different brain regions." Brain Research **177**(2): 407-409.

Schurr, A., Miller, J. J., Payne, R. S. and Rigor, B. M. (1999). "An increase in lactate output by brain tissue serves to meet the energy needs of glutamate-activated neurons." Journal of Neuroscience **19**(1): 34-39.

Schwartz, M. W., Figlewicz, D. P., Baskin, D. G., Woods, S. C. and Porte, J. D. (1992). "Insulin in the Brain: A Hormonal Regulator of Energy Balance*." Endocrine Reviews **13**(3): 387-414.

Schwartz, M. W. and Porte, D. (2005). "Diabetes, Obesity, and the Brain." Science **307**(5708): 375-379.

Schwartz, M. W., Woods, S. C., Porte, D., Jr., Seeley, R. J. and Baskin, D. G. (2000). "Central nervous system control of food intake." Nature **404**(6778): 661-671.

Secrest, A. M., Becker, D. J., Kelsey, S. F., Laporte, R. E. and Orchard, T. J. (2011). "Characterizing sudden death and dead-in-bed syndrome in Type 1 diabetes: analysis from two childhood-onset Type 1 diabetes registries." Diabet Med **28**(3): 293-300.

Segel, S. A., Paramore, D. S. and Cryer, P. E. (2002). "Hypoglycemia-Associated Autonomic Failure in Advanced Type 2 Diabetes." Diabetes **51**(3): 724-733.

Seppälä-Lindroos, A., Vehkavaara, S., Häkkinen, A.-M., Goto, T., Westerbacka, J., Sovijärvi, A., Halavaara, J. and Yki-Järvinen, H. (2002). "Fat accumulation in the liver is associated with defects in insulin suppression of glucose production and serum free fatty acids independent of obesity in normal men." The Journal of Clinical Endocrinology & Metabolism **87**(7): 3023-3028.

Sergeyev, V., Broberger, C., Gorbatyuk, O. and Hokfelt, T. (2000). "Effect of 2-mercaptoacetate and 2-deoxy-D-glucose administration on the expression of NPY,

AGRP, POMC, MCH and hypocretin/orexin in the rat hypothalamus." Neuroreport **11**(1): 117-121.

Sethi, J. K. and Hotamisligil, G. S. (1999). "The role of TNF alpha in adipocyte metabolism." Semin Cell Dev Biol **10**(1): 19-29.

Shaffer, A. L., Shapiro-Shelef, M., Iwakoshi, N. N., Lee, A. H., Qian, S. B., Zhao, H., Yu, X., Yang, L., Tan, B. K., Rosenwald, A., Hurt, E. M., Petroulakis, E., Sonenberg, N., Yewdell, J. W., Calame, K., Glimcher, L. H. and Staudt, L. M. (2004). "XBP1, downstream of Blimp-1, expands the secretory apparatus and other organelles, and increases protein synthesis in plasma cell differentiation." Immunity **21**(1): 81-93.

Shao, Y. and Sutin, J. (1992). "Expression of adrenergic receptors in individual astrocytes and motor neurons isolated from the adult rat brain." Glia **6**(2): 108-117.

Sherrington, C. (1906). The integrative action of the nervous system, CUP Archive.

Shi, J., Xiang, Y. and Simpkins, J. W. (1997). "Hypoglycemia enhances the expression of mRNA encoding β-amyloid precursor protein in rat primary cortical astroglial cells." Brain Research **772**(1–2): 247-251.

Shimizu, N., Oomura, Y., Novin, D., Grijalva, C. V. and Cooper, P. H. (1983). "Functional correlations between lateral hypothalamic glucose-sensitive neurons and hepatic portal glucose-sensitive units in rat." Brain Res **265**(1): 49-54.

Shintani, M., Ogawa, Y., Ebihara, K., Aizawa-Abe, M., Miyanaga, F., Takaya, K., Hayashi, T., Inoue, G., Hosoda, K., Kojima, M., Kangawa, K. and Nakao, K. (2001). "Ghrelin, an Endogenous Growth Hormone Secretagogue, Is a Novel Orexigenic Peptide That Antagonizes Leptin Action Through the Activation of Hypothalamic Neuropeptide Y/Y1 Receptor Pathway." Diabetes **50**(2): 227-232.

Shor-Posner, G., Azar, A. P., Jhanwar-Uniyal, M., Filart, R. and Leibowitz, S. F. (1986). "Destruction of noradrenergic innervation to the paraventricular nucleus: Deficits in food intake, macronutrient selection, and compensatory eating after food deprivation." Pharmacology Biochemistry and Behavior **25**(2): 381-392.

Sibson, N. R., Dhankhar, A., Mason, G. F., Rothman, D. L., Behar, K. L. and Shulman, R. G. (1998). "Stoichiometric coupling of brain glucose metabolism and glutamatergic neuronal activity." Proceedings of the National Academy of Sciences **95**(1): 316-321.

Silver, I. A. and Erecinska, M. (1997). "Energetic demands of the Na+/K+ ATPase in mammalian astrocytes." Glia **21**(1): 35-45.

Sima, A. A. (2010). "Encephalopathies: the emerging diabetic complications." Acta Diabetol **47**(4): 279-293.

Simpson, I. A., Chundu, K. R., Davies-Hill, T., Honer, W. G. and Davies, P. (1994). "Decreased concentrations of GLUT1 and GLUT3 glucose transporters in the brains of patients with Alzheimer's disease." Annals of Neurology **35**(5): 546-551.

Singh, P., Jain, A. and Kaur, G. (2004). "Impact of hypoglycemia and diabetes on CNS: Correlation of mitochondrial oxidative stress with DNA damage." Molecular and Cellular Biochemistry **260**(1): 153-159.

Skulachev, V. P. (1998). "Uncoupling: new approaches to an old problem of bioenergetics." Biochim Biophys Acta **1363**(2): 100-124.

Smith, A., Sturgess, W. and Gallagher, J. (1999). "Effects of a low dose of caffeine given in different drinks on mood and performance." Human Psychopharmacology: Clinical and Experimental **14**(7): 473-482.

Smith, A. I. and Funder, J. W. (1988). "Proopiomelanocortin Processing in the Pituitary, Central Nervous System, and Peripheral Tissues." Endocrine Reviews **9**(1): 159-179.

Snyder, S. H. and Kim, S. (2004). "No glial death with NO." Nature Cell Biology **6**: 17.

Sofroniew, M. V. (2009). "Molecular dissection of reactive astrogliosis and glial scar formation." Trends Neurosci **32**(12): 638-647.

Sohn, J.-W. (2015). "Network of hypothalamic neurons that control appetite." BMB Reports **48**(4): 229-233.

Song, Z., Levin, B. E., McArdle, J. J., Bakhos, N. and Routh, V. H. (2001). "Convergence of pre- and postsynaptic influences on glucosensing neurons in the ventromedial hypothalamic nucleus." Diabetes **50**(12): 2673-2681.

Späth-Schwalbe, E., Born, J., Schrezenmeier, H., Bornstein, S., Stromeyer, P., Drechsler, S., Fehm, H. and Porzsolt, F. (1994). "Interleukin-6 stimulates the hypothalamus-pituitary-adrenocortical axis in man." The Journal of Clinical Endocrinology & Metabolism **79**(4): 1212-1214.

Spiegelman, B. M. and Flier, J. S. (2001). "Obesity and the regulation of energy balance." Cell **104**(4): 531-543.

Sprague, J. E. and Arbeláez, A. M. (2011). "Glucose Counterregulatory Responses to Hypoglycemia." Pediatric endocrinology reviews : PER **9**(1): 463-475.

St-Pierre, J., Buckingham, J. A., Roebuck, S. J. and Brand, M. D. (2002). "Topology of Superoxide Production from Different Sites in the Mitochondrial Electron Transport Chain." Journal of Biological Chemistry **277**(47): 44784-44790.

Stahl, S. M. (1998). "Mechanism of action of serotonin selective reuptake inhibitors: Serotonin receptors and pathways mediate therapeutic effects and side effects." Journal of Affective Disorders **51**(3): 215-235.

Stanley, S., Wynne, K., McGowan, B. and Bloom, S. (2005). "Hormonal regulation of food intake." Physiol Rev **85**(4): 1131-1158.

Stanya, K. J., Jacobi, D., Liu, S., Bhargava, P., Dai, L., Gangl, M. R., Inouye, K., Barlow, J. L., Ji, Y., Mizgerd, J. P., Qi, L., Shi, H., McKenzie, A. N. and Lee, C. H. (2013). "Direct control of hepatic glucose production by interleukin-13 in mice." J Clin Invest **123**(1): 261-271.

Steffens, A. B., Scheurink, A. J., Luiten, P. G. and Bohus, B. (1988). "Hypothalamic food intake regulating areas are involved in the homeostasis of blood glucose and plasma FFA levels." Physiol Behav **44**(4-5): 581-589.

Steinman, M. Q., Gao, V. and Alberini, C. M. (2016). "The Role of Lactate-Mediated Metabolic Coupling between Astrocytes and Neurons in Long-Term Memory Formation." Frontiers in Integrative Neuroscience **10**(10).

Stephens, H. R. and Sandborn, E. B. (1976). "Cytochemical localization of glucose-6-phosphatase activity in the central nervous system of the rat." Brain Res **113**(1): 127-146.

Stincone, A., Prigione, A., Cramer, T., Wamelink, M. M., Campbell, K., Cheung, E., Olin-Sandoval, V., Grüning, N. M., Krüger, A. and Tauqeer Alam, M. (2015). "The return of metabolism: biochemistry and physiology of the pentose phosphate pathway." Biological Reviews **90**(3): 927-963.

Stone, E. A. and Platt, J. E. (1982). "Brain adrenergic receptors and resistance to stress." Brain Res **237**(2): 405-414.

Stosic-Grujicic, S., Stojanovic, I., Maksimovic-Ivanic, D., Momcilovic, M., Popadic, D., Harhaji, L., Miljkovic, D., Metz, C., Mangano, K., Papaccio, G., Al-Abed, Y. and Nicoletti, F. (2008). "Macrophage migration inhibitory factor (MIF) is necessary for progression of autoimmune diabetes mellitus." Journal of Cellular Physiology **215**(3): 665-675.

Stout, C. E., Costantin, J. L., Naus, C. C. and Charles, A. C. (2002). "Intercellular calcium signaling in astrocytes via ATP release through connexin hemichannels." J Biol Chem **277**(12): 10482-10488.

Strack, A., Sawyer, W., Platt, K. and Loewy, A. (1989). "CNS cell groups regulating the sympathetic outflow to adrenal gland as revealed by transneuronal cell body labelling with pseudorabies virus." Brain research **491**(2): 274-296.

Stumvoll, M., Goldstein, B. J. and van Haeften, T. W. (2005). "Type 2 diabetes: principles of pathogenesis and therapy." The Lancet **365**(9467): 1333-1346.

Su, Y., Lam, T. K., He, W., Pocai, A., Bryan, J., Aguilar-Bryan, L. and Gutiérrez-Juárez, R. (2012). "Hypothalamic leucine metabolism regulates liver glucose production." Diabetes **61**(1): 85-93.

Suadicani, S. O., Brosnan, C. F. and Scemes, E. (2006). "P2X7 receptors mediate ATP release and amplification of astrocytic intercellular Ca2+ signaling." Journal of Neuroscience **26**(5): 1378-1385.

Subramanian, A., Tamayo, P., Mootha, V. K., Mukherjee, S., Ebert, B. L., Gillette, M. A., Paulovich, A., Pomeroy, S. L., Golub, T. R. and Lander, E. S. (2005). "Gene set enrichment analysis: a knowledge-based approach for interpreting genome-wide expression profiles." Proceedings of the National Academy of Sciences **102**(43): 15545-15550.

Suh, S. W., Gum, E. T., Hamby, A. M., Chan, P. H. and Swanson, R. A. (2007). "Hypoglycemic neuronal death is triggered by glucose reperfusion and activation of neuronal NADPH oxidase." J Clin Invest **117**(4): 910-918.

Sutton, R., Keohane, M. E., VandenBerg, S. R. and Gonias, S. L. (1994). "Plasminogen activator inhibitor-1 in the cerebrospinal fluid as an index of neurological disease." Blood Coagulation & Fibrinolysis **5**(2): 167-172.

Suzuki, A., Stern, S. A., Bozdagi, O., Huntley, G. W., Walker, R. H., Magistretti, P. J. and Alberini, C. M. (2011). "Astrocyte-neuron lactate transport is required for long-term memory formation." Cell **144**(5): 810-823.

Swanson, L. W. and Kuypers, H. G. (1980). "The paraventricular nucleus of the hypothalamus: cytoarchitectonic subdivisions and organization of projections to the pituitary, dorsal vagal complex, and spinal cord as demonstrated by retrograde fluorescence double-labeling methods." J Comp Neurol **194**(3): 555-570.

Swanson, R. A., Ying, W. and Kauppinen, T. M. (2004). "Astrocyte influences on ischemic neuronal death." Current molecular medicine **4**(2): 193-205.

Syed, N. i. H. and Kennedy, C. (2012). "Pharmacology of P2X receptors." Wiley Interdisciplinary Reviews: Membrane Transport and Signaling **1**(1): 16-30.

Szepietowska, B., Zhu, W., Chan, O., Horblitt, A., Dziura, J. and Sherwin, R. S. (2011). "Modulation of beta-adrenergic receptors in the ventromedial hypothalamus influences counterregulatory responses to hypoglycemia." Diabetes **60**(12): 3154-3158.

Szepietowska, B., Zhu, W. and Sherwin, R. S. (2013). "β(2)-Adrenergic receptor agonist administration promotes counter-regulatory responses and recovery from hypoglycaemia in rats." Diabetologia **56**(11): 10.1007/s00125-00013-03009-00127.

Taborsky, G. J., Ahrén, B. and Havel, P. J. (1998). "Autonomic mediation of glucagon secretion during hypoglycemia: implications for impaired alpha-cell responses in type 1 diabetes." Diabetes **47**(7): 995-1005.

Takahashi, S., Izawa, Y. and Suzuki, N. (2012). "Astroglial pentose phosphate pathway rates in response to high-glucose environments." ASN neuro **4**(2): AN20120002.

Taniguchi, C. M., Emanuelli, B. and Kahn, C. R. (2006). "Critical nodes in signalling pathways: insights into insulin action." Nature Reviews Molecular Cell Biology **7**: 85.

Terpstra, M., Moheet, A., Kumar, A., Eberly, L. E., Seaquist, E. and Oz, G. (2014). "Changes in human brain glutamate concentration during hypoglycemia: insights into cerebral adaptations in hypoglycemia-associated autonomic failure in type 1 diabetes." J Cereb Blood Flow Metab **34**(5): 876-882.

Territo, P. R., Mootha, V. K., French, S. A. and Balaban, R. S. (2000). "Ca2+ activation of heart mitochondrial oxidative phosphorylation: role of the F0/F1-ATPase." American Journal of Physiology-Cell Physiology **278**(2): C423-C435.

Thaler, J. P., Yi, C. X., Schur, E. A., Guyenet, S. J., Hwang, B. H., Dietrich, M. O., Zhao, X., Sarruf, D. A., Izgur, V., Maravilla, K. R., Nguyen, H. T., Fischer, J. D., Matsen, M. E., Wisse, B. E., Morton, G. J., Horvath, T. L., Baskin, D. G., Tschop, M. H. and Schwartz, M. W. (2012). "Obesity is associated with hypothalamic injury in rodents and humans." J Clin Invest **122**(1): 153-162.

The Gene Ontology, C., Ashburner, M., Ball, C. A., Blake, J. A., Botstein, D., Butler, H., Cherry, J. M., Davis, A. P., Dolinski, K., Dwight, S. S., Eppig, J. T., Harris, M. A., Hill, D. P., Issel-Tarver, L., Kasarskis, A., Lewis, S., Matese, J. C., Richardson, J. E., Ringwald, M., Rubin, G. M. and Sherlock, G. (2000). "Gene Ontology: tool for the unification of biology." Nature genetics **25**(1): 25-29.

The Gene Ontology Consortium (2017). "Expansion of the Gene Ontology knowledgebase and resources." Nucleic Acids Research **45**(Database issue): D331-D338.

Thompson, R. H., Canteras, N. S. and Swanson, L. W. (1996). "Organization of projections from the dorsomedial nucleus of the hypothalamus: a PHA-L study in the rat." J Comp Neurol **376**(1): 143-173.

Thorens, B. and Larsen, P. J. (2004). "Gut-derived signaling molecules and vagal afferents in the control of glucose and energy homeostasis." Curr Opin Clin Nutr Metab Care **7**(4): 471-478.

Thurston, J. H., Hauhart, R. E. and Schiro, J. A. (1983). "Lactate reverses insulin-induced hypoglycemic stupor in suckling-weanling mice: biochemical correlates in blood, liver, and brain." J Cereb Blood Flow Metab **3**(4): 498-506.

Tian, Q., Stepaniants, S. B., Mao, M., Weng, L., Feetham, M. C., Doyle, M. J., Yi, E. C., Dai, H., Thorsson, V., Eng, J., Goodlett, D., Berger, J. P., Gunter, B., Linseley, P. S., Stoughton, R. B., Aebersold, R., Collins, S. J., Hanlon, W. A. and Hood, L. E. (2004). "Integrated genomic and proteomic analyses of gene expression in Mammalian cells." Mol Cell Proteomics **3**(10): 960-969.

Tinevez, J.-Y., Dragavon, J., Baba-Aissa, L., Roux, P., Perret, E., Canivet, A., Galy, V. and Shorte, S. (2012). Chapter fifteen - A Quantitative Method for Measuring Phototoxicity of a Live Cell Imaging Microscope. Methods in Enzymology. P. M. Conn, Academic Press. **506:** 291-309.

Toda, C., Santoro, A., Kim, J. D. and Diano, S. (2017). "POMC Neurons: From Birth to Death." Annual review of physiology **79**: 209-236.

Tomic, M., Jobin, R. M., Vergara, L. A. and Stojilkovic, S. S. (1996). "Expression of purinergic receptor channels and their role in calcium signaling and hormone release in pituitary gonadotrophs. Integration of P2 channels in plasma membrane- and endoplasmic reticulum-derived calcium oscillations." J Biol Chem **271**(35): 21200-21208.

Tong, Q., Ye, C., McCrimmon, R. J., Dhillon, H., Choi, B., Kramer, M. D., Yu, J., Yang, Z., Christiansen, L. M., Lee, C. E., Choi, C. S., Zigman, J. M., Shulman, G. I., Sherwin, R. S., Elmquist, J. K. and Lowell, B. B. (2007). "Synaptic Glutamate Release by Ventromedial Hypothalamic Neurons Is Part of the Neurocircuitry that Prevents Hypoglycemia." Cell Metabolism **5**(5): 383-393.

Tonkonogi, M., Krook, A., Walsh, B. and Sahlin, K. (2000). "Endurance training increases stimulation of uncoupling of skeletal muscle mitochondria in humans by non-esterified fatty acids: an uncoupling-protein-mediated effect?" Biochemical Journal **351**(3): 805-810.

Trautmann, A. (2009). "Extracellular ATP in the Immune System: More Than Just a “Danger Signal”." Science Signaling **2**(56): pe6-pe6.

Trayhurn, P. (2007). "Adipocyte biology." Obesity reviews **8**: 41-44.

Tsai, S., Shameli, A. and Santamaria, P. (2008). "CD8+ T cells in type 1 diabetes." Advances in immunology **100**: 79-124.

Tsigos, C., Papanicolaou, D. A., Defensor, R., Mitsiadis, C. S., Kyrou, I. and Chrousos, G. P. (1997). "Dose Effects of Recombinant Human Interleukin-6 on Pituitary Hormone Secretion and Energy Expenditure." Neuroendocrinology **66**(1): 54-62.

Turner, C. P., Blackburn, M. R. and Rivkees, S. A. (2004). "A1 adenosine receptors mediate hypoglycemia-induced neuronal injury." J Mol Endocrinol **32**(1): 129-144.

Turnley, A. M., Stapleton, D., Mann, R. J., Witters, L. A., Kemp, B. E. and Bartlett, P. F. (1999). "Cellular distribution and developmental expression of AMP-activated protein kinase isoforms in mouse central nervous system." J Neurochem **72**(4): 1707-1716.

Turovsky, E., Theparambil, S. M., Kasymov, V., Deitmer, J. W., del Arroyo, A. G., Ackland, G. L., Corneveaux, J. J., Allen, A. N., Huentelman, M. J. and Kasparov, S. (2016). "Mechanisms of CO2/H+ sensitivity of astrocytes." Journal of Neuroscience **36**(42): 10750-10758.

Ullrich, A., Bell, J., Chen, E. Y., Herrera, R., Petruzzelli, L., Dull, T. J., Gray, A., Coussens, L., Liao, Y.-C. and Tsubokawa, M. (1985). "Human insulin receptor and its relationship to the tyrosine kinase family of oncogenes." Nature **313**(6005): 756.

Ungerstedt, U. (1971). "Stereotaxic mapping of the monoamine pathways in the rat brain." Acta Physiol Scand Suppl **367**: 1-48.

Uysal, K. T., Wiesbrock, S. M., Marino, M. W. and Hotamisligil, G. S. (1997). "Protection from obesity-induced insulin resistance in mice lacking TNF-alpha function." Nature **389**(6651): 610-614.

Vaarala, O., Atkinson, M. A. and Neu, J. (2008). "The “Perfect Storm” for Type 1 Diabetes." The Complex Interplay Between Intestinal Microbiota, Gut Permeability, and Mucosal Immunity **57**(10): 2555-2562.

van der Meer, M. J. M., Sweep, C. G. J., Rijnkels, C. E. M., Pesman, G. J., Tilders, F. J. H., Kloppenborg, P. W. C. and Hermus, A. R. M. M. (1996). "Acute stimulation of the hypothalamic-pituitary-adrenal axis by IL-1ß, TNFα and IL-6: A dose response study." Journal of Endocrinological Investigation **19**(3): 175-182.

van der Meulen, T., Donaldson, C. J., Caceres, E., Hunter, A. E., Cowing-Zitron, C., Pound, L. D., Adams, M. W., Zembrzycki, A., Grove, K. L. and Huising, M. O. (2015). "Urocortin3 mediates somatostatin-dependent negative feedback control of insulin secretion." Nat Med **21**(7): 769-776.

van der Valk, J., Brunner, D., De Smet, K., Fex Svenningsen, A., Honegger, P., Knudsen, L. E., Lindl, T., Noraberg, J., Price, A., Scarino, M. L. and Gstraunthaler, G. (2010). "Optimization of chemically defined cell culture media--replacing fetal bovine serum in mammalian in vitro methods." Toxicol In Vitro **24**(4): 1053-1063.

Van Wagoner, N. J. and Benveniste, E. N. (1999). "Interleukin-6 expression and regulation in astrocytes." J Neuroimmunol **100**(1-2): 124-139.

Vannucci, R. C., Nardis, E. E., Vannucci, S. J. and Campbell, P. A. (1981). "Cerebral carbohydrate and energy metabolism during hypoglycemia in newborn dogs." Am J Physiol **240**(3): R192-199.

Vannucci, S. J., Reinhart, R., Maher, F., Bondy, C. A., Lee, W.-H., Vannucci, R. C. and Simpson, I. A. (1998). "Alterations in GLUT1 and GLUT3 glucose transporter gene expression following unilateral hypoxia–ischemia in the immature rat brain." Developmental brain research **107**(2): 255-264.

Varela, L. and Horvath, T. L. (2012). "Leptin and insulin pathways in POMC and AgRP neurons that modulate energy balance and glucose homeostasis." EMBO Rep **13**(12): 1079-1086.

Vaughan, D. E. (2005). "PAI-1 and atherothrombosis." Journal of Thrombosis and Haemostasis **3**(8): 1879-1883.

Velasquez, S. and Eugenin, E. (2014). "Role of Pannexin-1 hemichannels and purinergic receptors in the pathogenesis of human diseases." Frontiers in Physiology **5**(96).

Verkhratsky, A. (2006). "Calcium ions and integration in neural circuits." Acta Physiologica **187**(3): 357-369.

Verkhratsky, A. and Nedergaard, M. (2017). "Physiology of astroglia." Physiological reviews **98**(1): 239-389.

Verkhratsky, A., Rodríguez, J. J. and Parpura, V. (2012). "Calcium signalling in astroglia." Molecular and Cellular Endocrinology **353**(1): 45-56.

Verkhratsky, A. and Toescu, E. C. (2006). "Neuronal-glial networks as substrate for CNS integration." Journal of cellular and molecular medicine **10**(4): 826-836.

Vessby, B., Tengblad, S. and Lithell, H. (1994). "Insulin sensitivity is related to the fatty acid composition of serum lipids and skeletal muscle phospholipids in 70-year-old men." Diabetologia **37**(10): 1044-1050.

Vincent, V. A. M., Tilders, F. J. H. and Van Dam, A.-M. (1997). "Inhibition of endotoxin-induced nitric oxide synthase production in microglial cells by the presence of astroglial cells: A role for transforming growth factor β." Glia **19**(3): 190-198.

Virgintino, D., Monaghan, P., Robertson, D., Errede, M., Bertossi, M., Ambrosi, G. and Roncali, L. (1997). "An immunohistochemical and morphometric study on astrocytes and microvasculature in the human cerebral cortex." Histochem J **29**(9): 655-660.

Vlachaki Walker, J. M., Robb, J. L., Cruz, A. M., Malhi, A., Weightman Potter, P. G., Ashford, M. L. J., McCrimmon, R. J., Ellacott, K. L. J. and Beall, C. (2017). "AMP-activated protein kinase (AMPK) activator A-769662 increases intracellular calcium and ATP release from astrocytes in an AMPK-independent manner." Diabetes, obesity & metabolism **19**(7): 997-1005.

von Kügelgen, I., Späth, L. and Starke, K. (1994). "Evidence for P2-purinoceptor-mediated inhibition of noradrenaline release in rat brain cortex." British journal of pharmacology **113**(3): 815-822.

Vonend, O., Turner, C. M., Chan, C. M., Loesch, A., Carmen Dell'Anna, G., Srai, K. S., Burnstock, G. and Unwin, R. J. (2004). "Glomerular expression of the ATP-sensitive P2X7 receptor in diabetic and hypertensive rat models." Kidney International **66**(1): 157-166.

Voss, C. M., Pajęcka, K., Stridh, M. H., Nissen, J. D., Schousboe, A. and Waagepetersen, H. S. (2015). "AMPK Activation Affects Glutamate Metabolism in Astrocytes." Neurochemical Research **40**(12): 2431-2442.

Voutsinos-Porche, B., Bonvento, G., Tanaka, K., Steiner, P., Welker, E., Chatton, J.-Y., Magistretti, P. J. and Pellerin, L. (2003). "Glial glutamate transporters mediate a functional metabolic crosstalk between neurons and astrocytes in the mouse developing cortex." Neuron **37**(2): 275-286.

Waagepetersen, H., Bakken, I., Larsson, O., Sonnewald, U. and Schousboe, A. (1998). "Comparison of lactate and glucose metabolism in cultured neocortical neurons and astrocytes using 13C-NMR spectroscopy." Developmental neuroscience **20**(4-5): 310-320.

Wali, J. A. and Thomas, H. E. (2015). "Pancreatic Alpha Cells Hold the Key to Survival." EBioMedicine **2**(5): 368-369.

Wallenius, V., Wallenius, K., Ahrén, B., Rudling, M., Carlsten, H., Dickson, S. L., Ohlsson, C. and Jansson, J.-O. (2002). "Interleukin-6-deficient mice develop mature-onset obesity." Nature Medicine **8**: 75.

Walter, L., Dinh, T. and Stella, N. (2004). "ATP Induces a Rapid and Pronounced Increase in 2-Arachidonoylglycerol Production by Astrocytes, a Response Limited by Monoacylglycerol Lipase." The Journal of Neuroscience **24**(37): 8068-8074.

Walz, W. and Mukerji, S. (1988). "Lactate release from cultured astrocytes and neurons: a comparison." Glia **1**(6): 366-370.

Wang, D. D. and Bordey, A. (2008). "The astrocyte odyssey." Prog Neurobiol **86**(4): 342-367.

Wang, J., Li, G., Wang, Z., Zhang, X., Yao, L., Wang, F., Liu, S., Yin, J., Ling, E. A., Wang, L. and Hao, A. (2012). "High glucose-induced expression of inflammatory cytokines and reactive oxygen species in cultured astrocytes." Neuroscience **202**: 58-68.

Wang, R., Liu, X., Hentges, S. T., Dunn-Meynell, A. A., Levin, B. E., Wang, W. and Routh, V. H. (2004). "The Regulation of Glucose-Excited Neurons in the Hypothalamic Arcuate Nucleus by Glucose and Feeding-Relevant Peptides." Diabetes **53**(8): 1959-1965.

Wang, R. J. (1976). "Effect of room fluorescent light on the deterioration of tissue culture medium." In vitro **12**(1): 19-22.

Warburg, O. and Christian, W. (1936). "Optischer Nachweis der Hydrierung und Dehydrierung des Pyridins im Gärungs-Co-Ferment." Biochemische Zeitschrift **286**: 81.

Wasserman, D. H. (2009). "Four grams of glucose." Am J Physiol Endocrinol Metab **296**(1): E11-21.

Watts, A. G. and Donovan, C. M. (2010). "Sweet Talk In The Brain: Glucosensing, Neural Networks, and Hypoglycemic Counterregulation." Frontiers in neuroendocrinology **31**(1): 32.

Watts, A. G., Sanchez-Watts, G. and Kelly, A. B. (1999). "Distinct patterns of neuropeptide gene expression in the lateral hypothalamic area and arcuate nucleus are associated with dehydration-induced anorexia." J Neurosci **19**(14): 6111-6121.

Weaver, V. M., Petersen, O. W., Wang, F., Larabell, C., Briand, P., Damsky, C. and Bissell, M. J. (1997). "Reversion of the malignant phenotype of human breast cells in three-dimensional culture and in vivo by integrin blocking antibodies." The Journal of cell biology **137**(1): 231-245.

Wellen, K. E. and Hotamisligil, G. S. (2005). "Inflammation, stress, and diabetes." Journal of Clinical Investigation **115**(5): 1111-1119.

Wender, R., Brown, A. M., Fern, R., Swanson, R. A., Farrell, K. and Ransom, B. R. (2000). "Astrocytic Glycogen Influences Axon Function and Survival during Glucose Deprivation in Central White Matter." The Journal of Neuroscience **20**(18): 6804-6810.

Wiegers, E. C., Rooijackers, H. M., Tack, C. J., Heerschap, A., de Galan, B. E. and van der Graaf, M. (2016). "Brain Lactate Concentration Falls in Response to Hypoglycemia in Patients With Type 1 Diabetes and Impaired Awareness of Hypoglycemia." Diabetes **65**(6): 1601-1605.

Wilcox, G. (2005). "Insulin and Insulin Resistance." Clinical Biochemist Reviews **26**(2): 19-39.

Willcox, A., Richardson, S., Bone, A., Foulis, A. and Morgan, N. (2009). "Analysis of islet inflammation in human type 1 diabetes." Clinical & Experimental Immunology **155**(2): 173-181.

Williams, K. W., Margatho, L. O., Lee, C. E., Choi, M., Lee, S., Scott, M. M., Elias, C. F. and Elmquist, J. K. (2010). "Segregation of acute leptin and insulin effects in distinct populations of arcuate proopiomelanocortin neurons." J Neurosci **30**(7): 2472-2479.

Winder, W. W., Holmes, B. F., Rubink, D. S., Jensen, E. B., Chen, M. and Holloszy, J. O. (2000). "Activation of AMP-activated protein kinase increases mitochondrial enzymes in skeletal muscle." Journal of Applied Physiology **88**(6): 2219-2226.

Winkler, E. A., Nishida, Y., Sagare, A. P., Rege, S. V., Bell, R. D., Perlmutter, D., Sengillo, J. D., Hillman, S., Kong, P., Nelson, A. R., Sullivan, J. S., Zhao, Z., Meiselman, H. J., Wenby, R. B., Soto, J., Abel, E. D., Makshanoff, J., Zuniga, E., De Vivo, D. C. and Zlokovic, B. V. (2015). "GLUT1 reductions exacerbate

Alzheimer's disease vasculo-neuronal dysfunction and degeneration." Nature Neuroscience **18**: 521.

Winterbourn, C. C. and Metodiewa, D. (1994). "The reaction of superoxide with reduced glutathione." Archives of biochemistry and biophysics **314**(2): 284-290.

Wolosker, H., Balu, D. T. and Coyle, J. T. (2016). "The Rise and Fall of the d-Serine-Mediated Gliotransmission Hypothesis." Trends in Neurosciences **39**(11): 712-721.

Won, S. J., Yoo, B. H., Kauppinen, T. M., Choi, B. Y., Kim, J. H., Jang, B. G., Lee, M. W., Sohn, M., Liu, J., Swanson, R. A. and Suh, S. W. (2012). "Recurrent/moderate hypoglycemia induces hippocampal dendritic injury, microglial activation, and cognitive impairment in diabetic rats." Journal of Neuroinflammation **9**(1): 182.

Woods, S. C., Seeley, R. J., Baskin, D. G. and Schwartz, M. W. (2003). "Insulin and the blood-brain barrier." Current pharmaceutical design **9**(10): 795.

Wright, R. J., Newby, D. E., Stirling, D., Ludlam, C. A., Macdonald, I. A. and Frier, B. M. (2010). "Effects of Acute Insulin-Induced Hypoglycemia on Indices of Inflammation." Putative mechanism for aggravating vascular disease in diabetes **33**(7): 1591-1597.

Wu, Q., Boyle, M. P. and Palmiter, R. D. (2009). "Loss of GABAergic signaling by AgRP neurons to the parabrachial nucleus leads to starvation." Cell **137**(7): 1225-1234.

Wu, R., Zhang, Q. H., Lu, Y. J., Ren, K. and Yi, G. H. (2015). "Involvement of the IRE1alpha-XBP1 pathway and XBP1s-dependent transcriptional reprogramming in metabolic diseases." DNA Cell Biol **34**(1): 6-18.

Xiao, R.-P., Ji, X. and Lakatta, E. G. (1995). "Functional coupling of the beta 2-adrenoceptor to a pertussis toxin-sensitive G protein in cardiac myocytes." Molecular Pharmacology **47**(2): 322-329.

Xu, J., Song, D., Bai, Q., Zhou, L., Cai, L., Hertz, L. and Peng, L. (2013). "Role of Glycogenolysis in Stimulation of ATP Release from Cultured Mouse Astrocytes by Transmitters and High K+ Concentrations." ASN Neuro **6**(1): AN20130040.

Yabunaka, N., Nishihira, J., Mizue, Y., Tsuji, M., Kumagai, M., Ohtsuka, Y., Imamura, M. and Asaka, M. (2000). "Elevated serum content of macrophage migration inhibitory factor in patients with type 2 diabetes." Diabetes Care **23**(2): 256-258.

Yamada, E. W. and Huzel, N. J. (1985). "Ca2+-binding properties of a unique ATPase inhibitor protein isolated from mitochondria of bovine heart and rat skeletal muscle." Cell Calcium **6**(6): 469-479.

Yamauchi, T., Kamon, J., Minokoshi, Y. a., Ito, Y., Waki, H., Uchida, S., Yamashita, S., Noda, M., Kita, S. and Ueki, K. (2002). "Adiponectin stimulates glucose utilization and fatty-acid oxidation by activating AMP-activated protein kinase." Nature medicine **8**(11): 1288.

Yan, X., Shi, Z. F., Xu, L. X., Li, J. X., Wu, M., Wang, X. X., Jia, M., Dong, L. P., Yang, S. H. and Yuan, F. (2017). "Glutamate Impairs Mitochondria Aerobic Respiration Capacity and Enhances Glycolysis in Cultured Rat Astrocytes." Biomed Environ Sci **30**(1): 44-51.

Yang, C. F., Chiang, M., Gray, D. C., Prabhakaran, M., Alvarado, M., Juntti, S. A., Unger, E. K., Wells, J. A. and Shah, N. M. (2013). "Sexually dimorphic neurons in the ventromedial hypothalamus govern mating in both sexes and aggression in males." Cell **153**(4): 896-909.

Yang, D. D., Kuan, C. Y., Whitmarsh, A. J., Rincon, M., Zheng, T. S., Davis, R. J., Rakic, P. and Flavell, R. A. (1997). "Absence of excitotoxicity-induced apoptosis in the hippocampus of mice lacking the Jnk3 gene." Nature **389**(6653): 865-870.

Yi, C.-X., la Fleur, S. E., Fliers, E. and Kalsbeek, A. (2010). "The role of the autonomic nervous liver innervation in the control of energy metabolism." Biochimica et Biophysica Acta (BBA) - Molecular Basis of Disease **1802**(4): 416-431.

Yip, L. and Fathman, C. G. (2014). "Type 1 diabetes in mice and men: gene expression profiling to investigate disease pathogenesis." Immunologic research **58**(2-3): 340-350.

Yoon, J. C., Puigserver, P., Chen, G., Donovan, J., Wu, Z., Rhee, J., Adelmant, G., Stafford, J., Kahn, C. R. and Granner, D. K. (2001). "Control of hepatic gluconeogenesis through the transcriptional coactivator PGC-1." Nature **413**(6852): 131.

Yoshida, H., Matsui, T., Yamamoto, A., Okada, T. and Mori, K. (2001). "XBP1 mRNA Is Induced by ATF6 and Spliced by IRE1 in Response to ER Stress to Produce a Highly Active Transcription Factor." Cell **107**(7): 881-891.

Youle, R. J. and Van Der Bliek, A. M. (2012). "Mitochondrial fission, fusion, and stress." Science **337**(6098): 1062-1065.

Young, J. K., Baker, J. H. and Montes, M. I. (2000). "The brain response to 2-deoxy glucose is blocked by a glial drug." Pharmacology Biochemistry and Behavior **67**(2): 233-239.

Young, J. K. and McKenzie, J. C. (2004). "GLUT2 Immunoreactivity in Gomori-positive Astrocytes of the Hypothalamus." Journal of Histochemistry & Cytochemistry **52**(11): 1519-1524.

Young, M. D., Wakefield, M. J., Smyth, G. K. and Oshlack, A. (2010). "Gene ontology analysis for RNA-seq: accounting for selection bias." Genome Biology **11**(2): R14.

Yu, X., Carroll, S., Rigaud, J. L. and Inesi, G. (1993). "H+ countertransport and electrogenicity of the sarcoplasmic reticulum Ca2+ pump in reconstituted proteoliposomes." Biophysical Journal **64**(4): 1232-1242.

Yuan, P.-Q. and Yang, H. (2002). "Neuronal activation of brain vagal-regulatory pathways and upper gut enteric plexuses by insulin hypoglycemia." American Journal of Physiology-Endocrinology and Metabolism **283**(3): E436-E448.

Zamanian, J. L., Xu, L., Foo, L. C., Nouri, N., Zhou, L., Giffard, R. G. and Barres, B. A. (2012). "Genomic Analysis of Reactive Astrogliosis." The Journal of Neuroscience **32**(18): 6391-6410.

Zammitt, N. N. and Frier, B. M. (2005). "Hypoglycemia in Type 2 Diabetes." Pathophysiology, frequency, and effects of different treatment modalities **28**(12): 2948-2961.

Zhang, M., Buttigieg, J. and Nurse, C. A. (2007a). "Neurotransmitter mechanisms mediating low-glucose signalling in cocultures and fresh tissue slices of rat carotid body." The Journal of Physiology **578**(3): 735-750.

Zhang, Q. and Haydon, P. G. (2005a). "Roles for gliotransmission in the nervous system." Journal of Neural Transmission **112**(1): 121-125.

Zhang, X., Dong, F., Ren, J., Driscoll, M. J. and Culver, B. (2005b). "High dietary fat induces NADPH oxidase-associated oxidative stress and inflammation in rat cerebral cortex." Exp Neurol **191**(2): 318-325.

Zhang, X., Zhang, G., Zhang, H., Karin, M., Bai, H. and Cai, D. (2008). "Hypothalamic IKKβ/NF-κB and ER Stress Link Overnutrition to Energy Imbalance and Obesity." Cell **135**(1): 61-73.

Zhang, Z., Chen, G., Zhou, W., Song, A., Xu, T., Luo, Q., Wang, W., Gu, X.-s. and Duan, S. (2007b). "Regulated ATP release from astrocytes through lysosome exocytosis." Nature cell biology **9**(8): 945.

Zhao, H., Liu, Y., Cheng, L., Liu, B., Zhang, W., Guo, Y.-J. and Nie, L. (2013). "Mesencephalic Astrocyte-Derived Neurotrophic Factor Inhibits Oxygen–Glucose Deprivation-Induced Cell Damage and Inflammation by Suppressing Endoplasmic Reticulum Stress in Rat Primary Astrocytes." Journal of Molecular Neuroscience **51**(3): 671-678.

Zhou, G., Myers, R., Li, Y., Chen, Y., Shen, X., Fenyk-Melody, J., Wu, M., Ventre, J., Doebber, T. and Fujii, N. (2001). "Role of AMP-activated protein kinase in mechanism of metformin action." The Journal of clinical investigation **108**(8): 1167-1174.

Zhou, R., Yazdi, A. S., Menu, P. and Tschopp, J. (2010). "A role for mitochondria in NLRP3 inflammasome activation." Nature **469**: 221.

Zhou, Y., Lee, J., Reno, C. M., Sun, C., Park, S. W., Chung, J., Lee, J., Fisher, S. J., White, M. F., Biddinger, S. B. and Ozcan, U. (2011). "REGULATION OF GLUCOSE HOMEOSTASIS THROUGH XBP1-FOXO1 INTERACTION." Nature medicine **17**(3): 356-365.

Zhu, W., Czyzyk, D., Paranjape, S. A., Zhou, L., Horblitt, A., Szabo, G., Seashore, M. R., Sherwin, R. S. and Chan, O. (2010). "Glucose prevents the fall in ventromedial hypothalamic GABA that is required for full activation of glucose counterregulatory responses during hypoglycemia." Am J Physiol Endocrinol Metab **298**(5): E971-977.